Lightweight Aggregate Concrete

Science, Technology and Applications

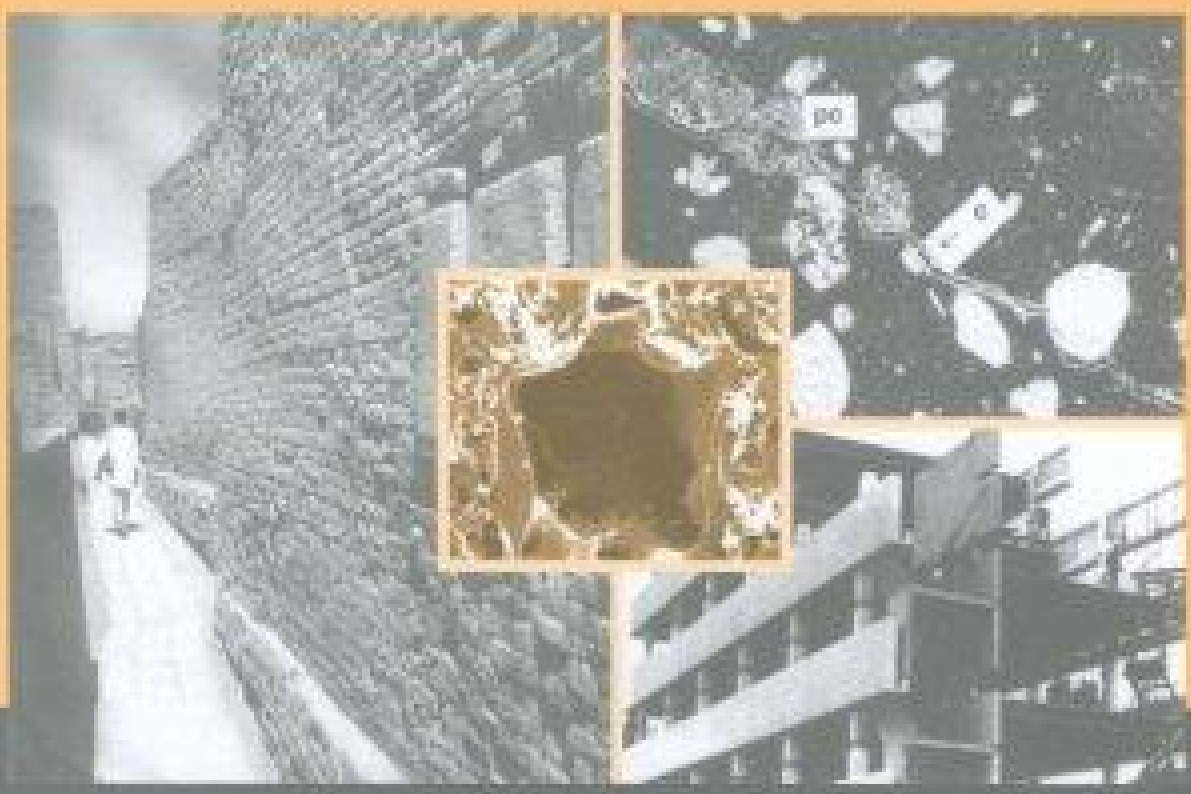

Satish Chandra
Leif Berntsson

Building Materials Series

LIGHTWEIGHT AGGREGATE CONCRETE

Science, Technology, and Applications

by

Satish Chandra and Leif Berntsson

Chalmers University of Technology
Göteborg, Sweden

NOYES PUBLICATIONS

WILLIAM ANDREW PUBLISHING
Norwich, New York, U.S.A.

Library of Congress Catalog Card Number: 2002021902
ISBN: 0-8155-1486-7
Printed in the United States

Published in the United States of America by
Noyes Publications / William Andrew Publishing
13 Eaton Avenue
Norwich, NY 13815
1-800-932-7045
www.williamandrew.com
www.knovel.com

10 9 8 7 6 5 4 3 2 1

NOTICE

To the best of our knowledge the information in this publication is accurate; however the Publisher does not assume any responsibility or liability for the accuracy or completeness of, or consequences arising from, such information. This book is intended for informational purposes only. Mention of trade names or commercial products does not constitute endorsement or recommendation for use by the Publisher. Final determination of the suitability of any information or product for use contemplated by any user, and the manner of that use, is the sole responsibility of the user. We recommend that anyone intending to rely on any recommendation of materials or procedures mentioned in this publication should satisfy himself as to such suitability, and that he can meet all applicable safety and health standards.

Library of Congress Cataloging-in-Publication Data

Chandra, S. (Satish)
Lightweight aggregate concrete / by Satish Chandra and Leif Berntsson.
p. cm. -- (Construction materials science and technology series)
ISBN 0-8155-1486-7 (alk. paper)
1. Lightweight concrete. 2. Aggregates (Building materials) I. Berntsson, Leif.
II. Title. III. Series.

TA439 .C445 2002
624.1'834--dc21 2002021902

CONSTRUCTION MATERIALS SCIENCE AND TECHNOLOGY SERIES

Editor

V. S. Ramachandran, National Research Council Canada

CONCRETE ADMIXTURES HANDBOOK; Properties, Science and Technology, *Second Edition:* edited by V. S. Ramachandran

CONCRETE ALKALI-AGGREGATE REACTIONS: edited by P. E. Grattan-Bellew

CONCRETE MATERIALS; Properties, Specifications and Testing, *Second Edition:* by Sandor Popovics

CORROSION AND CHEMICAL RESISTANT MASONRY MATERIALS HANDBOOK: by W. L. Sheppard, Jr.

HANDBOOK OF ANALYTICAL TECHNIQUES IN CONCRETE SCIENCE AND TECHNOLOGY; Principles, Techniques, and Applications: edited by V. S. Ramachandran and James J. Beaudoin

HANDBOOK OF CONCRETE AGGREGATES; A Petrographic and Technological Evaluation: by Ludmila Dolar-Mantuani

HANDBOOK OF FIBER-REINFORCED CONCRETE; Principles, Properties, Developments, and Applications: by James J. Beaudoin

HANDBOOK OF POLYMER MODIFIED CONCRETE AND MORTARS; Properties and Process Technology: by Yoshihiko Ohama

HANDBOOK OF THERMAL ANALYSIS OF CONSTRUCTION MATERIALS: edited by V. S. Ramachandran, Ralph M. Paroli, James J. Beaudoin, and Ana H. Delgado

LIGHTWEIGHT AGGREGATE CONCRETE; Science, Technology, and Applications: by Satish Chandra and Leif Berntsson

WASTE MATERIALS USED IN CONCRETE MANUFACTURING: edited by Satish Chandra

To Our Beloved Wives and Children

Acknowledgements

The authors thank first Prof. T. D. Bremner of the University of New Brunswick, Canada, for sending his papers. These have provided the inspiration and the framework for the contents of the book, especially the durability part. The authors also thank Mr. Tor Arne Hammer of SINTEF for permission to reproduce the literature from the proceedings of the International Symposium on Structural Lightweight Aggregate Concrete, held in Norway. Bipul K. Roy, England, sent the photographs, Spitzner Joachim of Liapor, Germany, sent the literature on lightweight aggregates and the status of the aggregates around the world, which we acknowledge with thanks. We are obligated to the Swedish Council of Building Research, Stockholm, and Swedish Leca, Linköping, for their support. We are indebted to D. Sesay of the Repro-department for reproducing the figures, and R. Sogdahl, Department of Environmental Inorganic Chemistry, Chalmers University of Technology, who scanned the photographs. We also thank Profs. G. Gustafson, Dean of the Faculty of Civil Engineering, and Thomas Hjärtberg, Dean of the Faculty of Chemistry, for their support. The authors appreciate the time Dr. V. S. Ramachandran, distinguished scientist, Canada, spent reviewing the book.

Finally, we thank our families, who were deprived of our time, as we were engrossed in our work. Their support is gratefully acknowledged.

Contents

Introduction

The use of lightweight aggregate concrete (LWAC) can be traced to as early as 3000 BC, when the famous towns of Mohenjo-Daro and Harappa were built during the Indus Valley civilization. In Europe, earlier use of LWAC occurred about two thousand years ago when the Romans built the Pantheon, the aqueducts, and the Colosseum in Rome. It is interesting to note that pumice is still used today as an aggregate for structural concrete in certain countries such as Germany, Italy, Iceland, and Japan. In some places, like Malaysia, palm oil shells are used for making lightweight aggregate concrete.

Earlier lightweight aggregates (LWAs) were of natural origin, mostly volcanic: pumice, scoria, tuff, etc. These have been used both as fine and coarse aggregates. They function as active pozzolanic materials when used as fine aggregates. These interact with the calcium hydroxide generated from the binder during hydration and produce calcium silicate hydrate which strengthens the structure and modifies the pore structure, enhancing the durability properties.

With the increasing demand and the non-availability of natural LWAs worldwide, techniques have been developed to produce them in factories. These are produced from the natural raw materials like expanded clay, shale, slate, etc., as well as from industrial by-products such as fly ash, bed ash, blast furnace slag, etc. The properties of the aggregates depend upon the raw materials and the process used for producing them.

Today, lightweight aggregates are produced in a very wide range of densities varying from 50 kg/m^3 for expanded perlite to 1000 kg/m^3 for clinkers. With these aggregates and high range water reducers, it is possible to make LWAC of 80 MPa 15 cm cube compressive strength.

Because of the practical advantages which it possesses, LWAC has, in recent years, become an important structural material and the demand for it is increasing. A savings in the weight of the superstructure means that foundations can be reduced in bulk, and time and expenses saved in erection and handling of components, so that smaller lifting equipment can be employed or larger precast units can be handled.

The low density results in high thermal insulation of buildings and, in some instances, the thickness of roofs and walls can be reduced. Where there is reduction in weight, a higher degree of thermal insulation will be achieved.

Nearly all LWACs are inherently fire resistant. In addition, depending upon the density and strength, the concrete can be easily cut, nailed, drilled, and chased with ordinary wood-working tools. One such example is 3L concrete developed at the Chalmers University of Technology, Göteborg, Sweden. The name is given on the basis of three properties: lightweight aggregate concrete, low density, and strength less than 20 MPa.

In the UK, clinker aggregate concrete was used in the construction of the British Museum in the early part of the 20th century. The output of clinker aggregates increased enormously in the ensuing decades, but its manufacture is now declining since oil and other fuels are more widely used for firing the furnaces. This trend is likely to continue and, as a result, the use of sintered pulverized fuel ash (fly ash) has been steadily increasing over the last decades. Besides this, other types of ashes have also been used for producing aggregates like bed ashes from boilers, etc.

In 1918, Stephen J. Hayde patented the lightweight aggregate "Haydite," the first one made by the expansion of shale, which came into production in the US. Synthetic aggregates of this type have been universally accepted, making satisfactory reinforced or prestressed concrete.

Other early applications are the ships built with the LWAC at the end of World War I, 1917. One of the famous ships was named *Selma*. After so many years of service in harsh climates, it is still in satisfactory condition. This speaks of the durability of lightweight aggregate concrete. In addition to the materials, the techniques adopted by the ship builders to construct the ship is equally important. It was so well constructed that some of the factors have become specifications for ship making.

The first building frame of reinforced LWAC in Great Britain was a three story office block at Bentford, near London, built in 1958. Since then, many structures have been built of precast, in-situ prestressed, or reinforced lightweight aggregate concrete.

With an increase in off-shore construction, and the general reluctance for using LWAC due to its low density and strength, the demand for improved strength has increased. This has led to the development of high strength structural lightweight aggregate concrete (HSLAC), specifically in Norway. The low strength of the aggregate has been balanced by using high strength cement mortar. Because this high strength matrix has a dense pore structure, it may decrease the insulating properties in comparison to the normal strength lightweight aggregate concrete.

The dense cement mortar matrix of the high strength LWAC also decreases fire resistance. However, this can be improved by modifying the pore structure using polymers, air-entraining agents, or polymer fibers. By the use of industrial by-products like fly ash, slag, and other types of ashes in making LWA, ecological and environmental problems are solved to some extent.

Lightweight aggregate is expensive, but the cost is calculated not just on the basis of aggregates or LWAC. Other costs involved are taken into consideration also, like working cost, reinforcement cost, transport cost, etc. Being lightweight, it is easy for the workers to handle and they complain less of back pain. The biggest advantage, which is generally not raised, is the enormous expenditure involved in medical aid to workers. Consequently, the contractor has to find substitute workers to avoid project delays. Another advantage is in the demolition cost. It takes less energy to demolish LWAC compared to normal concrete, as smaller equipment can be used. Apart from this, since it contains air, the amount of the waste will be less than when using normal concrete.

The bond between the aggregate and the matrix is stronger in the case of LWAC than in normal weight concrete. Cement paste penetrates inside the aggregates due to their porous nature. Thus, there is very little or no interfacial transition zone between the aggregates and the matrix, the weakest zone. It is a very important feature from the durability aspect of LWAC.

The use of lightweight aggregate concrete is increasing and research and development are going on worldwide to develop high performance structural lightweight aggregate concrete.

Preface

Lightweight aggregate concrete (LWAC) has its roots in the ancient period ca. 3000 years before the Christian Era. The aggregates used for making concrete were of volcanic origin. With time, the demand for LWAC increased and technologies were developed to produce the aggregates in factories. The raw materials used for producing lightweight aggregates (LWA) are natural minerals like clays, shales, and slates, as well as industrial by-products like fly ash, bed ash, blast furnace slag, etc. Synthetic organic aggregates, like polystyrene beads, are also used for making insulation concrete.

Today, lightweight aggregates are available in a wide range of densities, strengths, and sizes. This makes it possible to design concrete with a very wide spectrum, a concrete of very low density for insulation and, at the same time, a high strength concrete, more than 80 MPa 15 cm cube compressive strength, for structural purposes. The basic advantage of LWAC is its low density, which reduces the dead load and provides insulating properties. Along with this, it is easy to handle, and heavy duty tools are not required.

In spite of the increasing use and demand, there is still a lack of adequate explanations to understand the mechanisms responsible for the strength and durability properties of LWAC. This book is written to give an overall picture of LWAC, from the historical background, aggregate production, proportioning and production of concrete, to applications in structures.

Physical properties and chemical durability are described in detail. The physical properties include density, strength, shrinkage, and elasticity. Chemical durability includes resistance to acids, chloride ingress, carbonation, and freeze-thaw resistance. Fire resistance is also included, which is seldom considered, but is a very important aspect of the safety of the structure.

Microstructure development and its relation to the durability properties of LWAC generally are not highlighted in the literature. The development of bonds, the microstructure with different binder systems, and different types of lightweight aggregates are explained. They show how lightweight aggregate concrete differs from normal weight concrete. The chapters on chloride ingress and freeze-thaw resistance are detailed because of the use of LWAC in off-shore construction, especially in Norway.

The economical aspects of using LWAC are also reviewed. Emphasis is placed on the fact that although the cost of LWAC is high, the total cost of construction has to be considered, including the cost of transport, reinforcement, etc. When these are considered then LWAC becomes cheaper and attractive. The life cycle cost of the concrete is another consideration for calculating long-term savings on maintenance costs.

Some examples, from different parts of the world where LWAC is used successfully, are also included. This is an illustrative book that explains different phenomena involved in the design and the microstructure development of concrete in a very simple language. A glossary of the terminology and definitions is included to help practicing architects and engineers tailor a concrete that is resistant to the aggressive atmosphere to which it is often exposed.

Satish Chandra
Leif Berntsson

Göteborg, Sweden
1 June 2001

1

Historical Background of Lightweight Aggregate Concrete

1.0 INTRODUCTION

Lightweight Aggregate Concrete, LWAC, is not a new invention in concrete technology. It has been known since ancient times, so it is possible to find a good number of references in connection with the use of LWAC. It was made using natural aggregates of volcanic origin such as pumice, scoria, etc. Sumerians used this in building Babylon in the 3rd millennium B.C. (Fig. 1.1). The Greeks and the Romans used pumice in building construction. Some of these magnificent ancient structures still exist, like St. Sofia Cathedral or Hagia Sofia, in Istanbul, Turkey, built by two engineers, Isidore of Miletus and Anthemius of Tralles, commissioned by the Emperor Justinian in the 4th century A.D., (Fig. 1.2); the Roman temple, Pantheon, which was erected in the years A.D. 118 to 128; the prestigious aqueduct, Pont du Gard, built ca. A.D. 14; and the great Roman amphitheatre, Colosseum, built between A.D. 70 and 82 (Figs. 1.3, 1.4, and 1.5). In addition to building constructions, the Romans used natural lightweight aggregates and hollow clay vases for their "Opus Caementitium" in order to reduce the weight. This was also used in the construction of the Pyramids during the Mayan period in Mexico (Fig. 1.6).[1]

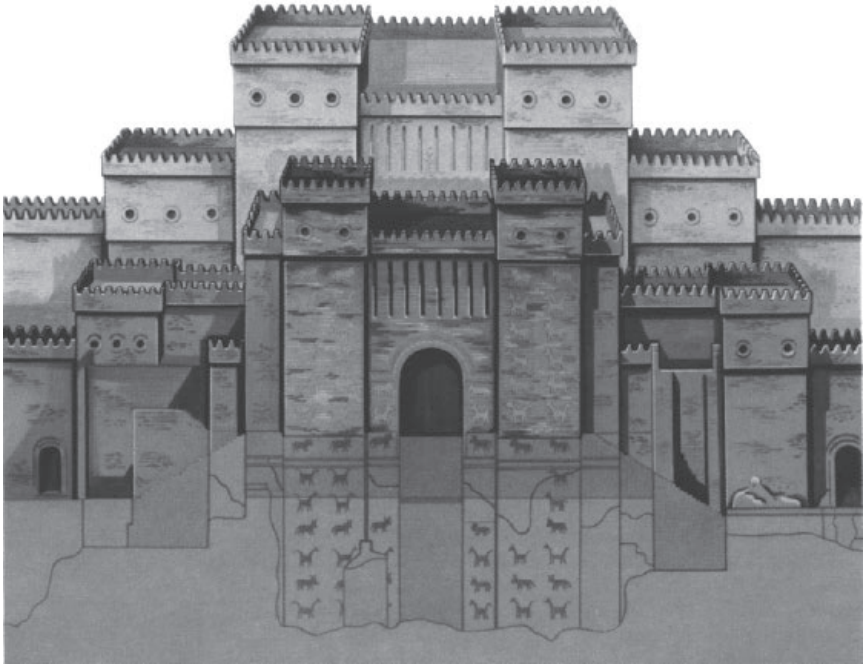

Figure 1.1. Babylon, Iraq, built by Sumerians in the 3rd millenium B.C.

Figure 1.2. St. Sofia Cathedral, Hagia Sofia, commissioned by the Emperor Justinian in the 4th century A.D. in Istanbul, Turkey.

Figure 1.3. The Roman temple, Pantheon, built in A.D. 118.

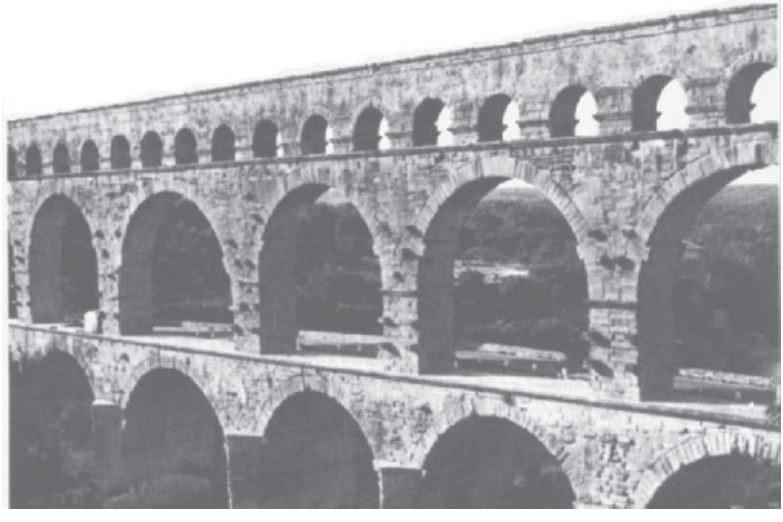

Figure 1.4. The prestigious aqueduct, Pont du Gard, built in ca. A.D. 14.

Figure 1.5. The great Roman amphitheatre, Colosseum, built between A.D. 70 and 82.

Figure 1.6. Pyramids in Mexico, built during the Mayan period, A.D. 624–987.

Porous clay bricks were produced long before the Christian era, during Indus Valley civilization ca. 2500 B.C.[2] These were used in the construction of two cities, Mohenjo-Daro and Harappa (Fig. 1.7). It is postulated that these porous bricks were crushed and used as the lightweight aggregates in the masonry. Although the origin of the LWAC is difficult to assess, it would not be an exaggeration to say that its roots are from the ancient period.

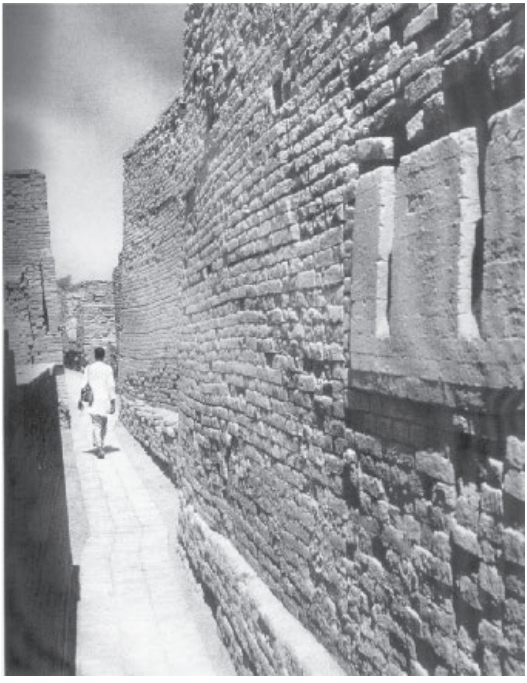

Figure 1.7. Mohenjo-Daro and Harappa, 2500 B.C.

With the increase in the demand of LWAC and the unavailability of the aggregates, technology for producing lightweight aggregates has been developed. In Germany, in the 19th century, porous clay pieces were produced by quick evaporation of water. Kukenthal from Braunschweig obtained a patent in 1880. The industrial use of natural lightweight aggregates in Germany was started in 1845 by Ferdinand Nebel from Koblenz who produced masonry blocks from pumice, with burnt lime as the binder.[3] In Iceland, pumice has been used in local building industries since 1928.

Concrete is mostly known as a grey material with good mechanical strength, but heavy and cold. It is generally understood that concrete is not necessarily just heavy, sharp-edged grey blocks. It can acquire any shape, color, density, and strength. The low density of pumice aggregates results in weight reduction of the structures and the foundations, and provides considerable savings regarding thermal insulation. The low density of the material results in high thermal insulation for buildings and, in some instances, the thickness of roofs and walls can be reduced. Where there is no reduction in thickness, a higher degree of thermal insulation will be achieved. The density, for example, can range from 300 to 3000 kg/m^3; thermal conductivity from 0.1 to 3 W/mK; and strength from 1 to 100 MPa or even more. The density is mostly controlled by the type of aggregate used. The strength is also partially dependent upon the type of aggregates used for making the concrete. A range of density and strength of concrete is given in Fig. 1.8.

Lightweight aggregates are the basic ingredient for making LWAC and their development through the ages is discussed here.

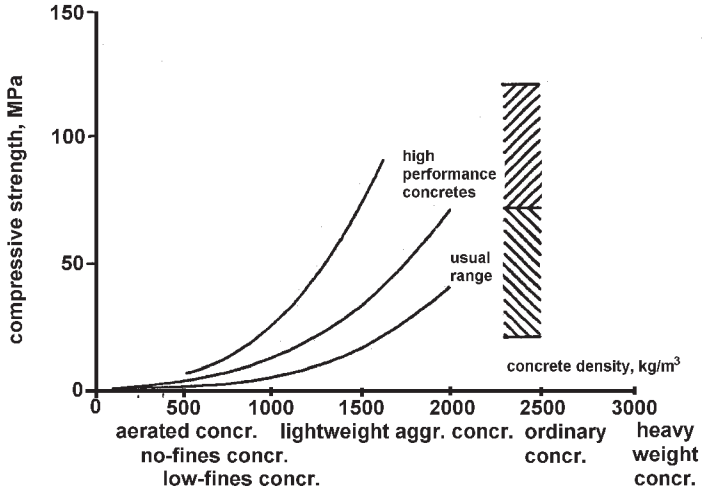

Figure 1.8. Weight and strength range of concrete.[3]

2.0 LIGHTWEIGHT AGGREGATES (LWA)

Lightweight aggregates can originate from natural resources or they can be man-made. The major natural resource is the volcanic material. Man-made or synthetic, aggregates are produced by a thermal process in factories.

2.1 Natural Aggregates

Volcanic Origin. When lava from a volcano cools down, it produces a spongy well-sintered mass. Since there is an abrupt cooling of the molten mass, the material freezes. With a sudden cooling of the molten magma, there is no crystallization, and the material acquires a glassy structure, a process similar to the production of the glass known as obsidian. It can be called a supercooled liquid, which has no crystalline phase. It is highly amorphous and has a glassy structure.

Lava is a boiling melt which may contain air and gases, and when it cools down, it freezes to a spongy porous mass. In other words, it produces lightweight material that is porous and reactive. This type of material is known as *volcanic aggregates*, or *pumice* or *scoria aggregates*. The aggregates are produced by mechanical handling of lava, i.e., crushing, sieving, and grinding.

Organic Aggregates; Palm Oil Shells. The use of agricultural waste as aggregates for the production of building materials has several practical and economical advantages. The palm oil industry which is important in many countries, such as Malaysia, Indonesia, and Nigeria, produces a large amount of waste which can be utilized in the production of building materials. Palm oil shells are produced in large quantities by the oil mills and can be used as aggregates in the production of lightweight concrete.[4] It is reported that, in 1989, world palm oil production reached about 9.6 million tons per year from a modest start in the early 1920s, due to the increasing demand for vegetable oil. Malaysia contributed 5.5 million tons per year from a palm oil cultivation of 1.85 million hectares during the same year, making it a major producer of palm oil. About 1.1 tons of shells, or 5.5% of the weight of the fresh fruit bunch, is produced annually from each hectare cultivated. The palm oil shells are hard and are received as crushed pieces as a result of the process used to release the oil. Palm oil shells have a bulk density of 620 kg/m^3 and a specific gravity of 1.25.

Though still not in commercial production of LWAC, these are used locally. There are two big advantages:

1. At present they have no commercial value.
2. Being locally available, the transport cost is nominal.

It is in the research and development stage. It is expected that soon these will be commercialized. (For details see Ch. 2.)

2.2 Synthetic Aggregates

Synthetic aggregates are produced by thermal treatment of the materials which have expansive properties. These materials can be divided in three groups

- Natural materials, such as perlite, vermiculite, clay, shale, and slate.
- Industrial products, such as glass.
- Industrial by-products, like fly ash, expanded slag cinder, bed ash, etc.

The most common types of lightweight aggregates produced from expansive clays are known as Leca and Liapor. Those made from fly ash are known as Lytag, etc. The bulk density of the aggregates varies greatly depending upon the raw materials and the process used for their manufacture. The development of lightweight aggregates in different parts of the world is reviewed below.

2.3 North America

Stephen John Hayde, of Kansas City, Missouri, was a contractor and brickmaker. He observed abnormal bloating in the bricks when burnt. This gave him the idea of making expanded clay pieces, e.g., aggregates, from this clay. He did tests for producing the aggregates and in February, 1918, received a patent on his process for the production of expanded shale aggregates in a rotary kiln.[5]

In 1920, the first commercial plant began operating in Kansas City, producing “Haydite” expanded shale aggregates. By the year 1941, there were seven plants in the USA and one plant in Canada. In 1952, the Expanded Shale, Clay and Slate Institute (ESCSI) was founded, and the

expanded clay aggregates became more and more attractive. By the year 1955, there were fifty-five producers in the USA and Canada. The output was 1.7 million cubic meters and increased to more than three million cubic meters in 1958. According to a report published in Germany in 1964 by Waltz and Wischers, 65% of the LWA production was based on shale, 29% on clay, and 6% on slate. Many well known producers started in the 1950s or early 1960s, for instance, Arkalite (clay, 1959), Utelite (shale, 1962), and Lehigh (shale, 1964). Mostly, the US plants produce LWA in a medium bulk density of 500 to 700 kg/m^3, which limits their use.

2.4 Europe

Not long after Hayde's patent in the USA, a patent was granted to Oskar Ohlsen on September 2, 1919, but it was not commercialized because of some disputes.[2]

In Germany, the first commercial production of expanded clay ensued between 1935 and 1939 at Sommerfeld/Niederlausitz and at Rudersdorf near Berlin. Some tests were conducted by the State Material Research Institute in 1938 to evaluate the suitability of the waste material from roof slate production, for use as aggregates for producing concrete.[6] But the results were not satisfactory and further investigations were recommended.

In general, however, Denmark can be looked at as the European birthplace of expanded clay. A plant was erected in 1939 at Rösnes near Kalundborg, producing Leca (Expanded Clay Aggregate) in a rotary kiln. The annual production capacity then was 20,000 m^3. Later, the plant moved to Hinge, where it now has six constructed kilns, with a capacity of 1.3 million m^3 per annum. The technical know-how was given to many countries. There are 35 kilns in operation, worldwide, following the Leca process with a capacity of six million m^3. The first German Leca plant started in February, 1956, near Itzehohe/Mittelholstein.

In the UK, until the 1970s, there was a fairly wide choice of lightweight aggregates for making structural lightweight concrete. Among the processed natural materials, there was regular production on a commercial scale of aggregates like Leca, Aglite (expanded shale, irregular in shape), and Solite (expanded slate-mainly rounded). Leca has a low density and, therefore, low strength. Owing to this, it is difficult to achieve a characteristic concrete strength of 20 N/mm^2. Aglite and Solite possess higher density and have higher strength. These could produce the range of

concrete strength suitable for most types of reinforced and pre-stressed concrete structures, although the application of Aglite concrete in pre-stressed structures has been scarce. Solite concrete can achieve high strength—grade 60 (60 MPa, cube compressive strength) or even higher—without much difficulty and is thus a suitable alternative component for pre-stressed concrete construction.

Processed industrial by-products include Lytag (sintered pulverized fuel ash, sintered PFA) and foamed slag (manufactured from molten blast furnace slag). The concrete made with the latter is relatively heavy, actually the heaviest of all LWAC, average density is in the region of 2000–2300 kg/m^3, so that the use of foam slag concrete was not very popular. Lytag, like Solite, can produce concrete encompassing a wide strength range from medium to high and even very high strength (such as 60 grade or over), and can be suitably and cost effectively used for all types of reinforced or pre-stressed concrete construction.

By the mid 1970s, however, the number of choices was limited. The production of Solite ceased because of environmental restrictions. Very soon the manufacture of Aglite also stopped, mainly for economic reasons. Foamed slag was virtually withdrawn from the market, although, in its place, a much improved aggregate known as *Perlite*—a pelletized expanded blast furnace slag—came into production. Perlite can produce medium to high strength concrete within a density range of 1700 to 2000 kg/m^3. However, only a relatively small portion of Perlite is actually used in structural concrete, the rest goes to the "block" manufacturing industry. Aggregates produced by sintering colliery tailings, known as Brag, was also manufactured for a short period, but production soon ended as the permission for production was not granted.

By 1994, there was a further decline in the manufacture of UK-produced LWA. Leca ceased production due to loss of clay extraction rights. Lytag had to close down two factories for the lack of ashes, a direct consequence of national policy on use of coal for thermal power generation. In fact, Perlite and Lytag are the only two LWA used in the UK. However, there are some imported aggregates which include Liapor, Granolux, Arlits (expanded clay, Spain), Aardelite (cold-bonded PFA from Holland), and Isotag.

The historical development in Europe was somewhat similar to North America, with many plants for expanded clay, shale, and slate being erected around the 1960s. For example, in 1955 and 1964 two plants started in Czechoslovakia (Bratislava and Vintirov) where international conferences on LWA were held in 1967 and 1968. Further developments ended due to the political uncertainty in 1968.

In western Europe, Liapor came into production in Germany (1967, 1969), France (1970), and Spain (1973). Many other countries started at about the same time or somewhat earlier, for example, Scandinavian countries.

Nevertheless, all production plants have not been successful. The main problems that they could not solve had to do with raw material, production process, quality, and marketing. Some production plants had too little capacity, not enough for the survival of the plant owner. In Germany, several plants were closed in the 1970s and 1980s. The production in the remaining plants was, however, raised. In Germany, an association of Lightweight Producers named BLZ (Bundesverband Leichtbetonzuschlag-Industrie) was founded in December, 1970. Six plants are in operation today.

In contrast to the USA, the Europeans used fly ash from coal thermal power stations as raw material, producing relatively heavy LWA of around 800 kg/m^3 bulk density. Started in the UK in 1960, sintered fly ash production was later established in 1973 in Germany and in 1985 in the Netherlands. In 1993, a plant was put up in the Netherlands to produce lime-bound fly ash aggregates which were made by steam curing. The density of these aggregates was 800 to 850 kg/m^3 for the grain sizes >4 mm.

2.5 Western and Middle Europe

For expanded clay, shale, and slate, thirty-two plants are currently installed; thirty of them were running in 1994. Additionally, there are five plants for LWA based on fly ash. In eight countries, as mentioned below by their symbols, there is only one plant. In Italy and Germany, there are five or more. The local distribution, as well as, capacity and sales in 1000 m^3 can be seen from the following list:[7]

	Capacity	**Sales 1994 m^3**
Eight countries with one plant each A, B, CH, CZ, E, P, S, SF	3,500	2,110
Ten countries with two or more plants D, DK, F, I, LV, LT, N, NL, PL, UK	10,450	5,190
Total	13,950	7,300

The ratio between the installed capacity and sales in most countries ranges between 50 and 80%, the lowest figures being below 20% in Latvia (LT), Lituania (LV), and Poland (PL). In some countries, the consumption per inhabitant is less than 10 liters per year, in others it exceeds 200 liters.

To the figures above, the volume of the natural LWA for pumice in Germany and Iceland should be added, i.e., 4.4 million m^3 in 1994. There have also been some million m^3 of scoria (D: 2.6 million m^3 with bulk density 800–1000 kg/m^3), but this volume was not completely used for concrete. The LWA for concrete in Western and Middle Europe might actually reach a total volume of about 12 million m^3.

2.6 Russia

The Russian LWA history began in the 1930s when Prof. Kostyrko started research on the production of LWA. The aggregate produced was named *Keramsit*. His work was interrupted by World War II, so the first rotary kiln was not installed before 1955 in Volgograd on a laboratory scale with 1 m^3/h output. Following are the statistics of the production of Keramsit in Russia;

1958:	174,000 m^3
1960:	690,000 m^3
1962:	2,850,000 m^3
1965:	7,750,000 m^3

In the 1980s, more than 300 plants were active with a capacity exceeding 30 million m^3 per year. Research and development was done in a special institute at Kujbysev,[7] but the real effective use was low. The bulk densities were high, only 10% of the production was below 400 kg/m^3, the average in 1987 being 498 kg/m^3

The grading was coarse with

0–5 mm	6.9 %
5–10 mm	17.1%
10–20 mm	45.5%
20–40 mm	10.8 %
mixed unscreened	19.7%

The energy consumption was enormous with 97 kg fuel plus 23.5 kWh per m^3.

There is no exact information about the actual production. But there is information[8] that fifty-three plants were producing Keramsit in 1995 in Russia, with sixteen plants in the Ukraine.

2.7 Other Continents

In the USA and Canada, there are fourteen companies, some of them owning five or more plants. The shipment in 1994 was about 4.6 million m^3 of expanded clay, shale, and slate combined. The production may increase. The sales volume is about 60–85% of the installed capacity.

In South America, there are two plants (Argentina and Venezuela). The same holds for Africa (Algeria, Egypt). In Japan, there are two plants with 1.2 million m^3 capacity and 750,000 m^3 shipment in 1994, mainly for structural concrete, the bulk density for 5/15 mm size being around 800 kg/m^3.

The summary of the number of plants in different continents is shown in the following table:[7]

			Total
Former Soviet Union	Russia Ukraine Others	>53 16 >2	 >71
Europe	Clay, shale, slate fly ash	32 5	 37
Africa		>2	
America	North South	25 2	
Asia	Japan Others	>2 >4	
Australia		?	35
Total			143

From the overall number of more than 140 plants, obviously half of them are operating in the former Soviet Union, one quarter in Europe and one quarter in the other continents.

Apart from the LWA from clay, shale, slate, and fly ash, there are also very light LWAs such as perlite and vermiculite. There are at least twelve plants operating in the eastern USA. The total amount of production of perlite in 1994 was 1.7 million m^3, with 0.6 million m^3 for vermiculite. Assuming an average bulk density of 100 kg/m^3, these figures lead to a combined volume of 23 million m^3 for perlite and vermiculite.[9]

3.0 CONCLUDING REMARKS

Lightweight aggregate concrete was used even before the Christian era. The concrete was made with natural volcanic aggregates of pumice and scoria. With time, because of the advantages of lightweight aggregate concrete, specifically its low density and thermal insulating properties, its demand has increased. In recent years, it has become an important structural material in off-shore construction. This has led to the development of synthetic lightweight aggregates which are made from natural raw materials like clay, slate, shale, etc., and from industrial by-products like fly ash, slag ashes, etc.

There has been some research and development work on the production of LWAC using organic natural aggregates such as palm oil and shales, but it is still not in commercial production.

There are many types of lightweight aggregates of mineral origin, ranging from weights below 50 kg/m^3 up to heavy types of 1,000 kg/m^3 or even more. They enable the production of concrete and mortars in very wide ranges with properties that will suit the requirements of different building industries. But the term *lightweight concrete* is not well defined, hence, is not used on a large scale.

REFERENCES

1. Rivera-Villareal, P., Ancient Structural Concrete in MesoAmerica, *ACI Spring Convention*, San Francisco, CA (Mar. 21, 1994)
2. Schmidt, H., Herstellung und Verwendnung von Blähtongranulat im Dpiegel der Literatur, *Die Ziegelindustrie*, Heft 21/22 (1970)

3. Landsverband Beton-und Bimsindustrie Rheinland-Pfalz e.v.: Bauen mit N, *Tagungsband zu Bimstagen* 30/31, (Mar. 1995)
4. Abdullah, A. A., Palm Oil Shell Aggregate for Lightweight Concrete, *Waste Material Used in Concrete Manufacturing*, (S. Chandra, ed.), Noyes Publications (1997)
5. ESCSI, *Lightweight Concrete*, Washington (Oct. 1971)
6. Staatliches Materialprufungsamt in Berlin-Dahlem, Prufungszeugnis II/ 3077 vom (Aug. 16, 1938)
7. Spitzner, J., A Review of the Development of Lightweight Aggregate, History & Actual Survey, *Proc. Int. Symp. Structural Lightweight Concrete*, Sandefjörd, Norway, pp. 13–21 (Jun. 20–26, 1995)
8. Stark, J., *Proc. Int. Synposium on Structural Lightweight Aggregate Concrete*, Sandefjörd, 1995, Paper by Spitzner., pp. 13–20 (1995)
9. Loughbrough, R., Minerals in Lightweight Insulation, *Industrial Minerals* (1991)

2

Production of Lightweight Aggregates and Its Properties

1.0 INTRODUCTION

Lightweight aggregate (LWA) can be divided in two categories:

1. Those occurring naturally and are ready to use only with mechanical treatment, i.e., crushing and sieving.
2. Those produced by thermal treatment from either naturally occurring materials or from industrial by-products, waste materials, etc.

The properties of LWAC are related to the properties of the aggregates used for producing them. This, in turn, depends upon the type of material and the process used for producing them. Generally, the strength and the density of concrete are considered when designing a structure. Specifically in the case of LWA, there is a vast variation in the density, so there will be a vast variation in the strength of the LWAC. The manual of Lightweight Aggregate Concrete[1] describes a number of aggregates that have been used and indicates an approximate range of densities and compressive strength for the resulting LWAC.

The natural materials used for producing LWA of the second category are: perlite, vermiculite, clay, shale, slate, etc. On the other hand, the industrial by-products used for producing LWA are pulverized fly ash (PFA), blast furnace slag (bfs), industrial waste, sludge, etc. These are produced by a process of either expansion (bloating) or agglomeration. Expansion takes place when the material is heated to fusion temperature at which point pyro-plasticity of the material occurs simultaneously with the formation of gas. Agglomeration occurs when some material fuses (melts), and the various particles are bonded together. To induce the expansion of the raw material, most artificial LWA undergo some type of heat treatment during their manufacture. The heat treatment is carried out in different types of industrial furnaces, such as rotary kilns, vertical shaft kilns, sinter strands, or foaming bed reactors, etc. A short description of the kilns follows.

2.0 INDUSTRIAL KILNS

2.1 Rotary Kiln

A rotary kiln used for manufacturing LWA is similar to the one used for manufacturing portland cement. It consists of a long cylinder lined with refractory bricks and capable of rotating about its longitudinal axis, which is inclined at an angle of 5° to the horizontal (Fig. 2.1). The length of the kiln depends upon the composition of the raw material to be processed and is usually thirty to sixty meters. The prepared raw material is fed into the kiln at the higher end, while firing takes place at the lower end. As the material moves to the heating zone, the temperature of the particles gradually increases and expansion takes place. Material is then discharged into a rotary cooler, where it is cooled by blowing cold air.

2.2 Vertical Shaft Kiln

In this process, the prepared raw material is fed into a vertical shaft kiln in batches. A hot jet of flue gases, entering at the center of the base of the combustion chamber, lifts the material upwards until the force of the upward jet is dispersed sufficiently to become less than the force of gravity.

Material falls down and rolls to the foot of the combustion chamber, which is in the shape of a funnel, where the flue gas again forces it upwards. This process is repeated a number of times over a period of about one minute for each batch.

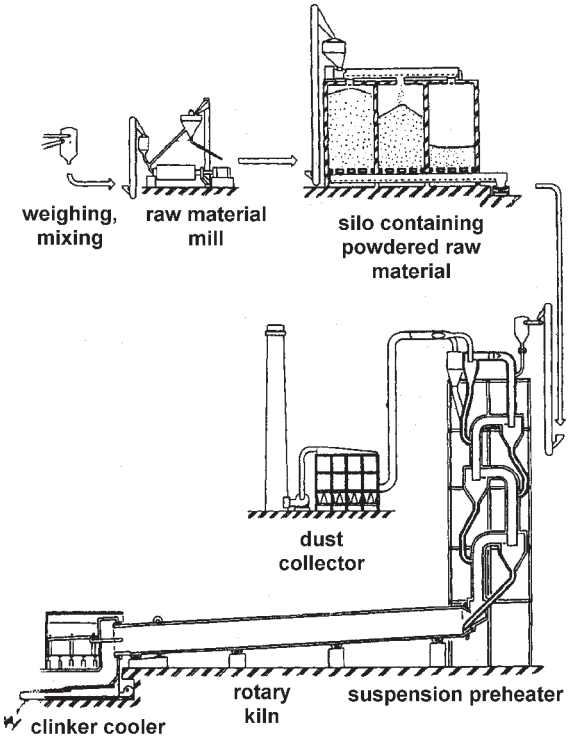

Figure 2.1. Rotary kiln for producing lightweight aggregates.

2.3 Sintered Strand

The prepared raw material is placed in loose layers, approximately 15–300 mm thick, on a moving sinter strand and carried, under drying and ignition hoods (fired by gas or oil), in such a manner that burning, initiated at the surface, continues through the full depth of the bed. The gases formed cause expansion; however, in some cases, the cellular structure results from the burning of the fuel grains and loss of moisture, and from fusion of the fine particles of the raw material.

2.4 Foaming Bed Reactor

In this process, used exclusively in the production of foamed blast furnace slag, the slag is poured onto a foaming bed consisting of a large number of water jets set in a concrete base. The water converts to steam on contact with the molten material and penetrates into the body of the material at which point it becomes superheated. Due to the rapid expansion that takes place, the material bloats to form a cellular structure. An alternative method includes spraying water onto the molten material when it is being tapped from the blast furnace, so that the material is cooled rapidly and steam becomes trapped within. In another method, the molten material is fed into a mill with revolving paddles and is treated directly with steam. A fluidized bed foaming reactor is shown in Fig. 2.2.[2]

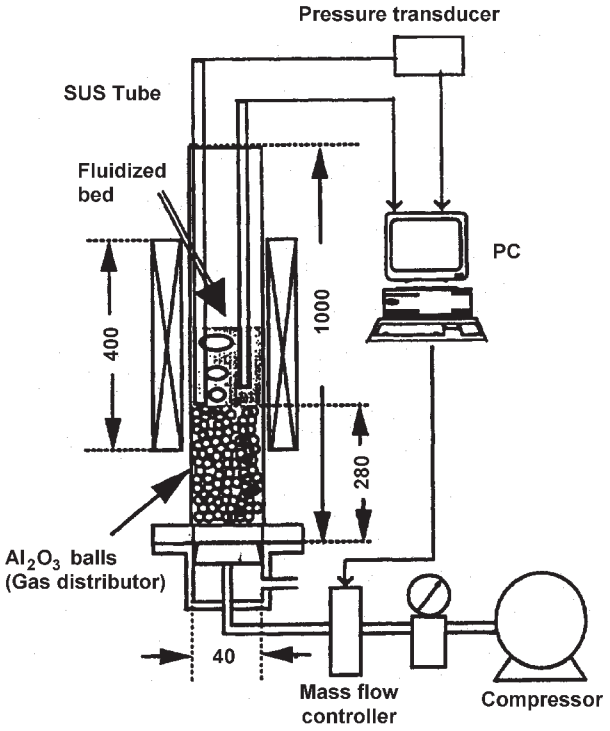

Figure 2.2. Fluidized bed foaming reactor.[2]

2.5 Cold Bonding

In this process, bonding is accomplished by the chemical reaction between lime and ash, which is due to the pozzolanic character of the ashes. Calcium silicate hydrates are produced as a result of this reaction. The production process is simple. A mixture of ash, lime, and water after mixing, is jointly transported towards a disk pelletizer, where spherical pellets are formed. To strengthen the still vulnerable "green pellets," they are embedded in a constant stream of ash and transported to curing silos. The energy released directly warms the pellets to a temperature of 85°C. After 15 hours, they leave the silos ready for screening.

3.0 NATURAL LIGHTWEIGHT AGGREGATES

Natural LWA are mostly of volcanic origin and, thus, are found only in certain parts of the world. Pumice and scoria are the oldest known LWA; they were used extensively in Roman time. These are light and strong enough to be used in their natural state, but their properties are variable. Pumice is formed when the molten SiO_2 rich lava from the explosive eruption of a volcano cools. Sudden cooling freezes the material existing at the molten state. There is no possibility of a crystallization process taking place. The principle is the same as in the production of glass, which is neither liquid nor solid. It is call "supercooled liquid." The low density of pumice is due to the presence of gas bubbles in the molten lava which become trapped on cooling. The voids are small and interconnected. Scoria is a similar material, but it is darker in color than pumice. It contains larger and more regular shaped shells that are not connected.

3.1 Pumice

The main sources of pumice in Europe are Iceland, Lipary Island in Italy, Yali in Greece, and the Rhineland in Germany. The lightweight aggregate concrete made with pumice has low density. This leads to a realative weight reduction of the structure and foundation, and thereby will reduce the dead load, a significant factor for high rise buildings. This is also a very attractive material for repairs of the old buildings, as it will not increase the total load of the structure.

With the use of fine pumice, it is possible to produce mortars with good insulating properties. It will provide considerable savings in thermal insulation. The LWAC is relatively porous, which could promote the corrosion of reinforcing steel. It is reported that its use in outdoors can create problems of reinforcement corrosion, but indoors should not be any problem.[3][4]

3.2 Palm Oil Shells

Low-cost building materials can be produced using inexpensive indigenous raw materials. Agriculture wastes, which are renewable, and found in abundance in many countries, present an interesting alternative to the traditional and sometimes to imported building materials, particularly for low-cost construction.[5] The use of agriculture waste as aggregates can provide an alternative to conventional methods for the production of lightweight concrete.

The material properties and structural performance of lightweight aggregate concrete with palm oil shells as aggregates are similar to the lightweight concrete produced using the more common aggregates such as clinker, foamed slag, and expanded clay. The palm oil shells are hard and are received as crushed pieces as a result of the process used for extracting the oil. They contain a large amount of fine particles which are removed by manual sieving. The shells are then air-dried before use. A typical particle size distribution curve for palm oil shells in comparison with the sand is shown in Fig. 2.3.[6]

The workability and compressive strength of lightweight concrete with palm oil shells as aggregates is affected by the proportion of palm oil shells and the water-to-cement ratio. The 28 day cube compressive strengths of the lightweight concrete vary between 5.0–19.5 MPa.

3.3 Crushed Burnt Bricks

In ancient masonries, crushed bricks or crushed sintered clays were used as aggregates. The densities of these aggregates were in the range of 1500–2000 kg/m^3. These aggregates form another category which is difficult to define. De Pauw, et al.,[7] classified them between the light-weight aggregate and the normal weight aggregate. However, some other characteristics, like porosity and water absorption, would classify them as LWA.

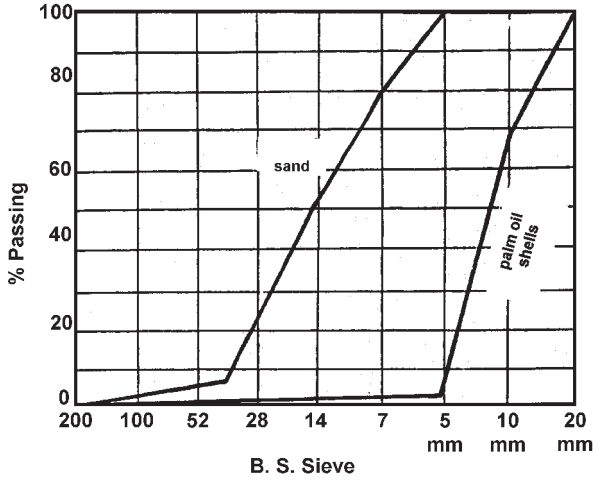

Figure 2.3. Particle size distribution curves for palm oil shells and sand.[6]

Burnt bricks were used in construction at Mohenjo-Daro, 2800 B.C., during the Indus Valley civilization. It is likely that during this time the bricks were crushed and the aggregates were used for making concrete. Lime was used as a binder. The crushed brick aggregates are porous and resemble, in structure, the sintered clay aggregates. The difference between the LWA produced today and the crushed bricks is the size and shape. The size of the aggregates in the former case is undefined; mostly these are edged, whereas the sintered clay aggregates are rounded due to their rotation in the rotary kiln. Sintered clay, shale, and slate aggregates are lighter than the crushed brick aggregates because the clay has bloating properties.

4.0 PRODUCTION TECHNIQUES

4.1 Natural Materials

Lightweight aggregates are made by a thermal process using natural materials like clay, shale, slate, perlite, and vermiculite. Unlike cement which has a calcium-rich feed going into the rotary kiln, lightweight

aggregates are made from silica-rich materials that release only modest amounts of CO_2.[8]

The production process of lightweight aggregate depends upon the raw materials used. Basically, there are two processes for making lightweight aggregates; namely a wet process and a dry process.

Wet process: similar to preparing clay for brick production—is more usual for soft clays.

Dry process: pelletizing or crushing is more common for harder shales and for slates.

Burning and Expanding. Burning and expanding are mostly done in rotary kilns at temperatures of about 1100° to 1200°C. Rotary kilns, preferably fired in a counter flow process, proven to be the most adequate equipment, are well known in the cement industry. Expansion depends upon the heating process. Thus, aggregates with varying bulk densities can be produced, for example, 300–800 kg/m^3 in grain sizes 4/8 or 8/16 mm (or others, as desired), from the same raw material. LWA produced by other processes give bulk densities only within a small range, mostly 500–600 kg/m^3. The LWA of a coarser grain size is lighter than the finer ones.

LWA from Perlite. Perlite is a glassy volcanic material with a water content of 2–6%. The industrial process of expanding the rock to form a lightweight aggregate consists of crushing the material to graded sizes and rapidly heating it to the point of incipient fusion. At this temperature, the water dissociates and expands the glass into a balloon-like shape of small bubbles to produce a cellular type of material. When perlite is quickly heated above 870°C, it expands and produces aggregates with a bulk density of 30–240 kg/m^3.

New LWA from Perlite (ASL). In Japan, new aggregates are developed which are made of perlite. These are called Asano Super Light (ASL). The aggregate is distinguished from the conventional ones by low absorption and high strength. It is chiefly made of perlite from Okushiri Island, Hokkaido, which is mixed with silicon carbide, SiC (foamed material), and bentonite (binder). An aqueous solution of lignin is also contained as a pelletizing aid. Perlite is suitable as an artificial lightweight aggregate since 80% of it is a glass phase which forms a uniform foam when adequately heated. The proportions of perlite, SiC, and bentonite by weight at the time of production are 95.5%, 4.3%, and 0.2%, respectively.[9]

Oven-dried specific gravity of the particle can be varied between 0.6 and 1.5 by adjusting the proportions of materials and production conditions. Taking into account the demand and ease of handling, two types of aggregates are produced based on oven-dried specific gravities of particles:

1. 0.85 ± 0.10
2. 1.20 ± 0.10

The 24 hour absorption is 5% or less.

LWA from Vermiculite. Vermiculite is a mineral of laminar formation, similar in appearance to mica but, unlike mica, it expands (exfoliates) rapidly when heated thereby radically reducing its density. The natural raw ore has a density of 600–1100 kg/m^3. The raw ore, as received from the mines, is first dried, crushed, and then graded. The grading process is carried out by the old method of "winnowing" in a stream of air. The individual grades of material are then rapidly passed through hot burners (1150–1250°C). They cause the vermiculite to expand and the formation of steam forces the laminate apart. The aggregate produced has a bulk density of 60–190 kg/m^3.

LWA from Expanded Clay (Leca™), Wet Process. Lightweight expanded clay aggregates (Leca™) are produced in a rotary kiln by a wet process, using bloating clay. They are produced in Sweden and Norway and are named Swedish Leca™ and Norwegian Leca™. They are made by mixing clay and water into a paste. The paste is fed into the higher end of the rotary kiln where it is broken into smaller granules by chains. Thus, they form aggregates of random size and shape while passing through the rotary kiln where they are sintered to a glassy material. The aggregates that come out of the kiln are sieved to different sizes.

Swedish Leca™. The expanded clay aggregates are made from fine particle clay which is poor in lime. It is mined in Gärstad outside Linköping in Sweden. The Swedish lightweight aggregate manufacturing company, AB Svensk Leca™, has rotary kilns and produces lightweight aggregate "Leca™."

The clay dries and expands in the rotary kiln at high temperatures, about 1100–1200°C, when it passes through the burning zone. The final product is expanded clay with a hard ceramic shell. Inside of these particles, there are holes of different sizes which are mostly interconnected.

The density and strength of the particles vary with the particle size. The smaller the size, the higher the density and strength. A relation between the size, density, and strength is given in Table 2.1

Table 2.1. Bulk Density and Strength of Swedish Leca™ of Different Sizes *(Svensk Leca™ AB)*

Size mm	Density kg/m^3	Compressive Strength MPa
2–6	400	1.50
4–10	310	1.15
4–12	300	1.15
8–14	270	0.85
8–20	260	0.85
12–20	260	0.75

The elasticity modulus for 12–20 mm packed material is 20 MPa and 10 MPa for filled material.

Norwegian Leca™. Norwegian Leca™ started the production of LWA based on expanded clay using one single kiln in 1954. The production capacity was less than 100,000 m^3 per year. Today, Norway's total production capacity of expanded clay is nearly 1 million m^3 annually, from four rotary kilns.

Since the start forty years ago, 18 million m^3 of LWA blocks have been produced and sold in Norway. If one takes this volume of LWA blocks and divides it by four million (population of Norway), it comes to 4.5 m^3 of LWA blocks per person. It means that, during the last forty years, consumption of Leca™ blocks was 4.5 m^3 or 20–25 m^2 per person.

German Liapor™, Dry Process. Lightweight aggregates produced by the dry process in Germany are known as Liapor™ after the name of the company producing them.

Liapor™ is produced from shale, a soft rock, which is crushed, dried, and milled into powder. It is homogenized and stored ready for pelletization. The process is quite similar to that of Lytag™ production. After the pelletization process for appropriate size, they are coated with finely powdered limestone. The pellets are spherical and have high green strength. These are then transported to a rotary kiln. In production, the pellets can be made to a predetermined size and the expansion can be controlled to produce particles of the required density. As the pellets are preformed, there is no fine fraction, as with Leca™.

Table 2.2. Bulk Density, Size, and the Moisture Content at Delivery of Some LWA[10]

Aggregate Fraction	Bulk Density kg/m^3	Particle Density kg/m^3	Moisture Content by wt%
Swedish Leca™			
2–6 mm	477(457)	875(838)	4.4
4–10 mm	327(318)	600(584)	2.8
Norwegian Leca™			
0–4 mm	845(765)	1392(1261)	10.4
4–8 mm	804(690)	1393(1196)	16.5
8–12 mm	786(709)	1319(1189)	10.9
Liapor™			
1–4 mm	514(511)	973(968)	0.5
4–8 mm	503(497)	908(897)	1.2
Liapor™ 6			
4–8 mm	606(606)	1052(1052)	0.03
Liapor™ 8			
4–8 mm	931(835)	1633(1465)	11.5
The value in the parentheses is of the dry particles.			

The density and the moisture ratio varies with the size of the aggregates. It is shown by the tests performed by Chandra and Berntsson.[10] The material properties of Swedish Leca™, Norwegian Leca™, and German Liapor™ are shown in Table 2.2.

Lightweight Expanded Slate Aggregates. The expanded slate aggregates are produced by the rotary kiln method.[11] Raw slate is fed from the storage silos into preheaters that allow the rock to heat up at a moderate rate, it then enters the upper end of the rotary kiln where it slowly revolves and moves toward the "firing zone" near the lower end of the kiln. The firing zone attains a temperature of 2000°F (1200°C). Here, the slate becomes sufficiently plastic to allow expanding gases to form masses of small unconnected cells. As the expanded slate cools, these cells remain, giving the aggregate its low unit weight and low absorption. The expanded material, called *clinker* at this point, leaves the lower end of the kiln and enters a forced-air cooling system.

From the cooler, the clinker is conveyed to a classifying area where it is crushed and screened. After blending, actual moisture content is adjusted to a predetermined level. The expanded slate aggregate is then tested for proper gradation, moisture content, specific gravity, and unit weight. After testing, the aggregates are stored.

There is a possibility of segregation in storage due to the variation in the size of the aggregate and, thereby, the bulk density. This is minimized using two procedures:

1. Coarse grade aggregates are stored in low-elevation stock-piles that feature a moisture control system
2. Fine grade aggregates are stored in low-height silos that feature a perimeter port feeding design

Some properties of expanded slate aggregates are given below.

Properties of Expanded Slate Aggregates

12.5 mm structural aggregates

Bulk Density

- Dry loose (ASTM C29) 50 lbs/cf (805 kg/m^2)
- Saturated surface dry loose 52 lbs/cf (833 kg/m^2)

Specific Gravity of the Particle

• Dry (ASTM C127)	1.45
• Saturated surface dry	1.52

Absorption

• Saturated surface dry (ASTM C127)	6%
• Under high pumping pressure of 150 psi (1033 kPa)	9.4%

Soundness

• Magnesium sulfate (ASTM C88)	0.01%
• Sodium sulfate (ASTM C88)	0.23%
• After 25 cycles freezing and thawing (AASHTO T 103)	0.22%

Toughness

• Los Angeles Abrasion (AASHTO T-96-B)	25%

4.2 LWA From Industrial By-Products

All lightweight aggregates are not produced using natural raw materials. Some are produced from industrial by-products like fly ash, slag, municipal waste, dredging waste, etc. It is a very important advancement as it will solve the environmental problem to some extent.

Expanded Pelletized Fly Ash Aggregates. Fly ash is a by-product of a thermal power station. The quality of the fly ash depends upon components of the burning process such as the temperature and heating rate. Experience has shown that the fly ash varies from the day shift to the night shift in the same thermal power station.[12] These factors influence the carbon content and the particle size. It can also vary the calcium content.

Depending upon the quality of fly ash, its use also varies. A high quality fly ash with a low carbon content is used as a mineral admixture in concrete production. Lower quality fly ash with a higher and variable carbon content is normally used in land filling. It is also used for making LWA by adding extra pulverized coal to bring the carbon content to about 12%, and then pan pelletizing and heat treating them on a traveling grate.

The aggregates produced are of high quality and high strength with low density. The aggregates produced from pulverized fly ash are known as PFA LWA. These have been widely used in the UK for the past three decades in construction of high-rise buildings and bridges. There is an increasing demand for lightweight aggregates, which has attracted the attention of researchers worldwide. This has resulted in the development of some new types of LWA. These are produced partially by using a combination of new material and partially by using new processes of pelletization and burning.

Pelletization and Burning. The manufacturing process of artificial LWA from fly ash is elaborated by Bijen.[13] The pellets are formed either by *agglomeration* or by *granulation*. Agglomeration is the term used for the entire field of consolidation of solid particles into larger shapes. The techniques applied to agglomerate fly ash can be divided as follows:

Granulation	disc (or pan) granulation, drum granulation, cone granulation, mixer granulation.
Compaction	uni-directional piston type compaction, roll pressing, extrusion and pellet mills.

Granulation. In the granulation techniques, agglomerates are formed without external compacting forces other than tumbling forces. The fly ash particles adhere together as a result of tumbling and capillary forces. In this process, the fly ash particles need to be moistened.

Cohesion forces between the particles increase with increasing amounts of wetting liquid. The states of cohesion can be described as follows with increasing amounts of liquid:

1. Pendular state
2. Funicular state
3. Capillary state

The state of liquid saturation reached with increasing interparticle forces is shown in Fig. 2.4.[14] For fly ash, the optimum water content is between 20 and 25%. The amount of water is a critical factor. Too little or too much bonding agent means insufficient cohesion forces can be developed, or muddy balls instead of pellets are formed. The balling occurs in two stages, first, the so-called seeds are formed, from which larger pellets then grow.

Compaction. The density of the pellets depends upon the process used to produce them. With compaction agglomeration the density of the pellets will, in general, be higher than that of the pellets produced with agitation granulation. This means that the porosity will be lower. The quantity of the bonding agent (water) has to be accurately adjusted to avoid squeezing the pellets.

Another device used for agglomeration of fly ash is the pellet mill. Figure 2.5 shows two types of pellet mills.[15] In this process, the materials are forced through open dies or holes. Normally, the pellets or briquettes formed are cylindrical with a fixed diameter and variable length.

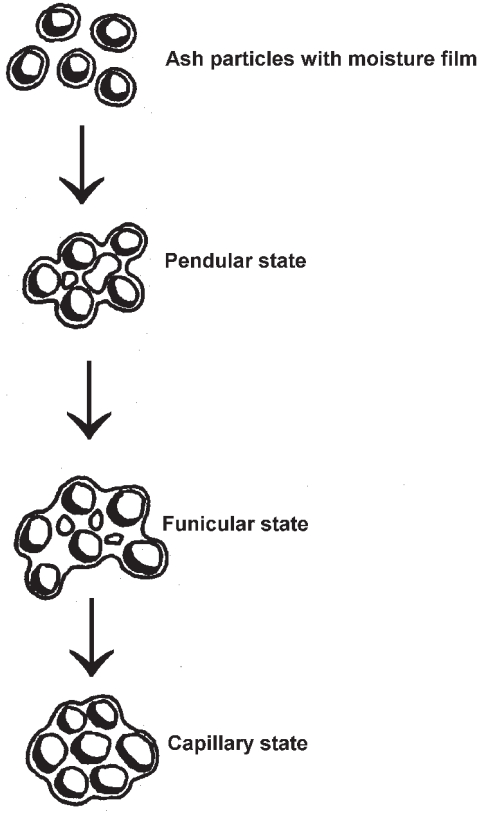

Figure 2.4. Diagrammatic representation of pellet formation.[14]

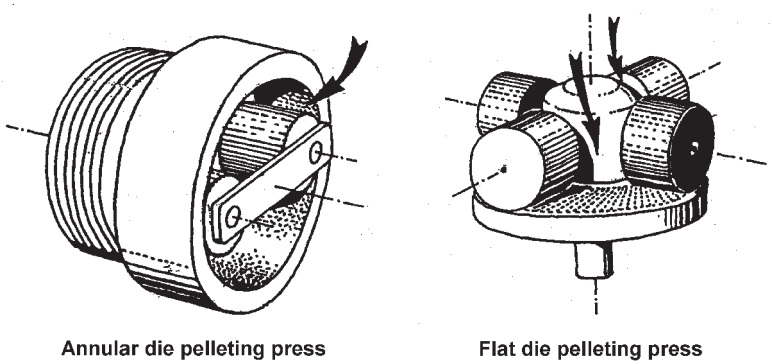

Figure 2.5. Pellet mills.[15]

Fly ash aggregates can also be produced by the extrusion method. Figure 2.6 shows two types of extruders.[15] This technique is well-known for the production of synthetic aggregates.

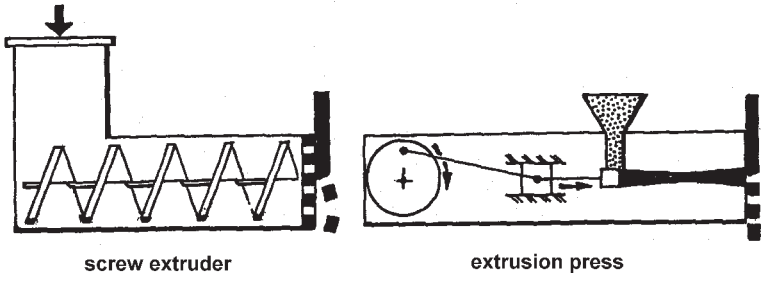

Figure 2.6. Extrusion press.[15]

Hardening. The green pellets, formed by agglomeration of fly ash particles, are too weak to be considered for use as aggregates. Therefore, the particles have to be bonded more firmly than by capillary forces.

For fly ash agglomeration, there are two types of bonding:

1. Bonding by a material bridge.
2. Embedding in a matrix formed by reaction of a bonding material with part of the fly ash particle.

The latter type of bonding could be considered an extreme case of the material bridge-type of bonding.

Figure 2.7 shows a schematic of these two types of bonding. Bonding by a material bridge happens in all well-known sintering processes. For matrix bonding the number of possible binders is very large. A division of the hardening process, based upon the temperature, is done as follows:

> 900°C	Sintering process (material bridge bonding)
< 250°C > 100°C	Hydrothermal process (matrix bonding under pressurized steam)
<100°C	Cold bonding process
<5°C	

Sintering. Sintering is usually done on grates. Here, the green pellets are transported in the form of a bed 200–300 mm thick on an endless belt through the sintering furnace. Figure 2.8 schematically shows a flow diagram for a sinter strand process.[16]

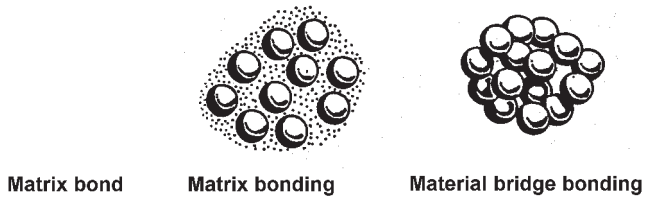

Figure 2.7. Two types of bonding.

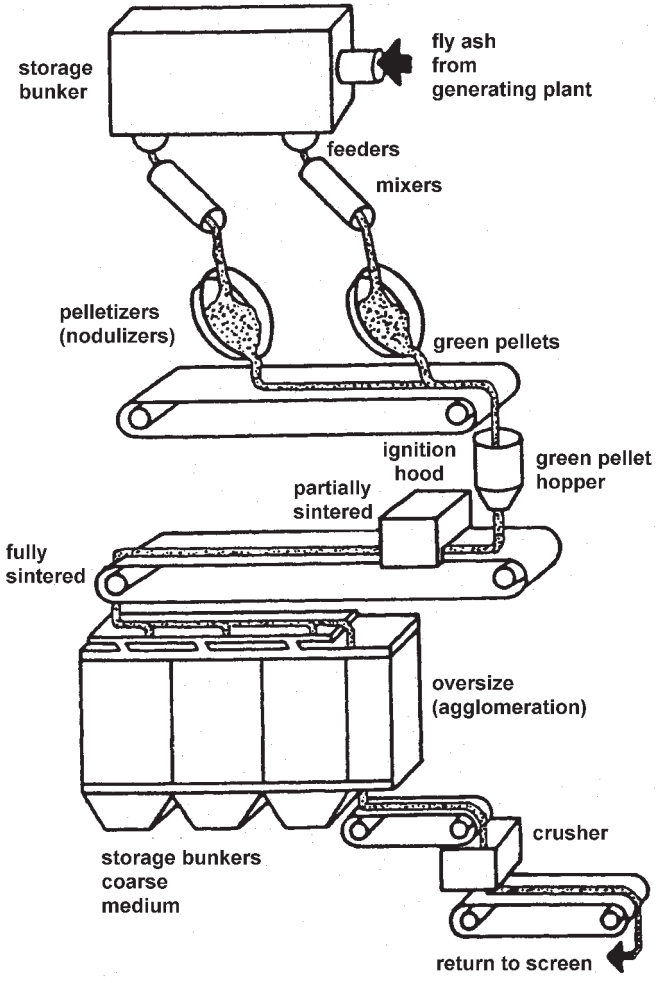

Figure 2.8. Schematic diagram of a sinter strand process.[16]

Hydrothermal Processes. In these processes, bonding is achieved by means of a chemical reaction of lime or portland cement with fly ash and water. The addition of a small quantity of gypsum can be an advantage. The hydrothermal processes are more or less related to ore-pelletizing processes such as the Swedish "COBO" process or American "MTU" process. A process developed in The Netherlands (Aardelite™) is shown in Fig. 2.9.[17] A typical composition of the pellets consists of 50% fly ash, 45% fine quartz, and 5% lime and water.

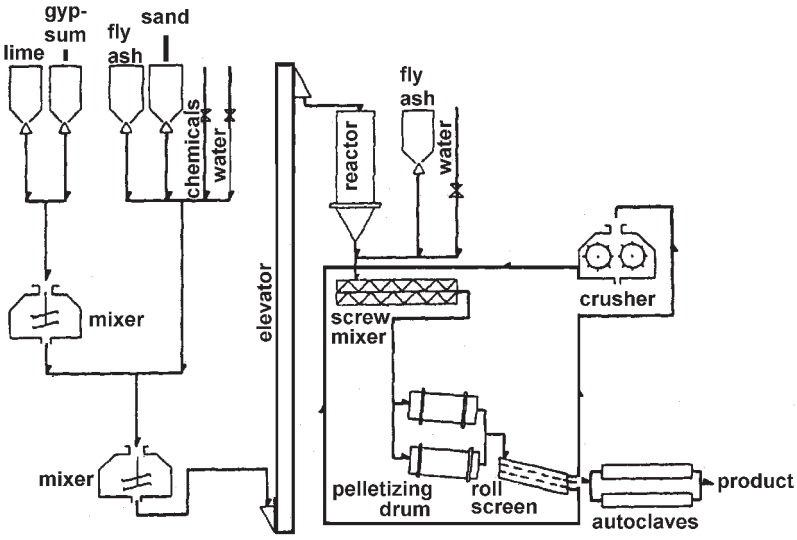

Figure 2.9. Flow sheet Aardelite™ autoclave process.[17]

Cold Bonding. Fly ash reacts chemically with calcium hydroxide due to its pozzolanic character at ordinary temperatures. The bonding obtained in this case is hydraulic bonding. It is generally less rigid than the bonding obtained with other types of bonding discussed, where the pellets are sintered at higher temperatures and have ceramic bonding. A flow sheet of the cold bonding process is shown in Fig. 2.10.[18]

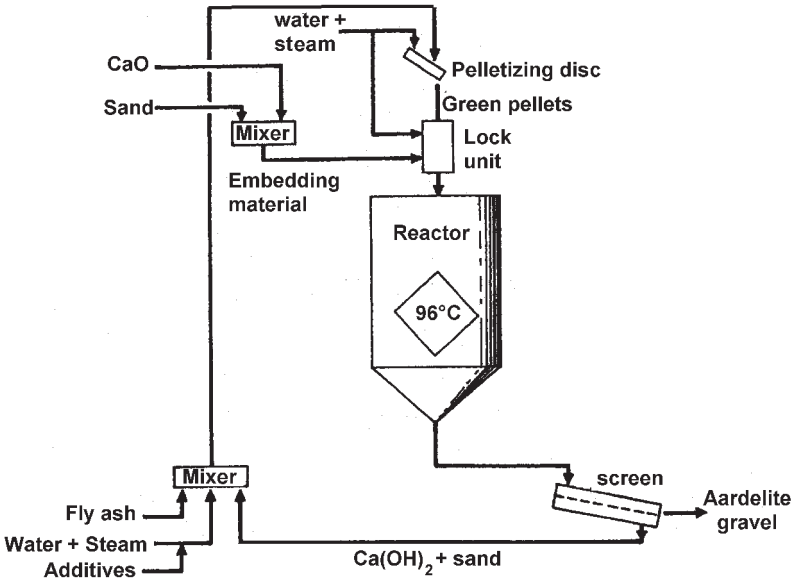

Figure 2.10. Flow diagram Aardellite cold bonded process.[18]

Production of Fly Ash Lightweight Aggregate, Lytag™. Lytag™ is the commercial name of sintered fly ash lightweight aggregate. It is produced by pyro-processing fly ash. The aggregate is formed as a result of agglomeration which takes place as the fly ash particles fuse and bond together. The transformation of fly ash to aggregate has long been established. However, in 1959, the Lytag™ process brought a new patented technique to fly ash conversion (Fig. 2.9). In this process, no bonding agents are used and no heat is applied prior to sintering. This method has been in operation in the UK for thirty-six years.

The dry fly ash is transferred pneumatically from the power station to storage silos at the plant site. A system of air slides and screw feeders transfers the ash to a mixer at a controlled flow rate. At this point water and, if necessary, additional fuel in the form of high carbon fly ash or coal, is added and mixed with the dry ash. These adjustments produce a homogeneous material containing sufficient energy to raise the temperature of the ash to the sintering point later in the process.

Pelletizing. The moisture-conditioned ash, as described above, is introduced to a large diameter flat disc pelletizer. On these slowly rotating inclined pans, the small particles of ash impact on each other. The pellets gradually grow in size due to compaction forces. The surface tension effects of further water added as a fine spray complete the agglomeration process. The finished pellets fall from the pelletizer and are fed to a moving steel conveyer: the sinter strand.

Sintering. ***Sinter Strand Process.*** The pellets are placed in a loose layer 200 to 250 mm thick. The sinter strand speed is automatically adjusted to ensure an even layer across and down its length. The pellets are immediately subjected to a temperature of approximately 1100°C in the ignition chamber which uses reprocessed oil to fire the carbon in the pellets.

The strand moves forward and the material comes out from the ignition chamber. The burn is pulled down slowly through the full depth of the pellet bed by down draft air employed along the entire 20 m length of the machine.

The burning of the fuel and loss of moisture creates a cellular structure bonded together by the fusion of the fine fly ash particles. The voids formed are generally interconnected and occupy 40% of the body of the pellet particles. When the mass of sintered pellets falls from the end of the sinter strand, it is in a relatively cool state at 100–200°C.

Grading and Storage. At the end of the strand, the finished pellets are either naturally or mechanically separated before passing over a primary screen to remove material that is less than 2.5 mm. Material above 2.5 mm is transported via conveyor for secondary screening to the required sizes for the appropriate market.

Traditionally, the secondary screening is carried out in purposely built screen houses. Current practice is to water spray the product as it emerges from the primary screens to control dust, before processing to final sizes on a mobile screen.

Quality Control. Quality control is done by checking for density and moisture content (a minimum of every 75 m^3 produced). Other parameters of secondary importance, such as loss on ignition (LOI), and chemical composition are tested on an annual basis.

Properties of the PFA LWA. ***Shape, Color, and Texture.*** The aggregates are spherical in shape and are of brown color with an internal black core. This is attributed to the carbon content and the state of oxidation of iron. The microstructure is smooth but, on the micro-scale, it is relatively rough with open pores. The structure of some pores of about 10–200 μm in size is shown in Fig. 2.11.[19] These figures show that the structure of the

pellet is largely porous and the pores are interconnected. The voids appear to have been formed by gases escaping through a molten material (Figs. 2.11a and 2.11b). The honeycombing is visible both within the void itself and around the void on the fracture surface, and the internal surfaces are smooth and curved. Figures 2.11c and 2.11d show voids which may have been formed during pelletizing process and then being fused into position during the sintering process.

Open pore structure allows moisture to enter and exit the aggregate. When mixed in concrete some of these pores on the surface of the particles are filled with cementitious products. In a mature specimen it is difficult, if not impossible, to define the aggregate to cement matrix interface.

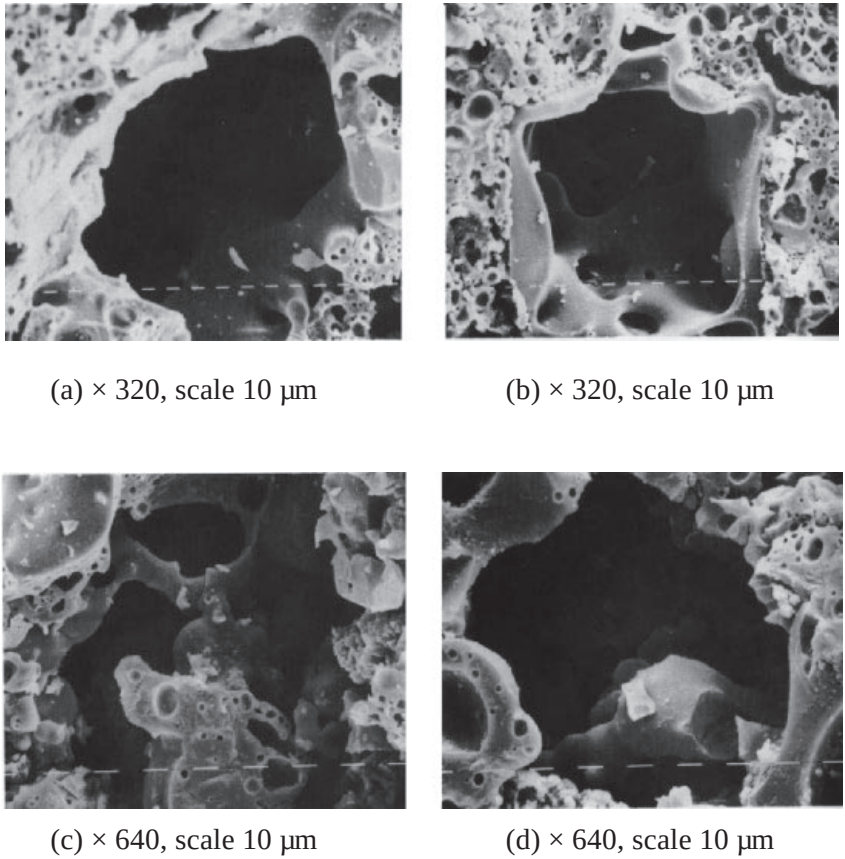

(a) × 320, scale 10 μm (b) × 320, scale 10 μm

(c) × 640, scale 10 μm (d) × 640, scale 10 μm

Figure 2.11. Microstructure of Lytag™ aggregate.[19]

The internal structure is a honeycomb of generally interconnected voids of varying size and shape amounting to 40% of the volume. This void space provides the reservoir for absorbed water and prevents the disruptive effects, for example, of ice formation if the aggregates are exposed to freezing. The air voids also act as an insulating material, enhancing the thermal properties of the finished concrete.

Microstructure and Water Absorption of Lytag™ Aggregate. Like other lightweight aggregates, the water absorption characteristics of Lytag™ follow two distinct phases:

1. The initial rapid absorption of water when dry aggregate is immersed.
2. The second phase is a much slower, prolonged period of absorption, tending towards a finite value after six to twelve months.

In terms of microstructure of Lytag™ aggregates, this two-phase phenomenon can be explained by the size range, structure, and distribution of the pores within a Lytag™ pellet. The pores range in size from approximately 200 μm down to less than 1 μm. The larger voids are highly interconnected and very few voids are discrete and completely sealed. The only ones which do tend to fit these latter criteria are those within the unreacted PFA xenospheres. Also, the pores are evenly distributed throughout the entire pellet with large, medium, and small pores being thoroughly mixed.

Even the larger voids are so small that they will only become saturated by capillary action but, on immersion in water, the saturation of these larger pores will be rapid. Therefore, within a few seconds of immersion the entire pellet will have water distributed throughout it by means of the larger and medium sized pores. The air in the voids has to be expelled during the second process. Capillary action over a period of time will saturate the smaller pores until eventually a state of equilibrium is reached. With some of the very small pores, however, it is possible that they will never become saturated under low pressure.

The above theory also applies, in reverse, to the drying out of a hardened lightweight concrete over a period of time. Water will tend to migrate relatively rapidly at first from the larger pores within the pellet into the concrete matrix so the hydration process continues, followed by the slower more prolonged dissipation of water from the smaller pores within the aggregate. This gradual loss of water over a period of time is believed

to enable the concrete to "self repair" internal microcracking, which is possibly caused by the application of loads to a member during the hydration process.

Density and Strength. The typical oven-dried bulk density of sintered fly ash aggregates lies in the range of 750 to 1100 kg/m^3. The larger the size of the pellets, the lower the bulk density and, more importantly, the lower the strength of the aggregate. The relationship between size and strength is a function of compaction and consequent void formation during burning. The larger pellets are less compacted in their outer layers with resultant larger voids.

Fly Ash Aggregates Produced by Rotary Kiln. Structural high strength concrete can be produced either by using mortar of very high strength, which compensates for the lower strength of the aggregates, or by using high strength aggregates, or both. But there are limitations. High strength mortar, though producing high strength, can have a deleterious effect on the durability properties. This created the need for the development of high strength LWA. Morishita, et al.,[20] developed a technique to produce tough and lightweight fly ash aggregate (TLA) using a rotary kiln. The production process is shown in Fig. 2.12.

TLA aggregates are produced using mainly fly ash as the raw material. Fly ash is mixed with 10% limestone powder and 5% bentonite and pelletized with water by a pan pelletizer to a diameter of 5 to 20 mm. The pellets are burned at 1200–1300°C in a rotary kiln with silica stone powder blown on the aggregate as an anti-adhesion agent. Some of the properties of the TLA are shown in Table 2.3.

The dry specific gravity of aggregate is in the range of 1.79 to 1.86, which corresponds to Class H in the classification of the specific gravity specified in the Japanese Standard, JIS A-5002 "LWA for Structural Concrete." The water absorption after 24 hours is about 2.5% in all samples and satisfies the value of less than 3% specified in the Japanese standard JIS A-5005 "Crushed Stones for Concrete." The aggregates produced are of high strength and can be used for making structural high strength concrete.

Sakai, et al.,[21] developed a new type of fly ash aggregate possessing high density and low water absorption. The specific mechanical properties of this aggregate are summarized here.

Specific Gravity. Oven-dried specific gravity of large grains (15–10 mm) is 1.96 and that of small grains (10–5 mm) is 1.92. The new LWA, therefore, has about 1.4 times the specific gravity of conventional fly ash aggregates.[22][23]

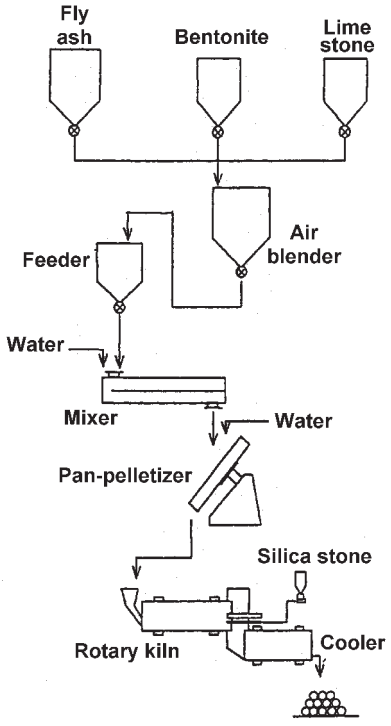

Figure 2.12. Schematic diagram showing the production of TLA aggregates.[20]

Table 2.3. Properties of Tough and Lightweight Fly Ash Aggregates, TLA[20]

	Absolute Dry Sp.Gr.	**Water Abs. 24 hrs%**	**Sound-ness Test %**	**Unit wt.**	**Loss Abras-ion %**	**Solid Content %**
Test value	1.79 to 1.86	2.52	0.1	1.15	13.2	64
JIS A-5002 SLWAC	L: <1.0 M: >1.0, <1.5 H: >1.5, -2.0		<20%			>60%
L-low, M-medium, H-high						

Water Absorption. Water absorption of large grains (15–10 mm) is 1.07% and that of the small grains (10–5 mm) is 3.15%. Larger sizes show less water absorption. When large and small sizes are mixed in the ratio of 4:6, its water absorption becomes 2.32, which is larger than crushed stone and river gravel, but lower than conventional fly ash aggregates.

40 Ton Crushing Value. 40 ton crushing value of the new LWA is 236%, which is much lower than conventional LWA and is expected to have higher strength capabilities for the concrete.[24]

Other Properties. The small particle fraction of the new LWA are uniform in size, i.e., the large grains and the small grains are 1.5 mm and 0.9 mm in diameter, respectively, and the percentage of the solid value of the new LWA is 62.1%. Maximum water absorption measured by two hours of boiling is 1.78% at large grains and 5.04% at small grains, which indicates that the new LWA has little voids or little cracks inside.

LWA from Biotite-Rhyolite by Fluidized Bed, ALA. A novel fluidized bed process has been developed to manufacture high performance Artificial Lightweight Aggregates, called ALA (particle diameter, 300–600 μm), with high yield.[2] The aggregates from this process are characterized by their very smooth surface, no open pores, uniformly dispersed closed bubbles, and excellent performance, i.e., lightweight, resistance to isostatic pressure, and low water absorption.

Two factors are important for the production of these aggregates:

1. Determination of the operating conditions of a fluidized bed reactor to produce ALA without agglomeration
2. Use of porous biotite rhyolite for producing lightweight aggregates

Raw Material and Pellet Preparation. The raw material used for ALA is porous biotite-rhyolite, which originates from lava. This material is produced on the Nijima Island of Tokyo. It is rich in SiO_2, and Al_2O_3 and contains a small amount of Fe_2O_3 (Table 2.4). The materials used for making pellets are shown in Table 2.5. These are very durable and have an especially high fire resistance.

Foaming Method. The silicon carbide foaming method consists of pulverization of the raw material, addition of a foaming agent, and burning. It is shown by a schematic chart in Fig. 2.13.

Powder of the composition shown in Table 2.4 is mixed in a drum granulator and then sieved through 0.25–0.5 mm. The raw pellets are heated for 30 minutes at 900–1000°C, to improve abrasion resistance during fluidization and to prevent breakage by rapid heating. Fine alumina

powder (d_p = 6.46 μm) is used to coat the raw pellets to prevent agglomeration.

The foaming agent, SiC, reacts with the SiO_2 in the melted raw material (1150–1190°C) under an oxidizing atmosphere, and evolves carbon monoxide gas in the glass matrix. This procedure has a potential to produce ALA with closed and uniformly sized bubbles.

Table 2.4. Analysis of Biotite-Rhyolite (wt%)[2]

SiO_2	Al_2O_3	Fe_2O_3	CaO	MgO	K_2O	Na_2O	LOI
78.7	12.3	0.87	0.85	0.09	2.73	4.01	0.39

Table 2.5. Materials Used for Making Biotite-Rhyolite Pellets[2]

Raw Material	Foaming Agent	Binder	Coating Powder
Biotite-rhyolite	Silicon Carbide	Bentonite	Fine alumina powder
96.8	0.2	3.0	10
Weight % coat powder of fine alumina not included in the base.			

SiC
Raw material → Fine Pulverization → Pelletization → Burning → ALA

Figure 2.13. Schematic chart for producing artificial lightweight aggregates, ALA.

The experimental set up of a fluidized bed reactor is shown in Fig. 2.14. A steel tube (inner diameter: 38 mm), adapted as a fluidized bed column, was placed in an electric arc furnace. A fixed bed of alumina balls (d_p = 2 mm, static bed height 0.28 m) was used as the gas distributor. The bed temperature was measured by using a K-type thermocouple immersed in the bed. The bed pressure drop was measured by a differential pressure sensor. Fluidization gas was supplied by a computer assisted system via a mass flow controller to maintain the excess gas velocity constant. Inert bed material was charged in the column up to a height of 30 mm and heated under fluidized conditions. When the bed temperature reached the predetermined temperature (1150–1190°C), raw pellets preheated to 900°C were introduced slowly into the fluidized bed over a period of 120 seconds, and then the fluidization was continued for 500–2000 seconds. The properties of LWA are shown in Table 2.6.

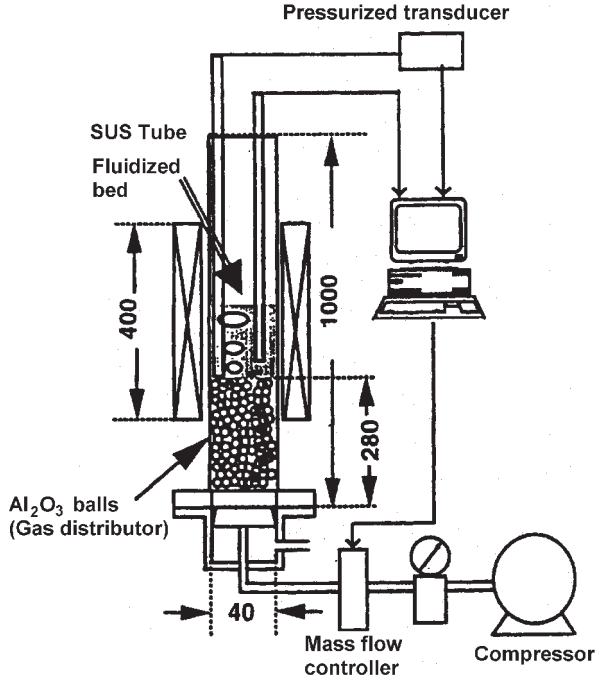

Figure 2.14. Laboratory scale fluidized bed forming reactor.[2]

Table 2.6. Properties of the Artificial Lightweight Aggregates Made by Fluidized Bed (F.B) and Rotary Kiln[2]

Aggregates	Mean Particle Diameter µm	24 hrs Water Absorption Ratio wt%	Apparent Density kg/m^3	Tensile Strength MPa
F.B 1190°C 500s	383	0.70	1051	5.83
F.B 1170°C 500s	349	0.19	1308	14.4
F.B 1150°C 500s	334	0.04	1520	18.2
F.B 1150°C 2000s	387	0.41	911	4.09
Rotary kiln Fine aggregate	398	19.24	1024	5.04

Aggregate Surface and Void Structure. A comparison of the surface and cross section of the ALA particles produced by the fluidized bed reactor and those produced by a rotary kiln are shown in Fig. 2.15, and the bubble structure is shown in Fig. 2.16.

The figures show that the fluidized bed particles are of spherical shape and smooth surface with almost no pore openings. On the contrary, the rotary kiln products have many pore openings on their surface and the intra-particle bubbles are more non-uniform, containing overgrown bubbles, than those contained in a fluidized bed product. These results indicate that the fluidized bed products would absorb little water and will have improved flowability and workability for casting concrete with ALA. Pore structure has shown that the closed bubbles become larger by coalescence. This also results in the decrease of the product's apparent density.

The fluidized bed is a very effective process for producing ALA aggregate of desired density by controlling the temperature. The aggregates have a smooth external surface, because the particle's surface melts without agglomeration by the fluidized bed sintering. These aggregates have shown higher resistance to mercury intrusion under isostatic pressure than those

produced by a rotary kiln. This implies that the fluidized bed product will have low water absorption and high strength. The properties of ALA aggregates produced by the fluidized bed and rotary kiln methods are compared in Table 2.6.

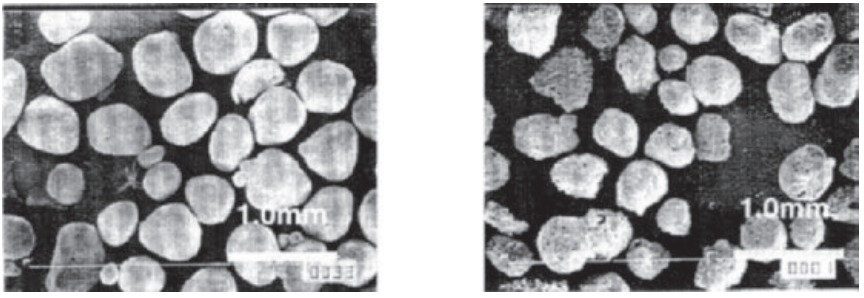

(a) external appearance

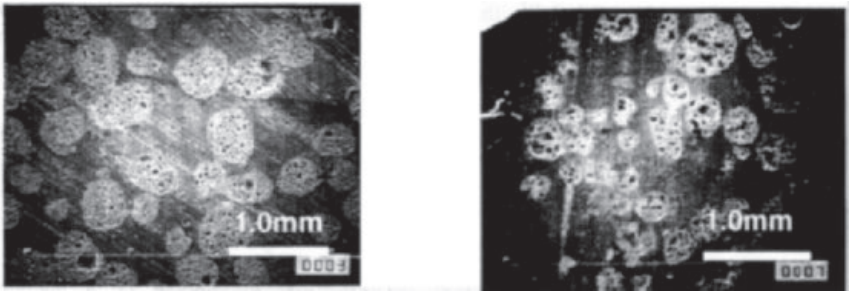

(b) cross-sections

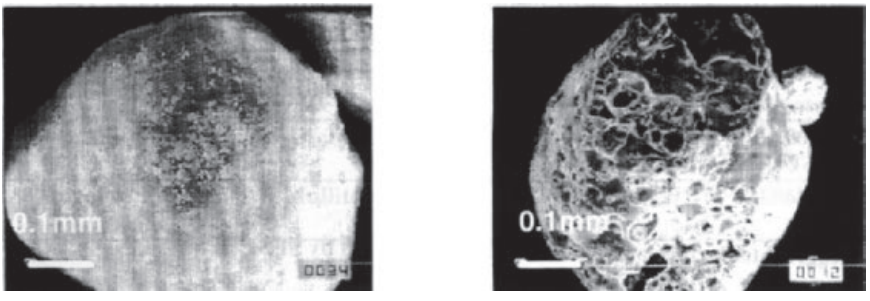

(c) magnified external surface

Fluidized bed products	Conventional rotary kiln products
1150°C 500s	Fine aggregate No. 4
(ρ_p = 1520 kg/m^3)	(ρ_p = 1024 kg/m^3)

Figure 2.15. ALA particles, cross-sections, and surfaces.[2]

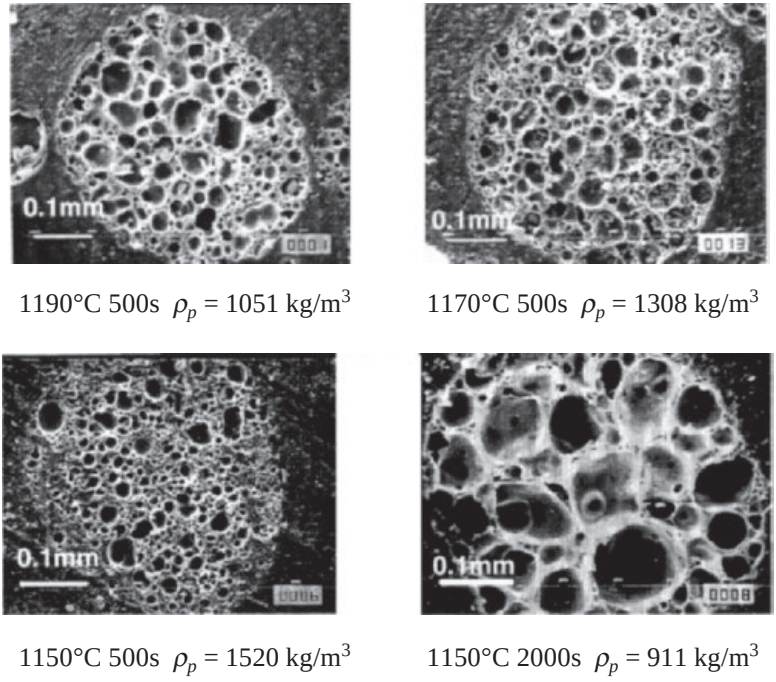

1190°C 500s ρ_p = 1051 kg/m^3 1170°C 500s ρ_p = 1308 kg/m^3

1150°C 500s ρ_p = 1520 kg/m^3 1150°C 2000s ρ_p = 911 kg/m^3

Figure 2.16. Bubble structure of ALA.[2]

Lightweight Aggregates from Blast Furnace Slag (Pelletized Slag). In the manufacture of steel, pig iron is produced together with slag. The amount by volume of slag produced is about the same as pig iron. The quantity of slag thus produced is very large, and it creates ecological and environmental problems. Hence, there is need for research to find uses for slag. Some slag is used after granulating and grinding as cement replacement material in the building industry. Apart from this, some of it is used in making lightweight aggregate. Due to the growing demand for aggregates worldwide, research is being carried out to develop the process and technique for producing good quality aggregates. Some of the processes used for making the LWA and their properties are described here.

LWA from Slag in Canada. A Canadian company, National Slag of Hamilton, has developed a method of pelletizing slag into a lightweight aggregate by directing the stream of molten slag that comes directly from the blast furnace tap hole onto a rotating finned drum. This finned drum rotating on a horizontal axis flings the molten slag up into the air where it is air cooled and then falls to the ground in discrete particles of expanded slag with a size and density that can be easily controlled. Normally, this

by-product of the steel industry, when run off into big pits and allowed to slowly air cool, is used as a low-value crushed aggregate. With the pelletization using the rotating drum, the end product can be used for lightweight concrete structural applications and for lightweight concrete masonry units. An example of its use is the sixty-eight floor Scotia Tower in Toronto which was built in 1988 and at 244 m is the highest building in Canada. It used 30,000 m^3 of expanded slag lightweight concrete for the lightweight composite floor deck and 100,000 tons for the lightweight slag masonry units.[25]

LWA from Slag in Russia. A process was developed to produce lightweight aggregates in the 1960s in Russia.[26] In this process, molten slag is introduced into a venturi-like tube system in which high pressure water and air are mixed in a turbulent flow with the molten slag. A modification of this technology in which the slag, after coming from the venturi, is cooled in a rotating drum and screened using a trammel screen attached to the rotating drum, was constructed in Chelabinsk, Russia, in the 1980s. The plant had an air-entrainment tower designed to fully treat the sulfur-rich exiting gases.

Generally, the production of expanded slag results in high SO_2 gas emissions that are not always properly treated. Also, leachate from slag aggregate piles has a high acid content and, therefore, care must be taken to minimize the effects on the environment. On the positive side, these LWAs are produced with essentially no additional energy than that required for regular aggregates, and in the area near blast furnaces, they provide a competitive source of aggregates for low density concrete and lightweight masonry units.

Expanded Slag Gravel, ESG-1. A new type of porous slag aggregates has been developed in Russia. These are made from the melted slag and are grouped in a class named "Expanded Slag Gravel (ESG)." These resemble the natural dense gravel in shape, hence, the name Expanded Slag Gravel. The manufacturing process has been described by Larmakovski.[27]

The technological complex for the production of the expanded slag gravel of the ESG-1 type consists of two production lines with a pore-forming apparatus and a drum-cooler granulator as the main elements for each line. One common steam-gas-dust cleaning system serves for both production lines. The principal scheme of one technological line of the operating complex at the Lipetsk metallurgical works in Russia is presented in Fig. 2.17.

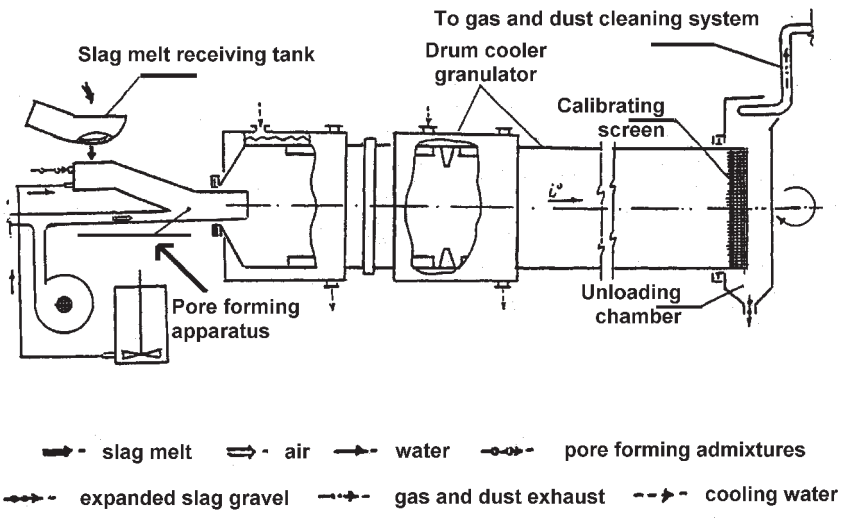

Figure 2.17. Schematic diagram showing the production of expanded slag gravel.[27]

The slag melt is normally fed into the inclined hydrochute of the water and air pore-forming apparatus directly from the runner system of the smelting furnace, (in particular, blast furnace) at T = 1400–1500°C. It is the best solution. The slag melts can also be fed to the pfa (pore forming apparatus) at T = 1300–1400°C by ladles in case the complex is at a remote distance from the furnace. The water jet penetrates the stream of the slag melt, resulting in a pore formation process. The mass of expanded (foamed) slag meets the stream of compressed air in the special run chamber of the pfa where the mass is dispersed and then injected into a rotating drum. In order to intensify the expanding (foaming) process in the slag melt and thus produce extra lightweight aggregates (ESG-1a) designated for the structural-thermal insulation concretes, not only physical (water-steam-air) pore forming is applied, but also an additional chemical addition (with the help of gas pore-forming admixtures). The chemical admixtures are fed into the slag melt together with water or air (depending upon the type of admixture).

The following processes take place in a revolving drum of up to 30 m in length.

At the entrance of the drum, the dispersed slag particles strike against a special screen which throws them onto the inner surface of the drum case where they reunite and form a still-movable mass, which gets some additional pore formation due to evaporation of water particles capsulated in the mass.

The expanded slag mass, together with some amount of dispersed slag particles, moves along the inclined drum case in a complex downward motion (spiraling down and forward). Moving in such a way, the slag mass is cooled by water jets from the nozzles located along the drum case, and then it is dispersed again by the drum's longitudinal ribs. In the process of the drum rotating, the dispersed expanded slag particles form shapes which are close to the form of natural gravel and are thrown out of the drum through the calibrated grate for further separation to fractions, 0–5, 5–10, and 10–20 mm.

The air-dried particle density of the ESG is 1.2–1.6 t/m^3 (depending on the chosen regime of the technological process and type, chemical compositions, and properties of the slag melt). At the end of the drum, there is an outlet pipe through which gases, water, steam, and dust are transferred to a special system to be cleaned mechanically and chemically. The productivity of each of the two production lines of the developed complex is 3–4 tons/minute of slag melt flow being processed or up to 200,000 m^3/year of the fractionated ESG-1.

Properties of Expanded Slag Gravel. Some important properties of the expanded slag aggregates produced by the above technology (a drum-cooler granulator) with the use of pore-forming admixtures (ESG-1a) or without them (ESG-1b) are shown in Table 2.7.

The characteristics of two varieties of ESG-1 are given compared to the characteristics of the EVS (expanded vesicular slag) aggregates produced from the same type of slag melt by the traditional technology which is well-known as Hydro-Screen Technology.

A comparative analysis of the data in Table 2.7 reflects the obvious advantages of ESG-1 produced according to the new technology, especially when using gas pore-forming admixtures (ESG-1a):

- Lower total intergrain volume of aggregate voids, provided for by a lesser volume of open pores on the surface of grains and a shape of the grain similar to that of the natural gravel.
- Lower density of the grain with approximately equal compressive strengths in concrete.
- Lower value of average size of intergrain pores; quite important to decrease thermal conductivity of concretes.

Table 2.7. Some Important Properties of the Expanded Blast Furnace Slag Aggregates Produced by Different Methods[27]

Production Process	Fraction of the Aggregates mm	Properties of the Aggregates		
		Total Intergrain Volume of Voids %	Bulk Density kg/m^3	Comp. Str. MPa
Hydro screen	5–10	52.3	780	1.15
EVS	10–20	52.5	746	1.05
Drum granulator/ ESG-1a	5–10	49.6	623	1.17
	10–20	50.9	608	1.12
Drum granulator/ ESG-1b	5–10	49.0	726	1.39
	10–20	50.1	715	1.31

ESG-1a–with pore forming admixture.
ESG-1b–without pore forming admixture.

Expanded Slag Gravel, Type ESG-2. The technological process of ESG-2 manufacture involves the following main operations.

In the case of ESG-1 production technology, the slag melt flowing from the running system of a blast furnace gets into the inclined vibrating feed plate and then drops into the pore-forming apparatus. But in the production of ESG-2, another variant of the pfa (pore forming apparatus) is developed and shifted along the vertical axis from one plate to another mounted on a vibrating frame. There are vertical water nozzles in the gaps between the plates.

The slag melt is partially pore-formed (foamed) under the influence of the water running out of the nozzles at the first level and moves lengthwise through the pfa (pore forming apparatus) installations. Then the melt is treated by water running out of the nozzles at the second level, etc. The number of pfa (pore forming apparatus) levels is characterized by the preset production capacity of the technological line (1–5 tons of processed slag melt per minute).

Further on, the foamed ductile (pyro-plastic) slag melt mass overflows onto the rotating blade drum and is dispersed by the co-impact with the blades. The pore-formed slag melt particles are thrown out into the surrounding environment of the working enclosed zone. Here, the particles assume the shape of a granule (pellet) in the air countercurrent due to the surface tension force. Then the particles cool to the temperature of crystallization and fall along the curve line onto transporting belts of the receiving bin. The mix of the cooled ESG granules of different sizes is delivered to the sorting installation for separation into 0–5, 5–10, and 10–20 mm fractions.

In contrast with the best world prototype technology of manufacturing, the so called “pelletized slag” (LITEX™) produced by National Slag Limited (Hamilton, Ontario, Canada),[28] one of the largest-scale slag processing companies in the world, the main advantages of this developed technology are the following:

- The environmental safety, due to significantly lower technological water consumption and correspondingly, 5–6 times reduced volume of steam gas exhausts in the atmosphere and its localization and neutralization.
- The possibility of obtaining more lightweight aggregate (particle density, 0.2–0.3 t/m^3 less) having pores of smaller

averaged size, that is provided for by permanent step-by-step contact of the slag melt with technological water on the above pore formation levels. The consequence is that uniform thorough treatment of the total slag melt volume by pore-forming agent takes place.

- The possibility of an amorphous phase content increases in the upper layer of the aggregate grain due to acceleration of granule cooling in the created air countercurrent. Correspondingly, it involves lowering thermal grain conductivity and improving bond strength of the aggregate grain to the hardened cement paste contained in the concrete.

Properties of Aggregates and Concrete. Some averaged statistical data on ESG-2 aggregates are the following:

- Bulk density for fractions of 10–20 mm, 550–600 kg/m^3 and 0–5 mm, 750–800 kg/m^3.
- Strength of grain is sufficient to obtain lightweight concrete with up to 20 MPa compressive strengths but when natural sand is used as a fine aggregate, then it reaches 40 MPa.
- Water absorption per hour is 6–10% by volume, when amorphous phase (glass) content is 50–70%.
- Coefficient of thermal conductivity in filling for fractions of 10–20 mm and 5–10 mm is 0.11–0.12 W/mK.

It must be emphasized that ESG-2 coarse aggregate with 550–650 kg/m^3 bulk density is equivalent in thermal conductivity to expanded clay gravel with 350–450 kg/m^3 bulk density. It is provided for by a considerably greater amorphous phase content and a smaller average size of ESG-2 intergrain pores.

ESG-2, with the above properties, is extremely effective to use within lightweight concrete which is designated for application in walls and masonry units. It may also be used to produce concrete for load bearing structures.

In the case of usage of gas pore-forming admixtures for additional foaming of slag melt, it is possible to obtain the ESG-2 with bulk densities not higher than 400 kg/m^3 (coarse fraction). This variety of ESG-2 will be effective for use in heat-insulating fillings.

The application of newly developed technologies of expanded slag aggregates (ESG) production at Russian metallurgical works, instead of the tractional hydroscreen technology of expanded vesicular slag (EVS) manufacture, made it possible:

- To meet environment requirements.
- To improve significantly the main properties of expanded slag aggregates and, hence, those of LWAC made on its basis. The cement consumption required is reduced by 11–15% for walls and masonry units; by up to 27% for bearing concrete structures, and the thermal conductivity of the cement is reduced by 11–29%. The durability, strength, and deformation properties are improved.

Lightweight Aggregates from Municipal Waste. ***NKK Process, Japan.*** In the incineration of domestic waste, ash is produced that can be converted into a slag, which is then converted into a lightweight aggregate as discussed in the previous subsection. The NKK corporation of Japan has three 100 ton/day incinerators and two 18 ton/day ash melting furnaces, the latter incorporating an innovative electric resistance ash-melting and slag recovery process.[29] This operates in the city of Hachioji while similar plants are operating in Ichinomiga, Ageo, and Morioka. The slag produced at the four cities is apparently only used as a land fill at the present time, but, in the future, could be converted into a lightweight aggregate.

In 1992, the NKK corporation began research on a "high temperature gasifying and direct-melting process" and in 1995 built a full-size pilot plant with a 24 ton/day capacity that subsequently processed 200 tons of municipal waste, car shredded dust, plastic waste, and incinerator ash in 200 days of operation. The waste is supplemented with coke and lime, with combustion in a three-stage furnace. The output is combustible gas and a slag material. The slag produced could apparently serve as the raw material to make an expanded pelletized slag for use in LWAC.

Sludge Ash Aggregates in the USA. In the USA, over five million tons of sewage sludge is produced annually.[30] About one fourth is used for making lightweight aggregates and the rest is for landfill disposal. Magdich[31] developed a method for treating 0.5 million tons of municipal sludge annually to produce about 300,000 tons of incinerated ash.

The flow chart for the production of pellets and slab aggregates from the sludge ash is shown in Fig. 2.18. The ash is first screened to 20 mesh (0.8 mm) and the lumps are removed. It is mixed with about 20% water and placed into a pelletizing unit set at 3/8 inch. The pellets are

dried overnight, loaded into stainless steel trays, and fired in a muffle at 1050–1110°C for different periods. The fired pellets are cooled to room temperature and later tested for specific gravity (sp. gr.). The variation in the specific gravity with temperature is shown in Table 2.8. The product with a specific gravity range between 0.8–1.4 was collected and subdivided into two fractions of lightweight I (sp. gr. = 1.1–1.4) and lightweight II (sp. gr. = 0.8–1.1) aggregates.

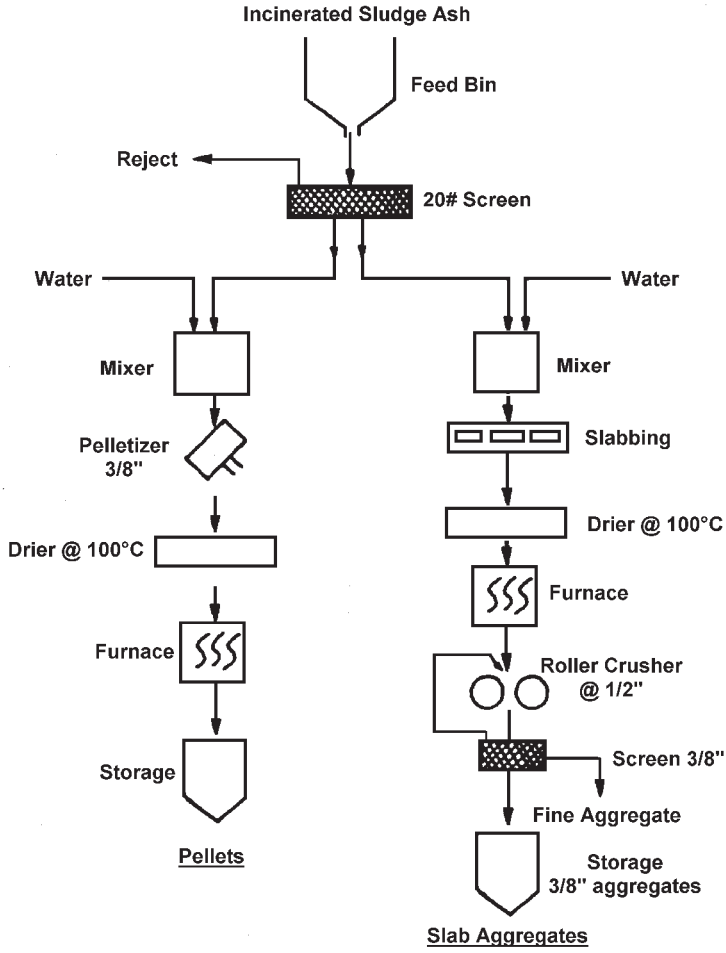

Figure 2.18. Schematic flow chart of the production of pellets and slab aggregates from sludge ash.[32]

Table 2.8. Variation in Specific Gravity of Sludge Ash Pellets[32]

Time min	Temperature °C				
	1060	1070	1080	1090	1100
10	1.55	1.34	1.04	0.77	0.79
15	1.41	1.24	0.80	0.65	0.68
20	1.35	1.12	0.71	0.58	0.59
25	1.30	1.08	0.65	0.55	0.57
30	1.27	0.98	0.63	0.54	0.52

Some of the properties of the aggregates are shown in Table 2.9, and their microstructure is shown in Fig. 2.19. These data show that the lightweight aggregates produced from sludge ash are stronger than the expanded clay aggregates. The reason could be the uniform size of pellets, their spherical shape, and low moisture absorption.

There is potential for producing lightweight aggregates from incinerated sludge ash that can be utilized in producing a moderate strength concrete.

Lightweight Aggregates from Dredging Waste. Maintaining adequate draft for shipping at wharfs near industrial sites requires periodic dredging. The dredge material frequently is silica-rich and highly toxic. Attempts have been made to dispose of these dredging wastes by pelletizing them by passing through an extruder and then burning them in a rotary kiln. One of the major disadvantages of the rotary kiln is the requirement of a large amount of air flowing up through the kiln beyond that needed for combustion. When the raw feed is fed into the high end of the kiln, it meets the exiting gases, and the liquids in the raw feed are converted into a gas and carried out of the kiln without entering the high temperature burning zone at the bottom end of the kiln. To alleviate this problem, various forms of two-kiln systems have been proposed in which the exiting gases from the first kiln are fed into the burning zone of the final second stage kiln. Another system uses the stainless steel rotating pipe as a kiln, and is externally heated to minimize the amount of gases that need to be treated. Although pilot plants that embody some or all of the above ideas have been built, no commercial operations are currently operating.

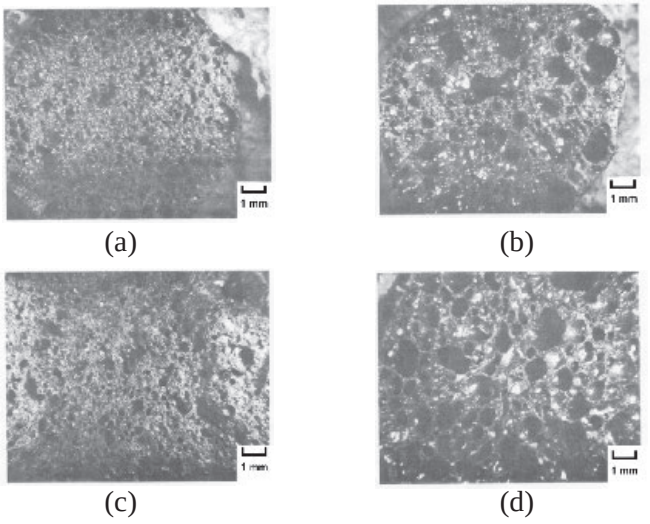

Figure 2.19. Sections showing pore size distribution of *(a)* lightweight I; *(b)* lightweight II pellets, *(c)* lightweight I *(d)* lightweight II slabs.[32]

Table 2.9. Specific Gravity, Bulk Density, Water Absorption and Fracture Strength of Pellets and Other Commercial Aggregates[32]

	Pellets		**Commercial**
	Lightweight I	**Lightweight II**	**Expanded clay**
Specific gravity	1.07	0.75	1.04
Bulk density	0.67	0.48	
Absorption (wt%)	2.49	2.88	
Fracture strength (lb)	120.0	42.8	35.93
Weight (gr)	0.66	0.31	0.34
Strength/weight ratios (lbs/gr)	183.0	140.0	112.0

Recovering and Recycling Liquid Combustible Waste. Many used fluids that normally pose a serious disposal problem, such as paint thinners, used motor oils, and spent cleaning fluids, have a high fuel level value. These fluids sometimes rival the fossil fuels that in the past were the only fuels used for firing rotary kilns. It has become common to obtain up to 80% of the total fuel from these "secondary combustible materials" in fueling lightweight aggregate kilns. The plants are normally designed to start up and shut down on conventional fuels such as natural gas and coal. The majority of the time they burn the secondary combustible fuels. If problems arise, they shift back to the gas or coal. Government regulations in North America control how these fuels can be disposed of in manufacturing lightweight aggregates. For waste fuels that need higher temperatures and longer resident times at high temperature, cement kilns are used. For a very limited amount of waste, special incinerators need to be dedicated only to the very toxic liquids where the CO_2 emissions are generated with no compensating benefit to society.

For both the cement, as well as the lightweight aggregate producing rotary kilns, the emissions rules are very strict and attention is to be given to the burning process that takes place at the lower end of the kiln. As the kiln revolves, the gases and objectionable particulate matter evolved in the burning zone move up the kiln; counter to the downward flow of the clay, shale, or the slate where they come in close contact. This long-term retention contributes to the efficient destruction of the hydrocarbons and other wastes and to the incorporation of the products of combustion into the raw feed for further exposure to the pyro-plastic aggregates and to the burning process again. Exiting gases pass through electrostatic precipitators, or fabric filters, or both. The kiln dust recovered can have some hydraulic properties and a significant amount of it is incorporated as a cement supplement for making masonry units.[26]

5.0 CONCLUDING REMARKS

Lightweight aggregates are produced from natural materials of volcanic origin like pumice and scoria by mechanical treatment. Lightweight aggregates are also produced by thermal treatment of either the natural raw materials like clay, slate, shale, etc., or industrial by-products like fly ash, slag, and sludge, etc. With the development of structurally high

strength lightweight aggregate concrete, the demand on the quality of the aggregates has increased. Intensive research is being carried out on the development of high strength, yet low density, aggregates with low water absorption and better thermal properties.

Lightweight aggregates from fly ash and slag are produced using different sintering processes. These are tough and have low water absorption. These will produce high-strength lightweight aggregate concrete of high durability.

REFERENCES

1. FIP, *Manual of Lightweight Aggregate Concrete, 2nd Ed.*, Surrey University Press, UK (1983)
2. Kimura, S., Kaniva, H., Horio, M., and Kimura, K., A Novel Fluidized Bed Manufacturing of High Performance Artificial Lightweight Aggregate, *Proc. 2nd Int. Symp on Structural Lightweight Aggregate Concrete*, Kristiansand, Norway, p. 613 (Jun. 18–22, 2000)
3. Dhir, R. K., Jones, M. R., and Munday, J. G. I., A Practical Approach to Studying Carbonation of Concrete, *Magazine of Concrete*, pp. 32–34 (Oct. 1985)
4. Dhir, R. K., Munday, J. G. I., and Cheng, H. T., Lightweight Concrete, Permeability and Durability, *Constr. Weekly*, 1, 22, pp. 10–13 (Aug. 1989)
5. Abdullah, A. A. A., Palm Oil Shell as Aggregate for Lightweight Concrete, *Waste MaterialsUsed in Concrete Manufacturing*, (S. Chandra, ed.) Ch. 10, Noyes Publ., Park Ridge, NJ (1997)
6. Abdullah, A. A. A., Basic Strength Properties of Lightweight Concrete Using Agricultural Wastes as Aggregates, *Proc. Int. Conf. on Low-cost Housing for Developing Countries*, Roorkee, (Nov. 1984)
7. De Pauw, P., Taerwe, L., and Desmyer, J., Concrete and Masonry Rubble as Aggregates for Concrete Something in Between Normal and Lightweight Concrete, *Proc. 2nd Int. Symp. on Structural Lightweight Aggregate Concrete*, Kristiansand, Norway, pp. 574–583 (Jun. 18–22, 2000)
8. Barnett, D. E., *Some Potential Bloating Shales from New Brunswick*, New Brunswick Research and Productivity Council, Fredericton, N.B, Research Note 9, p. 14 (Dec. 1967)
9. ASL, *Artificial Lightweight Aggregate Association*, Steel Fiber Reinforced Lightweight Aggregate Concrete, No.3 (Nov. 1998)

10. Berntsson, L., and Chandra, S., *Lightweight Aggregate Concrete for Inside House Construction,* Swedish Council for Building Research, R-13, Stockholm, Sweden (in Swedish) (1994)

11. Harmon, S. K., Physical Characteristics of Rotary Kiln Expanded Slate Lightweight Aggregate, *Proc. 2nd Int. Symp. on Structural Lightweight Aggregate Concrete*, Kristiansand, Norway, pp. 574–583 (Jun. 18–22, 2000)

12. Masuda, K., Yamada, K., Ohga, H., and Nagataki, S., Quality Control of Concrete with Fly Ash, *Proc. Durability of Concrete; Aspects of Admixtures and Industrial By-products, 2nd International Seminar,* Chalmers U. of Techn., Sweden, Swedish Council of Bldg Res., D9 (Jun. 1989)

13. Bijen, J. M. J. M., Manufacturing Processes of Artificial Lightweight Aggregates from Fly Ash, *The Int. J. Cement and Lightweight Concr.*, 8(3) (1986)

14. Harrison, W. H., and Munday, R. S., *An Investigation into the Production of Sintered PFA Aggregate,* Bldg. Res. Estab., Publ. CP 2/75 (1975)

15. Messman, C., and Tibbets, T. E., *Elements of Briquetting and Agglomeration,* Inst. of Briquetting and Agglomeration, Las Graces, NM

16. Lytag™ Production information, B.V. Vasin, Nijmegen

17. Aardelite™, A New Product, A New Challenge, Aarding, b.v, Nunspeet. The Netherlands

18. Spanjer, J. J., The Manufacturing of Artificial Gravel out of Fly Ash from Power-Stations, An Economical and Environment Friendly Alternative for Dumping, *Coal Technol.*, Europe, Conference, Amsterdam, (1983)

19. Swamy R. N., and Lambert, G. H., The Microstructure of Lytag™ Aggregates, *The Int. J. Cement Composite and Lightweight Concrete*, 3(4):273–285 (Nov. 1981)

20. Morishita, N., Yokoyama, H., Takada, S., Uji, K., and Ozawa, K., Characteristic of High Performance Aggregate Produced from Fly Ash Using a Rotary Kiln, *Proc, 2nd Int. Symp. Structural Lightweight Aggregate Concrete,* pp. 631–639, Kristiansand, Norway (Jun. 18–22, 2000)

21. Sakai, K., Tomosawa, F., Noguchi, T., and Sone, T., Evaluation of the New Type of Fly Ash Lightweight Aggregates, *Proc. Int. Symp. Structural Lightweight Aggregate Concrete,* Sandefjörd, Norway, pp. 640–649 (Jun. 20–24, 1995)

22. Zhang, H. M., and Gjörv, E. O., Development of High Strength Lightweight Concrete, High Strength Concrete, *2nd Int. Symp., ACI- SP, 121*, pp. 667–681 (1990)

23. Berra, M., and Ferrara, G., Normal Weight and Lightweight High Strength Concrete, A Comparative Experimental Study, *Proc. High Strength Concrete, 2nd Int. Symp., ACI-SP 121,* pp. 701–733 (1990)

24. Yoneda, S., Matsunaga, A., Igarashi, H., and Hamada, S., Properties of Lightweight Aggregate Made of Fly Ash Sources and Application to Deck Slabs Including Heat Pipes, *Extended Abstracts on the 45th Annual Meeting of the Cement Association of Jpn,* pp. 352–357 (1991)

25. Slag the All Purpose Construction Aggregate, MF 188-3 , *National Slag*, Hamilton, ON, Canada

26. Bremner, T. W., Lightweight Concrete-An Environmentally Friendly Material., *Int. Symp. Sustainable Development of the Cement and Concrete Industry,* Ottawa, Canada, pp. 523–530 (Oct. 1998)

27. Larmakovski, V. N., New Types of the Porous Aggregates and Lightweight Concretes with their Application, *Proc. Int. Symp. Structural Lightweight Aggregate Concrete,* Sandefjörd, Norway, (I. Haland, T. A. Hammer, and F. Fluge, eds.), pp. 363 (1995)

28. Emery, J. J., Pelletized Lightweight Slag Aggregates, *Proc. 2nd Int. Congress on Lightweight Aggregate Concrete,* Construction Press, London (1980)

29. NKK Annual Report NKK Corporation, 1-1-2 Marunouchi Chiyoda-kv, Tokyo Jpn, 100–8202, p. 44 (1998)

30. Padgett, L. E., Factors Affecting the Concentration of Heavy Metals in Municipal Sludge as Leachates, M.Sc. Thesis, Department of Civil Engineering; Notre Dame, Indiana (Jun. 1981)

31. Magdich, P., Literature Review of Sludge Ash Production and Disposal Factors Effecting the Trace Metals, Mineral Resources Research Centre, Internal Report; University of Minnesota, MN (1986)

32. Bhatty, J. I., and Reid, K. J., Moderate Strength Concrete from Lightweight Sludge Ash Aggregates, *The Int. J. Cement Composites and Lightweight Concrete,* 11(3) (Aug. 1989)

33. Dolby, P. G., Production and Properties of Lytag™ Aggregate Fully Utilized for the North Sea, *Proc. Int. Symp. Structural Lightweight Aggregate Concrete,* Sandefjörd, Norway, (I. Haland, T. A. Hammer, and F. Fluge, eds.), pp. 326–336 (1995)

3

Supplementary Cementing Materials

1.0 INTRODUCTION

The economic, practical, and technical benefits of high strength lightweight aggregate concrete have special attractions for applications in off-shore and marine structures, high-rise buildings, and long span bridges. A decreasing density without reducing strength, or increasing strength without increasing density, combined with high durability can lead to cost effective engineering solutions.

Modern concrete is based on portland cement comprising the basic minerals C_3S, C_2S, C_3A, and C_4AF. Though portland cement concrete has a lot of good properties, disadvantages are also associated with it: high energy required for producing cement, poor or lack of reaction with clay and dust particles, chemical interactions and formation of undesirable deleterious products, and the necessity of using both coarse and fine aggregates for attaining rich concrete. All these disadvantages are due to the fact that portland cement contains a large amount of calcium oxide (63–67%). As a result, the products of hydration, together with CSH, act as physically and

chemically active compounds; (3–4)$CaO \cdot Al_2O_3$(10–13)H_2O (calcium aluminate hydrate), (3–4)$CaO \cdot Al_2O_3 \cdot Fe_2O_3$(10–13)$H_2O$ (calcium alumino ferrite hydrate), $3CaO \cdot Al_2O_3 \cdot 3CaSO_4 \cdot 31H_2O$ [calcium aluminate calcium sulfate hydrate (ettringite)], (1.5–2)$CaO \cdot SiO_2 \cdot nH_2O$ (calcium silicate hydrate), etc.; the minerals that are almost nonexistent in nature. These interact actively with the surrounding environments and are, thus, subjected to various physical and chemical changes during the process of exposure.

These deficiencies in the properties of portland cement discourage its use in producing high performance concrete. With the development of industry, the increase in land as well as air traffic, and the increase in the global population, the atmosphere has become more polluted, thereby, more degrading to building materials. This has generated a demand for durability properties of concrete more than its high strength. In addition to this, with off-shore constructions where the concrete is exposed to very hostile climatic conditions, the demand for durability has further increased. This has led to the development of new binder systems which will fulfill the requirements set forth for the durability of concrete. Some new high performance cements have also been developed specifically in Norway where concrete of high performance is needed for off-shore construction and the marine environment.

It is known that the pozzolanic materials strengthen the mortar matrix and modify the microstructure. Pozzolanic materials of natural origin were used long before the invention of portland cement (patented in 1824). The Romans' binding materials were based on burnt limestone and ground volcanic materials, such as pumice from the neighborhood of the volcano Vesuvius, and from Thera or Santorini, named Santorin earth, from Greece. Another natural pozzolanic material from the Rhine river area in Germany known as "Trass" is also used for increasing the strength and durability properties of concrete. Pozzolanic materials are named as mineral admixtures, supplementary cementing materials, or cement replacement materials. Some of these materials are industrial by-products and agro-waste products. The most popular mineral admixtures are fly ash, blast furnace slag, and silica fume.

These supplementary cementing materials are known to contribute to properties of strength and durability. Silica fume has, for example, been extensively used to develop high strength lightweight aggregate concrete.[1]–[4] However, fly ash and slag are much more readily and widely available. These are used to enhance the durability properties, but they slow down the strength development of concrete in the early stage. Silica fume,

on the other hand, is highly pozzolanic and produces high strength material. When mixed together with fly ash and slag, it is capable of initiating rapid hydration at an early age while compensating for slower strength development.

To better understand the behavior of these binders, the hydration processes involved with their addition are discussed here. Some of the examples of LWAC made with their addition are also cited with special emphasis on strength and durability.

The hydration process of portland cement is well known and will not be discussed here in detail. However, based upon isothermal calorimetry, a classification of hydration has been done. It is shown schematically in Fig. 3.1.[5]

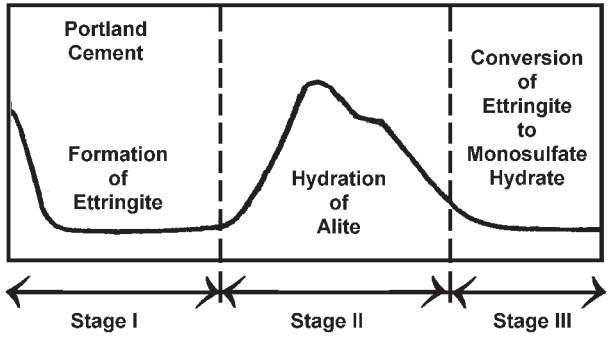

Figure 3.1. Classification of hydration stages by isothermal calorimetry.[5]

2.0 HIGH PERFORMANCE CEMENT

There are different types of cements varying in their mineralogical composition. Many of them are mixed with mineral admixtures. The addition of a mineral admixture like silica fume produces cement with high strength. This is of interest for off-shore construction where high strength and high performance are required.

As is well known, development is done to meet a need. A Norwegian cement company, NORCEM a.s., has developed high strength cement (NORCEM a.s. P30-4A/HS65). It is used in real structures and in research projects. In the 1970s, NORCEM a.s. started the optimization of portland

cement for the construction of off-shore platforms. The main objectives were to give a higher long-term strength and to reduce the heat of hydration. The latter was motivated by the fact that off-shore platforms (and also marine structures) typically have thick sections combined with a high binder content. The result was the development of a special high strength cement, designated as HS65 (28 day compressive strength, i.e., 65 MPa according to NS-EN 196). It has the following characteristic properties compared to the ordinary portland cement (P30):

- higher C_2S and somewhat lower C_3S
- higher fineness (appr. 400 m^2/kg for HS65 vs 350 m^2/kg for P30)
- lower alkali content (0.55% NaO-eq for HS65 vs 0.95% for P30)

The HS65 cement produces a concrete with about 25% higher 28 day compressive strength than a corresponding P30 cement.

Apart from special cements, silica fume, 5 to 8% by weight of cement, is added to all high performance LWA concretes in Norway. Silica fume is used not only to increase the strength, but to improve the durability, i.e., the resistance to reinforcement corrosion, to improve the ease of construction, and the resistance to segregation of LWA during mixing, transport, and placing. The guidelines of the Public Norwegian Roads Administration require a minimum silica fume content of 2% in concrete for marine bridges for durability reasons.

The required effective water/binder ratio has been somewhat lower than what is required for normal density concretes. This is done mainly to have extra security in order to fulfill the required maximum water/binder ratio because of the uncertainty about the amount of mix water absorption of the LWA. In most of the cases, the effective water/binder ratio is in the range of 0.35 to 0.38.

3.0 MINERAL ADMIXTURES

The most widely used mineral admixtures are fly ash, blast furnace slag, and silica fume. Sometimes rice husk ash is also used. Colloidal silica, a new product with the trade name Cembinder™, was recently developed. It is man-made and contains tiny pure silica particles in a dispersion form.

It is highly pozzolanic and has shown very promising results. The fly ash is generally used at replacement levels of up to 30%. For slag replacements, levels at around 40% and 70% are used for different applications. With these two minerals, the development of a microstructure during hydration is slightly modified from the pattern obtained without their addition. The replacement levels for silica fume are much lower, typically not more than 10%, but the effect on the microstructure development is very pronounced.[6] In the case of Cembinders, the amount used is very low, 2–4% of the weight of the binders and, thus, is used as a modifier.[7] All the mineral admixtures interact with calcium hydroxide and, thus, also have significant influence on the microstructure development.

The hydration process with the addition of a mineral admixture is different from that of pure portland cement. It depends upon the type of mineral admixture used. Blast furnace slag, for example, has a latent hydraulic property. It has to be activated. Fly ash "F" rich in iron, has a pozzolanic character whereas fly ash "C" is rich in calcium hydroxide. On the other hand, silica fume and rice husk ash have huge amounts of amorphous silica, and Cembinder is pure amorphous silica. Thus, it behaves like a reactive pozzolan.

3.1 Hydration of Fly Ash Cement

The effect of fly ash on the hydration of cement paste and concrete is still not well understood.[5] This is because fly ash is very inhomogeneous and its chemical composition may differ between two sources or even within one single particle. Fly ash particles, which are essentially inert in the early stages, are reported to enhance hydration of cement at later stages. These are slow reacting pozzolanic materials. For example, the amount of calcium hydroxide is high and the nonevaporable water, representing C-S-H formation, is low at an early age of cement paste hydration containing fly ash.[8] This pozzolanic reaction progresses with time, which is marked with a decrease in calcium hydroxide and an increase in C-S-H content. This phenomenon, which also occurs in the other finely divided non-reactive mineral powders, is attributed to the existence of these grains between the cement particles,[9] which results in increased space available for the growth of the hydration products.

In addition to enhanced cement hydration, fly ash by itself has the ability to react typically with Ca^{2+} and OH^- ions released from the cement to form secondary products. In this sense, as was mentioned before, class

F fly ash is a pozzolanic material. Class C fly ash, on the other hand, may contain higher amounts of CaO and some C_3A, C_2S, etc. It is able to hydrate by itself, and is of a more cementitious nature.

McCarthy and Tishmack[10] investigated fly ash from the Shawnee Pilot Plant, Paducah, KY, using bubbling bed atmospheric fluidized bed combustion technology (AFBC). They used high-sulfur bituminous coal, fly ash, and char. They have studied a paste of KY AFBC and char at a water-to-solid ratio of 0.45 cured at 100% R.H. for three months. It was shown that all the lime has been hydrated to portlandite, and much of the anhydride has hydrated to gypsum. The peaks in the XRD pattern were very sharp and distinct which indicates good crystal formation. Ettringite was identified and is a prominent hydration reaction product. There is also some calcite, which formed by partial carbonation of portlandite.

Besides the chemical interactions, fly ash also densifies the microstructure which is measured by mercury intrusion porosimetry. One of the examples of such densification is shown in Fig. 3.2,[11] for three types of fly ashes.

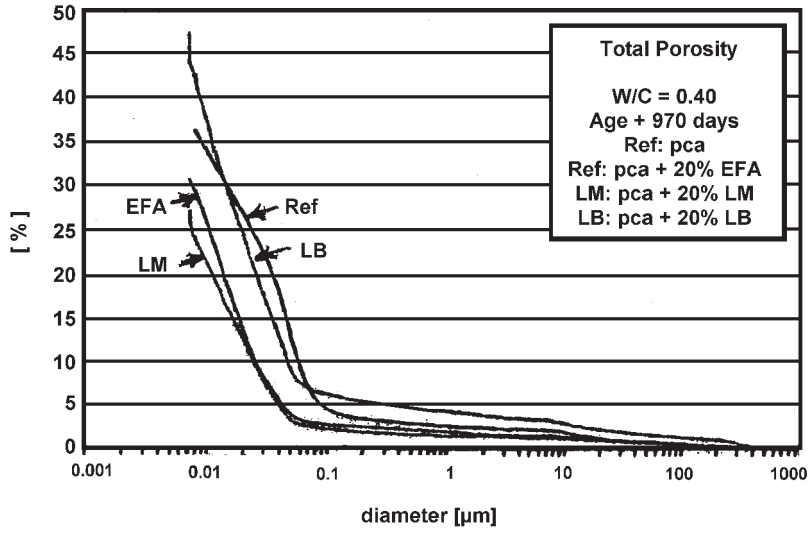

Figure 3.2. Pore size distribution measured by the mercury porosimetry of an ordinary portland cement and three fly ash composite cements (using fly ashes EFA, LM, and LB, respectively, in order of increasing particle size). Reference *(Ref)* is portland cement.[11]

3.2 Hydration of Blast Furnace Slag Cement

The principle hydration products formed in blast furnace slag cement are similar to those formed in portland cement; CSH gel, C_3AH_6, and AFt. Increasing slag content gradually results in the formation of C_2ASH_8 (incompatible with CH) and silicious hydrogarnets.[12] Pietersen[11] studied the interaction of slag with cement. His observations are shown in Figs. 3.3 and 3.4. Figure 3.3 shows a backscattered image of a reacted zone enveloping a slag grain in blast furnace slag cement hydrated for 90 days. Here the differences in composition along the slag edge are clearly visible. The two smaller maps represent XRD analyses of Mg and Al, respectively, and indicate the relative concentration of these elements at the slag edge due to the diffusion of calcium and silica.

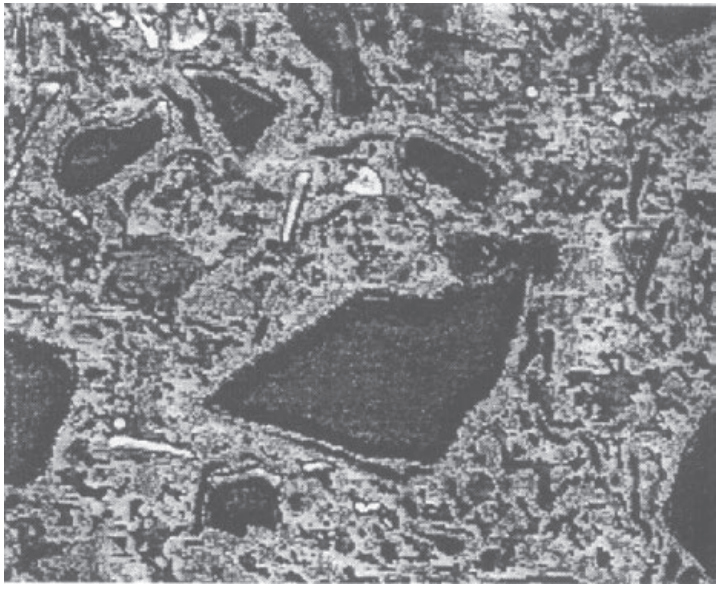

Figure 3.3. Backscattered image of a reacted zone enveloping a slag in blast furnace cement hydrated for 90 days.[11]

Figure 3.4. Scanning Transmission Electron Microscopy micrograph of a well-crystallized hydrotalcite-like phase which has developed within the original contours of a fully hydrated slag particle (ISH).[11]

Figure 3.4 shows that the Inner Slag Hydrate (ISH) indeed seems to have crystallized into well-formed platelets, presumably a hydrotalcite-like (HT) phase, which is known to be capable of forming in water-deficient regions. The apparent high internal porosity is noteworthy.

This figure clearly shows that a net transport of Ca, Si, and Al from the slag center has taken place; magnesium seems to act as a chemical "goalpost" as suggested by Feng, et al.[13] It is also evident that chemically different zones are formed approximately at the position of the original slag boundary; apparently these zones remain at their place, once they are formed, and may act as a chemical barrier or membrane. Feng and Glasser[14] have introduced the term ISH which reflects the inside of the reacting slag grain, and the term Outer Slag Grain (OSG) which stands for the additional hydrates formed outside of the original slag grain boundary.

The element transport mentioned above results in relatively porous, but isolated areas, formerly occupied by the interior of the slag grain (ISG). The densification of the slag cement paste outside the slag grains results in an overall reduced permeability. The total porosity of the blast furnace slag cement pastes changes only a little in this process relative to pastes without blast furnace slag. The densification of the microstructure of the paste is, of course, well known from the pore size distribution, as, for instance, measured by mercury porosimetry as is shown in the case of fly ash (Fig. 3.2).

3.3 Hydration of Silica Fumes

Silica fume contains particles as fine as 0.1 μm or less and has high surface energy; it partially dissolves in saturated CH solution within 5–15 minutes, and a SiO_2 rich hydrate is deposited in layers or films on the silica fume particles. C-S-H, having a C/S ratio of about 1, has been reported to form at 20°C in 24 hours after mixing with water and at 38°C in only 6 hours.[15] The reaction of silica fume with CH is affected by the specific surface area and the surface energy. Typically, the C-S-H produced with silica fume has a lower C/S ratio than that using fly ash. Since C-S-H with a C/S ratio of less than 0.8 is considered to be thermodynamically unstable, calcium silicate hydrate, once produced, is converted to a C-S-H variety having the lower limit of C/S, which coexists with excess silica containing very little calcium. This lower C/S ratio has been confirmed in reports by Taylor.[16] Diamond,[17] Glasser,[18] and Roy[19] stated that there is change in the composition of the pore solution with time. It shows that the hydration process takes place not only in the early stage, but it continues with time. After the early stage reaction, Li, et al.,[20] have shown that much silica fume remains unreacted after seven days. The silica fume particles surround each cement grain, densifying the matrix, and filling the voids with strong hydration products. Grutzeck, et al.,[15] reported that the Ca ion is actively dissolved from alite; its adsorption on the silica surface lowers the calcium ion concentration in the liquid phase, and the hydration of alite in the early age is accelerated. At the same time, the $CaSO_4$ content is also lowered and the hydration of the interstitial phases of C_3A and C_4AF are, therefore, accelerated. C-S-H formation by pozzolanic reaction is initiated at around ten hours, and it progresses in the period at 1–7 days. C-S-H with a low C/S ratio is produced, and the amount of $Ca(OH)_2$ remaining in the hardened paste is decreased.

3.4 Hydration of Cement with Colloidal Silica; Cembinder

Cembinders are aqueous silicic acid suspensions. They contain silicic acid particles expressed as silica in the range of about 8% to 60% silica by weight of solution. The specific surface area of the particles is in the range of 50 to about 200 m^2/g. Generally, the aqueous silicic suspension employed includes silicic acid particles which have a wide particle size distribution with the diameter of particles ranging from 5 to 200 nm.

Cembinder reacts chemically with the calcium hydroxide produced during hydration of portland cement and produces C-S-H. The reaction is spontaneous. Thus, its addition increases the early strength of concrete.[7] This reaction is marked by the consumption of calcium hydroxide determined after a particular interval by XRD and thermogravimetric analyses in a mixture of Cembinder™ and portland cement at 0.35 water-to-cement ratio. There is a significant decrease in the peak of calcium hydroxide after one day of hydration. This decreases with the increase in the amount of cembinder and time (Fig. 3.5). Similar observations were made by thermogravemetric analyses (Fig. 3.6), where weight loss between 105–400°C is related to the nonevaporable water representing C-S-H formation, and the weight loss between 400–500°C is related to calcium hydroxide. It is shown that the amount of nonevaporable water increased up to 7 days with a colloidal silica addition. Later, the increase is not substantial (Fig. 3.7). It shows that the reaction slows as most of the calcium hydroxide is already consumed.

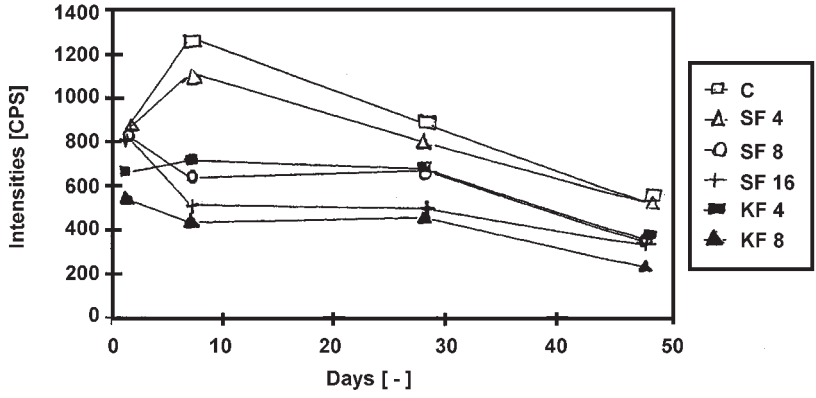

Figure 3.5. Quantity of calcium hydroxide calculated as counts per sec (at $2\theta = 18.10°$) C-Reference, SF4, SF8, and SF16 represents mixtures with 4, 8, and 16% condensed silica fume, and KF4, KF8 - 4 and 8% colloidal silica.[7]

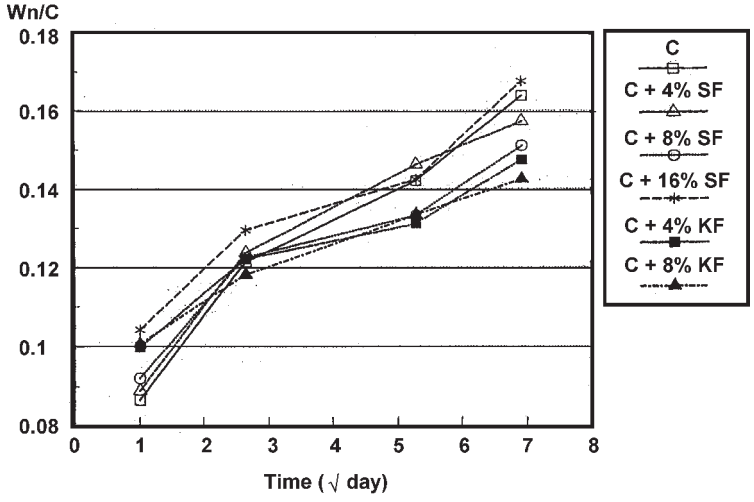

Figure 3.6. Weight loss of cement, between 105–400°C, with respect to time.[7]

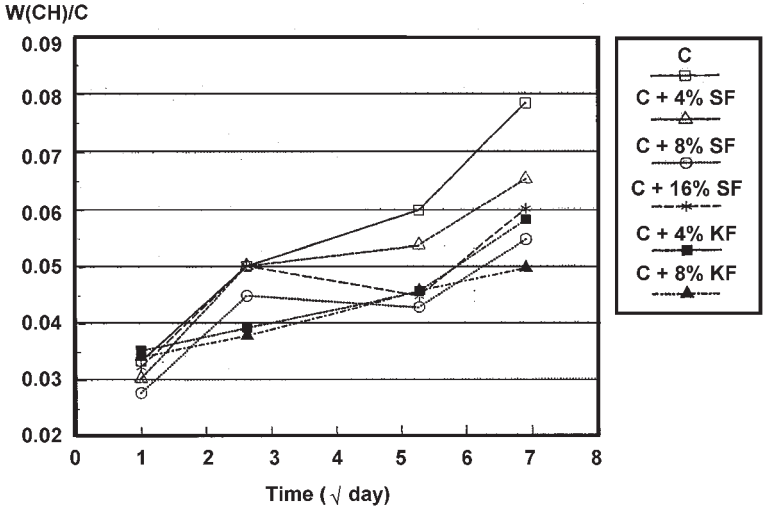

Figure 3.7. Weight loss of cement, between 400–500°C, with respect to time.[7]

Silica fume (SF) and colloidal silica (KF) are mixed with portland cement in a water-to-binder ratio of 0.35. The reactivity was determined by measuring the free CH at a particular interval. Figure 3.5 shows that the amount of CH substantially decreased in all the cases with respect to the reference sample except in the case of 4% SF where the difference is not so very large at seven days. This tendency continued even at the later stage, whereas with the addition of 8 and 16% SF, there is not much of a decrease at one day, but, at a later stage, a substantial decrease in the free CH is observed. In the case of colloidal silica, KF, the amount of free CH is significantly low even after 1 day. A 4% KF addition consumed 60% more CH after seven days than 4% SF. Colloidal silica has shown more reactivity in all the cases. This is attributed to its fine particle size and purity.

4.0 LWAC WITH A MINERAL ADMIXTURE

Swamy and Lixian[21] investigated lightweight aggregate concrete made with sintered fly ash aggregate (Lytag™), and mineral admixtures of fly ash, slag, and silica fume. Their work is reviewed here.

4.1 Details of the Materials Used

All the cementitious materials used in the mixes conformed to their respective BS Codes. The portland cement, ASTM Type I, had a specific surface of 365 m^2/kg, and a total equivalent sodium oxide alkali content of 0.83. The Bogue composition of portland cement consists of C_3S (48.6%), C_2S (23.9%), C_3A (8.5%), and C_4AF (9.1%). The slag had a fineness of 417 m^2/kg while the fineness of the fly ash expressed as the mass proportion of the ash retained on a 45 μm mesh was 7.6%. The silica fume was used in a dispersion form with 50% solid content.

Natural sand, with a fineness grade of 2.04, was used as fine aggregate. The coarse aggregate was the LWA made of sintered fly ash (Lytag™) with a maximum size of 14 mm. The aggregates were initially dried to a constant moisture content of 0.6%. The water absorptions of Lytag™ aggregate after 30 sec., 30 min., and 24 hrs were 9.0, 9.7, and 13.5%, respectively, and an average value of 12% was used for mix design purpose. The composition of the four types of LWAC is shown in Table 3.1, and the strength development in Tables 3.2 and 3.3. The amount of binder is 350 kg/m^3 for all types.

Table 3.1. Mix Proportions of LWAC[21]

No Free	Cement kg/m^3	SF kg/m^3	Slag kg/m^3	PFA kg/m^3	Sand kg/m^3	Lytag™ kg/m^3	W/B
N	350	—	—	—	635	715	0.4
F	300	20	—	30	635	715	0.4
S	300	20	30	—	635	715	0.4
SF	250	10	45	45	635	715	0.4

Table 3.2. Compressive Strength at Different Ages, MPa

Mix No.	Age of Concrete, days						
	1	3	7	28**	28*	180**	180*
N	31.3	36.6	48.0	53.8	59.0	61.1	61.7
F	27.3	34.3	42.8	48.0	53.8	59.9	62.1
S	25.0	39.1	41.7	50.4	55.6	63.2	65.6
SF	17.4	31.3	36.5	46.1	49.2	59.4	56.6
** Wet curing, * Wet/air curing							

Table 3.3. Flexural Strength with Time, MPa

Mix No.	Age of Concrete, days						
	1	3	7	28**	28*	180**	180*
N	4.35	5.01	5.52	5.73	2.97	5.48	5.55
F	3.78	4.96	5.33	5.75	2.60	5.77	5.80
S	4.44	5.11	5.27	5.95	2.91	4.93	5.25
SF	3.49	4.62	4.85	5.43	3.39	5.13	5.36
** Wet curing, * Wet/air curing							

4.2 Strength Properties

The addition of a highly reactive pozzolan, such as silica fume, can compensate for the loss of early age strength as is shown in Tables 3.2 and 3.3. The degree of compensation depends on the type of pozzolan and the mix design technique. Mixes F and S showed 10 and 20% lower compressive strengths at one day. However, at three days and beyond, compressive strength attained the level of the control mix N. These results demonstrate that PFA (pulverized fly ash) and slag had similar effects on the strength development of LWAC both at early and later stages.

A mixture of SF with a lower portland cement content and a relatively larger amount of cement replacement materials (replacement materials 28.6% of total binder compared to 14.3% in mixes F and S) produced 60% lower strength than the control mix N after 1 day, but at 28 days and after six months, nearly the same strength as mixes N, F, and S could be achieved.

Berntsson and Chandra[22] show that for a LWA concrete with 350 kg/m^3 cement and Swedish Leca™ (replacement by 30% slag) compressive strength after one day was 14% and after seven days was 41% of the 28 days strengths. The strengths after 1 day, 7 days, and 28 days were 27%, 43%, and 90% of the strength of concrete with 100% portland cement. This is attributed to the latent hydraulic properties of slag. Replacement with fly ash did not decrease the strength of the concrete. This may be due to the fly ash cement matrix. A 5 and 10% replacement of cement by condensed silica fume did show improvement in strength, but the increase was not significant.

With Liapor™ from Germany (replacement by 30% slag), compressive strength after 1 day was 7% and after seven days was 61% of 28 days. The strengths after 1, 7, and 28 days were 25%, 45%, and 90% of the strength of concrete with 100% portland cement, respectively.

There may be a more effective pozzolanic reaction with Swedish Leca™ compared to the German Liapor™. This may be due to the smooth surface of Swedish Leca™ compared to the rough surface of Liapor™ 5 and 6. The smooth surface contains a more glassy phase compared to the rough surface. This depends upon the sintering process and the temperature used for burning.

These results demonstrate the power of pozzolanic action of mineral admixtures such as PFA and slag, and the importance of mix design techniques to be able to tap and mobilize their ability to contribute to the strength of concrete.

The flexural strength data in Table 3.3 shows that at low replacement levels (14.3% of total binder) the flexural strength is scarcely affected at three days and beyond. The SF mix with 28.6% of the total binder replacement had a lower strength than the other mixes. By 28 days and thereafter, this mix had flexural strength (5.43 MPa) comparable to mixes N, F, and S (5.75 to 5.95 MPa).

The fly ash mix F showed the highest flexural strength at 6 months, compared to all other mixes, and this is considered to be due to the better bond between the fly ash LW aggregate and the fly ash cement matrix, as was reported earlier.[23]

4.3 Elastic Modulus

The elastic modulus of all the concretes containing supplementary cementing materials has a higher dynamic modulus than the portland cement concrete by about 10 to 15%. The F and S concrete mixes had almost the same dynamic modulus at all ages, whereas the SF mix with a lower portland cement content gave a slightly lower value than mixes F and S (Fig. 3.8). Similar results were obtained by Berntsson and Chandra.[22]

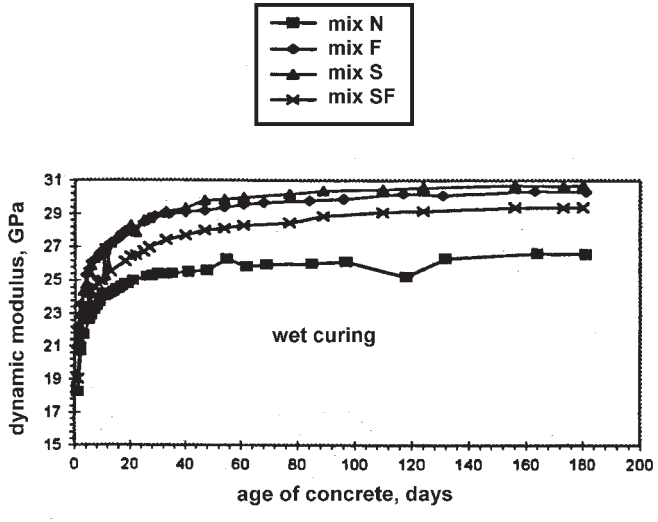

Figure 3.8. Development of elastic modulus with age.[21]

The effects of drying on the dynamic modulus of elasticity for the four concrete mixes show that once drying starts no further increase in dynamic modulus occurs (Fig. 3.9). There is a progressive reduction in the elastic modulus with time, and at six months, all the mixes had about the same value of dynamic modulus from 24 to 25 GPa compared to values of 29 to 31 at the same age for the concretes with mineral admixtures cured in water until the test.

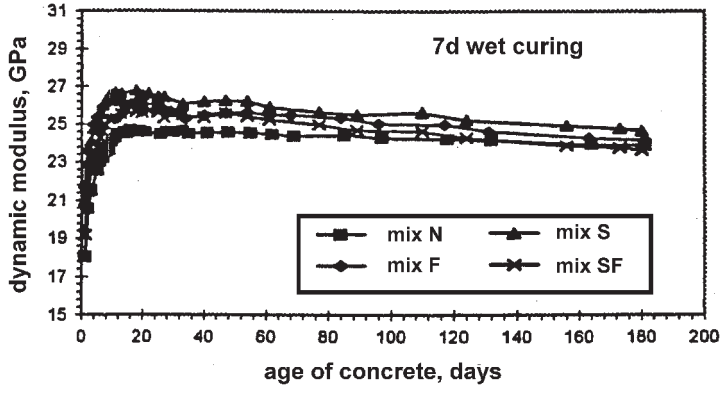

Figure 3.9. Effect of air curing on dynamic modulus.[21]

Two implications are as follows. The contribution to the long-term strength and stiffness of mineral admixtures depends greatly on the conditions that they have to continue their hydration process. In a drying environment, these conditions do not exist. Further, a drying environment prevents concrete with pozzolanic constituents from realizing its full potential and, further, because of the lack of continuing hydration, there is apparently a greater reduction in elastic modulus for these concretes compared to that of portland cement concrete. Whereas air drying has a negligible adverse effect on compressive strength and little long-term loss in flexural strength, the major impact of such environments is on a structural member's stiffness. In other words, structural stiffness is a major casualty, and cannot benefit from the incorporation of mineral admixtures in concrete unless special precautions are taken to ensure that the material is protected from the surrounding drying atmosphere, at least in the early stage of its life, to enable hydration to continue.

The influence of these mineral admixtures is discussed in detail in Ch. 6, hence it will not be discussed here. However, in short, it can be said that all the samples with mineral admixtures have shown a better pore structure than the portland cement mortar under both wet and dry curing conditions, except for the PFA mortar which showed, under the wet/air dry conditions, a slightly higher pore volume and porosity compared to portland cement mortar.

Further, it is confirmed that there is a pore refinement effect with the addition of cement replacement materials compared to that of normal portland cement mortar. This refinement occurs even when the mortar samples were exposed to prolonged air curing.

Fly ash is available in many parts of the world where coal is used in power generation. Apart from its universal availability, one of the unique features of the PFA lightweight aggregate concrete is the excellent aggregate-matrix bond that develops between the fly ash aggregate and portland cement or portland cement fly ash matrix.[23]

It is seen here that, unlike normal weight concrete, the mineral admixtures function somewhat differently. The reaction varies with the type of lightweight aggregates as they have different pozzolanic reactivity on the surface.

5.0 SUPERPLASTICIZERS (SP)

Superplasticizers are surface active agents and have water-reducing characteristics. These are also known as high range water reducers; fluidifiers, plasticizers, etc. This implies that it is possible to produce a concrete with lower water-to-cement ratio with their addition. High performance concrete (HPC) and high strength concrete (HSC) are generally made with high cementitious materials. It causes difficulties in obtaining good workability and homogeneous dispersion of the cementitious material. This problem can be overcome by adding more water. But this decreases the strength. This creates the necessity of using water-reducing admixtures. Concretes made with high cementitious materials and a low water-to-binder ratio may create other problems such as early age cracking because of autogeneous shrinkage. It occurs due to the loss of workability and the very quick drying at the open surface caused by the dual effects of lack of bleeding, and the lack of bleed water to move up to the surface. High

heat of hydration is another major factor causing thermal cracking with high cement content in concrete. It is reported that the addition of slag reduces the temperature rise during hydration. But it does not give early high strength to the concrete. However, a combination of a high range water reducer and a fine ground slag, which significantly improves the strength development, can be a possible solution.[24]

5.1 Influence of Cement Type on Superplasticizing Admixtures

It is now recognized that the superplasticizers behave differently with the same cement and different cements behave differently with the same superplasticizer. The various superplasticizers available are neither equivalent in their chemical characteristics nor in their functional properties. Even if the superplasticizer meets the standard specification, it does not mean that they are the same. The standard specification only defines minimum or maximum values of certain parameters so that a particular superplasticizer may meet the minimum standard, while the other may exceed this minimum specification by a large margin. This is the reason why superplasticizers sometimes work and sometimes they do not.

Superplasticizers behave differently with different cements, and different types of superplasticizers behave differently with the same cement. The difference with the cements mainly depends upon the sulfate and aluminate components in the cement. The type of sulfate in the cement has a major effect on the viscosity and yield. Claisse, et al.,[25] show that the anhydride gives substantially greater yield values than the gypsum. The type of superplasticizer has an influence on the workability of cement paste. For example, sulfonated naphthalene formaldehyde (SNF) condensates make the paste more workable than sulfonated melamine formaldehyde (SMF) condensates followed by lignosulfonates (LS). The influence of variation in the composition of clinker mineral is elaborated by Kinoshita and Okada.[26] They tested cements which varied in the clinker composition, i.e., C_3S, C_2S, C_3A, C_4AF, and in fineness, and tested with the superplasticizers synthesized in the laboratory (Methacrylic Water Soluble Polymers, MSPs). These superplasticizers varied in molecular weight. Comparison was done with a β-naphthalene based polymer. Cements used were low heat portland cement (L1), belite-rich portland cement (L2), ordinary portland cement (N), and early high strength portland cement (H).

Composition of the polymers and concrete are shown in Tables 3.4 and 3.5, respectively.

It has been shown that the apparent saturated adsorption of MSPs was significantly lower than that of NSF, and MSPs, with longer polyethylene graft chains, led to lower adsorption. This may be because MSPs with graft chains form a bulky, stereo-structural layer when adsorbed by cement particles. This is in contrast with the NSF, a copolymer in the shape of stiff chains forming a flatter layer on cement particles. In other words, MSPs are considered to produce strong stearic repulsion (entropy effect), rather than electrostatic repulsion, by being adsorbed by cement particles and forming a barrier, which provides an excellent cement-dispersing capability. It is also shown from the exothermic rate curves of cement pastes made with portland cement and a constant dosage of MSPs that the longer the polyoxyethylene (POE) chain, the weaker the set-retarding effect on hydration.

Table 3.4. Character of Superplasticizer[26]

Mark	**Kind of Superplasticizer**	**Mw[1] of polymer**	**Mw of POE[2] graft chain**	**Graft proportion of POE (%)**
MSP1	Methacrylic water-soluble polymer	37000	1000	240
MSP2	Methacrylic water-soluble polymer	43000	2000	340
MSP3	Methacrylic water-soluble polymer	43200	3000	340
NSF	β-naphthalene based polymer	2500	0	0

[1] weight-average molecular weight; [2] polyoxyethylene

Table 3.5. Mix Proportions of Concrete[26]

Type of Cement	W/B	Slump (cm)	Air Cont. %	Sand/ Coarse Agg. %	Unit Quantity (kg/m^3)					
					Binder			Fine Agg.	Coarse Agg.	
					Water W	Cement C	Silica Fume SF	S	G1	G2
L1	0.50	18	4.5	47.0	170	340	0	842	965	0
	0.35	21	4.5	40.9	170	486	0	684	1005	0
	0.20	65	1.0	41.6	135	608	68	694	0	984
L2	0.20	65	1.0	41.6	135	608	68	694	0	984
N	0.50	18	4.5	46.8	170	340	0	837	965	0
	0.35	21	4.5	40.6	170	486	0	676	1005	0
	0.20	65	1.0	41.6	135	608	67	694	0	984
H	0.50	18	4.5	46.7	170	340	0	837	965	0
	0.35	21	4.5	40.0	170	486	0	676	1005	0
	0.20	65	1.0	41.0	135	606	6	680	984	984

Flow values of cement paste made with normal portland cement and MSPs at W/C ratio 0.30 were similar. But when the W/C decreased to 0.25 and 0.20, the differences between the cement dispersing capabilities of MSPs became significant. Polyoxyethylene with the longest chain showed the highest dispersing capability. Further, it is reported that it needs a lower dosage of MSPs compared to NSF for good cement dispersion. With the use of MSP1 and MSP3, the fluidity of cement L1 was the highest followed by N and H. It was observed that at a W/C = 0.50, the fluidity-retaining capability of polymers with shorter graft chains is higher than that of the polymers with longer chains. However, the differences are narrowed in the range of low W/C ratio. MSPs impart the highest fluidity to low heat cement followed by normal cement and high early-strength cement. In the low W/C range, low heat cement requires a lower dose of MSP than normal cement. This curbs the adiabatic temperature rise of concrete without retardation in setting.

It is concluded that MSP3 and low heat cement used in combination make possible the production of high performance concrete having high fluidity, low heat of hydration, and high strength. Further, it is reported that the incompatibilities of cement/superplasticizers can be overcome by the use of a high molecular weight SP for normal alkali cement.[27] For low alkali cements, the use of a SP having a high residual sulfate content improves the rheology with time and decreases the SP dosage.

The time at which the SPs are added also plays an important role. It has been shown that the difference in the flow of cement paste with sulfonated naphthalene formaldehyde (SNF) or amino sulfonic acid base (AS) between simultaneous addition and later addition was larger than those with polycarboxylic acid base (PC) and lignosulfonate (LS).[28][29] Particularly, the flow of cement paste with SNF added later was larger than that added simultaneously. This increases slump and causes bleeding and segregation problems. This can be overcome by using some thickening agents. For coarsely ground cements having a low C_3A content, a small amount of a viscosity-enhancing agent, such as Welan gum, is recommended to prevent bleeding and segregation in high slump concretes.[30] In such cases, a higher dosage of SP can have better rheological properties.

6.0 CONCLUDING REMARKS

With the growing demand on the strength and durability properties of LWAC, different binder systems have been developed and used. These contained portland cement, fly ash, blast furnace slag, silica fume, and colloidal silica. Some of them are highly reactive pozzolans like silica fume and cembinder which produce material of early high strength. But at later ages, the strength with the addition of all mineral admixtures is of the same magnitude.

A mineral admixture addition to the portland cement-based concrete needs more water to produce the same slump as that of mineral admixtures. This problem is resolved by the addition of high-range water reducers, i.e., superplasticizers.

REFERENCES

1. Zhang, M. H., and Gjörv, O. E., Mechanical Properties of High Strength Lightweight Concrete, *ACI Mater. J.*, 88(3):240–247 (May–Jun. 1991)
2. Zhang, M. H., and Gjörv, O. E., Permeability of High Strength Lightweight Concrete, *ACI Mater. J.*, 88(3):240–247 (May–Jun. 1991)
3. Burge, T. A., *High Strength Lightweight Concrete With Condensed Silica Fume*, Am. Concr. Inst., 2:731–745, ACI Publ. SP 79 (1983)
4. Gjörv, O. E., Tan, K., and Zhang, M. H., Diffusivity of Chlorides from Sea Water into High Strength Lightweight Concrete, *ACI Mater. J.*, 91(5):447–452, (Sep.–Oct. 1994)
5. Roy, D. M., Fly Ash and Silica Fume Chemsitry and Hydration, *Proc. 3rd Int. Con. Fly Ash Slag, Silica Fume, and Natural Pozzolan*, Trondheim, ACI SP 114, 1:119–138 (1989)
6. Scrivener, K. L., The Microstructure of Concrete, *Material Science of Concrete*, (J. P. Skalny, ed.), pp. 127–157, American Ceramic Society (1989)
7. Chandra, S., and Bergqvist, H., Interaction of Colloidal Silica and Portland Cement, *Proc. 10th Int. Conf. on the Chemistry of Cement*, Sweden, (H. Justness, ed.), 3 ii:106–112 (Jun. 2–6, 1997)
8. Larbi, J. A., and Bijen, J. M., *Evolution of Lime and Microstructural Development in Fly Ash Portland System*, 178:127–138, Material Research Society (1990)

9. Yamazaki, K., Fundamental Studies of the Effects of Mineral Fines on the Strength of Concrete, *Transaction Jpn Soc. Civil Engineers,* (85):15–44 (1989)
10. McCartney, G. J., and Tismack, S., Hydration Minerology of Cementitious Coal Combustion by By-products, Advances in Cement and Concrete, *Proc. Eng. Foundation Conf.,* (Gruczeck, and Sarkar, ed.), pp. 103–121 (May 1994)
11. Pietersen, H. S., Reactivity of Fly Ash and Slag in Cement, Report, Delft U. of Techn., The Netherlands (Sep. 1993)
12. Atkins, M., Bennet, D., Dawes, A., Gasser, F. P., Kindness, A., and Read, D., *A Thermodynamic Model for Blended Cements,* Report No. DoE/HMIP/RR/92/005 (Dec. 1991)
13. Feng, Q. L., Lachowski, E. E., and Glasser, F. P., Densification and Migration of Ions in Blast Furnace Slag-Portland Cement Pastes, *Materials Research Society, Symp. 136,* pp. 263–272 (1999)
14. Feng, Q. L., and Glasser, F. P., Mass Transport and Densification of Slag Cement Pastes, *Materials Research Society, Symp. 178,* p. 87 (1990)
15. Grutzeck, M. W., Atkinson, S. D., and Roy, D. M., Mechanism of Hydration of Condensed Silica Fume in Calcium Hydroxide Solutions, *Proc. CANMET/ACI Int. Conf. Use of Fly ash, Silica Fume, Slag and other Mineral By-products in Concrete,* (V. M. Malhotra, ed.), ACI SP 79, pp. 643–669 (1983)
16. Taylor, H. F. W., Chemistry of Cement Hydration, Paper 2.1, *Proc. 8th Int. Con. Chemistry of Cement,* Rio de Janerio, Brazil, 1:82–110 (1986)
17. Diamond, S., Effect of Microsilica (Silica Fume) on the Pore Solution Chemistry of Cement Pastes, *J. Amer. Cer. Soc.,* 66(C):82–84 (1982)
18. Glasser, F. P., Diamond, S., and Roy, D. M., Hydration Reactions in Cement Pastes Incorporating Fly Ash and Other Pozzolanic Materials, *Materials Research Society, Proc. 86,* pp. 139–158 (1987)
19. Roy, D. M., Mechanism of Cement Paste Degradation Due to Chemical and Physical Factors, *Proc. 8th Int. Con. Chemistry of Cement,* Rio de Janerio, Brazil, 1:362–380 (1986)
20. Li, S., Roy, D. M., and Kumar, A., Quantitative Determination of Pozzolans in Hydrated Systems of Cement or $Ca(OH)_2$ with Fly Ash or Silica Fume, *Cem. Conc. Res.,* 15:1079–1086 (1985)
21. Swamy, R. N., and Lixian, W., The Ingredients for High Performance in Structural Lightweight Aggregate Concrete, *Proc. Int. Symp. Structural Lightweight Aggregate Concr.,* Sandefjörd, Norway, pp. 628–639 (Jun. 20–24, 1995)

22. Berntsson, L., and Chandra, S., *Structural Lightweight Aggregate Concrete for Inside House Construction*, Swedish Council of Bldg. Res., Report R 13, (in Swedish), Stockholm, Sweden (1994)

23. Swamy, R. N., and Lambert, G. H., The Microstructure of Lytag™ Aggregate, *The Int. J. Cement Composite and Lightweight Concr.*, 3(4):273–282 (Nov. 1981)

24. Swamy, R. N., The Magic of Synergy: Chemical and Mineral Admixtures for High Performance Concrete, *Proc. Int. Symp. The Role of Admixtures in High Performance Concr.,* Monterrey, Mexico, pp. 3–19 (Mar. 21–26, 1999)

25. Claisse, P. A., Lorimer, P., and Al-Omari, M. H., The Effect of Changes on the Properties of Cement Grouts with Superplasticizing Admixtures, *Proc. Int. Symp., The Role of Admixtures in High Performance Concr.,* Monterrey, Mexico, (J. G. Cabrera and P. Rivera-Villareal, eds.), pp. 19–33 (Mar. 21–26, 1999)

26. Kinoshita, M., and Okada, K., Performance of Methacrylate Water-soluble Graft Polymers with Different Types of Cements, *Proc. Int. Symp., The Role of Admixtures in High Performance Concr.,* Monterrey, Mexico, (J. G. Cabrera and P. Rivera-Villareal, eds.), pp. 34–47 (Mar. 21–26, 1999)

27. Page, M., Nkinamubanzi, P. C., and Aitcin, P. C., The Cement/ Superplasticizer Compatibility Headache for Superplasticizer Manufacturers, *Proc. Int. Symp. The Role of Admixtures in High Performance Concr.,* Monterrey, Mexico, (J. G. Cabrera and P. Rivera-Villareal, eds.), pp. 48–55 (Mar. 21–26, 1999)

28. Uchikawa, H., Sawaki, D., and Hanehara, S., Influence of Kind and Added Timing of Organic Admixture on Composition, Structure, and Property of Fresh Cement Paste, *Cement and Concrete Research,* 25:353–364 (1995)

29. Uchikawa, H., Function of Organic Admixture Supporting High Performance Concrete, *Proc. Int. Symp., The Role of Admixtures in High Performance Concr.*, Monterrey, Mexico, (J. G. Cabrera and P. Rivera-Villareal, eds.), pp. 69–96 (Mar. 21–26, 1999)

30. Ambroise, A., Chabannet, M., Rols, S., and Pera, J., Basic Properties and Effects of Starch on Self Leveling Concrete, *Proc. Int. Symp., The Role of Admixtures in High Performance Concr.,* Monterrey, Mexico, (J. G. Cabrera and P. Rivera-Villareal, eds.), pp. 377–386 (Mar. 21–26, 1999)

4

Mix Proportioning

1.0 INTRODUCTION

There are many ways to produce lightweight concrete. Of these, three main types can be identified. The first type is lightweight aggregate concrete with monolithic structure in which the lightweight aggregate is used instead of normal weight aggregate. The concrete may be used as structural concrete and non-load bearing concrete for heat insulation purposes. The second method relies on introducing large voids within the concrete mass and is known as aerated, foamed, or gas concrete. There are examples where lightweight aggregate has also been added to such mixes. The third type of low-density concrete is formed by omitting the fine aggregate, causing a large number of interstitial voids. Generally, coarse aggregate of normal density is used, but lightweight aggregate gives considerably reduced weight and better heat-insulation properties. This concrete is described as *no-fines concrete.*

A classification of lightweight aggregate concrete can be based on the density of the concrete. There may be a relation between the density and the compressive strength of lightweight aggregate concrete. A low density concrete has low strength and a high density often has high strength. Structural lightweight aggregate concrete normally has compressive strength from at least 10 to 70 MPa.

2.0 MIX PROPORTIONING OF NO-FINES LWAC

The no-fines concrete of lightweight aggregate normally is composed of coarse lightweight aggregate of fraction from 4 mm and upwards, for example, 4 to 8 or 10 mm. For no-fines, the fine aggregate is omitted and the concrete consists of cement, water, and coarse aggregate only. Quite often, there is an addition of a mineral admixture such as fly ash or slag and a small addition of filler or fine sand to the binder paste, mostly for economical and technical reasons.

No-fines concrete is a lightweight aggregate in bulk with the particles surrounded by a coating of cement paste or binder or mortar. The thickness may be about one millimeter and sometimes a little more; for that reason, large voids exist between the aggregate particles. When graded aggregate is used, a higher bulk density results compared to a one-size aggregate. The volume of voids is decreased, resulting in higher strength and thermal conductivity.

There are differences between rounded or spherical-shaped aggregate particles compared to sharp-edged crushed particles. Local crushing may take place at contact points of small areas, which lowers the strength of the concrete. Crushed aggregate does not have the dense particle surface layer as do industrial burned types.

The bulk density, in kg/m^3, of the fresh and compacted no-fines concrete is simply calculated as the sum of the bulk density of the compacted aggregate, the cement content, the water added, and the eventual addition of other fine particles, such as pozzolan, filler, or fine sand. The formula for bulk density of the fresh concrete can be written as:

Eq. (1) $$\gamma_{con} = (1+p)\gamma_A + C + W + m_{ma} \qquad (kg/m^3)$$

where p is the compaction degree of the concrete or the increase in the bulk density of the lightweight aggregate, γ_A is the bulk density of the loose aggregate, C is the cement content in kg/m^3, W is the added water content in kg/m^3, and m_{ma} is the amount of the other fine and dry particle addition in kg/m^3.

After proper storing and hardening, the bulk density and the compressive strength can be tested. The bulk density of the concrete should be calculated after drying at 105°C until a constant weight is attained. The bulk density of the dried concrete can be calculated as:

Eq. (2) $\gamma_{dry} = \gamma_{Adry} + C + W_n + m_{ma}$ (kg/m^3)

where γ_{Adry} is the bulk density of the dry, compacted lightweight aggregate and W_n is the chemically bound water after the hydration of the cement which is equal to the non-evaporable water.

The chemically bound water may be expressed as:

Eq. (3) $W_n = \alpha\ 0.25\ C$ (kg/m^3)

where α is the hydration degree which may be in the range of 0.7–0.8 after 28 days hydration in room temperature.

The compressive strength of the no-fines lightweight aggregate concrete varies according to the strength of the lightweight particles which, in turn, depends on the type or origin of the aggregate and the particle density, the compaction degree or the bulk density and the cement content. The water-to-cement ratio is not the main controling factor, and there is quite a narrow optimum water-to-cement ratio for any given aggregate or aggregate combination. A water-to-cement ratio higher than optimum would result in the cement paste draining away from the surface of the aggregate particles during compaction load and vibration. Too low a water-to-cement ratio would result in insufficient adhesive particle agglomeration. The actual compressive strength has to be determined by a normal compression test. It is better to use a trial test method than to create a theoretical method of proportioning that is based on the desired compressive strength.

It is not possible to propose an optimum water-to-cement ratio in advance, since it is affected by the water absorption of the aggregate and the existing water content of the aggregate. It is, therefore, recommended that a simple calculation for a trial mix composition be made. The following assumptions may be considered for calculation.

For 1 m^3 compacted concrete, p% of extra bulk volume of loosely compacted lightweight aggregate is needed because of the degree of compaction of the concrete. For example, assume p is 10% of the fraction 4–8 mm with the mean diameter d_{mean} = 5.6 mm and the particle density and bulk density of the lightweight aggregate are 584 and 318 kg/m^3, respectively.

The volume of aggregate particles (V_a) in 1 m^3 compacted concrete is:

$$V_a = 1.1 \times 318/584 = 0.599\ m^3$$

The ratio of bulk density and particle density is the volume of particles in 1 m^3 of loosely packed aggregate.

For *t* mm mean thickness of cement paste or mortar covering all the surfaces of the aggregate particles, the volume of cement paste or mortar, (assuming that the particles are spheres) will be:

Eq. (4) $$V_{pm} = 6V_a\, t/d_{mean} \qquad (m^3)$$

Natural aggregate particles are not spheres so the surface area is multiplied by a factor. For rounded particles, the factor is 1.1. Thus, with t = 0.25 mm, the volume of cement paste is:

$$V_{pm} = 1.1 \times 6 \times 0.599 \times 0.25/5.6 = 0.176\ m^3$$

In this case, fine sand (<0.25 mm) is added in the same volume as the cement to the mortar in order to stabilize the fresh structure of concrete and increase its strength. The volume of cement mortar can be expressed as the sum of cement, fine sand, and water as follows:

Eq. (5) $$V_{pm} = C/\rho_c + C/\rho_c + (W/C)\ C/\rho_w \qquad (m^3)$$

where ρ_c = 3200 kg/m^3 is the density of the cement and ρ_w = 1000 kg/m^3 is the density of the water.

Assuming that the effective water-to-cement ratio is 0.5, the cement content is calculated from:

$$0.176 = C \times (2/3200 + 0.5/1000)$$

$$C = 0.176\ /[(2/3200) + (0.5/1000)] = 156\ kg/m^3$$

$$W = (W/C)\ C = 0.5 \times 156 = 78\ kg/m^3$$

It is necessary to pre-soak dry aggregate. In practice, it is done by adding the water in the mixer before adding the other components. Assume that 15% by weight of the dry aggregate is added. The absorbed water content is:

$$0.15 \times 1.1 \times 318 = 52\ kg/m^3$$

The fresh density of the compacted concrete will be

$$156 + 78 + 156 \times 2600/3200 + 0.599 \times 584 + 52 = 799\ kg/m^3$$

where 2600 kg/m^3 is the particle density of the fine sand. The dry density will be:

$$156 + 0.7 \times 0.25 \times 156 + 127 + 349 = 659 \text{ kg/m}^3$$

The compressive strength, as well as thermal conductivity, are functions of density. If it is necessary to increase the strength of the concrete, normally the density must be increased. Consequently, the thermal conductivity will also be increased by about 0.03 W/(mK) for every 100 kg/m^3 increase of the dry density.

The increase in strength can be done in many ways, for example, by exchange for a lightweight aggregate of higher density and strength, by the addition of another fraction of lightweight aggregate of a smaller size, by adding fine normal sand or filler, and by adding more cement or mineral admixture.

The mechanism of strength development in the concrete involves the size of the contact area between particles. This area will be increased by the layer of paste or mortar around the particles so that the strength of the concrete reaches the strength of the lightweight particles themselves.

3.0 MIX PROPORTIONING OF STRUCTURAL LIGHTWEIGHT AGGREGATE CONCRETE

The aim of mix proportioning of the concrete is to present a formula or a recipe according to specifications. The procedure for proportioning is to combine different concrete ingredients based on their properties to attain the required properties of the fresh, as well as the hardened concrete. The properties for the concrete are chosen from the structural design and the requirements of safe and functional structures.

The requirements are mostly technical in nature, such as consistency, workability, compressive strength, density, freeze-thaw resistance, water permeability, thermal conductivity, and, not least, the service life of the structure. In many cases, there are requirements which are implicit and expected of good quality concrete, i.e., stability against segregation of aggregate, insignificant internal water bleeding, homogeneity after transportation, and compaction. Good economy is mostly the driving force of all kinds of concrete structures.

Lightweight aggregate concrete is quite similar to normal weight concrete except that the whole or a part of the aggregate consists of porous particles with density less than natural normal weight aggregate of rock origin, i.e., less than 2000 kg/m^3. In practice, the designation of lightweight concrete is classified according to standardized strength and density classes.

Structural lightweight aggregate concrete has a closed structure which means that all voids between the aggregate particles are filled with a binder component or cement paste. The surfaces of the aggregate particles have to transfer the distributed stresses from the surrounding binder. This is not the case in concrete with open structure or no-fines concrete where the internal stresses are concentrated at discrete contact points on aggregate particles.

The production procedure of lightweight aggregate concrete may often be more complicated than normal weight concrete. For example, it is necessary to take into consideration the water absorption of the porous aggregate from the fresh cement paste and that the lightweight aggregate particles have a lower density than the surrounding matrix, i.e., the cement paste. The absorption of water in the aggregate results in an increasing stiffness of the fresh concrete with time; the aggregate particles of low density may segregate by flowing to the upper surface of the concrete. Varying the density of the particles will also change the density and the strength of the concrete.

Particle density and water content may normally vary from time to time for different reasons. However, the properties of the lightweight aggregate concrete need to be based on oven-dried concrete and all the concrete ingredients. It will facilitate the whole analysis.

For practical reasons, the consistency or workability and the density of the freshly compacted concrete will reveal if the proportion of the concrete ingredients and their properties are as expected. If not, it may be necessary to analyze the recipe and make proper corrections for a new trial mix.

3.1 Basic Steps of Mix Proportioning

The concrete is regarded as a composite material. To simplify the procedure of proportioning, the ingredients are restricted to two main components, namely the binder and particles or, rather, cement mortar and coarse aggregate particles. The two main components are assumed to fully interact with each other.

The steps of the proportioning procedure and what is needed for the calculation are described below.

The Requirements of Concrete.

- Compressive strength and density of the hardened concrete for the design of the structure.
- Consistency or workability for production purposes and entrained air volume.

Other properties may be required for any specific application such as frost resistance, water impermeability, and the rate of chloride diffusion. For design work, formulas exist that are used, such as for tensile strength and the modulus of elasticity, based on density and compressive strength.

The Ingredients of Concrete.

- Binder, for example, type of cement and mineral admixture, i.e., silica fume, fly ash, and slag.
- Fine and coarse aggregate and its properties such as particle size distribution by sieve analysis, bulk density, and particle density of the lightweight aggregate, water content, and, eventually, water absorption.
- Chemical admixtures, such as plasticizers and air-entraining agents.

Combined Aggregate Particle Size Distribution Curve. The size distribution curve shall be constructed on the volume of particle density, and, for that reason, the particle density of the different size or fraction should be known. The combined particle size distribution curve is a modified Fuller's curve for continuous particle size distribution according to the formula:

Eq. (6) $$p = (d/D)^n$$

where p is the volume passing through a sieve of size d mm, D is the maximum size of the particles, and n is according to Table 4.1.

Mean Value of the Particle Density of the Lightweight Aggregate and Its Compressive Strength. The strength of the lightweight aggregate particle may be calculated using the empirical formula (Eq. 8) in which the particle density is needed.

Table 4.1. Exponent Coefficient According to the Fuller's Formula

Sieve mm	*n*
0.125	0.70
0.25	0.65
0.50	0.60
1	0.55
≥2	0.50

The Compressive Strength of the Mortar. The strength of the concrete is a function of the volume and strength of the mortar in the concrete and of the strength of the lightweight aggregate. The relation between the strength and the volume is shown in Fig. 4.1. The volume of lightweight aggregate particles of 2–12 mm size should be in the range of 40 ± 5% by volume. The water/cement ratio or water/binder ratio for the mortar is calculated according to the formula in Eq. (11a). The bulk density of the mortar is also needed for proportioning.

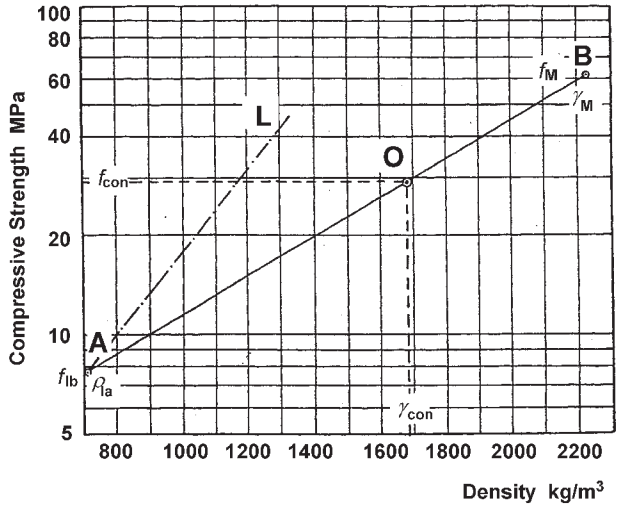

Figure 4.1. Diagram showing the relationships of density and compressive strength of lightweight aggregate, mortar, and concrete. The line *AL* describes the relationship between the density and strength of lightweight aggregate and point *B* represents the mortar. Point *O* is the density and strength of the lightweight aggregate concrete.

Volume of Cement Paste and Cement Content. The volume of cement paste or binder normally should be in the range of 0.28–0.35 m^3 for 1 m^3 concrete. The volume depends on the air volume and the strength. The cement content is calculated from the known volume and the water/cement ratio.

Consistency. The volume and the rheology properties of the cement paste influence mainly the consistency or the workability of the concrete. Even the water absorption of the lightweight aggregate should be taken into consideration, especially the change of the consistency with time. The consistency or workability may be measured by a slump test, flow table test, or another test which is suitable for lightweight aggregate concrete. During a flow table test, it is even possible to estimate the segregation stability.

Preliminary Mix. The amounts of the concrete ingredients are summarized and specified in weight as well as in volume for 1 m^3 of compacted concrete. It is preferable to add lightweight aggregates to the mixer by bulk volumes instead of by weight in case the density varies.

Trial Mix. The first mix of a new composition is a trial mix and the fresh density and consistency is tested. If the density differs too much from the calculated value, the composition is checked to see if there is any reason for the divergence in the calculation or properties of the ingredients. After that, it might be necessary to revise the composition of the concrete. Normally, the water absorption of the lightweight aggregate may cause a divergence of the density and the consistency. Too stiff a concrete mix needs a suitable plasticizer. More trial mixes are done until fresh concrete with the required properties is obtained. The preliminary testing procedure is followed by production of cylinders or cubes as specimens for testing, mainly for density and compressive strength after hardening.

Final Mix. The density and the compressive strength are tested at 28 days according to the existing standards. After testing, the specimens are dried to equilibrium in weight at 105°C, and the oven-dry density is calculated and noted, as well as the density of the fresh concrete and the density after storage.

3.2 Procedure of Proportioning

The procedure for calculating the composition of concrete with compressive strengths from about 10 to 40 MPa using different types of lightweight aggregates is given here. An example is also given showing how

to analyze concrete composition of up to 70 MPa or more of compressive strength. It should be emphasized that the density and the strength of the lightweight aggregate are related to the density and strength of the concrete. There are limitations in the selection of lightweight aggregates for producing concrete defined by its density and strength. For example, using a lightweight aggregate of low density and low strength to develop a concrete of high strength goes beyond the capabilities of the aggregate. The reverse is also true—a high density and strength aggregate should not be used to create a concrete of low density and low strength. Producing low-density concrete is possible by adding an air-entraining agent to create and attain a fixed volume of air bubbles. However, it is more advantageous to have air bubbles in the aggregate particles than in the cement paste.

3.3 Properties and Volume of Components and their Relations to the Properties of Concrete

Mean Compressive Strength of Concrete. The compressive strength may satisfy the following conditions:

Eq. (7) $$m \geq f_{ck} + \lambda \times s_n$$

where m is the mean strength of the set of samples

s_n is the standard deviation of the set of strength results from the samples

f_{ck} is the specific characteristic strength of the concrete

λ is a factor depending on the number of samples in the set of statistical analysis

The coefficient of variation is approximately 5–10% for the strength and 3–5% for the density. Standard deviation is the coefficient multiplied by the mean strength.

The Strength of the Lightweight Aggregate Particles. The recommendation is to design the concrete mortar with a compressive strength double that of the value of the strength of the lightweight aggregate. The mean compressive strength of the lightweight aggregate is calculated using the formula:

Eq. (8) $$f_{la} = a \cdot 10^{b\rho\,/1000}$$

where a and b are coefficients according to Table 4.2 and ρ is the particle density in kg/m^3.

For all types of lightweight aggregate, natural or factory produced, there are different relationships between the strength of the lightweight particles and the particle density. There are special methods to measure the particle strength of the aggregate. Because the particles interact with the surrounding matrix, the cement paste or mortar, the method is based on estimating the strength in concrete. The results are then used to evaluate coefficients a and b in Eq. (8).

The relationships among the strength of the mortar, the strength of the lightweight aggregate, the strength of the concrete, and the volume of the mortar or volume of the lightweight aggregate are calculated using:

Eq. (9a) $$\log f_{con} = v_{la} \cdot \log f_{la} + v_M \cdot \log f_M$$

or

Eq. (9b) $$\log f_M = (\log f_{con} - v_{la} \cdot \log f_{la})/(1 - v_{la})$$

where f_{con} is the strength of concrete
f_M is the strength of mortar
f_{la} is the strength of lightweight aggregate
v_{la} is the volume of the lightweight aggregate particles
v_M is the volume of mortar

Table 4.2. Coefficients a and b in Eq. (8)

Aggregate No.	*a*	*b*
1	1.52	1.14 (1.08, 1.03)
2	1.12	1.22 (1.16, 1.11)
3	1.00	1.25 (1.15, 1.14)
4	0.89	1.28 (1.22, 1.17)

In parenthesis, the value of b is for 5 and 10% water content in the aggregate. The value of b is not or is marginally influenced by the water content. Aggregate no.3 is for the bulk density of 300 kg/m^3. The lightweight aggregate is some type of high quality sintered clay. Other lightweight aggregates may have other values and shall be provided after the test.

The Compressive Strength of Mortar. The compressive strength of mortar can be calculated from Eq. (10). Here natural sand and ordinary portland cement are assumed to be used, and the specimens for mortar testing are of the same type and size as used for the testing of concrete.

Eq. (10) $f_M = A \cdot 10^{-B \cdot W/C}$

where A and B are experimentally evaluated coefficients.

With $A = 140$ and $B = 0.87$ (ordinary portland cement after 28 days and W/C or W/binder > 0.30), the compressive strength is:

$$f_M = 140 \cdot 10^{-0.87 \cdot W/C}$$

or

Eq. (11a) $W/C = \log(140/f_M)/0.87$

When W/C is >0.20 and <0.25, the following formula may be used:

Eq. (11b) $f_M = 160 \cdot 10^{-0.87 \cdot W/C}$

When W/C is between 0.25 and 0.30, A is to be interpolated.

According to accepted definition, the water/cement ratio is:

$$W/C = W \cdot 10^3/C$$

where W is the water content in m^3/m^3 and C is the cement content in kg/m^3. The formulae are valid for natural sand, not for lightweight sand, and for a water/cement ratio less than 0.8.

Sometimes air is entrained in the concrete, for example, if salt-frost resistance is required. In this case, Eq. (11a) is changed to

Eq. (11c) $W_a = \log(176/f_M)$

where W_a is defined as $(W + V_l) \cdot 10^3/C$; V_l is the volume of entrained air in m^3/m^3. The air volume shall not exceed 10% of the volume of concrete.

The Volume of Cement Paste. The volume of cement paste or binder in concrete should adhere to the principle of a constant paste-aggregate volume and should be about 30% of the volume of concrete. The volume of cement paste depends on many factors, for example, the type and shape of aggregate, consistency, stability of the concrete mixture, the strength of the mortar or concrete, and water absorption of the lightweight aggregate. According to the experience even from normal weight concretes, the volume of cement paste or binder may be in the range of 30 ± 2%. In some cases, especially for a very high strength concrete in which silica fume is added, the volume of the binder can reach up to 34%. Air-entrained concrete also influences the volume of cement paste: the small air bubble system changes the rheological properties of the fresh concrete and positively improves the workability.

Cement Content. The cement content is calculated using the formula:

Eq. (12) $$C = 1000 \cdot v_p/(0.31 + W/C)\ kg/m^3$$

where v_p is the volume of cement paste in concrete.

The Volume of Sand. The volume of sand is calculated from the formula:

Eq. (13) $$v_s = 1 - (v_p + v_{la} + v_{air})$$

where v_{la} is the volume of lightweight aggregate and v_{air} is the volume of air in the concrete. Normally, the air volume is 1.5–2% of the volume of concrete. For air-entrained concrete, the total air volume, as measured or calculated, is used in the formula.

The Bulk Density of the Concrete. The density of the concrete can be obtained by adding all the amounts of the ingredients in 1 m^3 of compacted concrete or may be calculated according to the formula:

Eq. (14a) $$\gamma_{con} = v_{la} \cdot \gamma_{la} + \gamma_M \cdot (1 - v_{lb})$$

or

Eq. (14b) $$\gamma_{con} = v_{la} \cdot \gamma_{la} + v_M \cdot \gamma_M$$

where γ_{con} is the bulk density of concrete

γ_{la} is the mean particle density of the lightweight aggregate

γ_M is the density of mortar

3.4 Examples of Calculations

The following calculations are examples of the proportioning method and may be used for specific requirements.

Example I. Lightweight aggregate concrete, strength class 25 MPa (LC25) and density class 1.6 (oven-dry density 1400–1600 kg/m^3), the mean bulk density of the aggregate is 500 kg/m^3 and particle density is 920 kg/m^3.

a. The mean compressive strength is calculated using Eq. (7).

$$m \geq f_{ck} + \lambda \cdot s_n$$

$m \geq 25 + 1.48 \cdot 0.07 \cdot m$

Standard deviation (s_n) is 7% and λ is 1.48 according to the number of samples in the set.

$m \geq 27.9$ MPa, i.e., 28 MPa

b. The strength of the lightweight aggregate particles is calculated from Eq. (8) using $a = 1.12$ and $b = 1.22$:

$f_{la} = a \cdot 10^{b\rho/1000} = 1.12 \times 10^{1.22 \times 920/1000} = 14.9$ MPa

c. The strength of the mortar

Equation (9b) is used to calculate the compressive strength of the mortar. The volume of the lightweight aggregate particles is chosen to be 40% (v_{la})

$\log f_M = (\log 28 - 0.40 \times \log 14.9)/(1 - 0.40) = 1.63$

$f_M = 42.6$ MPa

d. Water/cement ratio

Calculate the water/cement ratio using Eq. (11a).

$W/C = \log(140/f_M)/0.87 = \log(140/42.6)/0.87 = 0.59$

e. Volume of cement paste

The volume of the cement paste is chosen to be 0.30 (v_p)

f. Cement content

The cement content is calculated from Eq. (12)

$C = 1000 \cdot v_p/(0.31 + W/C) = 1000 \times 0.30/(0.31 + 0.59) = 333$ kg/m^3

g. Volume and weight of natural sand

The volume of sand is according to Eq. (13)

$v_s = 1 - (v_p + v_{la} + v_{air}) = 1 - (0.30 + 0.40 + 0.02) = 0.28$

The weight of natural sand is $0.28 \times 2650 = 742$ kg/m^3

h. Volume and weight of the lightweight aggregate

Volume of lightweight particle = 0.40 m^3/m^3

Weight of lightweight particle = $920 \times 0.40 = 368$ kg/m^3

Bulk volume of lightweight aggregate = $0.40 \times 920/500 = 0.736$ m^3/m^3

Water absorption, 3% of 368 kg dry aggregate = $0.03 \times 368 = 11$ kg/m^3

i. The composition of the concrete

In 1 m^3 of compacted concrete (dry materials) the composition is as follows:

Ingredients	**Weight (kg)**	**Volume (m^3)**
Ordinary PC	333	0.104
Eff. water 0.59×333	196	0.196
Absorbed water	11	——
Natural sand	742	0.280
Lightweight agg.	368	0.400*
Air		0.020
* 0.736 m^3 in loose bulk volume		

The water absorption of the lightweight aggregate particles from the cement paste in the fresh concrete is normally 75 to 100% of the absorption in pure water. For many lightweight aggregates, the water is absorbed very quickly during the first few minutes of contact with water. Thus, it might not be wrong to assume the same values for the free absorption in water during 30 minutes or sometimes up to 1 hour.

The density of the fresh compacted concrete should be 1650 kg/m^3.

During 28 days, the hydration degree, α, is deemed to be 0.7. The chemically bound water is calculated by $W_n = \alpha\, 0.25°C = 0.7 \times 0.25 \times 333 = 58$ kg/m^3. When 100% of the cement is hydrated $\alpha = 1.0$.

The density of the oven-dried concrete is the sum of the dry materials plus the chemically bound water. The oven-dry density will then be 1506 kg/m^3.

When the natural sand is replaced by lightweight sand, the density of the concrete is decreased. However, it is not necessary to change the whole part of natural sand, for example, half of the sand may be sufficient.

In the recipe above, all the natural sand is replaced with lightweight sand, size 0–4 mm, bulk density of 700 kg/m^3 and mean particle density of 1500 kg/m^3. The water absorption in the lightweight sand will be $0.03 \times 0.28 \times 1500 = 13$ kg/m^3. The weight of the lightweight sand is $0.28 \times 1500 = 420$ kg/m^3 instead of 742 kg/m^3 of natural sand. The mix proportions will be as follows:

Ingredients	Weight (kg)	Volume (m^3)
Ordinary PC	337	0.104
Eff. water 0.58 × 337	196	0.196
Absorbed water	24	——
Lightweight sand	420	0.280
Lightweight agg.	368	0.400*
Air		0.020
* 0.736 in loose bulk volume		

The density of the fresh concrete is 1341 kg/m^3 and the oven-dry density is 1179 kg/m^3. The strength of the concrete is insignificantly influenced by the lightweight sand, if any.

The consistency of the concrete with lightweight sand will generally be stiffer compared to concrete with natural sand. A superplasticizer may normally be added, sometimes in combination with an air-entraining agent. An increase of 1% air volume is equivalent to 5–6 liters per m^3 concrete of added water for the same consistency.

The principle of proportioning with regard to strength and density may be easy to grasp in a diagram in which the compressive strength is plotted as a function of the density, see Fig. 4.1. Point *A* represents the mean strength (7.7 MPa) and the mean particle density (710 kg/m^3) of the lightweight aggregate, and point *B*, a strength of (61 MPa) and the density (2230 kg/m^3) of the mortar. Point *O* is the location based on the composition of the concrete, namely the density (1683 kg/m^3) and strength (29 MPa). The length *AB* is divided into two parts according to the volume of mortar and volume of lightweight aggregate as follows:

$$AO/AB = v_M = 1 - v_{la} \text{ and } BO/AB = v_{la}$$

The line *AL* is obtained according to Eq. (8) and aggregate no. 3 in Table 4.2. The line *AB* is represented by the equation

$$\log f_{con} = 5.91 \times 10^{-4} \times \gamma_{con} + 0.4668$$

where f_{con} is the compressive strength of the concrete in MPa and γ_{con} is the density of the fresh concrete.

Example II. Proportioning of LWAC of 40 MPa Cube Compressive Strength (LC40) with 6% Entrained Air. The mean compressive strength at 28 days shall not be less than 45 MPa. The available lightweight aggregate has a particle density of 1100 kg/m^3 and a bulk density of 600 kg/m^3 and the strength of the aggregate is 26 MPa. It is convenient to start the procedure to find the composition of concrete without entrained air and add 5–10% silica fume to the weight of portland cement. In this example, it is convenient to use 7% silica fume. The object of adding silica fume is to increase the strength of the binder and avoid excessive heat development during the hydration process. This works because of the pozzolanic reactivity and dilution effect of silica fume, respectively. The proportioning with the same procedure as in the previous calculation resulted in a composition without entrained air as follows:

Ingredients	Weight (kg)	Volume (m^3)
Portland cement	394	0.123
Silica fume	28	0.013
Natural sand	723	0.273
Added water	184	0.171
Absorbed water	13	——
Lightweight agg.	440	0.400*
Air	—	0.020
* 0.736 in loose bulk volume		

The density of the fresh concrete is 1782 kg/m^3. During the mixing, air voids will be created after adding an air-entraining agent. At the same time, the consistency will be changed. A 1% increase in air volume has the same effect on the consistency as adding about 0.005 m^3/m^3 of water. Correction by addition of water shall be done in excess of the normal air volume, normally 2%. Air voids will also decrease the strength of the concrete. The water/cement (binder) ratio will be constant after air entrainment and the air volume to be added to the volume of water, is:

Eq. (15) $$(v_w + v_{air}) \cdot 1000/(C + \beta \cdot S)$$

The equation is written in order to compensate for the loss of strength because of the increase of air voids. Beta (β) is the factor of efficiency for the mineral admixture, for example, silica fume, and here $\beta = 2$ will be used.

The amount of binder, which is the sum of cement and silica fume, after entrained air is accounted for is:

Eq. (16) $$B_{air} = B_0 \left[(v_0 - \Delta v_{wa} + v_{air})/(v_0 + v_{0air})\right]$$

where B_0 is the weight of the binder without entrained air,

v_0 is the volume of effective water without entrained air,

Δv_{wa} is the volume of water reduction keeping a constant consistency,

v_{air} is the total volume of air in the air-entrained concrete,

v_{0air} is the volume of air in concrete without entrained air.

Calculate the amount of binder as shown below:

$$B_{air} = (394 + 2 \times 28)[(0.171 - 4 \times 0.005 + 0.060)/(0.171 + 0.020)] = 497 \text{ kg/m}^3$$

The cement content is calculated from the weight of the binder, which is the sum of cement and silica fume. The silica fume is 7% of the weight of cement, but 1 kg silica fume corresponds to 2 kg cement.

$C + 2 \times 0.07 \times C = 497$

$C = 436 \text{ kg/m}^3$

$S = 0.07 \times 436 = 30.5 \text{ kg/m}^3$

The weight of the binder is 466.5 instead of 497 kg/m^3

The water content is $0.171 - 0.005 \times 4 = 0.151 \text{ m}^3/\text{m}^3$

The ratio of volume of water plus air-to-binder is

$(0.151 + 0.060) \cdot 1000/(436 + 2 \times 30.5) = 0.425 \cong 0.43$

The effective water-to-binder ratio is

$0.151 \times 1000/(436 + 2 \times 30.5) = 0.304$

The volume of aggregate, sand, and lightweight aggregate is

$v_{agg} = 1 - (v_C + v_s + v_w + v_{air}) =$

$1 - [(436/3200) + (30.5/2200) + (151/1000) + 0.060]$

$v_{agg} = 0.639 \text{ m}^3/\text{m}^3$

The volume of natural sand is $0.639 - 0.400 = 0.239 \text{ m}^3/\text{m}^3$

The strength of mortar according to Eq. (9b) is

$\log f_M = (\log 45 - 0.40 \times \log 26)/(1 - 0.40)$

v_{la} is 0.40, see Example I(c)

$f_M = 65$ MPa

The ratio of the volume of water plus air to the binder is according to Eq. (11c):

$$\log(176/65) = 0.43$$

and calculated the same way as was done earlier.

The resultant mix is as follows:

Ingredients	Weight (kg)	Volume (m^3)
Portland cement	436	0.136
Silica fume	30.5	0.014
Natural sand	633	0.239
Added water	164	0.151
Absorbed water	13	——
Lightweight agg.	440	0.400*
Air	—	0.060
* 0,736 in loose bulk volume		

The density of the fresh concrete is 1704 kg/m^3 and of the oven-dried concrete is about 1620 kg/m^3. When the test specimens are stored under water from 1 to 28 days, the density of concrete will be about 1730 kg/m^3.

Example III. Proportioning of Extremely Low Weight Structural Lightweight Aggregate Concrete. The compressive strength will be at least 12 MPa and the density of fresh concrete should be about 1200 kg/m^3. Based on experience, the particle density of the lightweight aggregate, size 2–4 mm and 4–10 mm, will be 700 kg/m^3 with the bulk density of 385 kg/m^3 as the mean value. The proportion of the smaller fraction to the larger fraction aggregate particle is 3:2 to 1:1 by volume. Using a lightweight aggregate with a lower density is not advisable for structural concrete. The cement content should not be less than 350 kg/m^3 and the total air volume should be less than 10% of the volume of concrete.

The strength of the lightweight aggregate according to Eq. (8) and Table 4.2 is:

$$f_{la} = 1.00 \cdot 10^{1.25 \times 700/1000} = 7.5 \text{ MPa}$$

In order to obtain a concrete of density of about 1200 kg/m^3, it is necessary to replace a part of the natural sand with an expanded polystyrene particle of size 0.5–2 mm, of particle density 40 kg/m^3, and normally not more than 8% by volume of concrete. These particles have almost no strength and the compressive strength of concrete without polystyrene particles may be

estimated taking into the fact that the compressive strength is reduced by 4% for every volume percent of air bubbles or polystyrene particles added to the concrete. Without polystyrene particles, the compressive strength will be $12/(1–0.04 \times 7) = 16.7$ MPa. The volume of polystyrene particles is 7% in this case.

The first calculation procedure is to design the concrete composition without polystyrene particles or beads. The strength of the mortar is according to Eq. (9b) and Example Ic.

$$\log f_M = (\log 16.7 - 0.40 \times \log 7.5)/(1 - 0.40)$$

$$f_M = 28.5 \text{ MPa}$$

The ratio of the water volume plus air volume-to-cement is calculated according to Eq. (11c):

$$W_a = \log(176/f_M) = \log(176/28.5) = 0.79$$

The volume of cement paste is chosen as $v_p = 0.30$ the cement content is 350 kg/m^3, and the total air volume 0.090 m^3. The volume of water is

$$(v_w + 0.090) \cdot 1000/350 = 0.79$$

$$v_w = 0.187 \text{ m}^3/\text{m}^3$$

The volume of cement paste is

$$v_p = 350/3200 + 187/1000 = 0.30 \text{ m}^3/\text{m}^3$$

The total volume of aggregate is

$$v_{la} = 1 - (v_c + v_w + v_{air})$$

$$v_{la} = 1 - (350/3200 + 187/1000 + 0.090) = 0.614 \text{ m}^3/\text{m}^3$$

and the volume of sand is

$$0.614 - 0.400 = 0.214 \text{ m}^3/\text{m}^3$$

Replace 0.070 m^3 of the natural sand with the same volume of polystyrene particles. The mix proportion is as follows:

Ingredients	Weight (kg)	Volume (m^3)
Portland cement	350	0.109
Natural sand	381	0.144
Polystyrene	3	0.070
Added water	202	0.187
Absorbed water	15	——
Lightweight agg.	280	0.400*
Air	—	0.090
* 0.727 in loose bulk volume		

The strength of concrete without polystyrene, Eq. (9a):

$\log f_{con} = 0.40 \times \log 7.5 + 0.6 \times \log 28.5$ $f_{con} = 16.7$ MPa

The density of the fresh concrete is

$350 + 381 + 3 + 202 + 280 = 1216$ kg/m^3

and the density of the oven-dried concrete is about 1075 kg/m^3.

The strength of the concrete is $16.7 \times 0.72 = 12$ MPa.

The strength can be increased by adding a water-reducing agent.

Example IV. Analysis of High Strength Lightweight Aggregate Concrete. During the last decade, there has been great interest in high strength lightweight aggregate concrete for special applications, for example, in off-shore construction. An analysis is given here of a lightweight aggregate concrete composition, which has a compressive strength of at least 70 MPa.

The lightweight aggregate has a particle density of 1450 kg/m^3 and a bulk density of 800 kg/m^3. The composition is the following:

Ingredients	Weight (kg)	Volume (m^3)
Portland cement	430	0.134
Silica fume	37	0.017
Natural sand	590	0.223
Added water	202	0.174
Absorbed water	28	——
Lightweight agg.	625	0.430*
Superplasticizer	10	0.007
Air	—	0.015
* 0.780 in loose bulk volume		

The volume of mortar is 0.570 m^3/m^3 and the volume of lightweight aggregate is 0.430 m^3/m^3.

The strength of the lightweight aggregate is according to Eq. (8) and Table 4.2

$f_{la} = 1.52 \cdot 10^{1.14 \cdot 1.45} = 68$ MPa

The effective water-to-binder ratio is

$174/(430 + 2 \times 37) = 0.345$

The strength of the mortar is according to Eq. (10)

$f_M = A\ 10^{-BW/C} = 140 \times 10^{-0.87 \times 0.345} = 70$ MPa

With a rapid hardening cement, the compressive strength is multiplied by the factor 1.1, thus the 28 day compressive strength should be $1.1 \times 70 = 77$ MPa.

The compressive strength of the concrete is calculated according to Eq. (9a):

$\log f_{con} = v_{la} \log f_{la} + v_M \log f_M = 0.430 \times \log 68 + 0.570 \times \log 77 = 1.863$

$f_{con} = 73$ MPa

The density of the fresh concrete is 1894 kg/m^3.

Example V. Modifying of the Composition of Concrete. It is a normal procedure to adjust the mix proportion of the concrete composition after one or more trial mixings. The testing is combined with the optimization process, which includes the adjustment of the consistency or workability of the fresh concrete and the strength and the density in the hardened state and several other properties. It is also necessary to analyze the test results in order to find out the strength of the lightweight aggregate in concrete, which may differ from one aggregate to another. For analysis, it may be helpful to use the diagram shown in Fig. 4.1.

Changing the Density and Strength of Mortar. Figure 4.2 shows the result of decreasing the density ($\Delta\gamma_M$) and strength (Δf_M), which means that B moves to B'. The volume of mortar shall also be kept constant and the same lightweight aggregate is to be used. The density of the concrete will be

$$\gamma'_{con} = \gamma_{con} - v_M \cdot \Delta\gamma_M$$

where γ_{con} (kg/m^3) is the density of the concrete before the change, and $\Delta\gamma_M$ (kg/m^3) is the change of the density of mortar. The strength of the concrete after the change is

$$f'_{con} = f_{con} \times (f'_M / f_M)^{v_M}$$

where f'_M (MPa) is the strength of the mortar after the change and $v'_M = v_M$.

Changing the Density of the Lightweight Aggregate. When one type of lightweight aggregate is replaced by another type, for example, one of a higher particle density, or the distribution of the particle size has changed resulting in another mean density, the properties of the concrete will change. In Fig. 4.3, the lightweight aggregate density has been increased as has the strength of the aggregate. The volume of mortar should be kept constant and the same mortar should be used as before the change.

The density of the concrete is

$$\gamma'_{con} = \gamma_{con} + v_{la}\,\Delta\rho$$

where the $\Delta\rho$ is the change of the particle density.

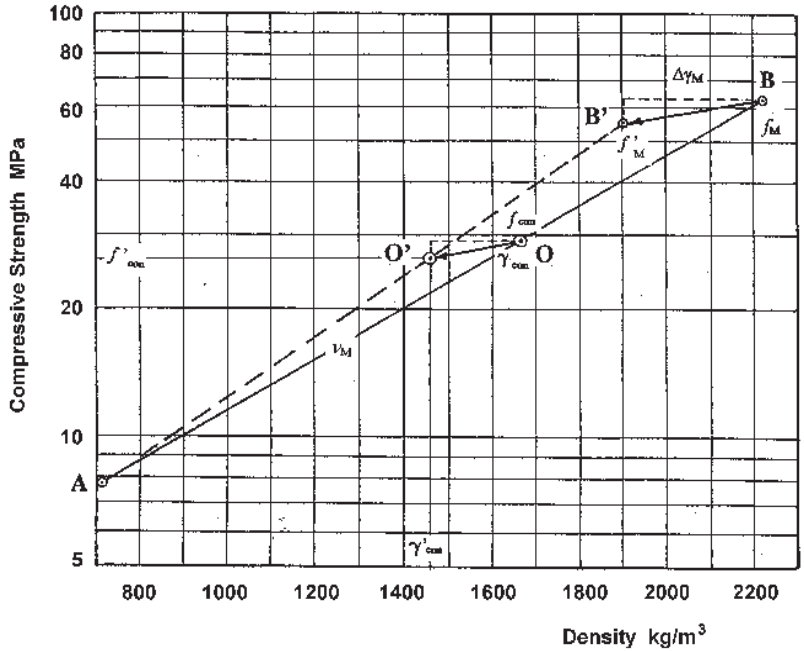

Figure 4.2. The graphic presentation of the density and the compressive strength of the lightweight aggregate concrete by decreasing the density ($\Delta\gamma_M$) and the strength of the mortar. The volume of mortar and lightweight aggregate is kept constant. The density and strength of the concrete will move from Point *O* (density and strength of concrete before the change) to Point *O´*(density and strength after the change).

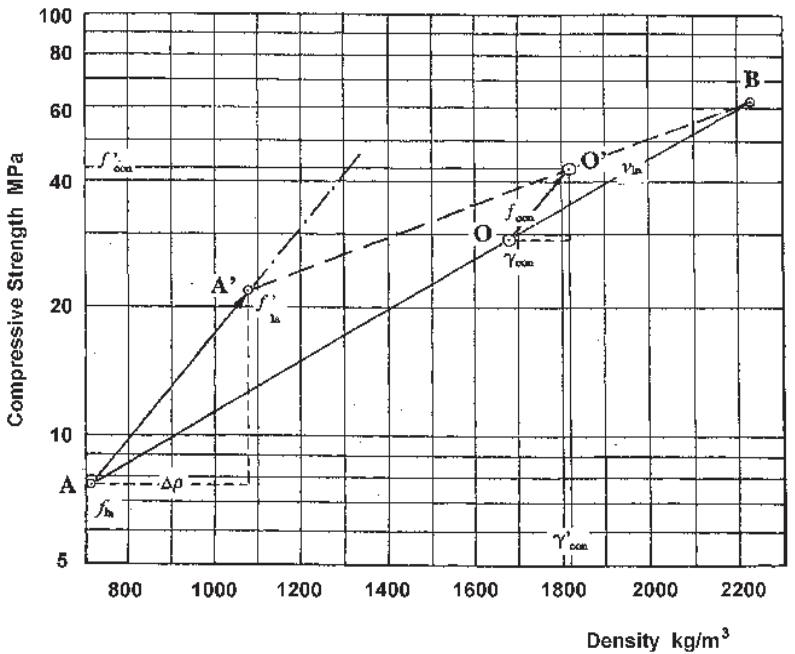

Figure 4.3. Graphic presentation of the density and the compressive strength of lightweight aggregate concrete when the particle density of the lightweight aggregate has increased $\Delta\rho$ from *A* to *A´*. The volume of the lightweight aggregate or mortar is kept constant and the composition of mortar is unchanged. The density and the strength of the concrete have moved from *O* to *O´*.

The strength of the concrete after replacing the lightweight aggregate is:

$$f'_{con} = f_{con} \times (f'_{la} / f_{la})^{v_{la}}$$

where f'_{la} is the particle density after replacing the lightweight aggregate.

4.0 CONCLUDING REMARKS

Lightweight aggregate concrete differs basically from the normal weight concrete due to its porous nature (mainly due to the aggregate particles) and lower strength. This fact is reflected on most of the properties, for example, on physical and mechanical behaviors. Normally, all concrete types are designed according to what concrete is sought, such as structural, load bearing, heat insulating, or on the whole, a high performance purpose.

The properties of lightweight aggregate concrete determine the type of lightweight concrete to be produced. When most of the lightweight aggregate, more or less, is manufactured by the use of industrial methods; the demands of the market control the type as well as the accessibility of the raw materials. In quite a few areas of the world, there is pumice, a material of volcanic origin, which is almost ready to be used directly in the production of mostly low strength concrete.

There are many ways or methods of designing lightweight aggregate concrete. First of all, what structure the concrete will be used for has to be decided, then the accessibility of different types of lightweight aggregate and the price restraints need to be known. No-fines concrete for block machine production or structural reinforced lightweight aggregate concrete for pouring on site or in the factory lead to at least two different ways of proportioning. However, common to both of them, the definite proportion of concrete ingredients is established after testing and corrections.

In calculating the optimal solution for the strength and density of the concrete at the start of the mix design process, the results are dependent on the strength, density, and size of the available lightweight aggregate. Sometimes, much is to be gained by changing one or two ingredients.

Based on the described proportioning methods, most of the lightweight aggregate concrete can be designed for different applications.

REFERENCES

1. ACI Committee 211, Standard Practice for Selecting Proportions for Structural Lightweight Concrete, *ACI 211.2-81*, Detroit, MI (1990)
2. Bache, H. H., Proportioning Lightweight Construction Concrete, (in Danish) *Betong Teknik,* Aalborg Portland, Denmark (1976)
3. Berntsson, L., *Proportioning of Lightweight Aggregate Concrete,* Swedish Council for Bldg. Res., Report R12:1994 (in Swedish) (1994)
4. Zhang, M., *Microstructure and Properties of High Strength Lightweight Concrete,* Report, The Norwegian Institute of Technology, Division of Bldg. Mater., Trondheim, Norway (Nov. 1989)

5

Production Techniques

1.0 INTRODUCTION

The production of lightweight aggregate concrete has been expanding, and now includes all types—from no-fines concrete of low density, mainly for block production, to structural concrete with densities from 1000 to 2000 kg/m^3 and compressive strengths up to 80 MPa. The production of all types of concrete is closely connected to the availability of lightweight aggregate, and economics dictate the use of lightweight aggregate concrete in place of normal weight concrete. Concrete is often placed by pumping in situ. There have been difficulties pumping lightweight aggregate concrete because the pump pressure forces water into the porous aggregate particles resulting in an increased stiffness in the concrete which blocks the pipes.

Some types of structural lightweight aggregate concrete have been successfully pumped by using a suitable chemical admixture. Lightweight aggregate particles have a low density due to their air voids. These air voids allow the particles to absorb water. However, quite a few voids are closed or sealed and have no connection to the surfaces and, therefore, are not absorbent. Knowing the absorbancy of the LWA before production is critical to the process because water absorbency plays an important role in

the way the concrete behaves in the fresh or wet state, mainly changing it to a stiffer consistency.

The different types of lightweight aggregate, natural and man-made, need to be carefully examined before use for the production of concrete. The properties of the aggregate, such as the bulk density, the particle density, the moisture content, and the size distribution by sieve analysis, are to be determined before production. Sometimes, it is necessary to do a chemical analysis for sulfur and chloride content. Many lightweight aggregates are manufactured rather than natural and, therefore, are reproducible and have a uniform quality, which is important at all production stages, i.e., mixing, placing, and compaction.

Lightweight aggregates have a lower strength than natural aggregates mainly because of the higher porosity which places a limitation on the strength attained by the concrete. As a rule, the water-to-cement ratio concept is used in the cement paste in concrete and is compatible with the strength of the lightweight aggregates. However, a very high-strength cement paste does not compensate for a lightweight aggregate of low density and strength when a specific compressive strength of concrete is sought, even if it may be feasible from a durability point of view.

In principle, the production of lightweight aggregate concrete and normal concrete is similar, but there are some exceptions which have to be taken into account for lightweight aggregate concrete. From experience, lightweight aggregate is not difficult to use. Nevertheless, the concrete is different and some methods need to be altered or modified.

2.0 LIGHTWEIGHT AGGREGATE AND ITS SUPPLY

2.1 Bulk Density and Particle Density

Normally, the manufacturer or the supplier provides the bulk density of the dry materials and, sometimes, proposals for mix proportion. The delivered lightweight aggregates are more or less wet and may also contain particles outside the stated fraction size. The moisture content can vary over a broad range of values from a few percent for manufactured materials up to 100% by weight for some types of pumice. The moisture at

the time of delivery depends, for example, on how long a time the aggregates were in stock and on the weather conditions when stored outdoors. The bulk density of wet aggregate or, preferably, the particle density must be known for the concrete mix and the weight of aggregate prior to batching. The tests for density and the moisture content need to be updated from time to time and always at the delivery of fresh materials.

2.2 Moisture Content of the Lightweight Aggregate

The absorption of water by the lightweight aggregate particles is significant in concrete production. It is, of course, desirable to prevent such an absorption during the concreting process. It is logical to soak the aggregate before mixing or to ask for delivery of very wet aggregates. However, this is not always a good solution for all concrete production. For house construction, a high water content in the lightweight aggregate results in a long drying time of the concrete components and high humidity indoors which creates problems for the other construction materials and for human beings. Another result of high water content in the lightweight aggregate is a lack of homogeneity in the cement paste of the concrete when compared to the vicinity of the surface of the particles and the bulk cement paste. When dry cement comes in contact with very wet aggregate particles, a cement paste layer of low water-to-cement ratio is produced on the surface. This results in irregularities in the concrete and creates a structure of higher permeability and low strength.

If the stiffening of the consistency over time is due to the absorption of water, the absorption may be reduced by soaking the aggregate. There are a number of methods used. They may be:

- Immerse the aggregates in water, sometimes in hot water at the production site.
- Continuous sprinkling of stockpiled aggregate with water.
- Storing and agitating the aggregate in a lagoon filled with water.
- Pre-wet the aggregate in the mixer at the beginning of the mixing process.
- Vacuum-soaking.

Pre-wetting in the mixer is the least effective method, but, it is commonly used. It may be successful because most of the water absorption is completed during the first few minutes of soaking.

The most effective method is vacuum-soaking. The process is finished after a short time, but the method is expensive. When the vacuum-treated aggregates are to be stored, they should continuously be sprayed with water to avoid having them dry out.

The water-soaked aggregates are necessary when the concrete is to be applied by high pressure pumping. Normally, the water-absorbed aggregates have no detrimental effect on strength and durability for high strength structural lightweight aggregate concrete. It should be emphasized that the water in the aggregate particles may be ignored when calculating the water/cement ratio of the concrete.

3.0 REMARKS ON MIX DESIGN

Lightweight aggregate concrete has a lower compressive strength than normal concrete with the same water/cement ratio based on the assumption that the lightweight aggregate particles have lower strength than the hardened cement paste. There are several advantages in using lightweight aggregates. These are due to their bond with the cement paste and closeness of their coefficients of thermal expansion and the modulus of elasticity compared to those of the dry cement paste. As a composite material, this type of concrete leads to a more homogenous and coherent material with a minimum of microcracking. The water absorbed by the aggregate particles may be an aid to extending the hydration of the cement and delaying and reducing crack formation caused by drying. Another advantage is that compatibility between the aggregate particles and the cement paste does not need to be taken into account for mix design, unlike normal concrete. On top of it all, there is a reduction in permeability, shrinkage cracking, and improved durability. At mix design, cement may be partially replaced by fly ash, ground-granulated blast furnace slag, and micro silica. All these influence the properties of fresh and hardened lightweight aggregate concretes.

3.1 Lightweight Fines

Normally, the lightweight aggregate is confined to the coarse fraction which means a particle size from 2 mm to 4 mm and sometimes even larger. Specifications call for even lower densities, and, in such cases, use of lightweight fines may be the optimal solution in place of natural sand for mortar. The lightweight sand is water absorbent, and needs more water for the same consistency, and has considerable variation in the particle size distribution, mainly caused by handling. Lightweight fines often lead to harsh mixes and, to overcome this effect, increased cement content is necessary. An extended mixing time may also have a positive influence on the rheological properties of the concrete mix.

3.2 Pumped Concrete and its Design

Pumping of fresh concrete has been widely used and the high pressure during pumping presses water into the porous lightweight aggregates. Usually, it is necessary to add a thickening agent to reduce the water movement and, after addition of a proper plasticizer, the workability is recovered. The types of lightweight aggregate, sand, and mineral admixtures influence the rheology changes under high pressure in the pipelines. Mineral admixtures, for example, ground-granulated blast furnace slag or fly ash, as a fines addition influences workability and is cost effective. For that reason, the thickening agent may be unnecessary. The workability needs to be of a high order, at least a 650 mm flow, and the cement content increased up to 100 kg/m^3, when fine lightweight aggregate is used. After mix design, trials are advisable in order to ensure that the performance is appropriate.

4.0 BATCHING

4.1 Aggregate Proportion

The aggregate proportion in the design mix is based on the volume as are all the other concrete constituents in the concrete mix. After mixing the concrete, the density of the compacted concrete seldom equals the

calculated density. The variation is a result of the following uncertain factors:

- The actual particle density of the lightweight aggregate.
- The water absorption of the aggregate.
- The air volume.

The bulk density of loosely packed lightweight aggregate must be measured after the delivery of the materials and even once per day during production. Based on the measured particle density and the bulk density, the ratio of bulk and particle density is calculated. This ratio is used to convert the measured bulk density to a calculated particle density which is used for the calculation of volume of the lightweight aggregate in the mix. The magnitude of the ratio depends on the size distribution and the geometric shape of the particles, normally between 0.52 to 0.58 for rounded particles, and is almost constant for the same type of material.

Failure to measure the bulk density and the moisture content of the lightweight aggregate may affect the density, strength, workability, and the volume of the mixed concrete. This moisture content contributes to the water content of the mix and contributes to the batched water. The density and the workability of the fresh concrete and the batching of water are the requirements for performance because the free water content greatly influences the workability or the consistency.

The final comparison of the probable concrete composition can be established from the value of the hardened and dried lightweight aggregate concrete. For this reason, some specimens are dried from time to time at 105°C after testing of the compressive strength.

4.2 Mixing Procedure

The mixing procedure for lightweight aggregate concrete is the same as for normal concrete and is produced in the same type of mixer or mixing plant. An alternate mixing procedure is to mix the concrete in two separate stages. According to the experience of many years, this method has been successful especially for low density structural lightweight aggregate concrete. In the first stage, the mortar is mixed, i.e., cement, sand, admixture, and about two-thirds of mixing water. In the second stage, the coarse aggregate is added with the rest of the water, and final mixing is done. The concrete mixed by this procedure is characterized by good homogeneity and high performance.

At times, lightweight dry fines cause the materials to form balls in the mixer. It can be avoided if less water is added at the start and then the amount is increased gradually.

The rate of water absorption during the mixing process is relatively rapid for small sized lightweight particles. There should not be much difference between mixes of lightweight fines and regular sand. In order to estimate the mixing time, the water-absorption curve for the actual materials can be studied. From the curve, it is evident that water absorption practically ceases after a few minutes for lightweight aggregate particles less than 8 or 10 mm. When necessary, the water added during mixing should include the water absorbed during transportation and water that may be added during compaction at the site.

In some cases, it is desirable to add extra water to the fresh concrete to compensate for the increased stiffness. But this should be done under strict supervision. Of course, the decision for such action needs to be well-founded and the increased stiffness should not have occurred for any other reasons, for example, decreased efficiency of the plasticizers or cement hydration.

4.3 Volume of the Concrete Mix

The yield or the delivered quantity of the mixed concrete may differ from the calculated or expected volume. The variations may be caused by miscalculation and malfunctioning or operation of the dosage and weighing equipment, but it is more likely that the variability in density of the aggregate is the result of changes in the aggregate itself and moisture content. To avoid errors, the bulk density and moisture content must be measured regularly and the batch weights adjusted accordingly.

In some concrete mixes, entrained air is included to improve the freeze-thaw durability and workability or to reduce the density of the concrete. Measuring the air volume in lightweight aggregate using the pressure method can be misleading. The volume of air in the empty voids in the lightweight particles is also included in the air content of the concrete. It is not a reliable value especially at a very high air content, such as up to 10% by volume of the concrete. Another method of measuring the air volume must be used.

5.0 TRANSPORTATION AND PLACING OF CONCRETE

5.1 Transportation

The transportation of lightweight aggregate concrete, factory produced, and ready-mixed lightweight aggregate concrete to a job site is almost the same as for normal concrete. As discussed earlier, the loss in workability between mixing and placing is more pronounced because of the absorption of water by the porous particles. Transportation equipment may lead to segregation and loss of homogeneity. This can be overcome by modifying the mix composition, keeping the concrete in a slow state of agitation or mixing periodically such as by the use of a truck mixer or more radically changing to other equipment for transportation. Attention must always be paid to possible delays, for example, due to a traffic jam, in transporting concrete under hot and dry conditions. In a cold climate, it is normal to increase the temperature of the fresh concrete during the mixing procedure, if necessary, even up to 30°C. It should be emphasized that the lower density of the lightweight aggregate concrete results in a lower specific heat than that of normal concrete and a higher loss of temperature with time.

Now, large quantities of concrete can be transported by means of pumping through pipelines over long distances especially to a location which is not easily accessible by other means. Pumping is an example of the end of one sort of transportation system and includes the placing operation. Pumping lightweight aggregate concrete is easily achievable using good pumping practices and ensuring that the mix composition and properties of the fresh concrete are adjusted to meet the requirements and needs of the materials used. Pumping of concrete that contains a high volume of entrained air, with about half the density of normal concrete, has not yet been successful.

5.2 Compacting, Finishing, and Curing

Compaction is a consolidation process that molds concrete within forms and around embedded parts to eliminate pockets of entrapped air. The operation can be carried out in many ways, mostly by mechanical methods

such as by internal vibrators, poker vibrators, and external vibrators rigidly clamped to the formwork. Compaction of precast concrete units in factory production is often executed by means of vibrating tables. The vibration characteristics vary from very low and high amplitudes to high frequency with small amplitudes. Poker vibrators have a high frequency, up to at least 200 Hz, and a high acceleration which, in turn, is a function of frequency and amplitude. Compared to normal concrete, lightweight aggregate concrete needs less compaction. Too intensive a vibration may lead to low homogeneity and loss of stability of the fresh concrete. As with similar normal concrete, the use of an impervious smooth mold increases the occurrence of air bubbles on the surface. This is even more likely for concrete containing lightweight aggregate fines. Very smooth steel forms may give better results after chemical etching.

Bleeding will normally be less than for normal weight concrete because the lightweight aggregate concrete contains a higher cement content compared with normal concrete of the same strength class. The water on the upper surface reduces the risk of plastic cracking caused by water evaporation and high negative water pressure in the capillary pores of the concrete. Less bleeding can logically give more early cracking, but, on the other hand, the absorbed water in the lightweight aggregate reduces such a risk.

A long vibration time for lightweight aggregate concrete, unlike normal weight concrete, does not cause concentration of cement paste or cement mortar on the top surface. Instead, the coarse aggregate particles have a tendency to rise and may leave the concrete creating a loose layer of lightweight aggregate. The driving force is the difference between the particle density of the particles and the cement paste including entrained air voids. The rate of movement is given by the Stokes' formula for spherical particles:

Eq. (1) $$v = 2\, r^2\, \Delta\rho\, g / 9\eta \quad \text{(m/s)}$$

where
- r = the radius of the particle (m)
- $\Delta\rho$ = the difference between the particle density and surrounding medium, cement paste or mortar (kg/m^3)
- g = acceleration due to gravity (m/s^2) and
- η = viscosity (dynamic) of the cement paste (Ns/m^2)

In the formula, it is shown that the size of the particles is raised to the second power and larger particles move faster than smaller ones. This effect will continue to exist until the concrete reaches its final set or, according to the formula above, until the viscosity increases to a sufficiently high value. The visible lightweight aggregate particles on the upper surface are a particular characteristic of this type of concrete which requires special consideration during finishing. Power floating at the proper time adjusted to the setting of the concrete may produce a smooth finish of high quality.

The object of curing is to achieve a concrete that hardens in such a way that all the required specifications will be met. The external climatic conditions, the concrete composition, and the properties of components influence strength development and other important durability properties. The surrounding temperature and moisture condition, as well as the heat insulation of the formwork, play a significant role in the early hydration and hardening. Normally, a high cement content, lower specific heat, and lower thermal conductivity than normal concrete will accelerate the exothermic heat development and the temperature in the concrete. Inside a monolithic structure, the temperature can reach much higher values than normal concrete. To reduce the heat development and the temperature rise, part of the portland cement should be replaced with ground-granulated furnace slag, pozzolan, or fly ash.

6.0 TESTING OF LWAC RELATED TO PRODUCTION

6.1 Density of the Fresh Concrete

Repeated testing of the density of the lightweight aggregate concrete in connection with the mixing is almost mandatory during continuous production, as well as at the start of a new production, new material, and a new concrete mix. Included in the density tests of the hardened concrete are several characteristics:

- The density of standard stored concrete specimens at the time of testing for strength.
- The density in situ of air-dried concrete or at equilibrium with the surrounding climate.
- The oven-dried density, temperature 105°C.

The fresh density and oven-dried density are specific and easily reproducible, and are unambiguous. Air-dried concrete varies with atmospheric conditions and will be different from place to place. This density, however, is the value the structural designer needs for calculation of the dead load of the structure. The air-dried density can be adopted based on the cement content, water/cement ratio, content of lightweight aggregate, and known isotherms for cement paste and lightweight aggregate at fixed relative humidity of air in the surroundings of the concrete structure concerned. The final air density equates to the oven-dried density plus 60–90 kg/m^3 depending on the cement content of the concrete. It is difficult to change the characteristic densities of the available lightweight aggregate concrete. It should be the duty of the designer to design within the limits of the materials available.

6.2 Workability

Workability testing should be carried out in the normal manner by slump test or, rather, flow table test. The slump test tends to underestimate the workability because of the lower density and less force for deformation. The flow table test is better suited to lightweight aggregate concrete and for flows of over 400 mm up to a maximum of 700 mm. The workability of lightweight aggregate concrete for pumping needs a value of flow that is higher than 600 mm. It is impossible in the beginning to visually judge the mix appearance but, after training, it may be possible to develop an eye for evaluating the workability of fresh concrete.

6.3 Strength Test and In Situ Testing

The same tests apply to lightweight aggregate concrete and normal weight concrete. Both cube and cylinder are well suited for compressive and splitting tensile strength for early, as well as for 28 days, strength.

The early strength, for example, 1 day relative to 28 day compressive strength, will definitely be higher for lightweight aggregate concrete than for normal concrete. The explanation of that is the influence the lower strength of the lightweight aggregate particles has on the development of the strength of concrete. The strength class of lightweight aggregate concrete is based on the 28 days strength. The form stripping can, however, be performed earlier than usual and may have a positive effect on the cost of construction.

The most reliable test method for compressive strength is an in situ test of cores drilled from the concrete structure. There are nondestructive methods such as the Schmidt Hammer, impact test, and ultrasonic test which must be used or combined with some caution. The lightweight aggregate particles are easily crushed by an impact test.

7.0 CONCLUDING REMARKS

The only difference between lightweight aggregate concrete and the normal weight concrete is the type of the aggregate. Natural rock mineral particles in normal concrete are replaced by porous aggregate particles of different origin and size. By this replacement, many properties are changed which influence the whole production of lightweight aggregate concretes.

For the production and use of LWAC, basic information about the properties of the lightweight aggregate and the use of a suitable test procedure for the aggregate material, as well as for the concrete, are important. It is necessary to understand the whole behavior of the fresh, as well as the hardened concrete, in order to select and find the optimal proportion of the constituents for a specific purpose.

6

Lightweight Aggregate Concrete Microstructure

1.0 INTERFACES IN CONCRETE

Concrete is a composite material consisting of relatively inert aggregate particles, with a wide size distribution and variable mineralogical composition, embedded in a matrix of hydrated cement paste (hcp). The hardened matrix itself is derived from hydration reactions between portland cement and water. However, in addition to portland cement, water, and aggregates, modern concretes generally contain at least some of the following additional ingredients:

- Chemical admixtures.
- Pozzolanic materials, such as fly ash, silica fumes, or blast furnace slag.
- Discontinuous fibers, made of steel, glass, or natural, synthetic, or organic materials, which are used in fiber-reinforced concrete.

In addition, structural concrete is almost invariably reinforced with steel-reinforcing bars or prestressed cables.

The presence of these materials give rise to a wide variety of interfaces in concrete. The principal ones are listed below.

1. The various phases that make up hcp.
2. The hcp and the still-unhydrated cement grains.
3. The hcp and the unreacted portion of the pozzolanic materials.
4. The hcp and the aggregate.
5. The hcp (or mortar) and the discontinuous fibers.
6. The hcp (or concrete) and the steel reinforcement.
7. The solid phases and either air or water, which will not be considered further in this review since they do not contribute directly to the mechanical behavior.

1.1 The Nature of the Interfacial Regions in Concrete

The bonds in the cementitious composite systems are the outcome of the combination of different mechanisms, such as van der Waal's forces, hydrogen bonds, and possibly chemical bonds. The nature of these mechanisms varies from system to system depending upon the chemical nature of the raw materials, the hydration conditions, etc. Mehta's[1] observations with regards to hcp are as follows:

> "The intrinsic nature of the bonding forces, both between the several hydration products, and within each remains variable and therefore indeterminate."

Scrivener and Pratt[2] reported:

> "The relative movement of the sand and cement grains during mixing, and possibly settling of the sand grains before the cement paste sets, may lead to regions of low paste density around the sand grains and to areas of localized bleeding at the interface in which large CH crystals precipitate."

It seems likely that, during the preparation and handling of concrete, artifacts are developed that influence the results. This is the root cause for the disagreement about the precise nature of the interfacial regions or their mechanical properties. Nevertheless, it is clear that the interfacial regions are, in general, profoundly different from the "bulk" cement paste,

in terms of morphology, composition, and density. There are generally large crystals in the interfacial zone, with a preferential orientation. But this should not be taken as the inherent property of interfaces; more likely it occurs because there is extra space at the interface due to the bleeding of water.

Many models of interfacial zones have been presented which vary from each other. A few of these models are shown in Fig. 6.1. Besides the other differences, it is shown that the thickness of the interfacial zone varies from 40 to 50 μm, with the major differences from the bulk paste occurring within the first 20 or 50 μm from the physical interface. Moreover, the weakest part of this interfacial zone lies not right at the physical interface, but 5 to 10 μm away from it, within the paste fraction.

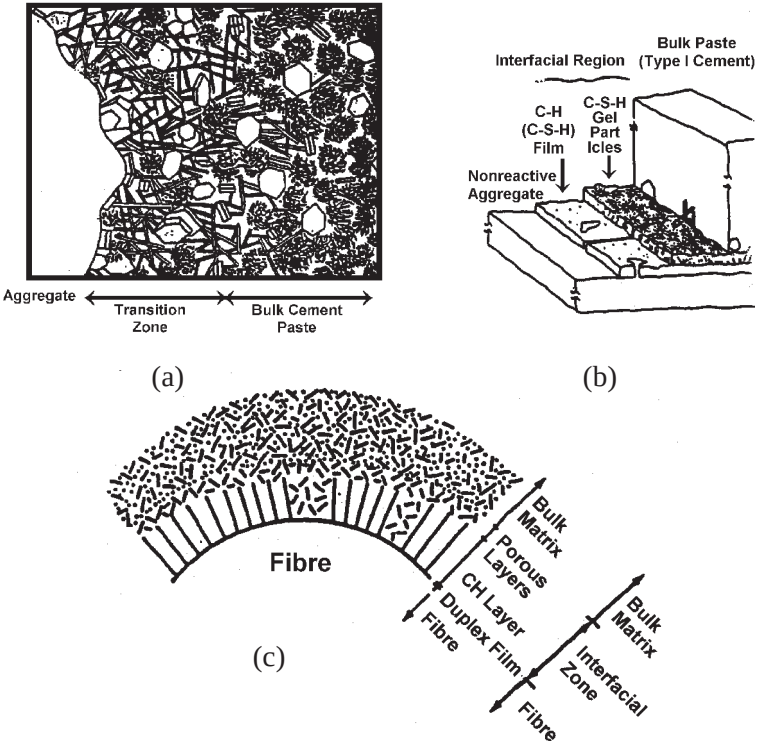

Figure 6.1. (*a*) Diagrammatic representation of the transition zone and bulk paste in concrete,[1] (*b*) interfacial region formed between a non reactive silica substrate and type I cement paste,[3] (*c*) interfacial zone at the steel fiber interface.[4]

Traditionally, it was assumed that the interfacial regions occupy only a small volume in concrete and, therefore, the properties of the bulk paste dominate concrete behavior. But a careful microscopic examination of the polished surfaces has revealed that the mean spacing between aggregate particles is only 75 to 100 μm.[5] Even though the variability is large, this suggests that, with an interfacial zone thickness equaling 50 μm, most of the hcp lies in the interfacial zone. Only a relatively small volume of bulk hcp exists.

1.2 Cement-Aggregate Bond

It is generally agreed that the interface between the hcp and the aggregate is the "weak link" in concrete. There are a number of observations that contribute to this belief:

1. The cement aggregate interfacial zone has an open morphology compared to the bulk hcp.
2. The interfacial zone contains large crystals of portlandite, $Ca(OH)_2$, preferentially oriented so as to create planes of weakness.
3. Bleed water often accumulates beneath the larger aggregate particles, creating additional planes of weakness.

Most microscopic examinations[6][7] have shown that the cracks in plain concrete propagate preferentially in the interfacial region, generally a few micrometers away from the aggregate surfaces themselves. However, whether the cracks initiate in this region, or at flaws in the bulk paste, is not known. The fact that cracks tend to occur in the interfacial region is consistent with the observations that the fracture toughness of the interface in regular concrete is considerably lower than that of either the aggregate or the bulk paste.[8][9] Even in the high strength concretes, where both the paste strength and the interfacial bond strength are presumably higher, cracks tend to follow the interfacial zone under tensile loading. Generally, they go through the aggregate particles only at a high loading rate.[10] In LWAC, on the other hand, the cracks tend to propagate in a straight line right through the aggregate particles in the crack path. This indicates that, in this case, the aggregates themselves are weaker than either the hcp or the interfacial regions.

Most studies of cement aggregate bond strength in tension, compression, or bending have shown that increasing the bond strength increases the concrete strength, but these increases tend to be moderate, in the range of 20 to 40% at best in going from "no bond" to "perfect bond." Apparently an increase in bond strength will improve the tensile strength more than the compressive strength[11] though this difference is not large. One simple relationship between bond strength and either compressive or flexural strength was developed by Alexander and Toplin,[12] based on a regression analysis of the data then available to them. It has the form

Eq. (1) $$\sigma = b_0 + b_1 M_1 + b_2 M_2$$

where σ = concrete strength in compression or flexure

b_0, b_1, b_2 = linear regression coefficients

480, 2.08, 1.02, respectively, for compression

290, 0.318, 0.162, respectively, for flexure

M_1 = modulus of rupture of the paste

M_2 = modulus of rupture of the aggregate-cement border

A plot of this equation is shown in Fig. 6.2. For the "no bond" situation, M_2 was equal to zero, for "perfect bond," M_2 was set equal to M_1. As may be seen, even upper and lower-bound cases are not very different. Moreover, a change in the flexural strength of the hcp has about twice as much effect on concrete strength as does a change in the bond strength.

There are a number of practical ways in which the bond between the hcp and the aggregate can be improved. It has been found that addition of silica fumes densifies the interfacial region and improves the cement aggregate bond. The improvement in bond strength is attributed to:

- Less free water (i.e., bleeding water) at the interface during specimen preparation.
- A reduction in the size of the transition zone due to the pozzolanic reaction between $Ca(OH)_2$ and the silica fume, and thus, a reduction in the preferred orientation of the $Ca(OH)_2$ crystals.[13]

The wall effect also results in higher porosity in the contact zone compared to the bulk cement paste.

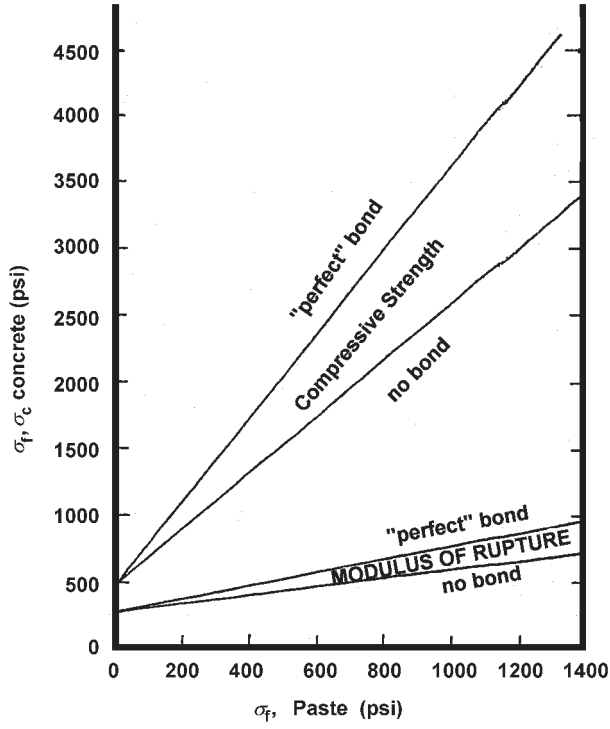

Figure 6.2. Effect of cement-aggregate bond strength on the compressive strength (σ_c) and flexural strength (σ_f) of concrete.[12]

1.3 Lightweight Aggregate-Cement Paste Interface

The interface is characterized by a mechanical interlocking in combination with a chemical interaction in the form of a pozzolanic reaction. The lightweight aggregates have a porous surface. Due to this, some part of the binder will penetrate into the aggregate, which will subsequently decrease the internal bleeding water zone. The phenomenon of surface bleeding in freshly placed concrete is due to a high permeability of unhydrated cement paste. A natural consequence of this phenomenon is laitence, which consists of a highly porous and weak film of mortar on the surface of hardened concrete. The phenomenon of internal bleeding is not

well known. It is illustrated in Fig. 6.3.[14] The internal bleed water is water that has not been able to reach the surface, therefore, it accumulates under coarse aggregate in concrete. Like the surface bleed water, the internal bleed water may contain fine particles of sand and cement, and gives rise to a porous cement paste matrix at the aggregate surface, a phenomenon similar to the surface laitence.

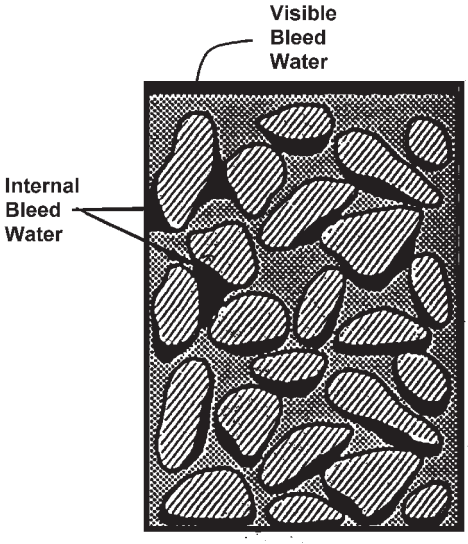

Figure 6.3. Schematic representation of bleeding in freshly-placed concrete.[14]

Surface bleeding and internal bleeding are closely interrelated in the sense that the factors influencing the former seem to affect the latter in the same manner. When the aggregates are porous or are of a pozzolanic character, as in the case of the lightweight aggregate (expanded clay, shale, etc.), or when the mineral admixtures are incorporated in the mix, the internal bleed water area will decrease. Figure 6.4 illustrates schematically how the presence of fine mineral admixture particles (0.1 μm diameter) between two cement grains would effectively reduce the size of the channels flow, thus considerably lowering the permeability and bleeding in a freshly-placed concrete. In addition to this, the chemical interaction of the

mineral admixture part of the bleed water will move into the porous LWA. It will further decrease the interfacial transition zone (ITZ). It is illustrated in Fig. 6.5. The bond between the aggregates will not be on the surface of the aggregates, as in the case of stone aggregates in regular concrete, but will move further inside the lightweight aggregate.

Idealized representation of freshly compacted concrete, showing surface bleeding and internal bleeding effects

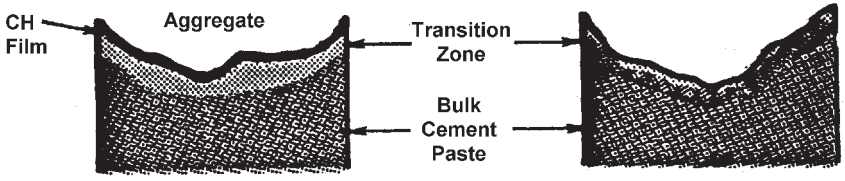

Idealized representation of the Transition Zone in Hardened Concrete

Figure 6.4. Schematic diagram representing reduction in the size and porosity of transition zone by addition of pozzolanic material.[14]

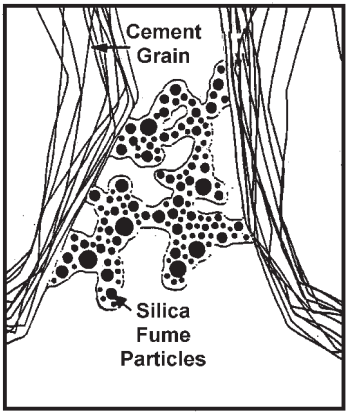

Figure 6.5. Schematic diagram representing blockage in channels of fluid flow by fine particles.[15]

2.0 PORE STRUCTURE OF LIGHTWEIGHT AGGREGATE

Lightweight aggregates are porous and have the ability to suction, so it is necessary to look into the pore structure of the aggregates itself. There are two types of pores in the lightweight aggregates: open and closed pores. Open pores are the pores that are interconnected and take part in the permeation, whereas the closed pores are sealed and not interconnected. Thus, they do not take part in the permeation. The total porosity of a material is the sum of the closed and open pores, whereas the permeability will depend only upon the interconnected pores. The simple way to assess the interconnectivity of the pores is by measuring the water absorption property.

2.1 Water Absorption

The connectivity of the pores in the aggregate is determined by immersing the aggregates in water for 24 hours and later completely saturating them under vacuum. The difference between the water absorption thus measured will indicate the fraction of non-interconnected pores. Sarkar, et al.,[16] have tested four LWA: Swedish Leca™, and Liapor™ 5, 6, and 8 of German origin. The particle densities of Liapor™ 5, 6, and 8 are 1000, 1080, and 1437 kg/m^3, respectively. It is reported that the water absorption was highest in the case of Liapor™ 8 and lowest in Swedish Leca™ (see Table 6.1), which implies that the Swedish Leca™ is least permeable and has less interconnected pores. Its interconnectivity is 46%, Liapor™ 8 has very few closed pores, and interconnectivity is calculated at 97%, thus, very few pores in Liapor™ 8 are completely sealed.

Sintered fly ash aggregates, Lytag™, have shown water absorption in the range of 13–14% according to Swamy and Lambert,[17] Bolendran[18] and Teychene.[19] It is further reported that the Lytag™ absorbs water very rapidly in the beginning. It slows down later, but continues for a long time. It can be as long as several months. Zhang and Gjörv,[20] who have also found open pores in German Liapor™, Norwegian Leca™, and UK Lytag™ aggregates, concluded from porosimetry measurements that over 30% of pores are open, and the closed pores represent only 4–7%.

Table 6.1. Water Absorption of Lightweight Aggregates[16]

Aggregates	Initial moisture (% by wt)	Water absorption (24 h)	Water absorption under vacuum	Inter-connectivity (%)	Density of aggregate	
					Surface dried (kg/m^3)	Wet (kg/m^3)
Sw. Leca™	0.04	10.2	22.2	46.0	735	836
Liapor™ 5	0.21	16.1	22.6	71.2	911	1072
Liapor™ 6	0.08	17.1	21.5	79.5	1155	1326
Liapor™ 8	0.69	21.0	21.6	97.2	1535	1745

Interconnectivity ratio of water absorption after 24 hours and under vacuum. Water absorption is calculated on the percentage of dry mass

Water absorption depends upon the size and type of the pores and the particle density. This is related to the degree of vitrification during the sintering of the aggregate and depends upon the process of production of LWA. Swedish Leca™ is made when the clay passing through the rotary kiln is broken into tiny pieces by chains inside the kiln. This makes a well-compacted dense structure, whereas Liapor™ is formed first in the specified size and then sintered. Thus, they form a particular structure before burning, so they are not as dense and have more interconnectivity. The process of manufacturing of lightweight aggregates is described in Ch. 2.

During sintering, the vitrification takes place on the surface of the aggregates where a layer of glassy phase is formed. This layer hinders further vitrification inside the aggregate. Thus, the structure on the surface is different from the interior of the aggregate.

For each type of clay, there exists an optimum firing temperature. At temperatures above this optimum, recrystallization starts while, at lower temperatures, the clay lattice structure may still exist. The typical firing temperature of lightweight aggregate is 1200°C, where sintering and devitrification takes place. The aggregates form a dense outer shell. The density and the thickness of the outer shell of lightweight aggregates may vary from one particle to another and even from one area to another in the same particle.

Microscopic study done on the outer surface of Swedish Leca™ and Liapor™, using an optical microscope, has shown a distinct, thick external shell in the Swedish Leca™, which also appears to be less permeable (Figs. 6.6*a–d*).[16] This indicates that the outer shell of Swedish Leca™ is partly responsible for its low water absorption. It was reddish brown in color with a glassy surface, suggesting iron enrichment. Iron, being a catalyst, forms a liquid phase at lower temperatures and cools down to a glass. Liapor™ 8, on the other hand, consists of an indistinct over-shell with a number of jagged features. The impermeable shell of Swedish Leca™ acts as a barrier for rapid capillary suction. Thus, water can enter the interior of these aggregates only under pressure, whereas the interconnected cellular structure of the external shell of Liapor™ 8 permits passage of water with relative ease. The external surface of Liapor™ 8, however, exhibits the most angular features, which can promote the formation of a better bond with the paste matrix.

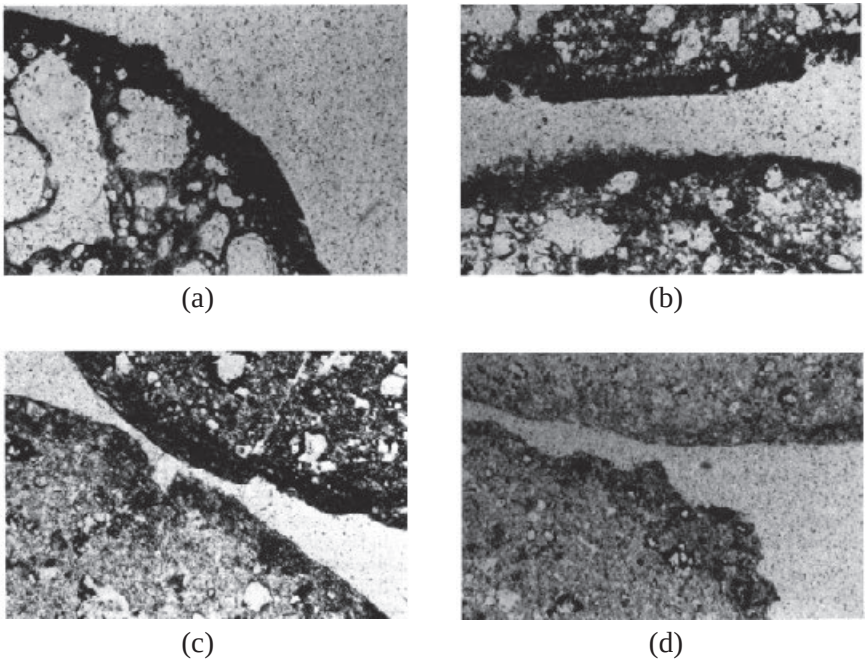

Figure 6.6. External surface of lightweight aggregates under transmitted-light polarizing microscope: (*a*) Swedish Leca™, (*b*) Liapor™ 5, (*c*) Liapor™ 6, (*d*) Liapor™ 8.[16]

3.0 MICROSTRUCTURE OF THE INTERFACIAL TRANSITION ZONE

Microstructure is usually studied using a scanning electron microscope with an energy dispersive x-ray analysis system. But Scrivener and Pratt[21] have shown that, from a backscattered electron image (BSEI) of the polished section of cement paste, it is possible to identify four components of the microstructure: anhydrous material, massive calcium hydroxide, other hydration products, and pores. Zhang and Gjörv[22] have studied the microstructure in the ITZ using a combination of microscopic analysis and backscattered electron image. The elemental x-ray dot maps of Ca and Si in conjunction with the BSEI from the same area provided a basis for distinguishing the aggregate phase (Si-rich) from the cement paste (Ca-rich). The composition of the LWAC used for this study is shown in Table 6.2.

Table 6.2. Mix Proportion of LWA Concrete[21]

No.	Type of Aggregate	Cement (g)	Aggregate (g-)	Water (g)	W/C /est.	Particle Density g/cm^3
1	Liapor™ 8	600	274	202	0.3	1.37
2	Liapor™ 7	600	250	203	0.3	1.25
3	Liapor™ 6	600	214	206	0.3	1.07
4	H.S.S. Leca™	600	260	211	0.3	1.30
5	Lytag™	600	288	217	0.3	1.44
H.S.S.Leca™ - high strength Swedish Leca™.						

Oxide Composition of Cement Used. SiO_2 = 22.2%, Al_2O_3 = 3.74%, Fe_2O_3 = 2.75%, CaO = 63.90%, MgO = 1.97%, SO_3 = 3.11%, K_2O = 0.64%, Na_2O = 0.26%, Free lime = 1.32%, Loss on ignition = 0.96%.

Mineral Composition of Cement Used. C_3S = 52.7%, C_2S = 24,2%, C_3A = 5.3%, C_4AF = 8.4%.

A portland cement, type Sp 30-4 A, was used which is a specially designed cement for Norwegian offshore concrete structures.

A typical microstructure of the interfacial zone for a composite of a Liapor™ 8 particle and cement paste is shown in Fig. 6.7. The BSEI and the elemental x-ray images for the interfacial zone between Liapor™ 8 aggregate and cement paste is shown in Fig. 6.8. The area to the left in the picture is an aggregate and the area to the right is cement paste. The pores in the aggregate and in the interfacial zone (black area) and the unhydrated cement particles (bright) can be easily distinguished.

The above observation demonstrates that for a LWA, with a very dense outer shell, the formation of a porous interfacial zone containing massive $Ca(OH)_2$ is possible. This is probably caused by the wall effect and localized bleeding, since water absorption by the dense shell is minimal.

The microstructure of the interfacial zone and the Ca, Si and S, x-ray images for the composite of Liapor™ 7, Liapor™ 6, high strength Leca™, Lytag™, and cement paste are shown in Figs. 6.9–6.16, respectively. In all the composite specimens, the cement paste and lightweight particles are well-bonded and almost no $Ca(OH)_2$-rich zone was observed near the aggregate particles. In some areas, where the aggregate was very porous, the calcium and sulfate penetrated the lightweight aggregate. In the isolated area where the aggregate was locally dense (Liapor™ 7, Fig. 6.9), a relatively porous interface zone is observed.

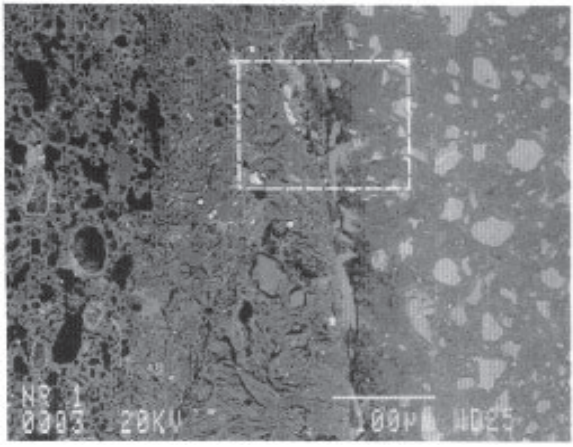

Figure 6.7. Microstructure of the interfacial zone between Liapor™ 8 aggregate and cement paste (200x).[22]

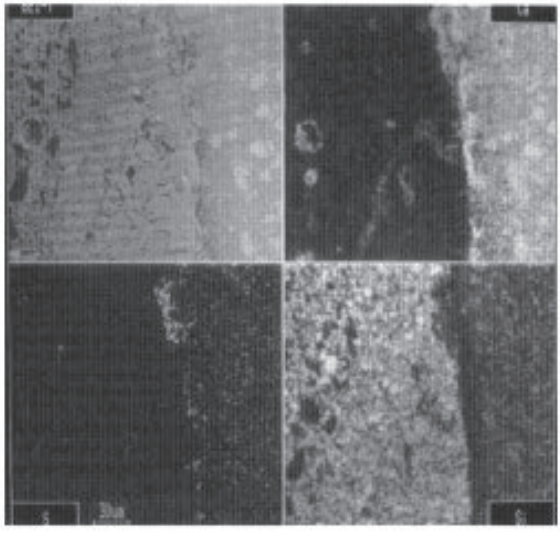

Figure 6.8. BSEI and elemental x-ray images for the interfacial zone between Liapor™ 8 aggregate and cement paste.[22]

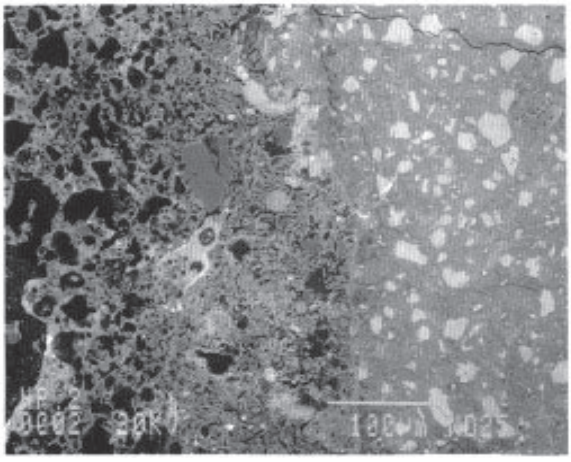

Figure 6.9. Microstructure of the interfacial zone between Liapor™ 7 aggregate and cement paste (200x).[22]

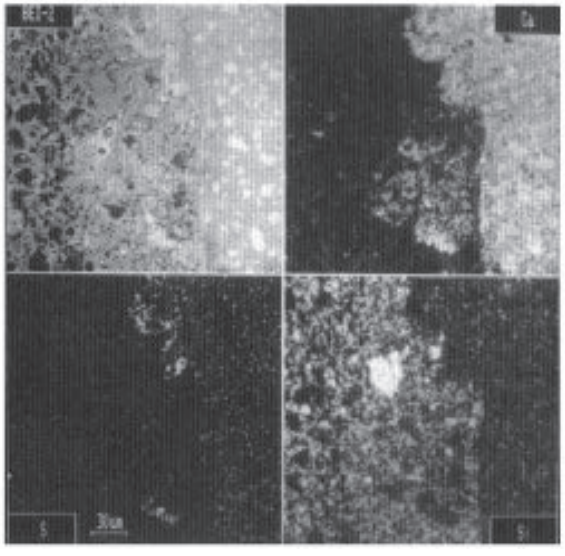

Figure 6.10. BSEI and elemental x-ray images for the interfacial zone between Liapor™ 7 aggregate and cement paste.[22]

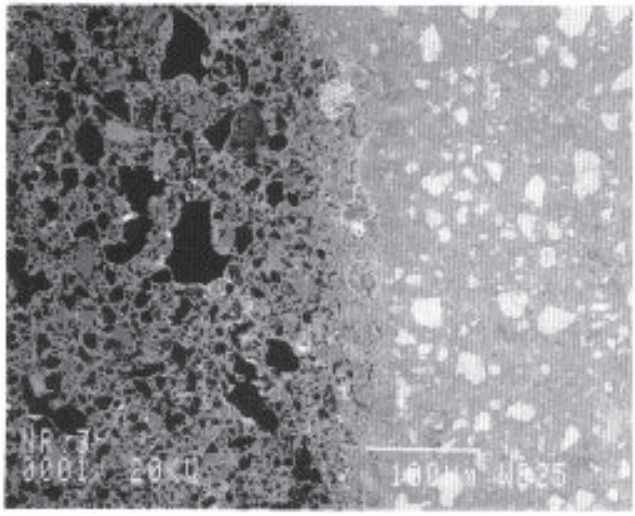

Figure 6.11. Microstructure of the interfacial zone between Liapor™ 6 aggregate and cement paste (200x).[22]

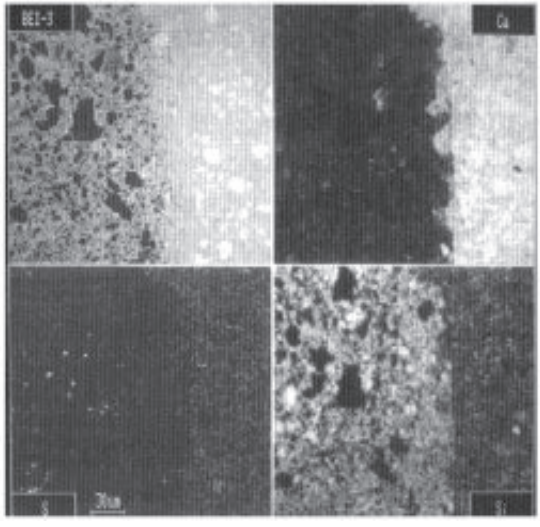

Figure 6.12. BSEI and elemental x-ray images for the interfacial zone between Liapor™ 6 aggregate and cement paste.[22]

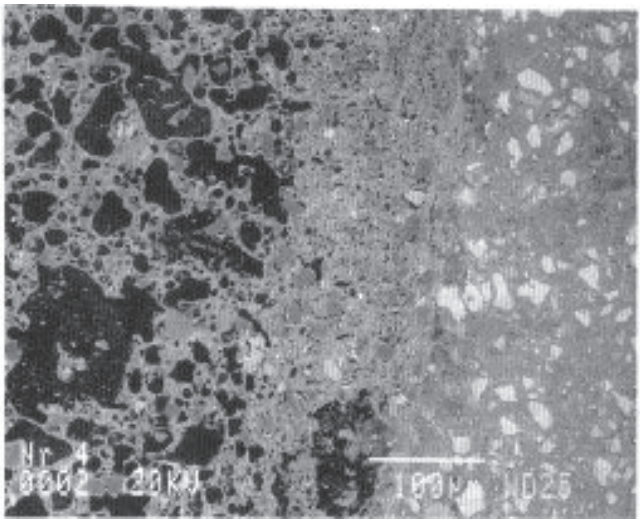

Figure 6.13. Microstructure of the interfacial zone between high strength Leca™ aggregate and cement paste (200x).[22]

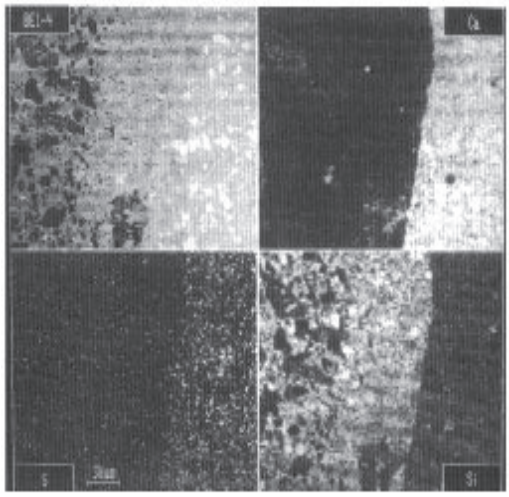

Figure 6.14. BSEI and elemental x-ray images for the interfacial zone between high strength Leca™ aggregate and cement paste.[22]

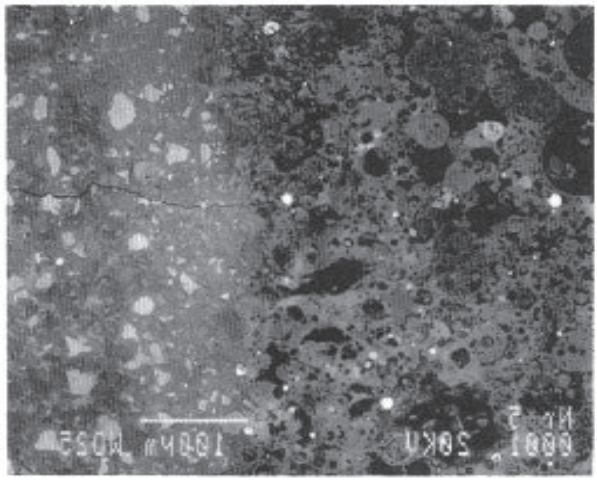

Figure 6.15. Microstructure of the interfacial zone between Lytag™ aggregate and cement paste (200x).[22]

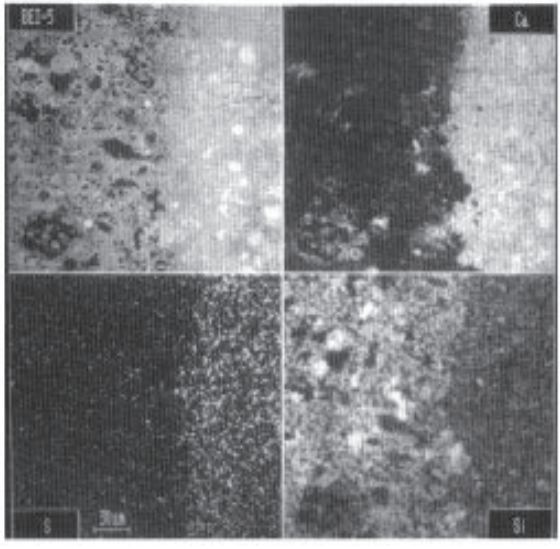

Figure 6.16. BSEI and elemental x-ray images for the interfacial zone between Lytag™ aggregate and cement paste.[22]

For the lightweight aggregate without a dense outer shell (Lytag™), the cement paste may penetrate the surface pores, thereby providing a good mechanical interlocking after hardening between the aggregate and paste.

The distinct difference in microstructure of the interfacial zone for Liapor™ 8 and the other aggregates (Liapor™ 7, Liapor™ 6, high strength Leca™, and Lytag™, Figs. 6.9–6.16) demonstrates the effect of the dense outer shell of the lightweight aggregate. As discussed earlier, the density and thickness of the outer layer of LWA may vary from one particle to another, and even from one area to another on the same particle. Therefore, the characteristic microstructure of the interfacial zone may also vary. It seems that for the increasing density of the outer layer of the LWA, the nature of the interfacial transition zone becomes more similar to that observed for the normal weight concrete aggregate. For more porous types of lightweight aggregates without a dense shell, such as Liapor™ 7, Liapor™ 6, high strength Leca™, and Lytag™, a better bond forms between the paste and aggregate partly due to a better microstructural zone and partly due to improved mechanical interlocking.

3.1 Microstructure of Old Concrete

The microstructures of some old concrete from the ships have not shown a distinct boundary between the aggregate and the cement paste. Instead, new phases develop on the contact point of the aggregate and the cement paste.

Scanning electron micrographs of concrete from some mature bridge decks have shown that the LWAs were extremely well-bonded to the cement paste matrix (Figs. 6.17–6.21) The concrete in Figs. 6.17, 6.18, and 6.19 is from the deck of a more than twenty year old bridge in Maryland. The concrete in Fig. 6.20 is from a core taken from a forty year old lightweight concrete bridge crossing the Cape Cod Canal in Massachusetts, and the sample in Fig. 6.21 is from a core taken from a twelve year old bridge in New York. These micrographs of the cement paste suggest a change from a plate-like structure in the mass of the cement paste to a more cubic structure at the aggregate-cement paste interface. This interface layer is 60 μm thick and tends to contain fewer voids and pores than does the cement paste further away from the interface.

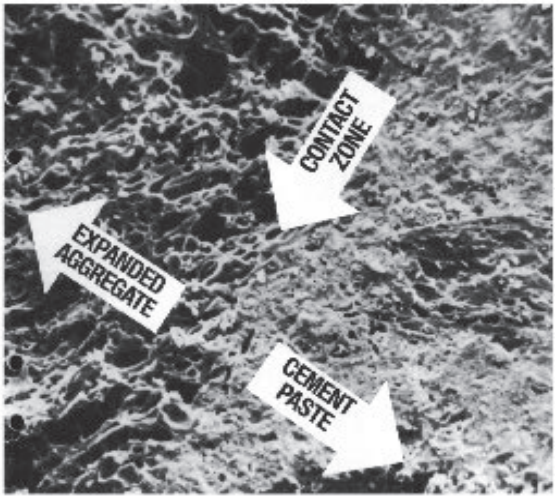

Figure 6.17. Contact zone between expanded aggregate and cement paste, Chesapeake Bay Bridge. Micrograph width is 500 μm.[23]

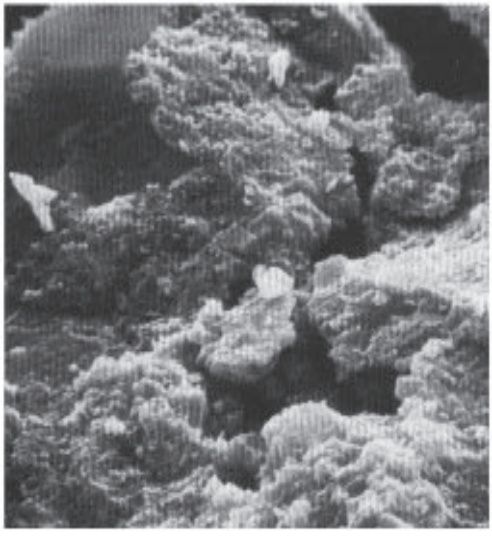

Figure 6.18. Fracture surface of concrete from the deck of the Chesapeake Bay Bridge; aggregate is on the top left. Micrograph width is 20 μm.[23]

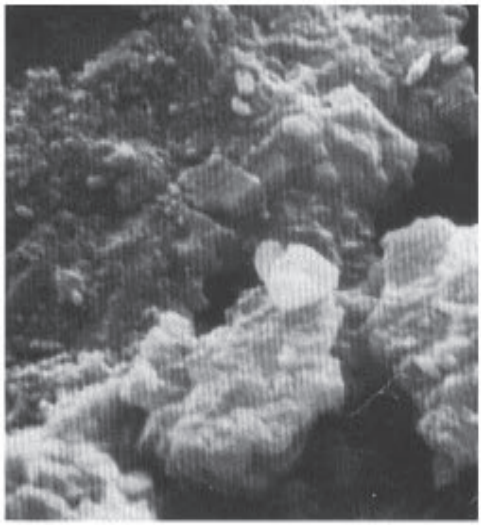

Figure 6.19. Interface in Fig. 6.18 at higher magnification, shows the dense surface layer adjacent to the expanded aggregate. Micrograph width is 10 μm.[23]

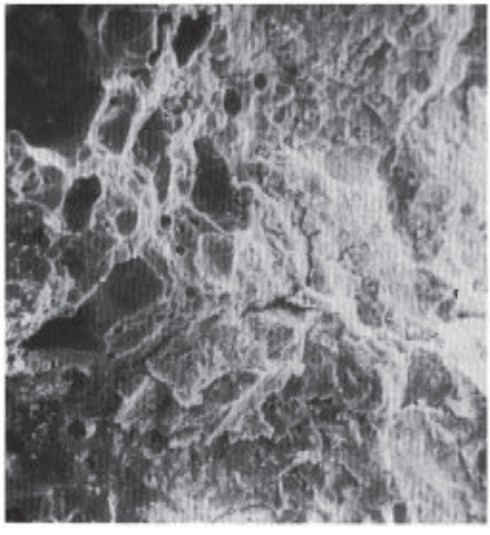

Figure 6.20. Contact zone between expanded aggregate and cement paste from the bridge deck over Cape Cod Canal, Massachusetts. Micrograph width is 550 μm.[23]

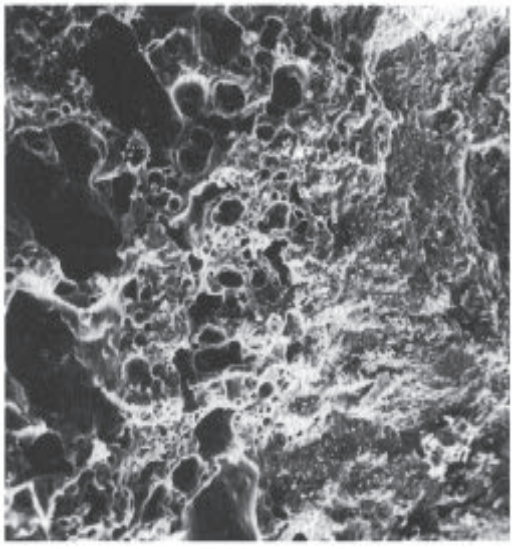

Figure 6.21. Contact zone between expanded aggregate and cement paste from the Coxsackie Bridge, New York. Micrograph width is 550 μm.[23]

When this concrete is subjected to applied stresses or volume changes, then stress concentration occurs at the weak aggregate-cement paste interface, leading to the formation of microcracks. In order to understand the mechanism by which the LWAC improves the performance, it is necessary to understand how these stress concentrations can be reduced.

When using expanded clay aggregates, the boundary between the two porous phases, the aggregate and the mortar, is difficult to identify, whereas the transition between dense aggregates, gravel, and porous hydrated cement paste is distinct. Moisture exchange can take place between the partially saturated lightweight aggregate and the still plastic mortar phase, thereby reducing the tendency of fresh lightweight concrete to develop thin films of water at the interface between the aggregate and cement paste.

Expanded clay aggregate-mortar interaction is both mechanical and chemical. In other words, the contact layer is not simply an interface between two substances, it contains new substances that are formed from

the interaction. The increase in cohesion is due to the chemical reaction between the products of cement hydration and the alumino-silicates at the surface of the LWA formed during production at high temperature.

Khokhorin[24] compared the hardness at and away from the contact zone for both expanded and dense aggregates. The microhardness of the mortar fraction outside that zone was considerably greater than the microhardness of the mortar fraction outside the zone when expanded aggregates are used.

Khokhorin's results are summarized as follows:

> "On the whole one should note that the quality as defined by cohesion, density, and strength of the contact zone of the concretes based upon porous aggregates is better than that of the contact zone of normal concrete based on dense aggregate."

3.2 Elastic Compatibility

Cracks are often found at the interface between the aggregate and the cement paste. But surprisingly enough, in the case of lightweight aggregate concrete one does not see them. The primary reason for the lack of bond cracks may be due to the similarity of elastic stiffness of the LWA and the remaining mortar fraction. Stress-strain curves of lightweight aggregate concretes are typically linear to levels approaching 90% of the failure strength, indicating the relative compatibility of the constituents and the reduced occurrences of microcracking. When microcracking is reduced, the disruptive forces that are generated due to the freezing of water-filled cracks will be reduced. Similarly, rapid movement of chloride will also be limited when microcracking is reduced.

It is important to emphasize that when entrained air is added to regular weight concrete, it increases the elastic mismatch between the dense aggregates and the air-entrained mortar while, in structural LWAC, the effect is to bring the elastic characterstics of the two phases closer together. In ordinary concrete, the stiffness of the aggregate is from two to more than six times the stiffness of the mortar, whereas in the concretes composed of structural grade lightweight aggregates, the two fractions are quite similar. Use of a large sized, rigid, dense aggregate in concrete mixtures with a high air content enlarges the stress concentrations at the interface between the aggregate and the matrix.

Goodier analyzed the stresses in and around a spherical inclusion embedded in an infinite matrix.[25] It shows how the stress concentrations change as the concrete progresses from the fresh condition to a mature, fully hydrated material. All concretes start with an infinitely stiff inclusion relative to the matrix with maximum and minimum principal stresses of 2.00 and 0.57 developing when an uniaxial unit compressive stress is applied.[26] The maximum compressive stress occurs at the top (pole) and the bottom of the inclusion when loaded vertically (through the poles) and the maximum principal tensile stress occurs approximately between the pole and the equator with the crack propagating out from the surface of the spherical inclusion.

With mature normal concrete, the stiffness of the cement paste matrix is about 50% and less of the stiffness of the aggregate inclusion and the stress concentrations are reduced to 1.33 and 0.15. With LWAC, the stiffness of the matrix tends to match the stiffness of the aggregate and the stress concentrations become about 1.000 and 0. When the stiffness of the matrix and the inclusion become equal, the concrete experiences uniform uniaxial compressive stress and could be expected to have a reasonably straight stress-strain curve up to failure with a stress-induced microcracking occurring only near ultimate strength.

Its practical implication is that the lightweight concrete tends to have a lower permeability to gases and aggressive liquids than does regular concrete when subjected to load. Nishi et al.,[27] reported that for both fresh water and sea water test programs, Japanese structural LWAC demonstrated greater resistance to penetration than the regular weight concrete. They have suggested that there is probably a formation of a coating layer of dense cement paste surrounding the particles of the artificial lightweight coarse aggregates.

3.3 Pozzolanic Interaction

A lightweight aggregate has a glassy surface, which is formed during the sintering process. This phase is amorphous, thus potentially reactive. In general, well sintered clays at high temperature work like pozzolanic material. This pozzolanic material interacts chemically with the calcium hydroxide produced during the hydration of cement. In a Russian study done by Khokhorin[24] pozzolanic reactivity of keramzite aggregates is reported. Scanning electron micrographs revealed new chemical formations at the interfacial zone between the lightweight aggregate and the matrix. Further, the microhardness tests of the interfacial zone between the

lightweight aggregate and the matrix indicated the width of the ITZ to be approximately 60 μm. The microhardness of the matrix within the ITZ was 9–15 MPa while outside it was 6–9 MPa. This shows that the newly formed product is hard.

The pozzolanic interactions were also studied by Zhang and Gjörv,[22] who reported that the reaction occurred, but the effect was not so pronounced. It may be that the concrete was made with a very low water-to-cement ratio, namely 0.3. Out of this, part of the water might have been absorbed by the aggregates. The actual water available for the hydration of the cement was not enough. This can be one of the reasons for non-effectiveness of the pozzolanic reaction.

3.4 Elemental Distribution

Sarkar, et al.,[16] studied the microstructures of LWAC compositions given in Table 6.3 and the cube compressive strength and density in Table 6.4. Zhang and Gjörv[22] also studied the microstructure, as described in Sec. 3.0. Though the LWA used in these two cases were the same, there was difference in the water-to-cement ratio and type of cement. The water-to-cement ratio was very low and the cement used was a special cement, one which is different from the standard portland cement (see Table 6.2).

Zhang and Gjörv[22] claimed the presence of a calcium-enriched paste-aggregate interfacial zone in some lightweight aggregate concretes, whereas this zone was indistinguishable from the x-ray mapping that was done by Sarkar, et al.[16] (See Fig. 6.22.) The aggregates were virtually devoid of calcium, although its concentration was extremely high in the paste region. Apart from cement hydrate components, calcium dissolution from the aggregates may have contributed to its high concentration in the paste region.

Other differences were also noted in the internal structure. For example, the potassium and iron distribution in the Swedish Leca™ was uniform (Fig. 6.22a), whereas potassium formed an external rim in the Liapor™ 5 aggregate (Fig. 6.22b).[16] Iron in this aggregate, however, was as evenly distributed in the solid spaces as in the Swedish Leca™. The Liapor™ 6 concrete showed an unusually dense concentration of both potassium and sulfur in the paste (Fig. 6.22c). Solubility test results (Table 6.5) confirm a high dissolution rate of these ions from the Liapor™ 6 aggregate compared with the Swedish Leca™. The concrete composition using Swedish Leca™, Liapor™ 5, and 6 are shown in Table 6.3, no. 3, 6, and 8, respectively.

Table 6.3. Composition and Slump of Lightweight Aggregate Concrete[16]

No.	Aggregate type	Aggregate volume(m^3/m^3) A[a]	B[b]	Sand kg/m^3	Cement kg/m^3	CSF kg/m^3	BSF kg/m^3	Adm.[c]	W/C,W/B[d]	Slump mm
1	Sw. Leca™	0.167	0.167	863	400	-	-	0.20[e]	0.44	30
2	Sw. Leca™	0.163	0.163	851	444	-	-	0.63[f]	0.44	170
3	Sw. Leca™	0.192	0.129	823	444	22	-	0.60[f]	0.45/0.42	42
4	Liapor™ 5	0.159	0.159	838	384	-	-	0.30[e]	0.51	60
5	Liapor™ 5	0.163	0.163	826	259	-	109	0.30[e]	0.85/0.60	40
6	Liapor™ 5	0.153	0.153	804	337	34	-	0.36[e]	0.64/0.58	60
7	Liapor™ 6	0.171[g]	0.170	845	342	34	-	0.36[e]	0.51/0.46	30
8	Liapor™ 6	0.158[g]	0.157	804	385	-	-	0.30[e]	0.56	160
9	Liapor™ 8	0.178[g]	0.178	873	445	-	-	0.40[e]	0.42	80

a Size 2–6 mm for Swedish Leca™ and 1–4 mm for Liapor™

b Size 4–10 mm for Swedish Leca™ and 4–8 mm for Liapor™

c Adm., Chemical admixture, calculated on the weight of binder (%dry wt)

d W/C=water/cement ratio, W/B = water/binder ratio

e Chemical admixture, lignosulphonate

g Liapor™ 5

f Chemical admixture, melamine type

BSF Blast furnace slag

CSF Condensed silica fume

Table 6.4. Compressive Strength and Density of LWA Concrete of the Composition Shown in Table 6.3[16]

No.	Aggregate type	Compressive strength MPa			Density kg/m^3
		1 day	7 days	28 days	
1	Swedish Leca™	17.2	24.6	26.2	1544
2	Swedish Leca™	23.6	28.0	32.9	1567
3	Swedish Leca™	24.0	29.9	36.4	1619
4	Liapor™ 5	19.6	29.5	34.8	1634
5	Liapor™ 5	13.6	31.8	38.1	1714
6	Liapor™ 5	13.1	28.1	35.1	1661
7	Liapor™ 6	18.5	31.6	42.3	1635
8	Liapor™ 6	18.6	32.8	35.6	1620
9	Liapor™ 8	19.6	37.3	40.6	1619

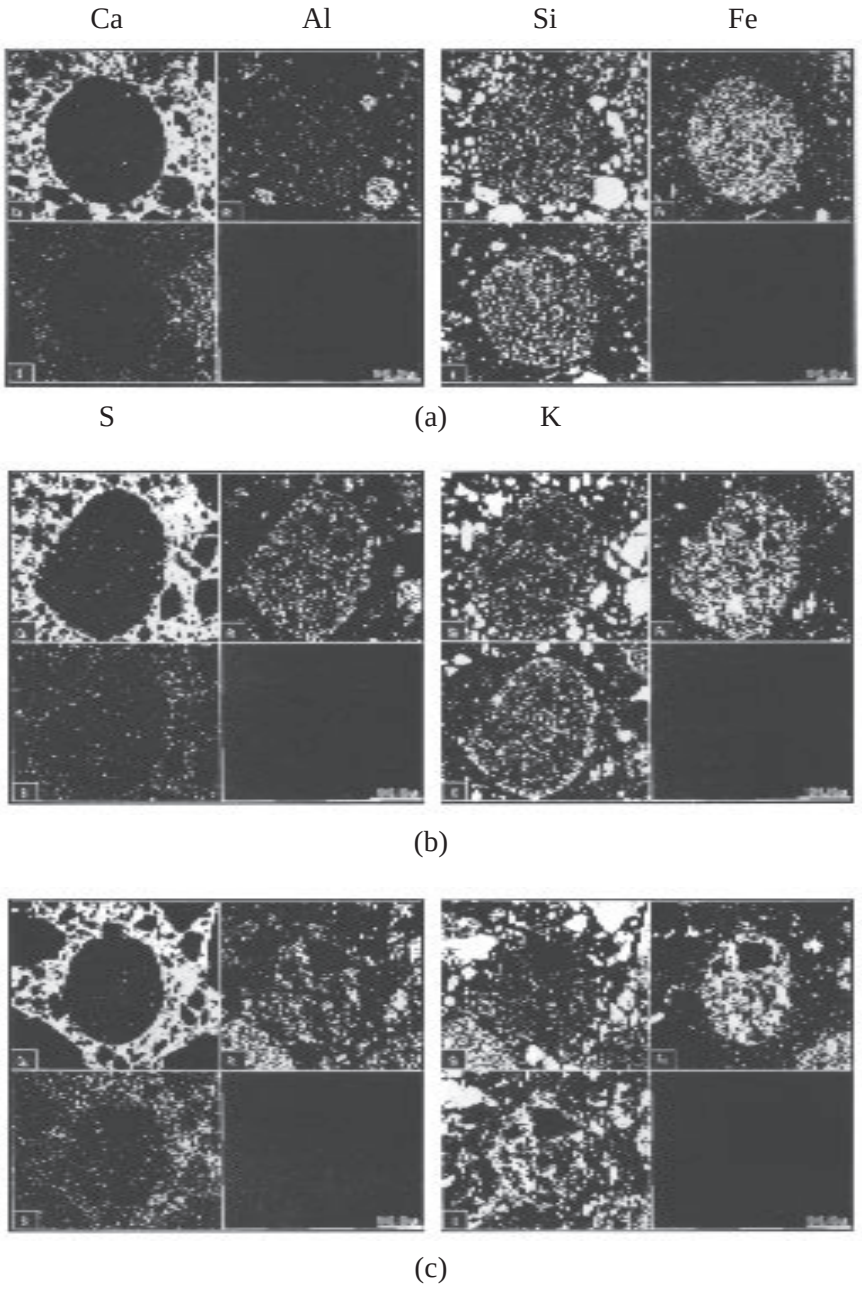

Figure 6.22. Elemental x-ray maps of Ca, Al, S, Si, Fe, and K, (*a*) Swedish Leca™ concrete composition 3, (*b*) Liapor™ 5 concrete composition 6, (*c*) Liapor™ 6 concrete composition 8. The composition is given in Table 6.2.[16]

Table 6.5. Solubility of Selective Ions (mg/litre) of Lightweight Aggregates[16]

Aggregates	Si	Al	Fe	Mg	Ca	Na	K	SO_4
Sw. Leca™	3.3	1.7	0.1	0.4	610	10.0	9.0	40.3
Liapor™ 5	3.4	0.8	0.1	0.3	700	14.5	58.4	385.0
Liapor™ 6	3.3	0.9	0.1	0.4	660	16.8	54.7	423.6
Liapor™ 8	4.2	1.0	0.1	0.3	530	9.0	35.8	453.3

The partially matching patterns of aluminum and silicon distribution in these aggregates suggest aluminum silicate as one of the mineral components, whereas iron is either located in silicate minerals or occurs individually, and its likely composition is hematite. This confirms the presence of these minerals, which was indicated by XRD. The exact location of quartz could not be precisely determined from x-ray mapping. The dark coloration in the external shell may be partly related to optical isotropism as a result of the presence of semi-amorphous and amorphous phases.

Some of the sulfur visible in the x-ray maps of the other concretes could have resulted from the use of chemical admixtures, which are sulfonated compounds relatively rich in sulphur. Similar findings were reported earlier in high strength concrete containing a superplasticizer.[28] Zhang and Gjörv, who also reported high concentration, concluded this to be due to the ettringite formation. The aluminum distribution, however, failed to demonstrate a preponderance of aluminum, another major component mineral in this zone.

4.0 INTER-RELATION OF MICROSTRUCTURE AND THE STRENGTH OF LWAC

Strength and microstructures are generally studied separately, and there is not much literature showing the dependence of the microstructure on the strength of concrete. Sarkar, et al.,[16] studied the microstructure and

the strength of LWAC of the compostion shown in Table 6.3 and the strength of the respective concretes shown in Table 6.4, and have correlated the microstructure to the strength.

Strength of concrete, in general, is related to its microstructure, but this is not the only factor responsible for strength development. A number of other related factors, such as batch composition, dosage, and type of chemical admixtures, water-to-cement or water-to-binder ratio, porosity, density, etc., also play dominant roles. Careful microstructural examination, however, does reveal the importance of the external and internal structure of lightweight aggregates in the development of paste-aggregate bond, the effect of water-to-cement ratio, and mineral admixtures on the porosity of paste.

The typical fracture surface (Fig. 6.23) of Swedish Leca™ aggregate concrete (composition 3), shows a 10–20 μm smooth impermeable external shell of the aggregate, in addition to a strong paste-aggregate bond. The compactness of the paste is due to the use of 5% silica fume by weight, and low water-to-binder ratio in the concrete. Silica fume is known for its high pozzolanicity and micro-filler action. It contributes to enhancing the early strength. In the case of Liapor™ 6 (composition 8, Table 6.3), an intimate bond between the paste and aggregate is evident (Fig. 6.24).

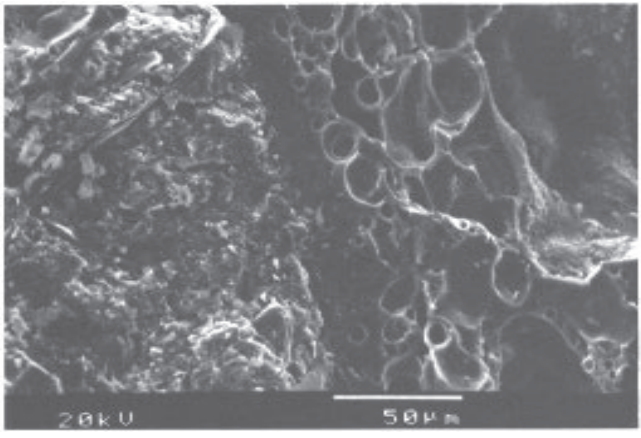

Figure 6.23. The paste aggregate microstructure of Swedish Leca™ aggregate concrete, (composition 3, Table 6.3) showing the thick impermeable external surface, dense paste and strong paste-aggregate bond.[16]

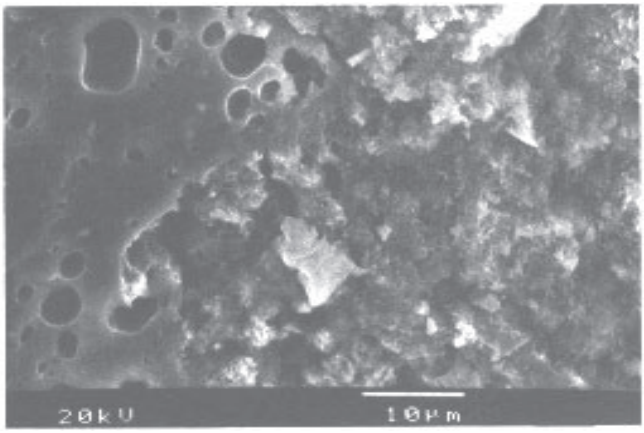

Figure 6.24. The strong bond between the rough external surface of Liapor™ 6 aggregate and paste (composition 8, Table 6.3). The paste is porous.[16]

This agrees with the hypothesis that the rough external surface of lightweight aggregate can act as an anchor for the paste. The roughness of the surface can be clearly seen in Fig. 6.25. The porous nature of the paste is due to the relatively high water-to-cement ratio (0.54). Some ettringite crystals are developed in the vacant spaces of the paste-aggregate interfacial zone (Fig. 6.26).

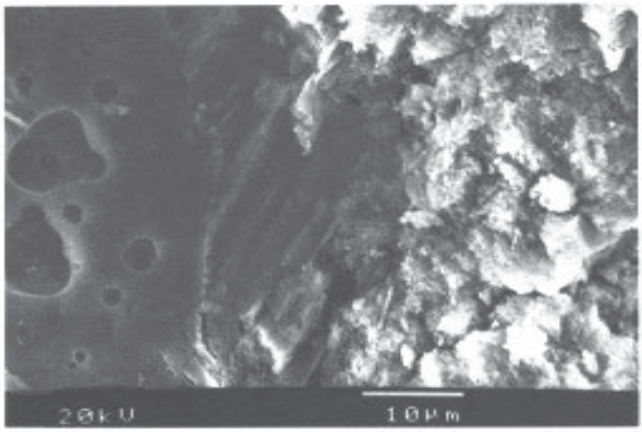

Figure 6.25. The rough external surface of Liapor™ 6, (composition 8, Table 6.3).[16]

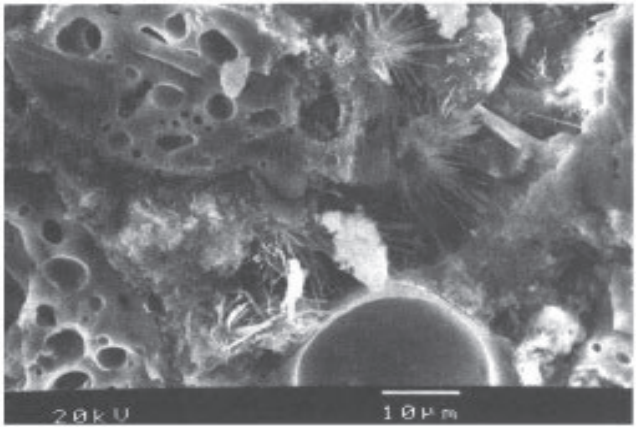

Figure 6.26. Ettringite needles formed in the paste-aggregate interfacial zone of concrete with Liapor™ 8, (composition 8, Table 6.3).[16]

The high interconnectivity and absence of the dense external shell of the Liapor™ 8 aggregate is seen in Fig. 6.27 (composition 9, Table 6.3). However, the extremely rough surface of this aggregate helps to form a much stronger bond, which directly imparts high strength. The paste of this concrete, which has a water-to-cement ratio of 0.42, is not as porous as that of concrete 7.

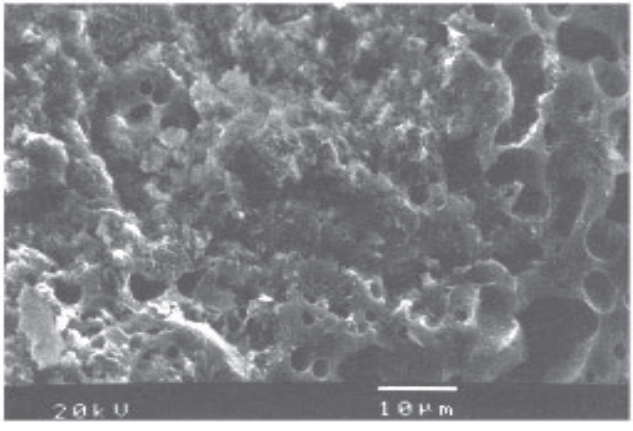

Figure 6.27. Interlocking nature of paste-aggregate bonding in Liapor™ 8 concrete, (composition 9, Table 6.3).[16]

Concrete 6, made with Liapor™ 5, has also shown a strong bond (Fig. 6.28). The paste is dense, as in concrete 2, by virtue of its content of 10% by weight of silica fume. The impermeable shell and rough exterior of Liapor™ 5 are also distinctly visible.

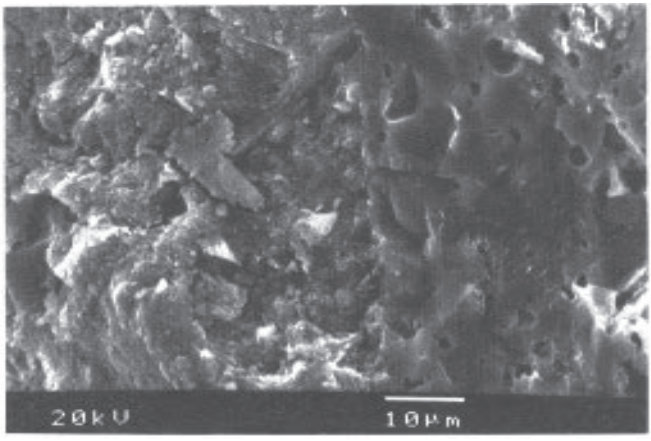

Figure 6.28. The paste-aggregate bonding in Liapor™ 5 concrete (composition 6, Table 6.3). The impermeable external shell of the aggregate and the dense paste are also visible.[16]

4.1 Influence of Water-to-Cement Ratio

The influence of the water-to-cement ratio or water-to-binder ratio and particle density of the lightweight aggregate used (Table 6.3) are seen in concrete 6 and 7. In principle, the strength of the lightweight aggregate concrete is related to the density of concrete. The strength increases when the density increases, assuming that the lightweight aggregate and water-to-cement ratio is unchanged. Concrete 7 has greater strength than concrete 6, despite the higher density of the latter. The explanation of this is the lower water/cement ratio in concrete 7, and the higher density of the aggregate. The particle density of Liapor™ 6 is 1052 kg/m^3 and is higher than that of Liapor™ 5 which is 897 kg/m^3.

Silica fume appears to have little effect on the early strength of concretes made with aggregates with a rough external surface (Liapor™ 5 and 6). Some positive influence on the early strength seems to occur in mixes containing the Swedish Leca™, which has a smooth surface.

A 30% weight replacement of cement by slag, together with Liapor™ 5 aggregate, develops a low early strength, but 28 day strength is higher than that of some of the other concretes in the series. This is because of the latent hydraulic properties of slag, which helps to enhance the late age strength. Concrete 5 also has a high density.

Oriented calcium hydroxide crystals that are normally present at the paste-aggregate interface in conventional concrete could not be detected in the fracture specimens of the lightweight aggregate concretes. One reason is that the calcium hydroxide reacts slowing the pozzolanic effect, and the other is that the water absorption capacity of the lightweight aggregate lowers the water content in the paste-aggregate interfacial zone.

5.0 CONCLUDING REMARKS

The microstructure study of lightweight aggregate concretes reveals that the paste-aggregate bonding is dependent on the nature of the external shell of the aggregate. Mechanical interlocking plays an important role in strengthening the interface. Absence of the oriented calcium hydroxide crystals at the interface is related to the water absorption by the aggregate. It is demonstrated that distinct refinement of the interfacial zone can be obtained, provided the other factors are optimized.

There is some microstructural evidence of pozzolanic activity of LWA, which is possible due to the chemical reaction. About 10% by weight addition of silica fume helps to improve the early strength in some cases, whereas positive evidence of the latent hydraulicity of slag was noted in the concrete containing 30% by weight of cement replacement.

REFERENCES

1. Mehta, P. K., *Concrete Structures, and Material*, p. 38, Prentice Hall, NJ (1986b)
2. Scrivener, K. L., and Pratt, P. L., A Preliminary Study of the Microstructure of the Cement/Sand Bond in Mortars; *Proc. 8th Int. Congress on the Chemistry of Cement*, Finep, Rio de Janerio, Brazil, 1:466-471 (1986)

3. Langton, C. A., and Roy, D. M., Morphology and Microstructure of Cement Paste/Rock Interfacial Regions, *Proc. 7th Int. Congress on the Chemistry of Cement*, Editions Septima, Paris, VIII:VII-127–132 (1980)
4. Bentur, A., Gray, R. J., and Mindess, S., Cracking and Pull out Process in Fiber Reinforced Cementitious Materials, paper 6.2, *Developments in Fiber Reinforced Cement and Concrete*, RILEM, Vol. 2, (R. N. Swamy, R. L. Wagstaffe, and D. R. Oaklay, eds.) (1986)
5. Diamond, S., Mindess, S., and Lovell, J., On the Spacing Between Aggregate Grains in Concrete and the Dimension of the Aureaole of Transition, *Liaisons Pates de Ciment Materiaux Associes*, RILEM Colloquium, pp. C 42–46 ,Toulouse, France (1982)
6. Mindess, S., and Diamond, S., The Cracking and Fracture of Mortar, *Mater. Construction (Paris)*, 15(86):107–113 (1982a)
7. Mindess, S., and Diamond, S., A Device for Direct Observation of Cracking of Cement Paste or Mortar under Compressive Loading within a Scanning Electron Microscope, *Cem. Concr. Res.*, 12(5):569–576 (1982b)
8. Hillemeier, B., and Hilsdorf, H. K., Fracture Mechanics Studies on Concrete Compounds, *Cem. Concr. Res.*, 7(5):523–536 (1977)
9. Ziegeldorf, S., Fracture Mechanics Parameters of Hardened Cement Paste, Aggregate and Interfaces, *Fracture Mechanics of Concrete*, (F. H. Wittmann, ed.), Elsevier, Amsterdam (1983)
10. Bentur, A., and Mindness, S., The Effect of Concrete Strength on Crack Patterns, *Cem. Conc. Res.*, 16(1):59–66 (1986)
11. Maso, J. C., The Bond Between Aggregates and Hydrated Cement Paste, *Proc. 7th Int. Congress on the Chemistry of Cement*, Editions Septima, Paris, I:VII 1/3–1/15 (1980)
12. Alexander, K. M., and Taplin, J. H., *The Structure of Concrete*, Cement and Concrete Association, London (1964)
13. Monterio, P. J. M., and Mehta, P. K., Interaction Between Carbonate Rock and Cement Paste, *Cem. Conc. Res.*, 16:127–134 (1986)
14. Mehta, P. K., Influence of Pozzolanic Admixture on the ITZ in Concrete, *Durability of Concrete-Aspects of Admixture and Industrial By-products*, Int. Seminar, April 1986, Göteborg, Sweden, D1-1988, Swedish Council for Building Research, Stockholm, pp. 67–81 (1988)
15. Hjorth, L., Micro-Silica in Concrete, *Nordic Concrete Research*, 1:901–918 (1982)
16. Sarkar, S. L., Chandra, S., and Berntsson, L., Interdependence of Microstructure and Strength of Structural Lightweight Aggregate Concrete, *Cement and Concrete Composite*,14:239–248 (1992)

17. Swamy, R. N., and Lambert, G. H., The Microstructure of Lytag™ Aggregates, *Int. J. Cem. Comp. Lightweight Concrete*, 3(4):273–282 (1981)

18. Bolendran, R. V., PhD Thesis, University of Wales Institute of Science and Technology, p. 387 (1980)

19. Teychene, D. C., Lightweight Aggregates–Their Properties and Uses in Concrete in the U.K., *Proc. 1st Int. Congress on Lightweight Concrete*, 1:23–37 (May 1968)

20. Zhang, M. H., and Gjörv, O. E., Characteristics of Lightweight Aggregates for High Strength Concrete, *ACI Materials Journal*, 88:273–282 (1991)

21. Scrivener, K. L., and Pratt, P. L., Backscattered Electron Images of Polished Sections in the Scanning Electron Microscope, *Proc. 6th Int. Conf. Cement Microscopy*, New Mexico, USA, pp. 145–155 (Mar. 26–29, 1984)

22. Zhang, M. H., and Gjörv, O. E., Microstructure of Interfacial Transition Zone between Lightweight Aggregate and Cement, *Cem. Conc. Res.*, 20:610–618 (1990)

23. Holm, T. A., Three Decades of Durability, *The Military Engineers*, (Sep.-Oct. 1983)

24. Khokhorin, N. K., *The Durability of Lightweight Concrete Structure Members*, KvibySlev, USSR (1993)

25. Goodier, J. N., Concentration of Stress Around Spherical and Cylindrical Inclusions and Flaws, *J. Applied Mechanic, Transactions of ASME*, 55:A-39–A-44 (1933)

26. Bremner, T. W., and Holm, T. A., Elastic Compatibility and the Behavior of Concrete, *ACI Mater. J. Res.*, 83:(2) (Apr. 1986)

27. Nishi, S., Oshio, A., Sone, T., and Shirokeni, S., Water Tightness of Concrete Against Sea Water, *J. Central Research Laboratory*, Onada Cement Company, Tokyo, Jpn., 32(104):40–53 (1980)

28. Aitcin, P. C., Sarkar, S. L., and Datta, Y., Microstructural Study of Different Types of Very High Strength Concretes, *Proc. Materials Research Society Symp.*, MRS, Pittsburgh, 85:261–272 (1987)

29. Mehta, P. K., Hardened Cement Paste-Microstructure and its Relationship to Properties, *Proc. 8th Int. Congress on the Chemistry of Cement*, Finep, Rio de Janerio, Brazil, 1:113–121 (1986a)

30. Zhang, M. H., and Gjörv, O. E., Pozzolanic Reactivity of Lightweight Aggregate, *Cem. Conc. Res.*, 20:884–890 (1980)

7

Physical Properties of Lightweight Aggregate Concrete

1.0 INTRODUCTION

Physical properties are properties of concrete which keep the integrity of the structure. Strength is the cardinal property of concrete. It is the base property used by the architects for designing structures. In importance, strength is closely followed by density. Lightweight aggregate concretes are of various types, depending upon the composition of the mortar matrix and the aggregates used. The properties of the aggregates also vary significantly depending upon the raw materials used for making them and the technique adopted to produce them. When the concrete hardens, it changes in volume. This is significant for the stability of the structure and is determined by measuring the length changes over time. The following physical properties are reviewed in this chapter:

Density and Strength

Elasticity

Shrinkage and Creep

Thermal Conductivity

Abrasion Resistance

2.0 DENSITY AND STRENGTH

The relationship between the size and strength of LWA made by heat treatment is a function of compaction and void formation during burning. The larger pellets are less compacted in their outer layers with resultant larger voids. Furthermore, the larger the size of the pellets, the lower the bulk density and, more importantly, the lower the strength of the aggregate.

In general, the strength of LWA can be related to the resulting concrete strength and is often referred to as the "ceiling strength." A relationship between the type of aggregate, density and strength of concrete, and its field of utilization is shown in Fig. 7.1.[1]

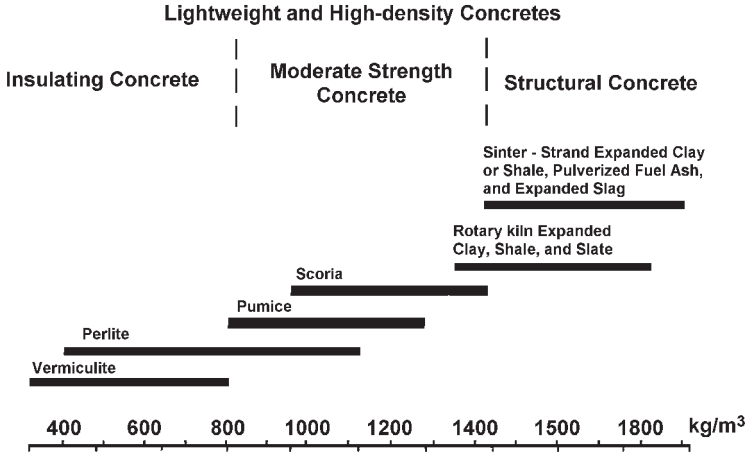

Figure 7.1. Typical ranges of densities of concretes made with various lightweight aggregates.[1]

The density and, thereby, the strength of lightweight aggregates depend upon the raw material used for making them. Even the aggregates produced from the same raw material, but using different production techniques, can vary in their density and strength. This makes it difficult to specify the density of different types of aggregates produced from the particular raw material. The air-dry particle densities of some of the lightweight aggregates are given in Table 7.1.

Table 7.1. Air-Dry Densities (Loose) of Lightweight Aggregates

Aggregate Type	Air-dry Density	
	kg/m^3	lb/ft^3
Clinker	720 – 1040	45 – 65
Sintered pulverized ash	770 – 960	48 – 60
Foamed slag	560 – 960	35 – 60
Expanded clays and slag	320 – 960	20 – 60
Expanded slate	560 – 860	35 – 54
Pumice	480 – 880	30 – 55
Palm oil shell	550 – 650	34 – 45
Diatomite	450 – 800	28 – 50
Wood particles	320 – 480	20 – 30
Expanded perlite	80 – 120	5 – 20
Expanded vermiculite	60 – 160	4 – 10

Apart from the density of the aggregates, the density of the concrete also depends upon the grading of the aggregates, their moisture content, mix proportions, cement content, water-to-binder ratio, chemical and mineral admixtures, etc. Besides the material, it also depends upon the method of compaction, curing conditions, etc. Usually the low density concretes are suitable only for non–load-bearing applications, such as partitions, screeds, and for insulating purposes, whereas compacted lightweight concretes with densities varying from 1550 to 1850 kg/m^3 (85 to 115 lb/ft^3) can usually be reinforced or prestressed and used in load-bearing structures. Lightweight concretes with intermediate densities varying from 800 to 1350 kg/m^3 (50 to 85 lb/ft^3) are extensively used in precast blockwork for load-bearing and heat-insulating walls.

Insulating building blocks are made with low strength aggregates. One example is Maplelite building blocks produced with pumice aggregates. The standard block has an average compressive strength of 3.5 MPa, but can be manufactured with strengths up to 7.0 MPa. The average density of the Maplelite block is 978 kg/m^3 at 3% moisture content, with oven-dry density at 950 kg/m^3. Thermal conductivity of these blocks is 0.20 W/mK at 3% moisture content.

Different classes of lightweight aggregate concretes have been developed at the Chalmers University of Technology, division of Building Materials, with the densities varying from 800 to 1300 kg/m^3 and the compressive strengths varying between 7.3 MPa and 25.5 MPa.[2]–[4] Structural lightweight aggregate concrete was also developed having a density of 1650 kg/m^{3}and strength up to 45 MPa.

Properties of the lightweight aggregate concretes are discussed here in comparison to normal weight concrete, K40, having a cube compressive strength of 40 MPa. Compositions of these lightweight aggregate concretes are shown in Table 7.2. The concretes of series X are made using pumice and polystyrene aggregates and 3L concrete is made using expanded clay aggregate, Swedish Leca™. Specifications for the material used are listed.

Table 7.2. Composition of Lightweight Aggregate Concrete[3]

Ingredients	Concrete Type*				
	K40	XL	XT	XB	3L
Cement	399	270	310	300	342
Water	184	133	156	149	176
CEMOS	0	3	3	3	3
Fine aggregates: 0–8 mm	988	0	0	0	0
Stones: 8–16 mm	749	0	0	0	0
Sand: 0–2 mm	0	184	246	257	422
Leca™: 2–4 mm	0	0	0	0	241
Leca™: 4–8 mm	0	0	0	0	165
Pumice	0	483	538	435	0
Polystyrene	0	7	4	5	0

* The values shown are in kg/m^3.

- Cement used was ordinary portland cement supplied by Cementa AB, Slite, Sweden.

- Sand: 0–4 mm
- Lightweight aggregates:

  Expanded polystyrene beads, 0.5–2 mm, delivered by Brännebruna AB. The density of the polystyrene beads was 50 kg/m^3.

  Pumice aggregates, 2–19 mm, were wet sieved. The aggregates were left for 3 days, and the moisture ratio at casting was 50–80%.

  Leca™, 2–4 mm, and Leca™, 4–8 mm, expanded clay aggregates supplied by Swedish Leca™ AB. The particle density of the aggregates of more than 2 mm size was 700 kg/m^3.

  Normal aggregates used were fine aggregates, 0–8 mm, and stones of 8–16 mm size.
- CEMOS: a chemical admixture supplied by BOFORS AB. Sweden.

Lightweight aggregates do not mix homogeneously. This problem was solved by using a very special chemical admixture, "CEMOS." It is an asphalt-modified acrylic polymer dispersion. It works as a dispersing agent, water reducer, and hydrophobing material. The densities and the compressive strengths of these concretes are shown in Table 7.3 at different ages. The density, strength, thermal conductivity, and drying shrinkage of some of the concretes made with vermiculite and perlite aggregates are shown in Table 7.4. The density, strength, and modulus of elasticity of some of the concretes made with various types of aggregates are shown in Table 7.5. The strength of concrete is not related only to its density, it is related to factors like the strength of the mortar matrix, strength of the aggregates, and the bond between the aggregates and the matrix. Further, it is noticed that the general concept, "More cement produces higher strength concrete," does not hold true. For example, in the use of foamed slag, with a cement content of 740 kg/m^3, concrete of 31.5 MPa strength and 2000 kg/m^3 density was produced, whereas, in the case of Solite™ aggregates, 540 kg/m^3 cement has produced a concrete of 42.0 MPa with a density of only 1650 kg/m^3, i.e., a concrete with about 40% less cement, which reduces the cost. Further, it lowers the density by 20% and produces a concrete with 25% higher strength with a larger volume of concrete, which will further reduce the cost.

Table 7.3. Density (D in kg/m^3) and Compressive Strength of Concrete (S in MPa)[4]

Concrete Type	1 Day		7 Days		28 Days		180 Days	
	D	S	D	S	D	S	D	S
XL	1080	1.8	960	5.5	870	7.8	820	7.4
XB	1200	3.3	1100	7.7	1015	9.6	940	11.7
XT	1255	2.9	1160	8.3	1050	10.7	955	11.5
3L	1350	10.7	1350	21.8	1360	25.4	1300	27.0
K40	2320	15.3	2330	36.2	2335	46.4	2250	52.4
Thermal conductivity of X-concrete at 105°C is 16 W/mK.								

Table 7.4. Some of the Typical Properties of Insulating Lightweight Aggregate Concrete[5]

Aggregate Type	Cement: Aggregate (by volume)	Air-dry Density kg/m^3	Minimum 28 day Cube Strength MPa	Thermal Conductivity W/mK	Drying Shrinkage %
Vermiculite	1:8 1:6 1:4	400 480 560	0.70 0.95 1.23	0.094 to 0.158	0.35 to 0.45
Perlite	1:7 1:6 1:5 1:4	400 480 560 640	1.40 2.17 3.43 4.83	0.098 to 0.155	0.14 to 0.20

Table 7.5. Some of the Typical Properties of Lightweight Aggregate Concrete[5]

Aggregate Type	Quantity per m^3 of Concrete				Air-dry Density kg/m3	Min. 28 Day, Cube Strength MPa	Modulus of Elasticity $N/mm^2 \times 10^6$
	Cement	Aggregates					
		Fine	Medium	Coarse			
Leca™	310	0.65	—	0.65	1000	7	0.011 to 0.018
	370	0.65	—	0.65	1200	10.5	
	460	0.6	0.6	—	1300	16	
	360	0.4	—	0.8	1350	14	
	360	0.45	—	—	1500	16	
Aglite™	300	0.7	0.7	—	1600	21	0.014 to 0.018
	440	0.65	0.7	—	1650	26.5	
	480	0.65	0.7	—	1700	31.5	
Solite™	390	0.65	—	0.8	1600	21	0.011 to 0.018
	450	0.6	—	0.8	1600	28	
	490	0.6	—	0.8	1650	35	
	540	0.6	—	0.8	1650	42	

Table 7.5. *(Cont'd.)*

Aggregate Type	Quantity per m^3 of Concrete				Air-dry Density kg/m^3	Min. 28 Day, Cube Strength MPa	Modulus of Elasticity $N/mm^2 \times 10^6$
	Cement	Aggregates					
		Fine	Medium	Coarse			
Lytag™	320	0.57	—	0.73	1600	21	0.014 to 0.018
	380	0.49	—	0.77	1700	26	
	480	0.41	—	0.78	1800	31.5	
Foamed slag	470	0.73	—	0.73	1800	16	0.014 to 0.021
	500	0.76	—	0.69	1900	21	
	740	0.52	—	0.52	2000	31.5	

The interrelation of compressive strength with the water-to-binder ratio, density, and age of the specimen is shown in Figs. 7.2–7.7. The properties of the aggregates used in this study are shown in Table 7.6.[6] For good comparison, dry aggregates were used in all the batches.

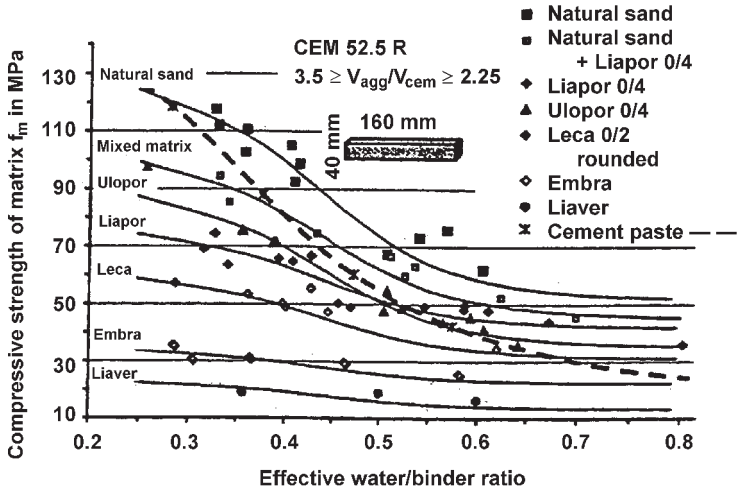

Figure 7.2. Relationship between water/binder ratio and compressive strength of different matrices.[6]

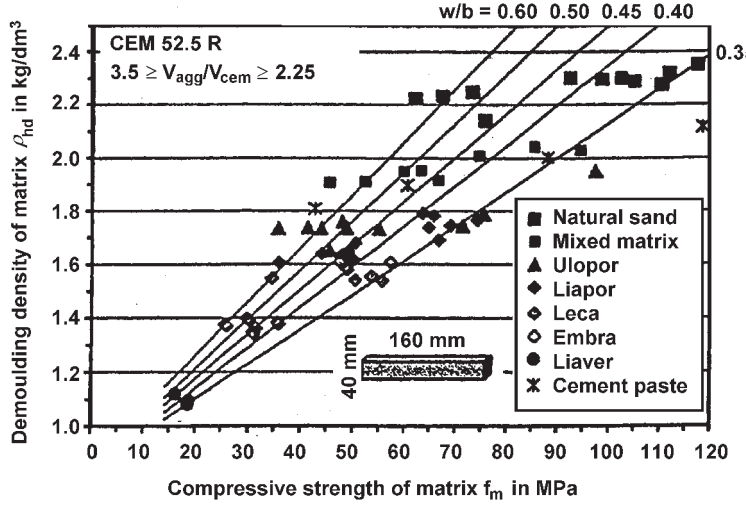

Figure 7.3. Relationship between demolding density and compressive strength of different matrices.[6]

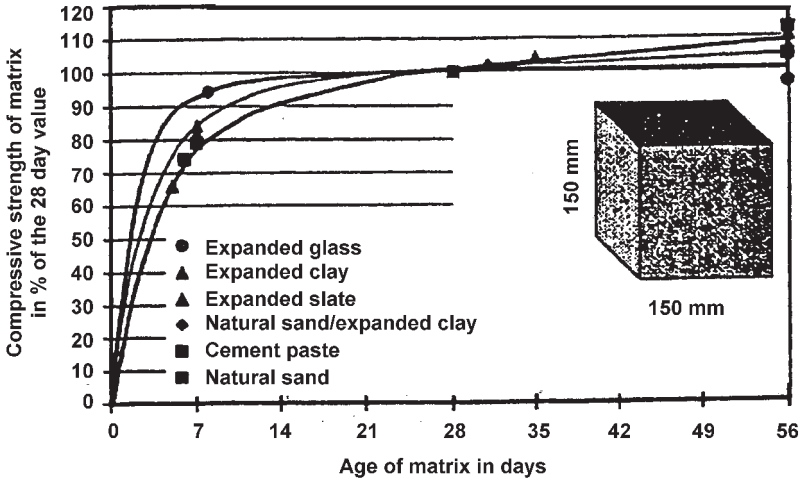

Figure 7.4. Development of compressive strength of different matrices over time.[6]

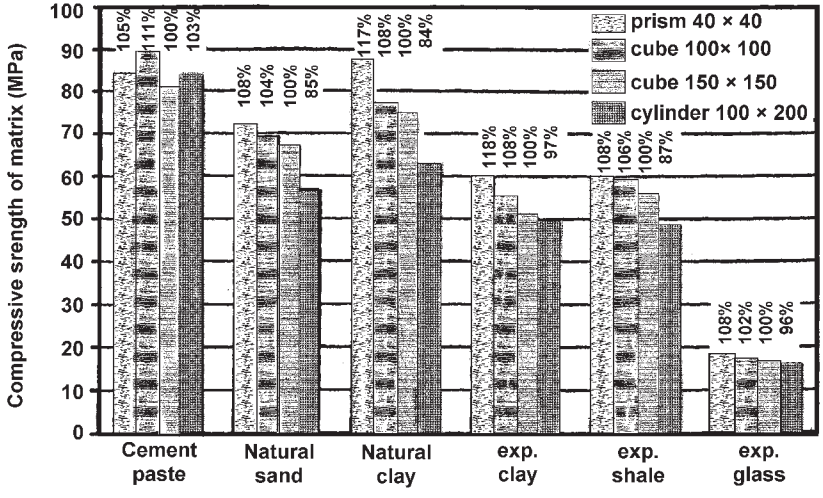

Figure 7.5. Influence of specimen shape of different matrices on compressive strength.[6]

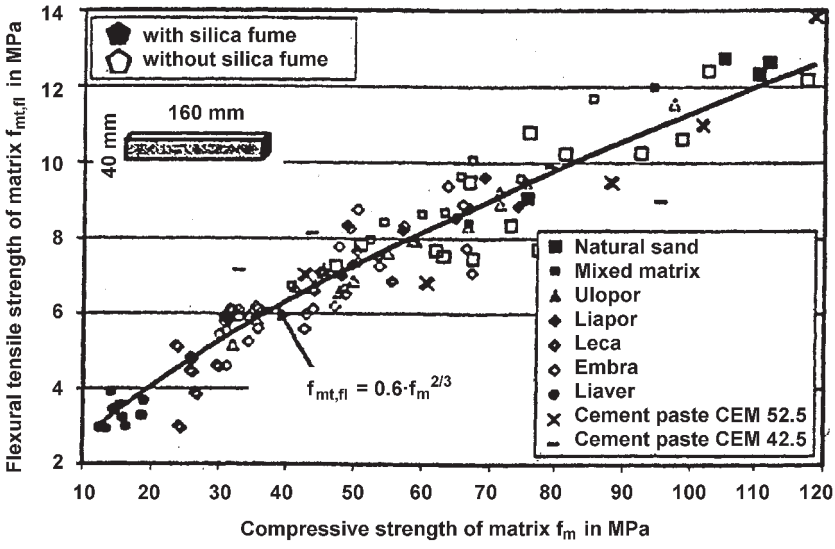

Figure 7.6. Relationship between compressive and flexural tensile strength of different matrices.[6]

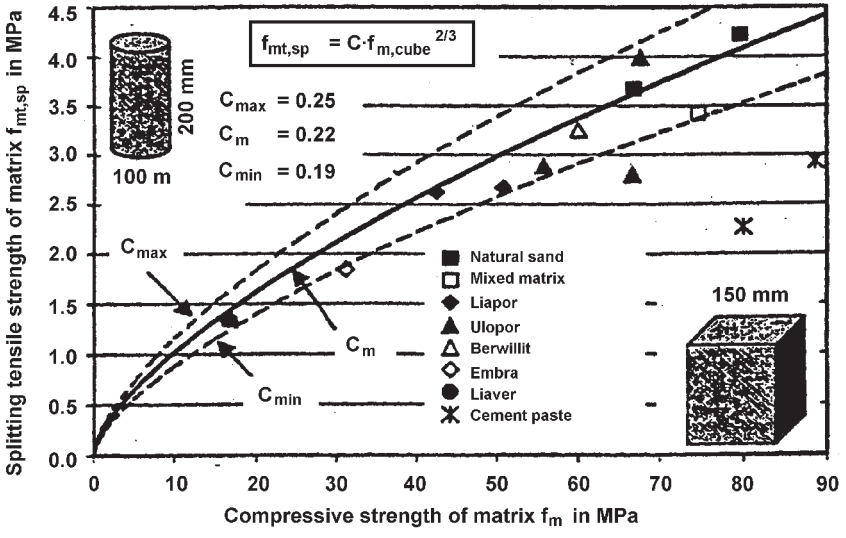

Figure 7.7. Relationship between compressive and splitting tensile strength of different matrices.[6]

Table 7.6. The Properties of the Aggregates Used[6]

	Fine Aggregate	Producer	Particle Geometry	Aggregate Size		Particle Density, kg/m^3		Water Absorption, M%
1	Natural sand		rounded	0/2		2.63		0
2	Natural sand + Liapor™, each 50% by volume			0/2	0/4	2.63	1.5	4.8
3	Expanded shale	Uloper	crushed	0/2	2/4	1.7	1.4	6.2
4	Expanded clay	Liapor™	crushed	0/4		1.5		4.8
5	Expanded clay	Leca™	rounded	0/2		1.3		4.7
6	Expanded clay	Embra	rounded	0/4		0.79		4.6
7	Expanded glass	Liaver	rounded	0.25/0.5/1/2/4		0.54–0.29		4.4

The workability and compressive strength of the lightweight aggregate concrete made with palm oil shells is affected by the proportion of palm oil shells and the water-to-cement ratio. The 28 day cube compressive strengths vary between 5.0–19.5 MPa.

Variations in workability and compressive strength values of the lightweight concrete with different proportions of palm oil shells, sand, and water-to-cement ratios are shown in Figs. 7.8 (a, b, and c). These data are summarized in Table 7.7.

The replacement of natural sand by lightweight fine aggregates reduces the compressive strength of the matrix (Fig. 7.2). The loss of strength is more pronounced with the decreasing density of the matrix (Fig. 7.3). Simultaneously, the influence of the effective water-to-binder ratio becomes more significant in the case of a matrix of a lower density.

The gain in strength with decreasing water/binder ratio is reduced with a decreasing density of the fine aggregate (Fig. 7.2). Hence, the lighter or rather weaker aggregates reduce the beneficial effect of the stronger cement paste. This finding is comparable to the known relationship between the compressive strength of the matrix and the LWAC. Finally, the influence of the cement grade on the matrix strength is reduced with the decreasing density of the fine aggregate.

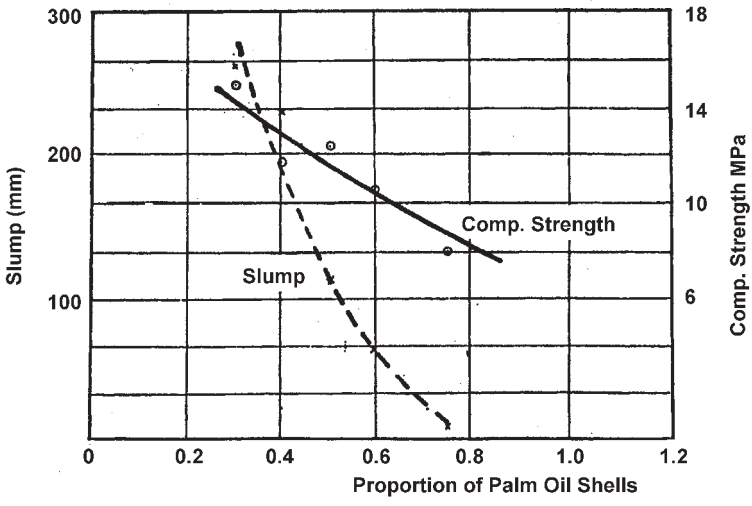

(a)

Figure 7.8. *(a)* Variation of slump and compressive strength with different proportions of palm oil shells. *(b)* Variation of slump and compressive strength with different proportions of sand. *(c)* Variation of slump and compressive strength with different water-to-cement ratios.[7]

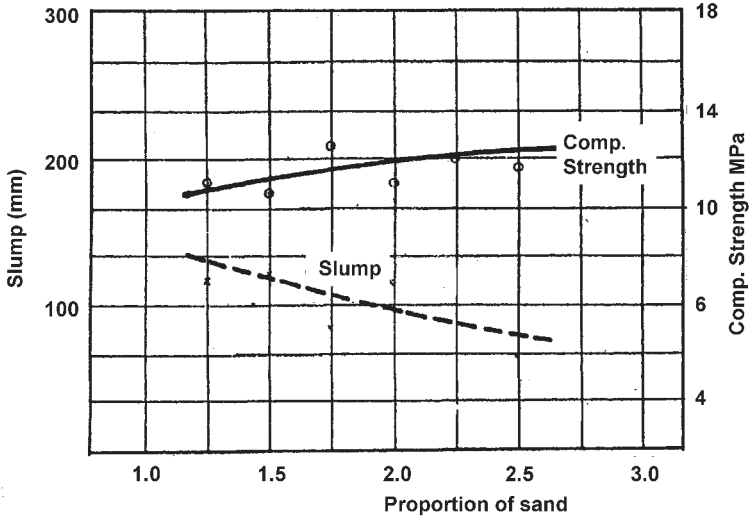

(b)

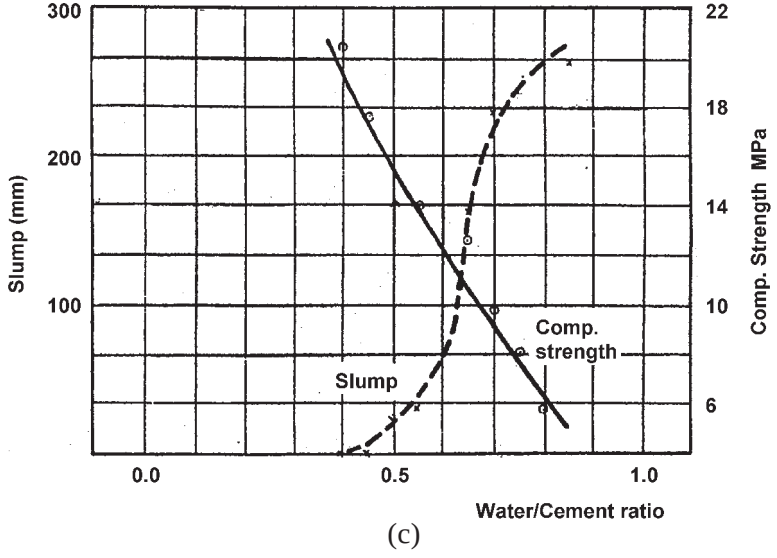

(c)

Figure 7.8. *(Cont'd.)*

Table 7.7. Workability and Compressive Strength with Different Proportions of Palm Oil Shells[7]

Mix Proportion*	Slump, mm	Air-dry Density, kg/m^3	Compressive Strength, MPa	
			7 days	28 days
1:1.5:0.5–1.0/0.6	200–0	1890–1725	10.0–2.5	15.0–5.5
1:2.0:0.5–1.0/0.6	230–5	1930–1780	8.0–2.0	11.5–5.0
1:2.5:0.3–0.75/0.6	260–10	1985–1895	9.5–5.5	15.5–8.0
1:1.25–2.5:0.6/0.6	115–60	1905–1935	7.0–8.0	11.0–11.5
1:2.0:0.6/0.40–0.85	0–260	2050–1840	16.5–0	20.5–0
* Mix proportion—cement:sand:palm oil shells/water-to-cement ratio.				

The development of the matrix compressive strength over time is faster, or equal in case of lightweight fine aggregates, in comparison to natural sand (Fig. 7.4). Particularly fine aggregate with a low particle density prevents a significant strain gain after a few days of placing. This result can be explained with the help of Fig. 7.2. The matrix with weak aggregates almost reaches the ceiling strength even with a high water-to-binder ratio.

The influence of the specimen shape on the compressive strength of different matrices is shown in Fig. 7.5. The rating was done on the basis of prisms.

Test specimens with the greatest dependence on shape were found in the case of the mixed fine aggregates (50 vol% each of natural sand and expanded clay fine aggregate). The selection of two aggregates with different stiffnesses seems to support the formation of microcracking, which makes the lateral expansion restrain due to the loading plates of the testing machine more effective.

The tensile strength of the matrix depends on the same parameters as the compressive strength. Therefore, a strong relationship between the tensile and compressive strength is expected. It is confirmed by the results presented in Figs. 7.6 and 7.7. The relationship is independent of the type of fine aggregate.

The compressive strength and the workability of lightweight aggregate concrete depend upon the proportion of aggregates, sand, and the water-to-binder ratio. This effect was illustrated by Abdullah[7] for lightweight aggregate concrete made with the addition of palm oil shells.

The mix proportion, density, and compressive strength of the concrete made with palm oil shells are shown in Table 7.7. It is seen that increase in the proportion of palm oil shells substantially decreases the slump, but not as much as compressive strength (Fig. 7.8a).

An increase in the proportion of sand decreases the slump, however, the decrease is not substantial. The compressive strength, on the other hand, increases, but the increase is not significant (Fig. 7.8b). The water-to-cement ratio has a significant influence on both the slump and the compressive strength. The slump increases and compressive strength decreases with the increase in the water-to-cement ratio (Fig. 7.8c).

Structural lightweight aggregate concrete was developed by Berntsson and Chandra[8] using expanded clay aggregates, Liapor™, and Swedish Leca™. High strength was achieved with the use of a superplasticizer and mineral admixture such as condensed silica fume, and blast furnace slag. The composition of the concrete and the strength development results are shown in Tables 7.8 and 7.9, 100 mm cubes were used for strength test.

The composition of the concrete tested was:

Ordinary portland cement	425 kg/m^3
Sand	850 kg/m^3
Swedish Leca™: 2–6 mm	310 l/m^3 (bulk volume)
Swedish Leca™: 4–10 mm	310 l/m^3 (bulk volume)
W/C	0.395
Superplasticizer	1% to the weight of cement

It is also shown that the density and the strength decrease with an increase in the amount of lightweight aggregates. Table 7.10 shows the density after normal curing. The compressive strength shown is after 28 days, both measured as well as calculated. A large deviation has been noted between the measured and calculated strength in the case of mortar. With the addition of a lightweight aggregate, which increases to one third the volume of the concrete, the compressive strength decreases to almost half of the mortar strength. The average bulk density of the lightweight aggregate is somewhat lower than 400 kg/m^3 (390 kg/m^3).

Table 7.8. Composition of Structural Lightweight Aggregate Concrete[8]

No.	Aggregate Type	Aggregate Volume in m^3/m^3		Sand, kg/m^3	Cement, kg/m^3	CSF, kg/m^3	BSF, kg/m^3	Admix-ture[c]	W/C W/B[d]	Slump, mm
		A[a]	B[b]							
1	Swedish Leca™	0.163	0.167	863	400	—	—	0.20[e]	0.44	30
2	Swedish Leca™	0.163	0.163	851	444	—	—	0.63[f]	0.44	170
3	Swedish Leca™	0.192	0.129	823	444	22	—	0.60[f]	0.45/0.42	42
4	Liapor™ 5	0.159	0.159	838	384	—	—	0.30[e]	0.51	60
5	Liapor™ 5	0.163	0.163	826	259	—	109	0.30[e]	0.85/0.60	40
6	Liapor™ 5	0.163	0.153	804	337	34	—	0.36[e]	0.64/0.58	60
7	Liapor™ 6	0.171[g]	0.170	845	342	34	—	0.36[e]	0.51/0.46	30
8	Liapor™ 6	0.158[g]	0.157	804	385	—	—	0.30[e]	0.56	160
9	Liapor™ 8	0.178[g]	0.178	673	445	—	—	0.40[e]	0.42	80

a Size 2–6 mm for Swedish Leca™ and 1–4 mm for Liapor™
b Size 4–10 mm for Swedish Leca™ and 4–8 mm for Liapor™
c Chemical admixture calculated on the weight of binder (dry wt%)
d W/C = Water-to-cement ratio, W/B= water-to-binder ratio
e Chemical admixture, lignosulfonate base
f Chemical admixture, melamine base
g CSF—Condensed Silica Fume; BSF—Blast Furnace Slag; Liapor™ 5

Table 7.9. Development of Compressive Strength[8]

No.	Aggregate Type	Compressive Strength, MPa			Density, kg/m^3
		1 day	7 days	28 days	
1	Swedish Leca™	17.2	24.6	26.2	1544
2	Swedish Leca™	23.6	28.0	32.9	1567
3	Swedish Leca™	24.0	29.9	36.4	1619
4	Liapor™ 5	19.6	29.5	34.8	1634
5	Liapor™ 5	13.6	31.8	38.1	1714
6	Liapor™ 5	13.1	28.1	35.1	1661
7	Liapor™ 6	18.5	31.6	42.3	1635
8	Liapor™ 6	18.6	32.8	35.6	1620
9	Liapor™ 8	19.6	37.3	40.6	1619

The densities mentioned here are after drying at 105°C for cubes cured for 28 days.

Table 7.10. Density and Strength of Concrete with Different Amounts of Leca™[8]

No.	Volume of Leca™ l/m^3	Slump, mm	Density,* kg/m^3	Compressive Strength,* MPa	
				Measured	Calculated
1	620	35	1660	32.2	32.2
2	464	45	1835	34.5	38.0
3	310	80	1905	39.3	45.0
4	155	80	2050	50.0	53.0
5	0	—	2265	75.0	64.0

* Density and strength shown are determined after 28 days.

2.1 High Strength Lightweight Aggregate Concrete

High strength lightweight aggregate concrete can be made in two ways:

1. By using pozzolanic materials like condensed silica fume (CSF) together with the cement, and using high-range water-reducing chemical admixtures.
2. By using high strength lightweight aggregates.

Recently, some special expanded slag aggregates were developed in Russia. These are called Expanded Slag Gravel (ESG) as they resemble gravel. With these aggregates, a lightweight aggregate concrete having 60 MPa cube compressive strength can be produced.[9]

The structural properties of lightweight aggregate concrete (LWAC) can differ significantly from normal weight concrete (NC) and depend upon the type of aggregates used and its characteristics. Some of the properties of LWAC are described here in relation to NC.

Density. The density of structural LWAC varies from 1200 to 2000 kg/m^3 compared with 2300 to 2400 kg/m^3 for NC. Most properties of LWAC can be related to density which is influenced by the cement content, density of the aggregates, entrained air, moisture content of the aggregates, and the environmental conditions such as wetting and drying. A relationship between the density and compressive strength of LWAC made with different aggregates is shown in Fig. 7.9.[10]

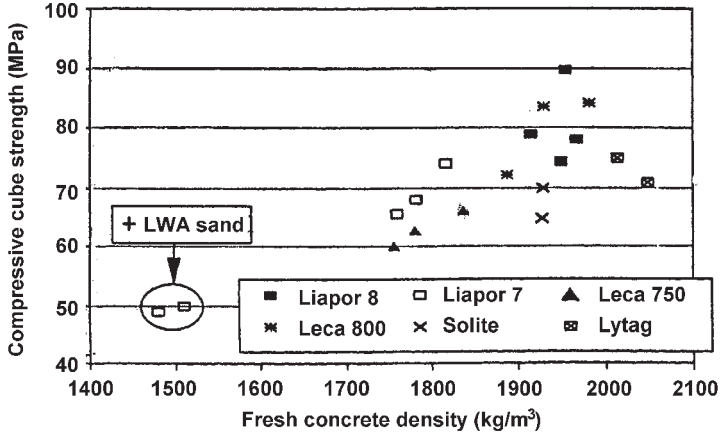

Figure 7.9. Compressive strength versus fresh density for LWA concrete mixtures with different types of LWA.[10]

Compressive Strength. The compressive strength of LWAC depends upon a number of parameters including the type of aggregate, the free water/cement ratio, the cement content, and the age of the concrete. The strength generally increases with increasing aggregate density. The good aggregate-cement bond and the similarity between the stiffness of the aggregate and matrix in LWAC result in an efficient mix with a strength approaching maximum theoretical strength.

Due to the water absorption of lightweight aggregates, the water-to-cement ratio in LWAC mixes is not directly comparable to NC. However, the effect of free water in the mix is similar to that in NC. Generally, the compressive strength reduces as free water increases.

De Pauw, et al.,[11] defined different types of water in the lightweight aggregates, and established a relationship between them. When working with the lightweight aggregates, the following quantities are to be considered:

W_{tot} Total amount of water in concrete mix.

W_{agg} The amount of water initially present in the aggregate.

W_{abs} The amount of water absorbed by the aggregate during mixing of the concrete.

W_{free} The amount of water available in the cement paste when mixing the concrete.

W_{add} The amount of water added when mixing the concrete.

The following relationships are valid:

Eq. (1) $$W_{tot} = W_{agg} + W_{abs} + W_{free}$$

and

Eq. (2) $$W_{add} = W_{abs} + W_{free}$$

In the case of NC for a given workability, compressive strength increases with cement content. On average, a 10% higher cement content results in a 5% higher compressive strength. The enhancement in strength, however, depends on the specie type of aggregate used.

The compressive strength of LWAC increases with time in a similar way to NC. However, the increase is less affected by poor curing and

a dry environment. The reserve of water within the pores of the lightweight aggregate particles prolongs the internal curing. The use of silica fume and superplasticizers in the mixture improves the cement paste strength and can result in compressive strengths of up to 100 MPa.

2.2 Compressive Strength and Absorptive Value of the Aggregates

Bilodeau, et al.,[12] showed the compressive strength dependence upon the absorptive value of the aggregates. The concretes were made with six different types of aggregates. The compressive strength of the concretes (batch A) ranged from 50.1 to 67.7 MPa at 28 days, and from 52.4 to 76.0 MPa at 1 year (Tables 7.11 and 7.12). The concrete made with aggregate II reached the highest compressive strength, whereas the concrete made with aggregate V showed the lowest values. The highest compressive strength of 60 to 65 MPa at 28 days was reached with only three of the six lightweight aggregates. It might have been possible to obtain that level of strength with aggregates III and VI by slightly modifying the mixture proportions as indicated by the long-term strength of the concrete made with those two aggregates. It appears that it would not have been possible to reach the target strength with the highly-absorptive aggregate V.

Two main factors probably explain the differences in the compressive strength of the concretes:

1. The effective water-to-cement ratio of the mixture.
2. The strength of the coarse lightweight aggregates.

The uncertainty about the effective W/C ratio increases with the increase in the absorption by the lightweight aggregate, and this explains why the strength of the concrete is almost a function of the absorption value of the lightweight aggregate in this study. The exception to this is the concrete made with aggregate II. This concrete shows the highest compressive strength in spite of the fact that aggregate II has an absorption value somewhat equivalent to that of aggregates III, IV, and VI, and significantly higher than that of aggregate I. In this case, the main factor controlling the strength of the concrete was probably the strength of the lightweight aggregate. The strength of the aggregate was possibly the limiting factor for the maximum strength of the concrete of mixtures 4 and 5 which almost did not show any strength development after 28 days, indicating that the maximum strength capacity of the aggregates was possibly reached at that

point. This low strength increase over time may also depend on the increase of stresses on the lightweight aggregate particles after shrinkage of the cement paste.

Table 7.11. Mixture Proportion of LWAC[12]

No.	Batch	LWA[a]	AEA,[b] ml/m^3	SP,[c] l/m^3	Fibers, kg/m^3	Slump, mm
1	A	I	85	8.9	0	90
	EF		55	5.0	1.5	135
2	A	II	55	5.9	0	190
	EF		45	4.5	1.5	80
3	A	III	40	6.2	0	100
	EF		45	4.4	1.5	115
4	A	IV	40	5.8	0	140
5	A	V	40	3.3	0	170
6	A	V	165	7.0	0	145

a LWA - lightweight aggregate
b AEA - air-entraining agent
c SP - superplasticizer

Table 7.12. Physical Properties of Concrete[12]

No.	Batch	LWA	Air, %	Density, kg/m^3	Compressive Strength, MPa				
					1d	7d	28d	91d	365d
1	A	I		1917	52.4	61.1	63.3	67.9	71.3
	EF		5.5	1922			63.2		
2	A	II		1947	48.9	59.4	67.7	72.7	76.0
	EF		5.5	1885			71.9		
3	A	III	5.5	1900	41.4	52.1	56.3	59.6	61.3
	EF			1895			53.9		
4	A	IV	5.3	1935	42.7	53.2	61.6	61.6	63.3
5	A	V	4.5	1920	41.1	48.3	50.1	50.8	52.4
6	A	VI	4.5	2000	40.7	51.4	57.5	59.8	na

2.3 Loss in Strength

Water absorption of the lightweight aggregates influences the properties of the concrete. It is reported that there is a loss of strength when the LWAC is made using dry lightweight aggregates.[13] It is postulated that there will be an exchange of water and air between the aggregate and the paste during the period of setting. In a microstructural study of the hardened concrete, air bubbles form a rim around the transition zone between the LWA and the paste (Fig. 7.10). This air evacuation from the LWA is the cause of the strength decrease. This is overcome by remixing the concrete. By so doing, the aggregates get wet and the air bubbles, which come out when the water goes in, get dispersed and behave like normal air bubbles created by the use of an air-entraining agent.

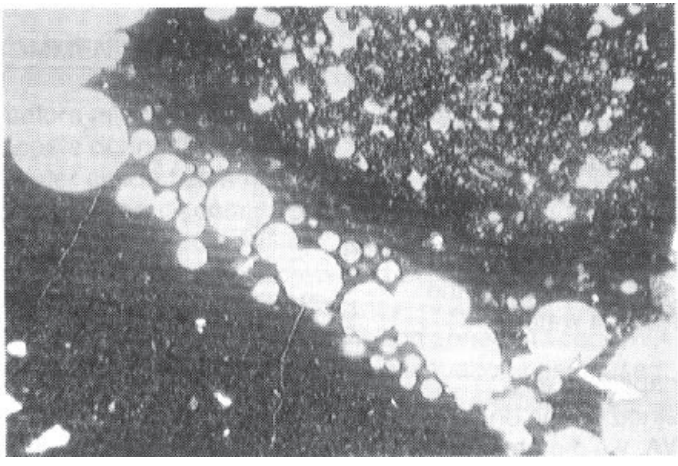

Figure 7.10. Micrograph showing the rim of air bubbles in the transition zone, LWA sample (4.8 × 3.1 mm) is in the upper right hand corner, and cement paste in the lower left corner.[13]

Punkki and Gjörv[14] have shown that the water absorption by the lightweight aggregate does not only depend upon the aggregate properties, but also on the moisture condition of the aggregate, the mixing procedure of the concrete, and the properties of the fresh cement paste. It is reported that 60 minutes after mixing, two types of high-strength concrete absorbed 3.5 to 4.0% and 4.5 to 5.5% water, respectively, while the absorption in pure

water was 6.9% and 7.0%, respectively. Absorption by the aggregates significantly decreases the workability, whereas it increases the compressive strength, in particular, the early strength. After one day, the use of dry aggregate gave approximately 10 MPa higher compressive strength than with the use of pre-wetted aggregate. This is in contradiction to the results reported by Helland and Maage,[13] but as explained earlier, it may be due to a different mixing schedule. After 28 days, however, no effect in the concrete with the lowest water-to-binder ratio was observed. At the highest water-to-binder ratio, the pre-wetted aggregate concrete gave approximately 6 MPa lower strength than that with the dry aggregate.

Pre-wetting significantly increases the capillary suction of the concrete. Thus, a pre-wetting of the most dense aggregate reduces the capillary resistance number by approximately 10% and increases the capillary number and the suction porosity by approximately 5% and 23%, respectively.

In contrast to the microstructures showing a rim of the air bubbles by Helland and Maage,[13] no such air bubbles on the aggregate surface could be observed by Punkki and Gjörv. Thus no adverse effect of the expelled air from the dry aggregate could be detected in the micrographs. However, some specimens typically showed a porous transition zone between the aggregate and the cement paste. This effect was observed in the concrete with pre-wetted aggregate and more so in the case of dense lightweight aggregate, and in the concrete with the highest water-to-binder ratio (Fig. 7.11).

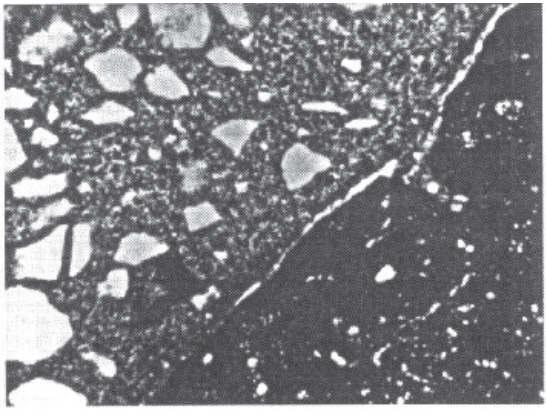

Figure 7.11. Micrograph of concrete with pre-wetted lightweight aggregate (sample width 2.5 mm).[14]

3.0 ELASTIC COMPATIBILITY AND MICROCRACKING

Concrete can be considered as a particulate composite in which the aggregate particles are embedded in a portland cement-based matrix. With normal concrete, the aggregates act as stiff and strong inclusions in a relatively flexible and weak cement paste matrix.

When this concrete is subjected to applied stresses or volume changes, then stress concentration occurs at the weak aggregate-cement paste interface, leading to the formation of microcracks. In order to understand the mechanism by which the performance of LWAC improves, it is necessary to understand how these stress concentrations can be reduced.

When using expanded clay aggregates, the boundary between the two porous phases, the aggregate and the mortar, is difficult to identify, whereas the transition from dense aggregates to gravel and to porous hydrated cement paste is distinct. Moisture exchange can take place between the partially saturated lightweight aggregate and the plastic mortar phase, thereby reducing the tendency of fresh lightweight concrete to develop thin films of water at the interface between the aggregate and the cement paste.

Expanded clay aggregate-mortar interaction involves both mechanical and chemical forces. In other words, the contact layer is not simply an interface between two substances, but contains new substances that are formed from the interaction. The increase in cohesion is due to the chemical reaction between the products of cement hydration and the aluminosilicates at the surface of the LWA formed during production at high temperatures.

Khokhorin[15] compared the hardness at and away from the contact zone for both expanded and dense aggregates. The microhardness of the mortar fraction at that zone was considerably greater than the microhardness of the mortar fraction outside that zone when expanded aggregates were used. When dense aggregates were used, no difference could be observed. Khokhorin's results can be quoted as follows:

> "On the whole one should note that the quality as defined by cohesion, density and strength of the contact zone of the concretes based upon porous aggregates is better than that of the contact zone of normal concrete based on dense aggregate."

3.1 Elastic Compatibility

Cracks are often found at the interface between the aggregate and the cement paste. Surprisingly enough, in the case of lightweight aggregate concrete, they are not observed. The primary reason for the lack of bond cracks may be due to the similarity of elastic stiffness of the LWA and the mortar fraction. Stress-strain curves of lightweight aggregate concretes are typically linear to levels approaching 90% of the failure strength, indicating the relative compatibility of the constituents and the reduced occurrences of microcracking. When the microcracking is reduced, the disruptive forces that are generated due to the freezing of water-filled cracks will be reduced. Similarly, rapid movement of chloride ions will also be limited when microcracking is reduced.

It is important to emphasize that when entrained air is added to normal weight concretes, it increases the elastic mismatch between the dense aggregates and the air-entrained mortar, while in structural LWAC the effect is to bring the elastic characterstics of the two phases closer together. In ordinary concrete, the stiffness of the aggregate is from two to more than six times the stiffness of the mortar, whereas in the concretes composed of structural grade lightweight aggregates, the two fractions are quite similar. Use of large, rigid, dense aggregates in concrete mixtures with a high air content increases the stress concentrations at the interface between the aggregate and the matrix.

Goodier[16] analyzed the stresses in and around a spherical inclusion embedded in an infinite matrix. His work shows how the stress concentrations change as the concrete progresses from the fresh condition to a mature, fully hydrated material. All concretes start with an infinite stiff inclusion relative to the matrix with maximum and minimum principal stresses of 2.00 and 0.57 developing when an uniaxial unit compressive stress is applied.[17] The maximum compressive stress occurs at the top (pole) and the bottom of the inclusion when loaded vertically (through the poles) and the maximum principal tensile stress occurs approximately between the pole and the equator with the crack propagating out from the surface of the spherical inclusion.

With mature normal concrete, the stiffness of the cement paste matrix is about 50% of the stiffness of the aggregate inclusion and the stress concentrations are reduced to 1.33 and 0.15. With LWAC, the stiffness of the matrix tends to match the stiffness of the aggregate and the stress concentrations are about 1.00 and 0. When the stiffness of the matrix and

the inclusion become equal, the concrete experiences uniform uniaxial compressive stress and can be expected to have a reasonably straight stress-strain curve up to failure with stress-induced microcracking occurring only near ultimate strength. Its practical implication is that the lightweight concrete tends to have a lower permeability to gases and aggressive liquids than normal concrete when subjected to load. Nishi[18] reported that for both fresh water and sea water test programs, Japanese structural LWAC demonstrated greater resistance to penetration than the normal weight concrete. They have suggested that there is probably the formation of a layer of dense cement paste surrounding the particles of the artificial lightweight coarse aggregates.

3.2 E-Modulus of Matrix

The modulus of elasticity (E-modulus) of concrete depends upon the modulus of elasticity of the matrix, type of aggregates, the effective water-to-binder ratio, and the volume of the cement. The water-to-binder ratio controls the E-modulus of the cement paste, which ranges from about 12,000 to 26,000 MPa, furthermore, the lower value can be reduced by air-entraining agents. The influence of the aggregate on the E-modulus of the matrix is illustrated in Fig. 7.12. The stiffness of the matrix increases with the increasing density of the sand. For the relationship of E-modulus and compressive strength, it has to be distinguished between matrices with natural sand and LWA (Fig. 7.13). The details of the aggregates used are given in Table 7.13.

The stress and strain behavior was studied on mixes designed with two different volume ratios between aggregates and binder. In the case of expanded clay and shale, this modification shows almost no effect. This means that the combination of cement paste with an expanded clay aggregate results in an almost homogeneous material, which minimizes microcracking because of the better elastic compatibility of the components. Consequently, the stress-strain diagram of a matrix with expanded clay is characterized by a nearly linear ascending branch and less ductility in the post-failure region (Fig. 7.14). In contrast with expanded clay, a higher content of natural sand increases the E-modulus of the matrix considerably. This observation is attributed to the discrepancy in the stiffness, which supports the crack formation. The result is a bending stress-strain relationship in compression (Fig. 7.14). However, the elastic compatibility of matrices with natural sand becomes better with lower water/binder ratios, as seen in Fig. 7.15 for the high-strength matrix.

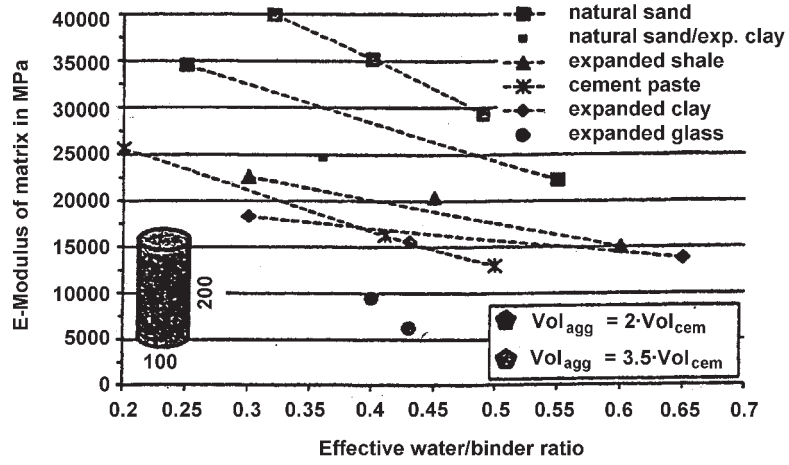

Figure 7.12. Dependence of E-modulus of different matrices on the water/binder ratio and the share of aggregate.[6]

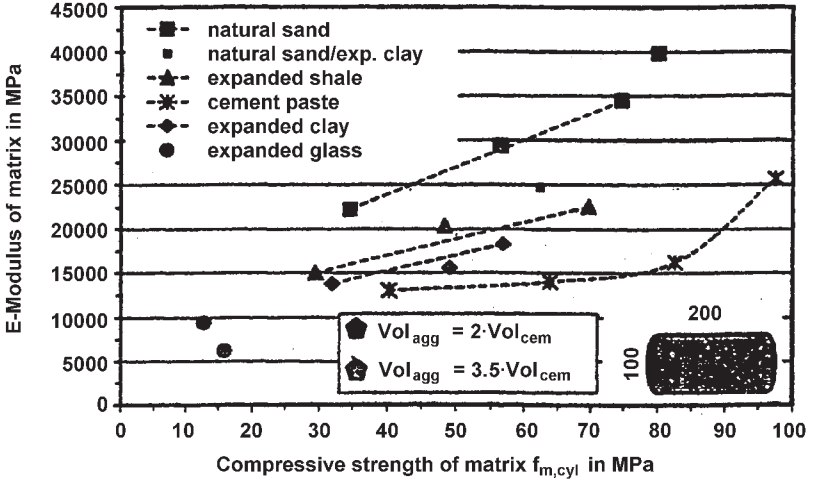

Figure 7.13. Relationship between E-modulus and compressive strength of different matrices.[6]

Table 7.13. The Properties of the Fine Aggregates[6]

	Fine Aggregates	Producer	Particle Geometry	Aggregate Size	Particle Density (P_a), kg/m^3	Water Absorption, M%
1	Natural sand		rounded	0/2	2.63	0
2	Natural sand + Liapor™ each 50% vol %			0/2 0/4	2.63 1.5	4.8
3	Expanded shale	Ulopor	crushed	0/2 2/4	1.7 1.4	6.2
4	Expanded clay	Liapor™	crushed	0/4	1.5	4.8
5	Expanded clay	Leca™	rounded	0/2	1.3	4.7
6	Expanded clay	Embra	rounded	0/4	0.79	4.6
7	Expanded glass	Liaver	rounded	0.25/0.5/1/2/4	0.54–0.29	4.4

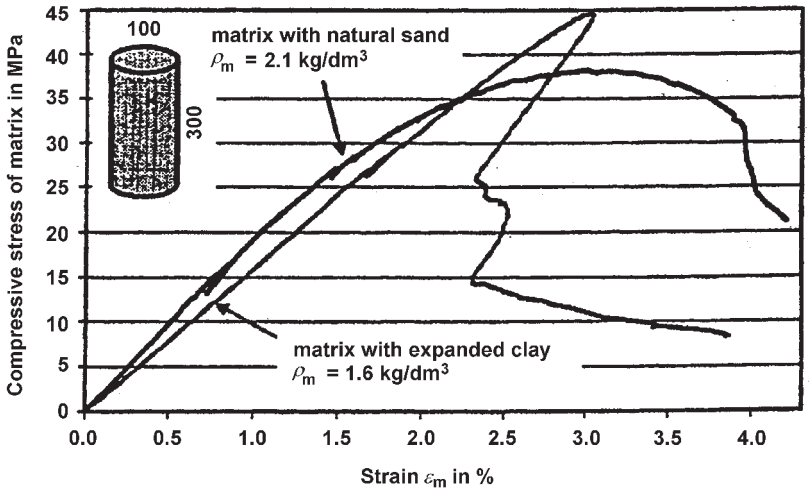

Figure 7.14. Typical stress-strain diagram of a matrix with natural sand and lightweight sand.[6]

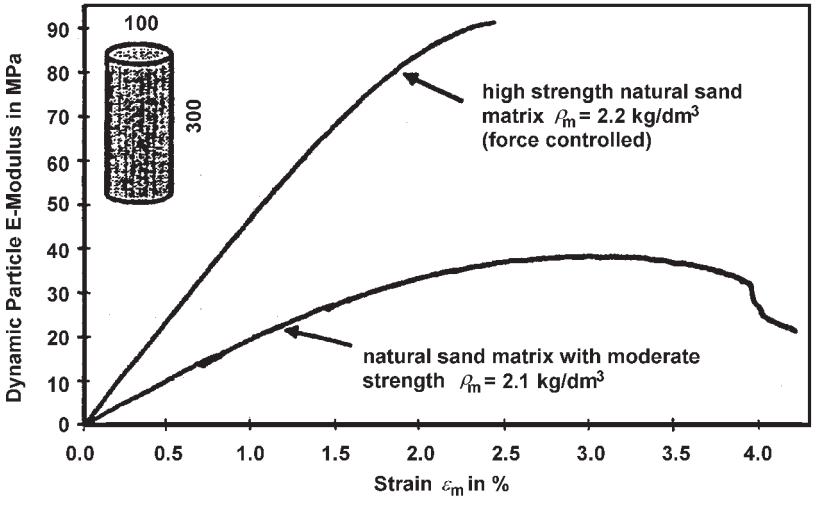

Figure 7.15. Comparison between high and moderate strength matrix with natural sand.[6]

3.3 Modulus of Elasticity of Aggregates

The modulus of elasticity of LWA has been studied on the individual particles of different lightweight aggregates.[20] The diameter of the particles was 12–16 mm. Because of the small dimensions of the particles, only the dynamic modulus was of interest. The values obtained scatter considerably around a parabola corresponding to Eq. (3):

Eq. (3) $$E_{dyn.a} = 8000\ \rho_a^2$$

where ρ_a is the particle density of the aggregate in kg/dm^3.

The results shown in Fig. 7.16, indicate a lower and an upper value for natural lightweight aggregate and expanded shale lightweight aggregates. These experiments were repeated by Müller-Rochholz.[21] In his experiments, the precision was higher, thereby the standard deviations can be reduced. Nevertheless, a good agreement can be achieved. Alternatively to the approach of Shultz, he suggested a linear relationship between the particle density and the dynamic E-modulus of lightweight aggregates (Fig. 7.17).

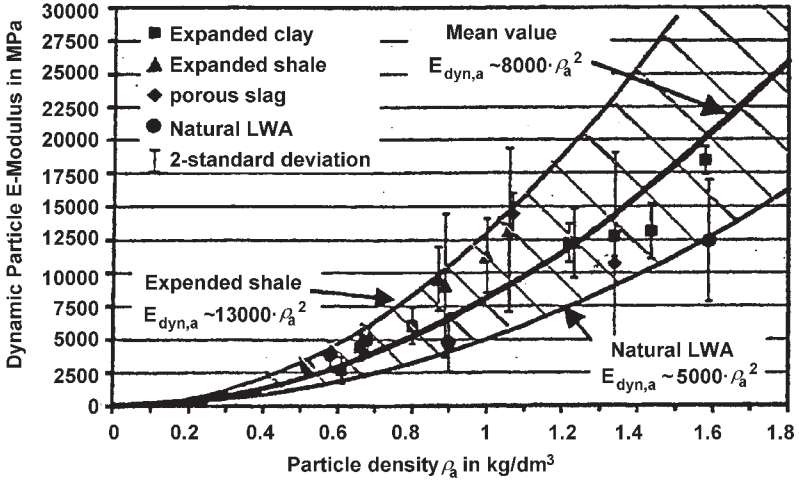

Figure 7.16. Dynamic E-modulus of different lightweight aggregates in dependence of the particle density.[20]

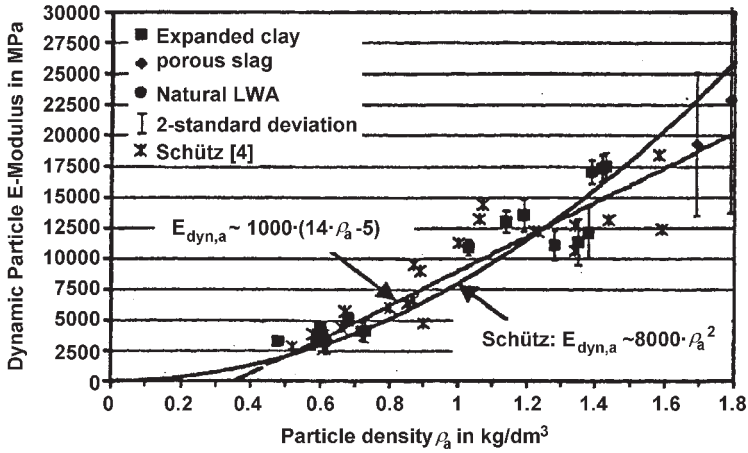

Figure 7.17. Dynamic E-modulus of different lightweight aggregates and its dependence on the particle density.[21]

Eq. (4) $E_{dyn.a} = 1000\ (14 \cdot \rho_a - 5)$

where ρ_a is the particle density, or

Eq. (5) $E_{dyn.a} = 100\ (27 \cdot \rho_b - 5)$

where ρ_b is the bulk density in kg/dm^3 of the aggregates.

In comparison to lightweight aggregates, dense natural aggregates are considerably more rigid. For quartz, the modulus of elasticity is approximately 60,000, for limestone 80,000, and for basalt it is over 100,000 MPa.

It is seen from both investigations that the dynamic E-modulus is dependent on the particle density.

4.0 SHRINKAGE AND CREEP OF LIGHTWEIGHT AGGREGATE CONCRETE

Drying shrinkage and creep of concrete have been studied for a long time and various theories have been proposed regarding their mechanisms. With regard to drying shrinkage, there is the capillary tension theory, the surface adsorption theory, and the interlayer water theory; for creep, there

is the visco-elastic theory, the seepage theory, and the viscous flow theory.[22]–[24] In most of these theories, the behavior of moisture contained in concrete is considered to be an important factor that influences shrinkage and creep. With regard to drying shrinkage in the range of relative humidity from 40% to 100%, the capillary tension theory is dominant. According to this theory, the drying shrinkage is caused by the capillary tension occurring in the moisture existing in the pores in cement paste.[24][25] The stress due to capillary tension in concrete is considered to be governed by the pore volume and pore size distribution. However, experimental estimations of the stresses due to capillary tension and the relationship between the stress and the mechanism of drying shrinkage have not been sufficiently studied. At a relative humidity less than 40%, the shrinkage deformation at drying is mostly caused by loss of structural water and adsorbed water in the cement paste.

With regard to the mechanism of creep of concrete, a great part of the mechanism can be explained by the visco-elastic theory. This theory considers that the cement paste is a composite material which consists of the frame structure and the visco-liquid filling the pores of cement paste, and that creep is the elastic deformation of the former delayed by the resistance due to viscosity of the latter. Therefore, it is considered that pore structures in cement paste, namely pore volume and pore size distribution, are closely related to not only drying shrinkage, but also to creep of concrete.

4.1 Shrinkage

There are several kinds of shrinkage: autogenous or chemical shrinkage, drying shrinkage, and carbonation shrinkage.

Drying shrinkage occurs when the concrete dries. The negative pressure in water is caused by the capillary meniscus, which gives compressive stresses in the solid cement paste. This process causes compaction, and the deformation increases with the decrease of the capillary radius.

Carbonation shrinkage occurs due to the interaction of calcium hydroxide and calcium silicates with carbon dioxide. Ramachandran and Feldman[26] were the first to observe that length changes, about 40% of that of portland cement, when calcium hydroxide compacts were exposed to CO_2(0.1 MPa, 50% RH). Further work by Swenson and Sereda[27] showed similar characteristics in shrinkage relative humidity curves. Maximum shrinkage occurred at approximately 50% RH at an age of 19 days for $Ca(OH)_2$, and 42 days for portland cement. Both the systems showed low

shrinkage at high and low humidities. This is in accordance with the intensity of carbonation at different relative humidities as is discussed in Ch. 8. Besides calcium hydroxide, C-S-H and C_3S paste also contributes to shrinkage. The carbonation shrinkage of C-S-H alone is significantly larger than the shrinkage of C_3S paste. Several theories of carbonation shrinkage have been proposed.

Ramachandran and Feldman's hypothesis suggests that the points of contact of $Ca(OH)_2$ crystals, and that the crystallites are pulled together into the holes by van der Waal forces. Secondary hysteresis observed in $Ca(OH)_2$- H_2O isotherms is due to the trapping of water in these holes. In Power's theory,[28] the shrinkage force is provided by menisci, but according to Ramachandran and Feldman's hypothesis,menisci forces are not necessary as van der Waals surfaces are sufficient to induce shrinkage on carbonation. It is suggested that the contribution shrinkage involves silica polymerization similar to that described by Lentz.[29]

Alexander and Wardlaw[30] found that normal atmospheric levels of CO_2 caused about one third of the carbonation shrinkage compared to a 100% CO_2 atmosphere. Klemn and Berger[31] found that accelerated curing through high levels of carbon dioxide produced different effects than normal curing. This indicates that the effect of a high concentration of CO_2 on concrete is basically different from that of a low concentration of CO_2. These differences are due to the different chemical processes involved. One of the implications of this is that the accelerated tests using very high concentrations of CO_2 may not be a valid method for modeling long-term behavior and service life assessment of concrete structures.

Drying shrinkage significantly affects the total shrinkage deformation and is a direct cause of cracking. Shrinkage depends upon the type of cement and its contents, water-to-binder ratio, and the aggregates.

The drying shrinkage of concrete is mostly affected by properties of LWA and the aggregate content, because almost three-quarters of the volume of concrete is made up of aggregate. The properties of LWA differ greatly with the material used for making them and the production technique. In the case of normal concrete, the aggregates have a higher modulus of elasticity and the volume change of the cement paste causes microcrack development, although the shrinkage is not as much. In the case of lightweight aggregate concrete, the shrinkage is greater. Since aggregates are less stiff, they accommodate the movement caused by the volume change. This results in less microcrack formations. So in order to understand the shrinkage of lightweight aggregate concrete, it is necessary to

study the influence of deformability of LWA because of the reduced restrained behavior.

4.2 Drying Shrinkage Test

Drying shrinkage of some of the LWAC was tested by the accelerated test method described below. Some of the aggregates used were steam cured and air-dried. The physical properties of the aggregates are shown in Table 7.14

Table 7.14. Physical Properties of LWA[32]

Aggregate Type	Bulk Density, kg/m^3	Particle Density, kg/m^3	Voids Ratio, %	Comp. Strength, MPa	Water Abs.%, 1 hr
Steam-cured fly ash	766	1311	41.6	6.09	27.0
Air-cured fly ash	795	1405	43.4	5.50	23.9
Super lightweight expanded clay	539	898	40.0	4.12	9.3
Sintered fly ash	693	1260	45.9	8.01	14.1
Expanded clay	742	1370	45.8	6.91	11.7

The 40 × 40 × 160 mm prism specimens were cast and demolded after 24 hours and stored in water at 20°C for 28 days, then tested. These specimens were dried at 50°C until a constant weight was attained. The shrinkage was calculated from the difference in the specimen length between wet and dry states. The composition of the concrete was:

- Mortar matrix composition: cement:sand:water = 1:1.5:0.42.

- The volume fraction (absolute volume fraction) of LWA in concrete V_a: 0 (control mortar), 0.1, 0.2, 0.3, and 0.4.
- Crushed limestone aggregate with particle size 5–10 mm was used in the control concrete.
- Fine aggregate used was natural sand, of fineness modulus 2.1.

The shrinkage of concrete with different types of LWA at various particle densities is shown in Fig. 7.18. The results are represented as relative shrinkage Sc/Sm (the ratio of shrinkage of concrete to the shrinkage of control mortar). The relationship between the shrinkage of concrete and volume fraction of LWA is shown in Fig. 7.19.

At the same volume fraction of aggregate, the shrinkage of LWAs is higher than that of crushed limestone concrete. The shrinkage of concrete with burned LWA is less than that with non-burned fly ash LWA.

Similar to crushed limestone, the burned LWA can reduce the shrinkage of concrete. The shrinkage of concrete decreases as the content of burned LWA increases. But, the non-burned fly ash does not necessarily reduce the shrinkage of the concrete. The air-cured fly ash aggregates have little influence on the shrinkage of concrete, while the steam-cured fly ash aggregate results in higher shrinkage as the volume fraction of aggregate increases.

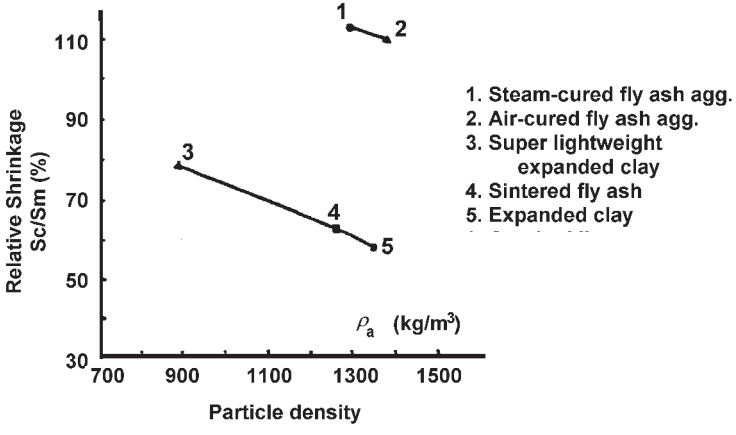

Figure 7.18. Relative shrinkage versus particle density (V_a = 0.4).[32]

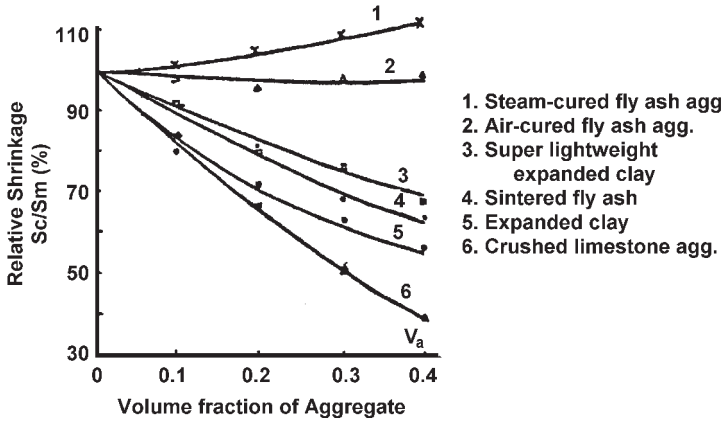

Figure 7.19. Relationships among the relative shrinkage of concretes and the volume fraction of aggregates.[32]

With regard to the LWAs produced by the same method (burned or non-burned), the shrinkage of concrete decreases as the particle density of aggregate increases. The shrinkage of concrete relates well to the particle density of aggregate. This relationship does not fit with the lightweight aggregates produced by different methods (see LWAs 3, 1, and 2, in Fig. 7.19).

There is no clear relationship between the shrinkage of concrete and the cylinder compressive strength of concrete (Table 7.14), but the lowest shrinkage of the sintered fly ash concrete has the highest strength.

It is concluded that the shrinkage of concrete with LWA is normally higher than that of ordinary aggregate. However, the burned LWA is superior to the non-burned LWA in decreasing the shrinkage of concrete. This is explained on the basis of the elastic modulus of the aggregates used (Table 7.15).

Table 7.15 shows that the elasticity of the burned aggregate (Nos. 4 and 5) is higher than that of the non-burned aggregate (Nos. 1 and 2), when their particle densities are almost similar. Therefore, the burned LWA has its advantage in reducing the shrinkage of concrete when compared to the non-burned lightweight aggregate. The difference between non-burned and burned LWA is due to the ceramic bond in the particles, which develops during the sintering process at high temperatures.

Table 7.15. Elastic Modulus of the LWAs

No.	Type of Aggregate	Elastic Modulus (GPa)
1	Steam-cured fly ash	14.44
2	Air-cured fly ash	15.96
3	Super lightweight expanded clay	13.85
4	Sintered fly ash	19.82
5	Expanded clay	20.69

Further, super lightweight expanded clay aggregate has a lower particle density than the other ones tested. Its modulus of elasticity is lower and its restraining influence on shrinkage of the concrete is also less. On the other hand, when comparing its restraining influence on concrete shrinkage to that of non-burned fly ash aggregates at the same volume fraction, the former shows higher values than the latter. Hence, other factors, the density of the particles and the shrinkage of the aggregate particle, may also influence the shrinkage of concrete. Liu, et al.'s,[32] results also infer:

- The shrinkage of the concrete with the burned lightweight aggregate (Sa) is less than that of the non-burned aggregates.
- When Sa > Sm, (Sm is the shrinkage of control mortar), the more of this kind of non-burned aggregate in concrete, the higher the shrinkage of concrete.
- When Sa = Sm, the shrinkage of concrete is related weakly to the volume fraction of aggregate (air-cured fly ash aggregate).
- When Sa < Sm, the shrinkage of concrete decreases as the volume fraction of LWA increases.

The drying shrinkage, and even the creep, also depend upon the process of manufacturing the lightweight aggregate concrete. Bijen[33] has shown that the fly ash aggregates produced by "cold bonding" are, in general, less rigid than that obtained with the other types of bonding. Moreover, the drying shrinkage and creep of the bonding material are greater. These negative aspects can, however, be alleviated or even overcome by using compaction agglomeration techniques. In general, the lower the porosity, the lower the shrinkage and creep.

Van der Wegen and Bijen[34] have tested the shrinkage and creep of lightweight aggregate concrete made with Aardelite™ and Lytag™ aggregates. Aardelite™, unburned, and Lytag™, burned, are fly ash aggregates. The composition and properties of fresh LWAC are shown in Table 7.16. The 100 × 100 × 400 mm specimens were cast for testing.

Table 7.16. Mix Proportions and Properties of Fresh Concrete[34]

Concrete Mix	Unit	Lytag™	Aardelite™	River gravel
Portland blast furnace cement	kg/m^3	390	378	366
Water free	kg/m^3	207	198	216
Water absorbed by coarse aggregate	kg/m^3	70	91	0
River sand	kg/m^3	735	752	730
Coarse sand	kg/m^3	559	652	1006
Total	kg/m^3	1961	2071	2318
Slump	mm	100	120	100
Flow (DIN 1048)	mm	420	440	420
Air content	%v/v	3.8	2.1	0.9
Apparent density measured	kg/m^3	1966	2074	2309
Apparent density calculated	kg/m^3	1961	2071	2318

The drying shrinkage specimens were demolded 24 hours after casting and subsequently stored in saturated lime-water at 20°C until an age of 7 days. They were then stored at 20°C and 50% RH. Although the modulus of elasticity of the Lytag™ is about 18% lower than that of gravel concrete and has a similar amount of cement (but a somewhat smaller water/cement ratio) as river gravel concrete, the drying shrinkage after 210 days was about half of that of the gravel concrete (Fig. 7.20). This difference is probably due to the initial water content of the coarse aggregate. It is known

that the water content of porous aggregates greatly influences the rate of drying.[35] The buffer water content of theporous aggregate slows down the drying shrinkage. This means that the Lytag™ concrete could continue to shrink even after the shrinkage of the gravel concrete has stabilized.

Aardelite™ concrete showed the largest shrinkage in spite of its smaller volume of cement and a lower water-to-cement ratio. Moreover, Aardelite™ also has a buffer water capacity even higher than that of Lytag™, hence, at least in the early days of drying shrinkage, behavior similar to that of Lytag™ concrete can be expected.

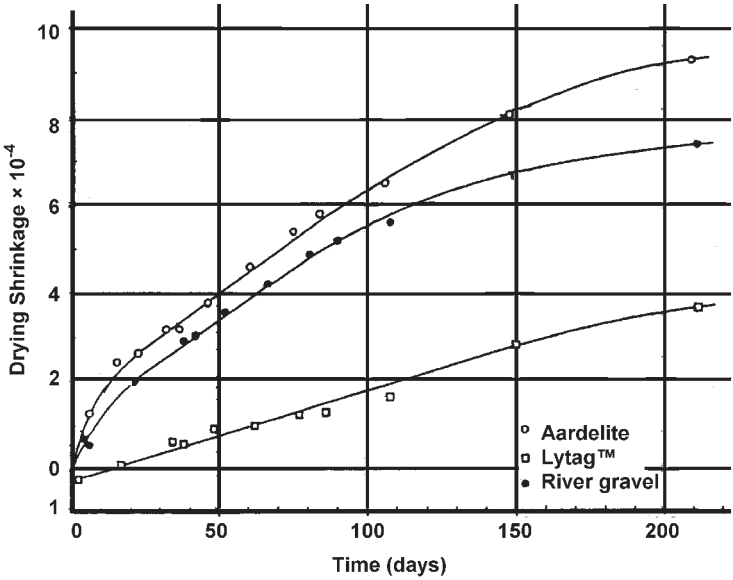

Figure 7.20. Shrinkage of LWAC made with Aardelite™ and Lytag™ aggregates.[34]

Apart from the smaller restraining effect of the Aardelite™ particles (because of its lower modulus), the higher shrinkage of Aardelite™ concrete is probably due to the shrinkage of the Aardelite™ aggregate itself. It is known that autoclaved lime-silica materials show drying shrinkage, in contrast to a sintered ceramic material such as Lytag™ and dense natural aggregate.

Kovalenko and Terentyev[36] used Haydite aggregates in the foamed concrete, and have shown that the introduction of Haydite into the foam concrete mix, even without formation of the compact frame, leads to a considerable decrease in shrinkage from 30% or more (Fig. 7.21).

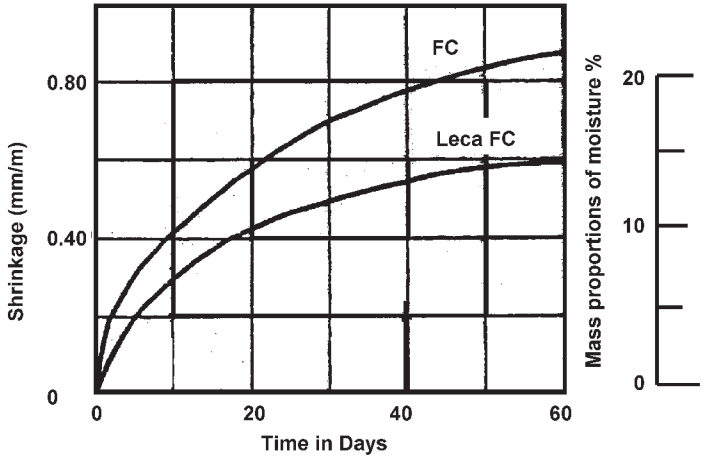

Figure 7.21. Shrinkage of concrete with Haydite aggregates (FC = foamed concrete).

Abdullah has used palm oil shell aggregates in lightweight aggregate concrete.[7] The shrinkage strain versus time curves for lightweight concrete using palm oil shells in comparison with the curve for normal concrete are shown in Fig. 7.22.[37] The LWA curve shows that the shrinkage rate decreased after about 60 days. However, the shrinkage of lightweight concrete using palm oil shells was about five times that of normal concrete. A semi-log plot of the same curve is shown in Fig. 7.23.

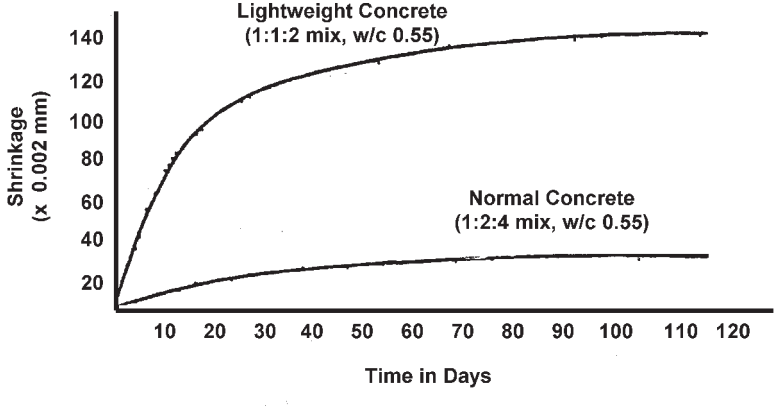

Figure 7.22. Shrinkage of lightweight concrete using palm oil shells as aggregates in comparison with normal concrete.[7]

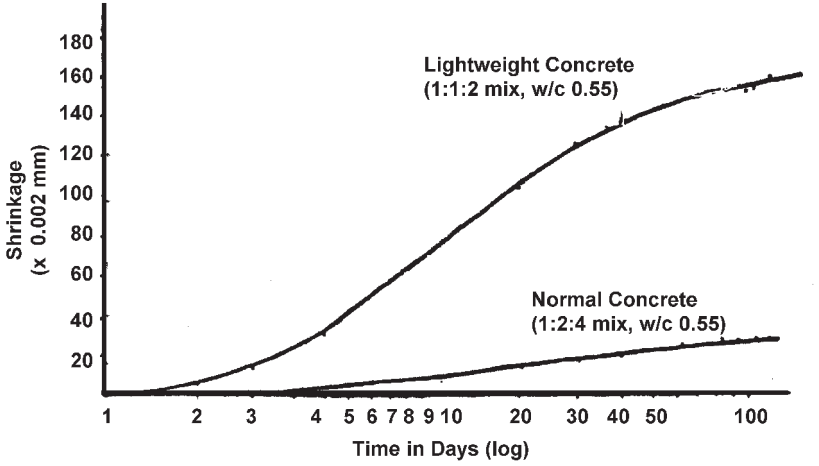

Figure 7.23. Semi-log plot of shrinkage of lightweight concrete using palm oil shells as aggregates in comparison with normal concrete.[7]

Nobuta, et al.,[38] tested the shrinkage of high strength lightweight aggregate concrete made from:

- FA—Lightweight aggregate made from fresh ash.
- LA—Lightweight aggregate made from conventional expansive shale.
- NA—Normal crushed stones.

They have shown that the length variation ratio at the age of 1 year depends on the type of aggregate, and tends to be large corresponding to the order of FA < LA < NA (Fig. 7.24). The symbols in the figure show water-to-cement ratio (%), type of aggregate, and slump values (cm). In cases with a water/cement ratio of 50% and slump of 18 cm, the length variation ratios for FA, LA and NA were 0.062%, 0.080% and 0.090%, respectively. The unit water amounts were 167 kg/m^3, 176 kg/m^3, and 183 kg/m^3, respectively, and the correlation with the unit water amount can also be observed. In the cases with a water/cement ratio of 40% and target slump of 21 cm, the length variation ratio for FA and NA were 0.064% and 0.093%. The unit water amounts were the same, which were 165 kg/m^3, but the water-to-cement ratio in the case of FA was smaller.

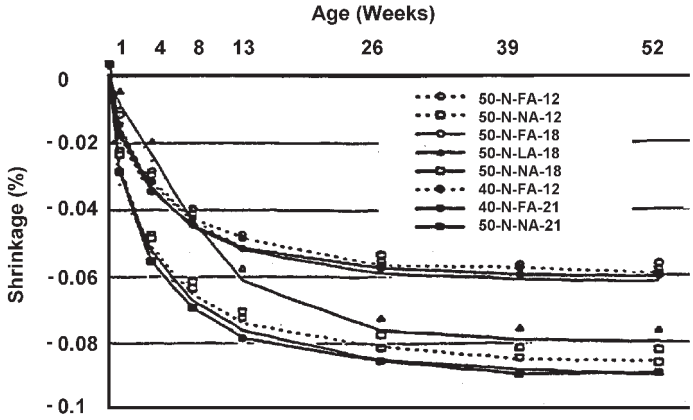

Figure 7.24. Drying shrinkage of lightweight aggregate concrete.[38]

There seems to be a good correlation between the E-modulus and the compressive strength of the LWA concrete. The results indicate no considerable influence of the LWA type on compressive strength.

The internal water reservoir of LWA concrete, due to the possible initial LWA moisture and mix water absorption, reduces the rate of drying shrinkage compared to the normal density concrete. For the same reason, the autogenous shrinkage is nearly eliminated. Consequently, when using dry LWA, the LWA with a high water absorption gives the lowest shrinkage.

Dhir, et al.,[39] have shown that the drying shrinkage of Aglite, "All light," lightweight aggregate concrete, as that of normal concrete, increases with its design strength, i.e., cement content. It is shown that for the range of effective water/cement ratio considered, the drying shrinkage values of concretes made with Aglite are generally comparable to those obtained with class I crushed rock and gravel aggregates. Thus, Aglite aggregate concrete is comparable to normal concrete.

4.3 Creep

Creep of concrete is understood as an increase in strain with time at a constant sustained stress level. Creep of concrete under drying conditions is calculated as the difference between the total time dependent on

deformation of the loaded specimen and the shrinkage of a similar unloaded specimen cured in the same conditions at the same time. Drying shrinkage and creep are not independent phenomena to which the principle of superposition can be applied in practice. Drying creep is calculated as the difference between the creep in air and the creep in water, i.e., without shrinkage, namely basic creep. The rate of primary creep decreases with time. It is proportional to the applied load when the stress is not more than 40% of the compressive strength of concrete.

4.4 Creep Test

Van der Wegen and Bijen[34] have tested creep deformation on the concrete made with the lightweight aggregates, Aardelite™, and Lytag™ of the composition shown in Table 7.16. The creep was determined from 100 × 100 × 400 mm prisms. The specimens were demolded 24 hours after casting and subsequently stored in saturated lime-water of 20°C until the age of 7 days. The specimens were then stored at 20°C and 50% RH and loaded at 28 days at a compressive stress of 10 MPa. The results are shown in Fig. 7.25. It is shown that although LWAC with Lytag™ had a somewhat smaller water-to-cement ratio than the gravel concrete, both showed similar creep characteristics probably due to the smaller elastic modulus of the Lytag™ concrete.

The Aardelite™ concrete showed the highest creep, which cannot be entirely accounted for by its lower modulus. It is suggested that the Aardelite™ particles themselves possess a larger creep deformation than the Lytag™ particles, since the creep of the sintered materials is generally much smaller than that of the autoclaved lime-silica materials.

The LWAC made with Lytag™ exhibited a higher elastic modulus, smaller drying shrinkage and creep, and a larger expansion than the Aardelite™ concrete, although their mix compositions were almost similar, but a larger expansion compared to gravel concrete. That means the Poison's value is larger.

Abdullah[7] has tested creep of LWAC made with palm oil shell aggregates. The creep test was performed according to ASTM. A load equivalent to a stress of 6.0 N/m^2 was applied to three 150 mm diameter cylinders made using lightweight concrete with palm oil shells as aggregates. The instantaneous strain was obtained by deducing the initial reading from the final reading immediately after loading. Readings were taken six

hours later, then daily for one week, weekly for one month, and monthly for nine months. Strain readings on the control specimens were taken according to the same time schedule. The total strain divided by the average stress provided the total strain per unit stress. This total strain per unit stress was plotted on semi-log coordinate paper. Figure 7.26 shows a large creep compared to normal concrete. The creep rate for lightweight aggregate concrete using palm oil shells did not achieve a constant value after three months. This may be a cause for concern when using lightweight concrete with palm oil shells as structural concrete.

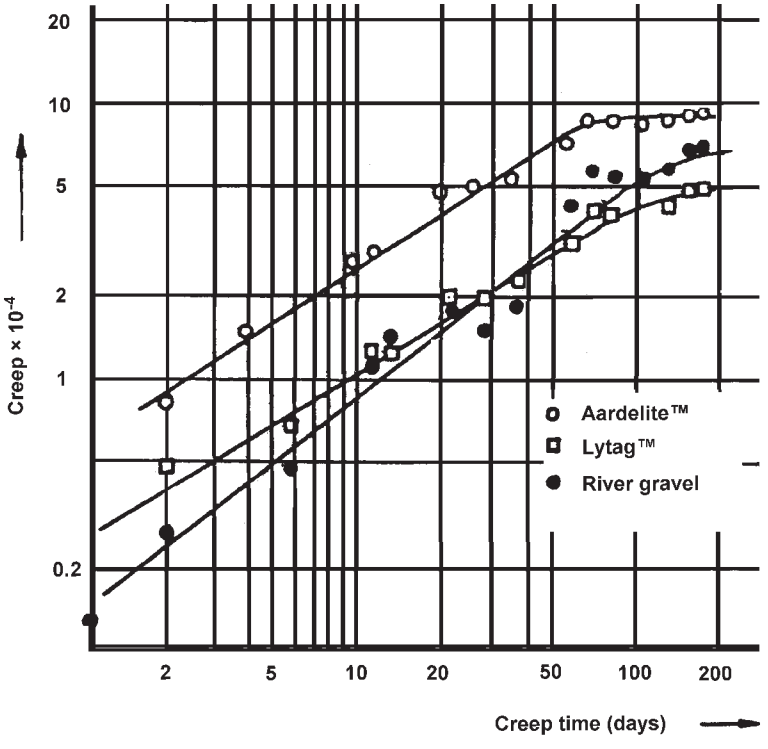

Figure 7.25. Creep deformation of LWAC made with Aardelite™ and Lytag™ aggregates.[34]

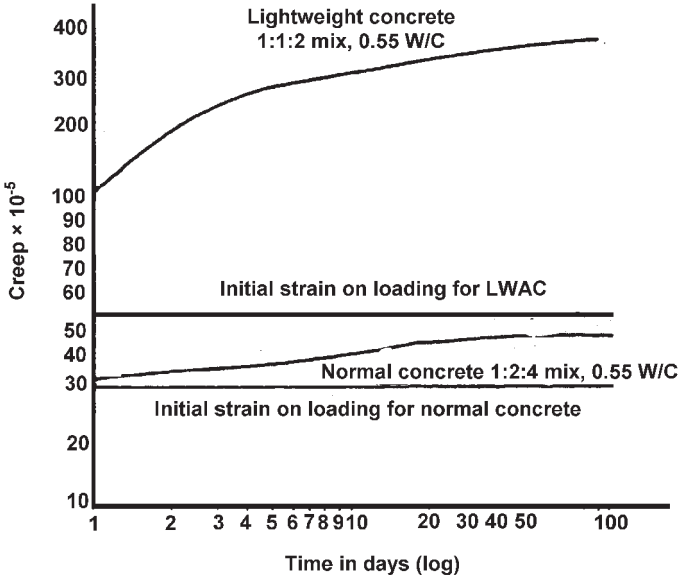

Figure 7.26. Creep of lightweight concrete using palm oil shell aggregates in comparison with normal concrete.[7]

4.5 Concluding Remarks

The mechanism of drying shrinkage of concrete of low to high strength in the range of medium to high relative humidities can be explained by the capillary tension theory.

Drying creep becomes smaller with the increase in compressive strength of concrete, and is caused by the stress due to the difference in capillary tension between drying shrinkage and creep specimens.

Drying creep of high strength concrete is very low, because the difference in capillary tensions between drying shrinkage and creep specimens does not arise. Drying creep is larger for low strength concrete because the capillary tensions of creep specimens are larger than that of drying shrinkage specimens.

5.0 THERMAL CONDUCTIVITY OF LIGHTWEIGHT AGGREGATE CONCRETE

Thermal behavior of lightweight aggregate concrete is related to its thermal conductivity and density which, in turn, is influenced by its pore structure, i.e., the air-void system, aggregates, and the matrix. Thus, the thermal conductivity will depend upon the pore structure of the lightweight aggregates and the cement paste matrix. Air is one of the best insulating materials. It implies that the thermal conductivity of a dense concrete (less the air voids) is more than that of the porous concrete. Thermal conductivity of a dry building material is increased by adding water to it. Wet concrete transmits heat better than dry concrete, because the thermal conductivity of wet concrete is 24 times that of the air. The heat passes through water 15 times faster than through the stationary air. For this reason, the thermal conductivity value of insulating concrete drops when it gets wet.

5.1 Influence of the Aggregates

Lightweight aggregates are produced by heat treatment during which they expand and produce a porous cellular structure. The pore structure and density of the aggregates depend upon the raw material and the process used to produce them. Porosity and density are interrelated, the higher the porosity, the lower the density. Higher porosity has more air. As a result of the above mentioned structure, thermal conductivity decreases with an increase in air content. It suggests that the light porous aggregates will produce concrete of low thermal conductivity, whereas the heavy dense aggregates will produce concrete of a higher thermal conductivity. Thermal conductivity of lightweight aggregate concrete made with different aggregates is shown in Table 7.17. EVS and ESG are expanded slag aggregates. EVS is made by hydro-screening, and ESG is produced by a drum granulating process.[9] The 28 days compressive strength of EVS and ESG concretes was 5.0, whereas vermiculite, perlite, and Swedish Leca™ concrete had a strength of 0.95, 2.17 MPa, and 32 MPa, respectively.[8] The thermal conductivity values mentioned here are to be compared with the thermal conductivity of dense concrete which is about 1.7 W/mK.

Table 7.17. Thermal Conductivity of Lightweight Aggregate Concrete[8]

Aggregate Type	Air-dry Density kg/m^3	Thermal Conductivity Coefficient W/mK at Moisture Content	
		0%	5%
Vermiculite	400	0.09	0.158
Perlite	310	0.098	0.155
EVS	1420	0.28	0.36
ESG-1a	1280	0.31	0.36
ESG-1b	1400	0.31	0.39
Swedish Leca™	1550	0.68	–

Table 7.17 shows that the thermal conductivity of concrete decreases with a decrease in the air-dry density of the concrete, which consequently depends upon the type of material used for making the aggregate. In the case of EVS and ESG, the material is the same—blast furnace slag—yet there are variations. These variations are attributed to the geometry and the morphology of the aggregates, which is different because EVS and ESG were produced by two different processes. Roughly rounded ESG aggregates, with a few small pores instead of the angular EVS aggregates with large open pores, promote a more uniform porous structure of the mortar components. This has a greater quantity of small pores. It is substantiated by determining the pore size distribution of the expanded slag concrete (Table 7.18).

Table 7.18. Pore Size Distribution of Hardened Mortar Component of Expanded Slag Concrete[40]

Aggregate Type	Content of Pores (% of Porosity of the Hardened Mortar Part of Concrete) Within the Size Range (μm)			
	1–60	70–120	150–300	>350
EVS	5	8	57	30
ESG	22	35	31	12
28 days cube compressive strength 5.0 MPa.				

The number of small pores (of the size up to 120 μm) in the hardened mortar component of the concrete, made with the use of ESG is about 57% in contrast to the one made with EVS which reaches a value only to 13%.

5.2 Effect of Mortar Matrix

The properties of the cementing matrix depend upon the binders used. Binders can be only portland cement or a combination of portland cement and mineral admixtures. Mineral admixtures can be fly ash, silica fume, blast furnace slag, etc. Besides this, chemical admixtures, like superplasticizers and air-entraining, agents are also used. Mineral admixtures modify the pore structure of the matrix and consequently produce a concrete with uniformly dispersed pores. Especially when an air-entraining agent is used, pores are created, thereby the density of concrete is reduced. To assess the influence of silica fume (SF) and fly ash (FA) on thermal conductivity, some lightweight concretes were made with expanded perlite and pumice aggregates.[40] The composition of the concrete is given as:

Total dosage of portland cement
(PC, PC + SF, or PC + FA) = 200 kg/m^3

Six main groups of mixes were cast with expanded perlite aggregate (EPA) and pumice aggregates (PA) in different proportions. They are named as:

- A (100% PA)
- B (80% PA+ 20% EPA)
- C (60% PA + 40% EPA)
- D (40% PA + 60% EPA)
- E (20% PA + 80% EPA)
- F (100% EPA)

For each group, separately 0, 10, 20, and 30% SF and FA, by weight of PC, were used. The superplasticizer used was sulfonated naphthalene formaldehyde condensate blended with some other air-entraining admixtures.

The thermal conductivity and the dry unit weight are given in Table 7.19 and the relationship between mineral admixtures SF and FA and thermal conductivity of mixes A, B, C, D, E, and F are presented in Figs. 7.27–7.32. Concrete was made by mixing the pumice (PA) and EPA aggregates in different proportions. The relation between the ratio of EPA and thermal conductivity is given in Fig. 7.33, and the relationship of the dry unit weight and thermal conductivity in Fig. 7.34.

Table 7.19. Thermal Conductivity and the Dry Unit Weight of Concrete of All Groups[40]

LWC Groups	A: 100% Pumice Aggregate (PA) LWC						
	A0	**A1**	**A2**	**A3**	**A1***	**A2***	**A3***
Thermal Conductivity (W/mK)	0.1378	0.3099	0.2981	0.285	0.285	0.283	0.2787
Oven-dried Unit weight (kg/m^3)	1154.3	1138.9	1125.6	1114.3	1153.4	1130	1125
LWC Groups	**B: 80% PA + 20% Expanded Perlite Agg. (EPA) LWC**						
	B0	**B1**	**B2**	**B3**	**B1***	**B2***	**B3***
Thermal Conductivity (W/mK)	0.2947	0.2994	0.2709	0.2408	0.2666	0.2586	0.2398
Oven-dried Unit weight (kg/m^3)	928.3	911.4	903.5	896.4	925.7	920.4	910.3
LWC Groups	**C: 60% PA + 40% EPA LWC**						
	C0	**C1**	**C2**	**C3**	**C1***	**C2***	**C3***
Thermal Conductivity (W/mK)	0.269	0.2498	0.251	0.2479	0.265	0.2564	0.249
Oven-dried Unit weight (kg/m^3)	858.8	854.5	850	845	855.4	853	852.9

(Cont'd.)

Table 7.19. *(Cont'd.)*

LWC Groups	D: 40% PA + 60% EPA LWC						
	D0	**D1**	**D2**	**D3**	**D1***	**D2***	**D3***
Thermal Conductivity (W/mK)	0.261	0.2517	0.2192	0.2207	0.2558	0.2457	0.2256
Oven-dried Unit weight (Kg/m^3)	755	743.3	738.15	735	753	750	748.4
LWC Groups	**E: 20% PA + 80% EPA LWC**						
	E0	**E1**	**E2**	**E3**	**E1***	**E2***	**E3***
Thermal Conductivity (W/mK)	0.1985	0.1979	0.1887	0.1826	0.1934	0.193	0.1924
Oven-dried Unit weight (Kg/m3)	602.98	597.8	588.3	584	602.9	598.4	589.2
LWC Groups	**F: 100% EPA LWC**						
	F0	**F1**	**F2**	**F3**	**F1***	**F2***	**F3***
Thermal Conductivity (W/mK)	0.1797	0.172	0.1552	0.1558	0.1676	0.1643	0.1472
Oven-dried Unit weight (Kg/m3)	479.8	457.6	441.2	435.1	472.2	468	463.1

Note: 0, 1, 2, 3, following letters show the percentage of SF, respectively, 0, 10, 20, 30% replacement of PC and 1*, 2*, 3* show the percentage of FA 10, 20, 30% replacement of PC for each group.

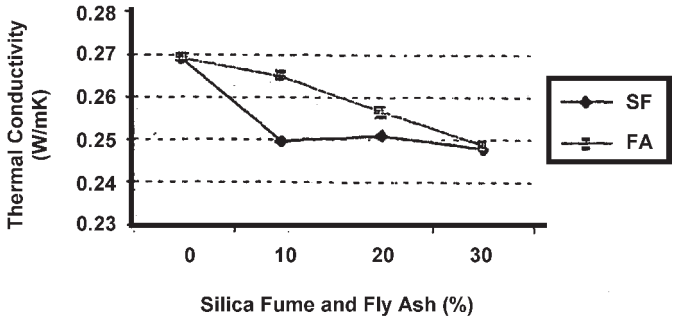

Figure 7.27. Relationship between admixture content and thermal conductivity of sample A.[40]

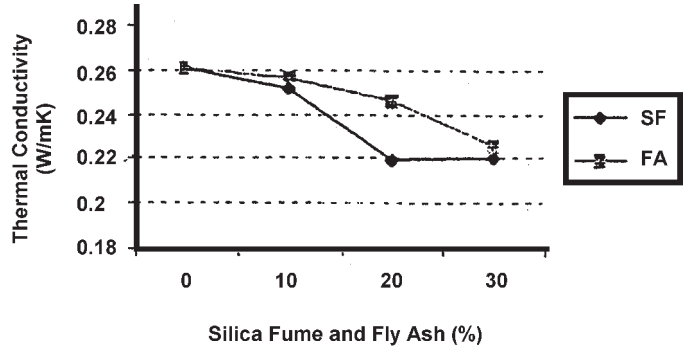

Figure 7.28. Relationship between admixture content and thermal conductivity of sample B.[40]

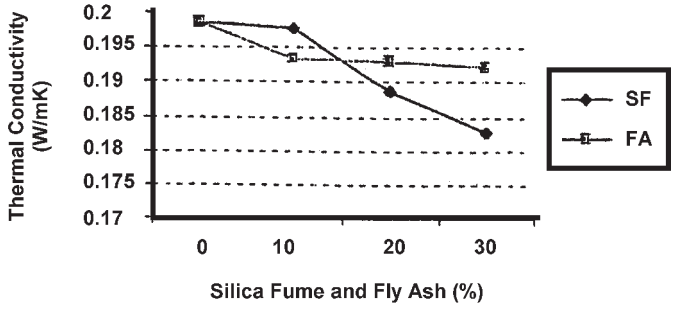

Figure 7.29. Relationship between admixture content and thermal conductivity of sample C.[40]

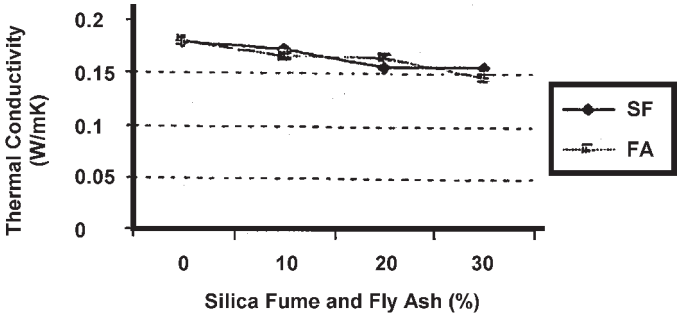

Figure 7.30. Relationship between admixture content and thermal conductivity of sample D.[40]

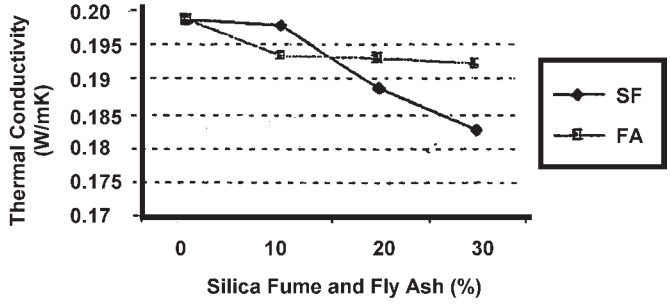

Figure 7.31. Relationship between admixture content and thermal conductivity of sample E.[40]

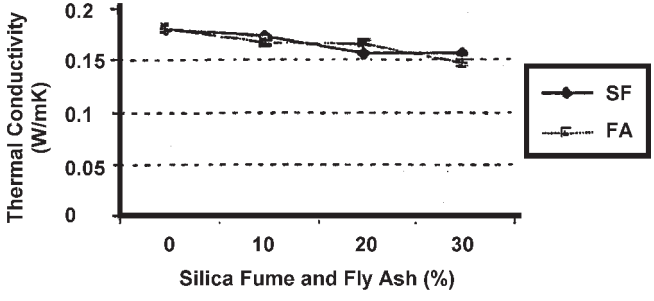

Figure 7.32. Relationship between admixture content and thermal conductivity of sample F.[40]

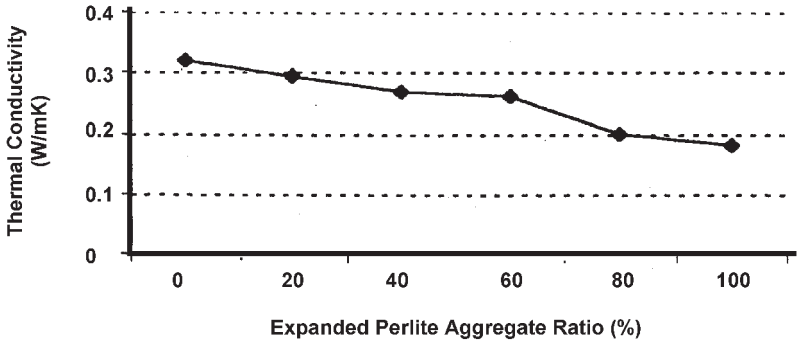

Figure 7.33. Relationship between EPAs ratio and thermal conductivity.[40]

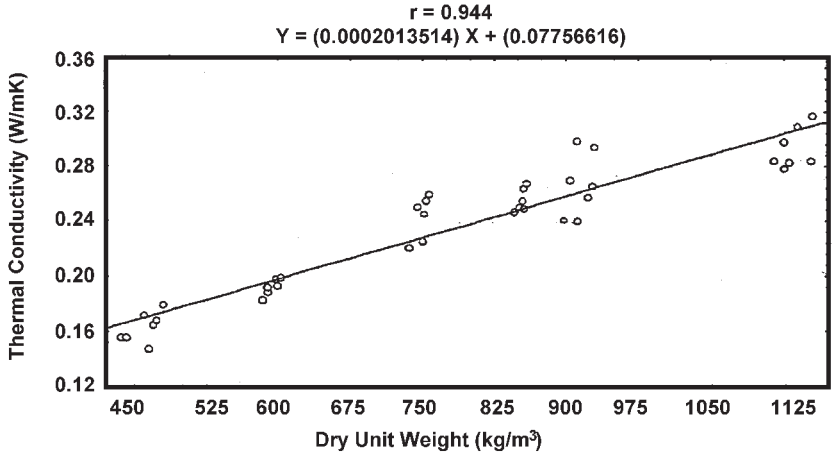

Figure 7.34. Relationship between dry unit weights and thermal conductivity.[40]

SF and FA reduce the thermal conductivity of group A (Fig. 7.27). The reduction in thermal conductivity shown by 10, 20, and 30% SF for group A are 2, 5, 6, and 10% compared to their corresponding control sample, respectively. The reduction due to FA (10, 20, and 30%, replacement of PC) for the same group are 10, 11, and 12%, respectively. This is

because the density decreased with increasing SF and FA content. The low density of LWAC with SF and FA is related to the high air content[41] and amorphous texture of SF and FA.[42][43] The difference between the FAs percents are very high.

For group B (20% EPA and 80% PA), both at 30% SF and FA, thermal conductivity decreased by 18.3 and 18.6%, respectively. The reductions due to FA (10, 20, and 30%) for group B are 9.5, 12.2, and 18.6%, respectively. The effect of FA is greater than the SF for group B at 10 and 20%, but at 30% replacement of PC both have about the same reduction effect. The results are shown in Table 7.18 and Fig. 7.28.

In general for all groups, both SF and FA decreased the thermal conductivity of samples with the increasing of SF and FA content. The reduction due to SF and FA showed the fluctuation. This may be due to the testing conditions and the moisture content of the samples. In any case, both SF and FA decreased the thermal conductivity significantly. The reduction due to the FA is greater than the silica fume. The reduction of thermal conductivity is because of low density of LWAC with SF and FA content and amorphous texture. The low density is related to the high air content of SF and FA.

EPA (replacement of PA) decreased the thermal conductivity of LWAC. For 20, 40, 60, 80, and 100% replacement of PA, other ingredients and conditions were constant. The reductions were 7.3, 15.4, 17.9, 37.5, and 43.5% compared to their corresponding control specimens.

These results reveal that the silica fume (10, 20, and 30% by weight of portland cement), FA (10, 20, and 30% by weight of portland cement), and EPA (20, 40, 60, 80, and 100% of exchange with PA) were effective in decreasing the thermal conductivity of the lightweight aggregate concrete up to 43.5%. This is mainly due to the relatively low thermal conductivity of these admixtures and the aggregate EPA, and the low density of the LWAC produced.

The amorphous texture of the admixture also may be the cause of the reduction because the phonons average free pathway in the amorphous ceramics is shorter than in crystalline ceramics. For this reason, the thermal conductivity of amorphous ceramics is low. For instance, the crystal textured SiO_2s thermal conductivity is 15 times higher than that of the amorphous SiO_2s thermal conductivity.[43]

5.3 Concluding Remarks

Thermal conductivity of lightweight aggregate concrete is related to its pore structure or air-void system. With air as the insulating material, concrete of a higher porosity and a lower density will have a lower thermal conductivity. The air-pore system in the LWAC depends upon the binder system and the chemical admixtures used. With the addition of silica fume and fly ash, thermal conductivity is decreased. The reduction is more pronounced in the case of FA than SF at 10 and 20% replacement, but at 30% replacement, it is approximately the same.

Porous aggregates produce a LWAC with a lower thermal conductivity, but it is not only the total air content which governs thermal conductivity. The geometry of the pores and their distribution play a decisive role in thermal conductivity.

6.0 ABRASION RESISTANCE

It is logical to conclude that the lightweight aggregate concrete will not have adequate abrasion resistance. This is based upon the fact that aggregates are not as strong as stone. However, this is incorrect since the abrasion of concrete does not only depend upon the lightweight aggregates, but also upon the strength of the matrix and the bond between the aggregates and the cement paste. In structural lightweight aggregate concretes, the high strength of the mortar compensates for the low value of the aggregate, and the bond between the mortar and the cement paste is much stronger compared to the bond in normal weight concrete. The bond in the lightweight aggregate concrete is not only on the surface of the aggregates, it penetrates the surface. Apart from this, the surface of the aggregate may be reactive, which leads to the pozzolanic reaction between the calcium hydroxide produced from the portland cement hydration and reactive silica. This makes the bond still stronger. Some tests have been performed by Chandra and Berntsson[8] to test the abrasion resistance of structural lightweight aggregate concrete.

The lightweight aggregate concrete used had the following composition:

Ordinary portland cement	425 kg/m^3
Sand	850 kg/m^3

Swedish Leca™: 2–6 mm	310 l/m^3
Swedish Leca™: 4–10 mm	310 l/m^3
Water-to-cement ratio	0.395
Superplasticizer, Mighty™ (A naphthalene formaldehyde based superplasticizer)	1% to the weight of cement

The fresh density of the concrete was 1750 kg/m^3. The concrete had a slump of 140 mm and the compressive strength at 28 days was 37.0 MPa. For comparison, normal concrete was made with the following composition:

Ordinary portland cement	275 kg/m^3
Sand	1060 kg/m^3
Stones: 8–12 mm	385 kg/m^3
Stones: 12–16 mm	385 kg/m^3
Water	203 kg/m^3
W/C	0.74

The 28 days cube compressive strength of the concrete was 32.5 MPa. The test was performed according to the Swedish Standard SS 1372 41. The apparatus used in the test differed from the one mentioned in the standard in that the load on each wheel was 330 N instead of 130 N and the number of rotations per minute was 67 instead of 60. The apparatus is shown in Fig. 7.35. The conditions of the plates made for the test were 1.1 × 1.1 × 0.25 m. The plates after the test are shown in Fig. 7.36. The results are shown in Table 7.20.

The test results show that the abrasion depth of the normal concrete was 1.9 mm after 800 rotations and 2.6 mm after 1600 rotations. For lightweight aggregate concrete, the abrasion depth after 800 rotation was 1.3 mm and after 1600 rotations, was 1.7 mm. This means that the abrasion resistance of lightweight aggregate concrete is better than the normal concrete tested. The abrasion depths are shown in Fig. 7.36. These results are contrary to normal expectations. The fact behind the strong resistance of lightweight aggregate concrete is the strength of the cement paste, which is two times higher than the strength of cement paste in the normal weight concrete. This is due to the higher amount of cement (3%) in lightweight aggregate concrete compared to the normal concrete and the low water-to-cement ratio, 0.74 in the case of normal concrete, and 0.40 in the case of lightweight aggregate concrete.

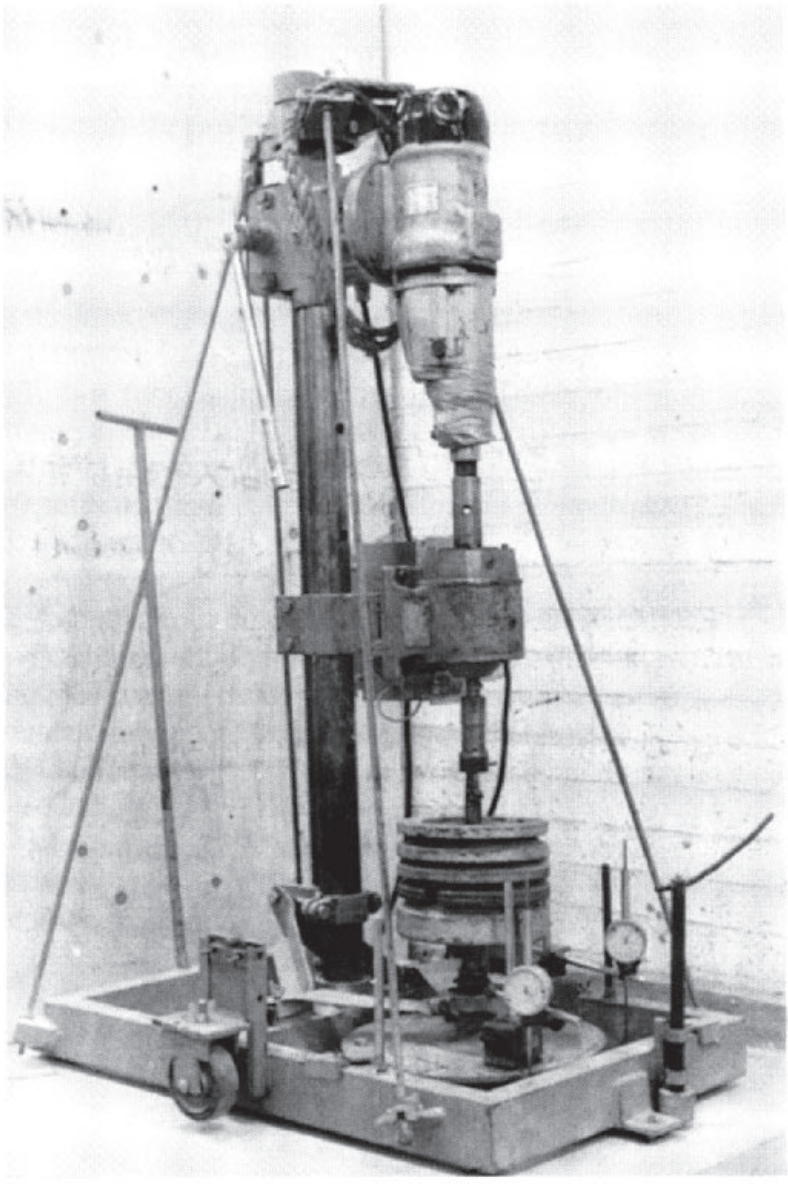

Figure 7.35. Apparatus for measuring abrasion resistance.[8]

Table 7.20. Abrasion Depth Measured During the Test[8]

No. of Rotations	Normal Concrete, mm			Lightweight Concrete, mm		
	Max	Min	Middle	Max	Min	Middle
800–1	1.04	2.64	1.84	0.86	1.56	1.21
800–2	1.24	2.73	1.99	0.93	1.94	1.43
1600–1	1.36	3.91	2.63	1.16	2.20	1.68
1600–2	1.40	3.89	2.65	1.19	2.31	1.73

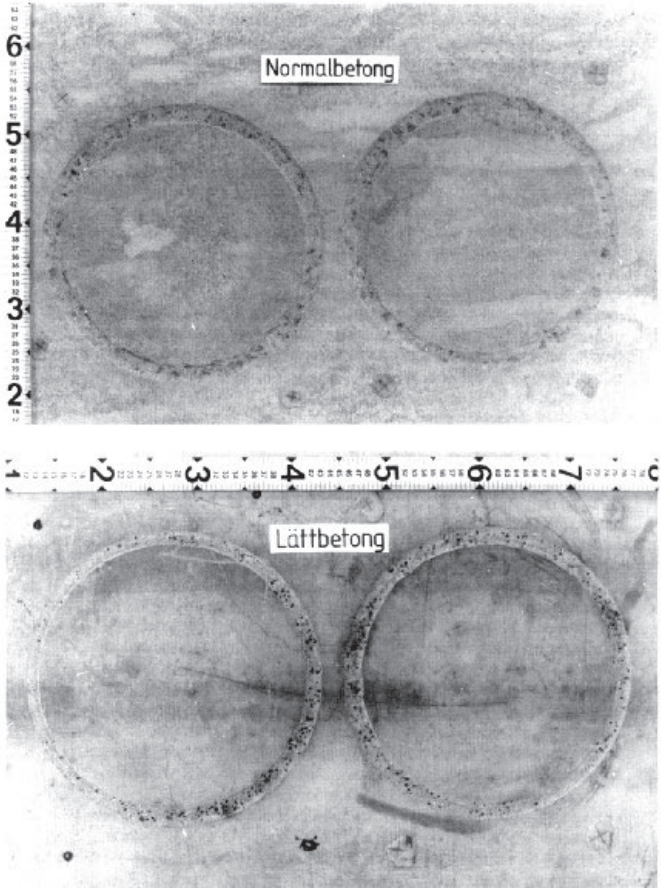

Figure 7.36. The plates after testing for abrasion resistance.[8]

6.1 Concluding Remarks

It is demonstrated that the lightweight aggregate concrete, in spite of the low strength of the aggregates, can have higher abrasion resistance compared to the normal construction concrete. This depends upon the cement mortar matrix. Structural high-strength lightweight aggregate concretes are produced using a high-strength cement matrix. Aggregates are also available today which have higher strength than the expanded clay aggregate Leca™. These can be used to produce abrasion resistant concrete.

REFERENCES

1. Dolby, P. G., Production and Properties of Lytag™ Aggregate Fully Utilized for the North Sea, *Proc. Int. Symp. Structural Lightweight Aggregate Concrete*, Sandefjörd, Norway, (Holand, et al., ed.) pp. 326–336 (Jun. 20–24, 1995)
2. Berge, O., Iceland Pumice; Some Significant Properties of Pumice as Aggregates, Internal Report 83:1, Building Materials, Chalmers University of Technology, Gothenburg, Sweden (1983)
3. Rodhe, M., Some Observations during Mortar Mixing of Iceland Pumice, Internal Report 84:2, Building Materials, Chalmers University of Technology, Gothenburg, Sweden (1984)
4. Rodhe, M., Properties of Fresh and Hardened X-Concrete, Internal Report 86:3, Building Materials, Chalmers University of Technology, Gothenburg, Sweden (1986)
5. C & CA., An Introduction to Lightweight Concrete, Cement and Concrete Association, Technical Advisory Series, SIB C1 96, London (1970)
6. Faust, T., Properties of Different Matrices and Lightweight Aggregate Concrete, *Proc. 2nd Int. Symp. Structural Lightweight Aggregate Concrete 2000*, Kristiansand, Norway, pp. 502–511 (Jun. 2000)
7. Abdullah, A. A. A., Palm Oil Shell Aggregate for Lightweight Concrete, *Waste Materials Used in Concrete Manufacturing*, (S. Chandra, ed.) Noyes Publ., Park Ridge, NJ (1995)
8. Chandra, S., and Berntsson, L., Structural Lightweight Aggregate Concrete, Swedish Council of Bld. Research, Report R13 1994, Stockholm, Sweden (1994)

9. Larmakovski, V. N., New Types of the Porous Aggregates and Lightweight Concretes with their Application; *Proc. Int. Symp. Structural Lightweight Aggregate Concrete*, Sandefjörd, Norway, (I. Haland, T. A. Hammer, and F. Fluge, eds.) p. 363 (1995)
10. Sandvik, M., and Hammer, T. A., The Development and use of High Performance LWAC in Norway, *Proc. 1st Int. Symp. Structural Lightweight Aggregate Concrete*, Sandefjörd, Norway, (I. Haland, T. A. Hammer, and F. Fluge, eds.) pp. 617-662 (Jun. 20–24, 1995)
11. De Pauw, P., Taerve, L., and Desymyter, J., Concrete and Masonry Rubble as Aggregates for Concrete, Something in between Normal and Lightweight Concrete, *2nd Int. Symp. Structural Lightweight Aggregate Concrete 2000*, Kristiansand, Norway, pp. 660–669 (1995)
12. Bilodeau, A., and Hoff, O., *Proc. Int. Symp. Structural Lightweight Aggregate Concrete*, Sandefjörd, Norway, (I. Haland, T. A. Hammer, and F. Fluge, eds.) p. 363 (1995)
13. Helland, S., and Maage, M., Strength Loss in Unremixed LWA-Concrete, *Proc. Int. Symp. Structural Lightweight Aggregate Concrete*, Sandefjörd, Norway, (Holand, et al., ed.) pp. 533–540 (Jun. 20–24, 1995)
14. Punkki, J., and Gjörv, O. E., Effect of Water Absorption by Aggregates on Properties of High Strength Lightweight Concrete, *Proc. Int. Symp. Structural Lightweight Aggregate Concrete*, Sandefjörd, Norway, (I. Haland, T. A. Hammer, and F. Fluge, eds.) pp. 604–616 (Jun. 20–24, 1995)
15. Khokhorin, N. K., The Durability of Lightweight Structural Members, *Kuibyshev*, U.S.S.R (in Russian) (1973)
16. Goodier, J. N., Concentration of Stress Around Spherical and Cylindrical Inclusions and Flaws, *J. Appl. Mec., Trans. of ASME*, 55:A-39–A-44 (1933)
17. Bremner, T. W., and Holm, T. A., Elastic Compatibility and the Behavior of Concrete, *Journal, ACI*, pp. 244–250, March-April 83-85 (1986)
18. Nishi, S., Oshio, A., Sone, T., and Shirokuni, S., Water Tightness of Concrete Against Sea Water, *J. Central Res. Lab.*, Onoda Cement Co., Tokyo, 32(104):40–53 (1980)
19. Faust, T., Softening Behavior of Lightweight Aggregate Concrete, *2nd Int. Symp. Structural Lightweight Aggregate Concrete* Kristiansand, Norway, pp. 522–530 (Jun. 2000)
20. Schütz, F. R., *Ein-fluss der Zuschlagelastizität auf die Betondruckfestikeit*, Dissertation, TH Aachen, Germany (1970)
21. Müller-Rochhoilz, J., *Ein-fluss von Liechtzuschlagen*, Betong+Fertigteil-Technic, Heft 10 (1979)

22. Nagataki, S., and Yonekura, A., The Mechanisms of Drying Shrinkage and Creep of Concrete, *Trans. Jpn. Concr. Inst.*, 5:127–140 (1983)

23. Iwasaki, N., *Properties of Concrete*, pp. 126–127, Kyoritsu Publishing, (Japanese) (1975)

24. Neville, A. M., *Creep of Concrete, Plain, Reinforced, and Prestressed*, North Holland Publishing Company, Amsterdam (1973)

25. Powers, T. C., Wittman, F., Feldman, R. F., Sereda, P. J., Mills, R. H., and Coutino, S., Session 6 Final Report and Conclusion, *RILEM J Mater. Con.*, 2(8):153–162 (1969)

26. Ramachandran, V. S., and Feldman, R. F., Length Change Characterstic of $Ca(OH)_2$ Compacts on Exposure to Water Vapor, *J. Appl. Chem*., 17:328 (1967)

27. Swenson, E. G., and Sereda, P. J., Mechanism of Carbonation Shrinkage of Lime and Hydrated Cement, *J. Appl. Chem.*, 18:111 (1968)

28. Powers, T. C., A Hypothesis on Carbonation Shrinkage, PCA, *Res. Dep. Bull. 146* (1962)

29. Lentz, C. W., Effect of Carbon Dioxide on Silicate Structures in Portland Cement Paste , *30th Cong. Industrial Chemistry*, Brussels, Comte Rendu II Gr., VII, S17, 455, 1965,1 (1965)

30. Alexander, K. M., and Wardlaw, J., A Possible Mechanism for Carbonation Shrinkage and Grazing, Based on the Study of Thin Layers of Hydrated Cement, *Aust. J. Appl. Sci.*, 10(4):470 (1959)

31. Klemn, W. A., and Berger, R. R., Accelerated Curins of Cementitious Systems by Carbon Dioxide, *Cement and Concrete Research*, 2(5):567 (1972)

32. Liu, X., Yang, Y., and Jiang, A., The Influence of Lightweight Aggregates on The Shrinkage of Concrete, *2nd Int. Symp. Structured LWAC*, Kristiansand, Norway, pp. 555–562 (1995)

33. Bijen, J. M. J. M., Manufacturing Processes of Artificial LWA from Fly Ash, *Int. J. Cem. Comp. Lightweight Concrete*, 8(3):191–199 (1986)

34. van der Wegen, J. L., and Bijen, J. M. J. M., Properties of Concrete made with Three Types of Artificial Coarse Aggregates, *Int. J. Cem. Comp. Lightweight Concrete*, 7(3):159–167 (1985)

35. Rostasy, F. S., Teichen K. T., and Alda, W., Ueber das Schwinden und Kriechen von Leichtbeton bei Unterschiedlicher Korneigenfeuchtigheit, *Beton*, 24(6):223–235 (1974)

36. Kovalenko, N. V., and Terentyev, A. Y., Lightweight Expanded Clay Aggregate Foam Concrete, Investigation, Production, Construction, *Proc. Int. Symp. Structural Lightweight Aggregate Concrete*, Sandefjörd, Norway, (Holand, et al., ed.) pp. 397–417 (Jun. 20–24, 1995)

37. Abdullah, A. A. A., Basic Strength Properties of Lightweight Concrete Using Agricultural Wastes as Aggregates, *Proc. Int. Conf. on Low-cost Housing for Developing Countries*, Roorkee, (Nov. 1984)

38. Nobuta, Y., Satoh, K., Hara, M., Sogoh, S., Takimoto, K., Applicability of Newly Developed High Strength Lightweight Concrete for Civil Structure, *2nd Int. Symp. Structural Lightweight Aggregate Concrete*, Kristiansand, Norway, pp. 396-405 (Jun. 2000)

39. Dhir, K., Mays, R. G. C., and Chua, H. C., Lightweight Structural Concrete with Aglite Aggregate: Mix Design and Properties, *Int. J. Cem. Comp. Lightweight Concrete*, 6(4):249–262 (1984)

40. Demirboga, R., Gül, R., Habib, U., and Düzgün, A. O., The Effects of Silica Fume and Fly Ash on the Thermal Conductivity of Lightweight Aggregate Concrete, *Proc. 2nd Int. Symp. Structural Lightweight Aggregate Concrete*, Kristiansand, Norway, pp. 483–501 (Jun. 2000)

41. Fu, X., and Chung, D. D. L., Effects of Silica Fume, Latex, Methylcellulose, and Carbon Fibers on the Thermal Conductivity and Specific Heat of Cement Paste, *Cement and Concrete Research*, 27(12):1799–1804 (1997)

42. Onaran, K., *Malzeme Bilimi (Materials Science), S 174*, Bilim Teknik Yayinevi, Istanbul, Turkey (1993)

43. Postacioglu, B., *Baglyici Maddeler, Agregalar, Beton, Cilt. I. Baglayici Maddeler*, Matbba Teknisyenleri Basimevi, Istanbul, Turkey, pp. 63–66 (1986)

8

Durability of Lightweight Aggregate Concrete to Chemical Attack

1.0 INTRODUCTION

Chemical durability is defined as the resistance of concrete against the gases, chemicals, and temperature variations which interact chemically with the binder components of the concrete causing deterioration. Lightweight aggregate concrete is made using different types of cements, mineral admixtures, and aggregates. These material variations influence the degree and rate of deterioration. The following types of chemical attack are discussed in this chapter.

Acid Resistance

Alkali-Aggregate Reaction

Carbonation and Corrosion

Chloride Ion Penetration

Extensive research data on the chemical durability of normal weight concrete are available whereas not much information is available on the chemical durability of LWAC. Besides, there are different types of concrete, ranging from low density insulating concrete to high strength structural concrete. This makes it difficult to collect data and assess the

durability of each concrete systematically against the different chemicals and other environmental conditions to which it is exposed. Nevertheless, the mechanisms involved in some of the deterioration processes are explained and the relevant examples are reviewed.

2.0 ACID RESISTANCE

Acids attack hardened concrete in different ways. The effect differs from acid to acid and is related to the type of LWAC. Chandra[1] has tested the durability of LWAC against three acids; hydrochloric acid, sulfuric acid, and lactic acid. A review of the results and the mechanisms involved follows.

The composition of the lightweight aggregate concrete tested is shown in Table 8.1. The table shows that the chemical admixture "CEMOS" is used. It is an asphalt-modified acrylic polymer dispersion. Its function is threefold:

1. To help disperse the aggregates.
2. To work like an air-entraining admixture.
3. To create hydrophobicity.

Mortar prisms of 6 × 6 × 12 cm size were cast and cured for 5 days in water and later in the climate room at 55% RH and 20°C. The samples tested were cast in and cut with exposed aggregate surfaces. Comparisons were done with normal weight concrete.

Solutions of 15% hydrochloric acid (HCl), 5% sulfuric acid (H_2SO_4), and 5% lactic acid (CH_3 CHOH COOH) were made and the specimens were continuously immersed in these solutions. The cement used was Swedish ordinary portland cement, C_3S-64%, C_2S-13%, C_3A-8%, C_4AF-10%, specific surface-337 m^2/kg.

LWA is an expanded clay aggregate produced in a rotary kiln. The aggregate is a regularly rounded particle with a dense skin. The particle density is about 800 kg/m^3 for 2–4 mm and 700 kg/m^3 for 4–12 mm. The percent of the polymer admixture CEMOS is calculated on the basis of its solid content.

Weight changes were noted at specific intervals. The test method followed for the hydrochloric and sulfuric acid was the same as described by DePuy.[2] In all cases, concentrations of the acid solutions (pH) were kept constant by titrating against sodium hydroxide (NaOH) using methyl red as an indicator.

Table 8.1. Concrete Composition, Density, and Compressive Strength[1]

Type of Concrete	No.	Adm. (%) to Cement Weight	Cement kg/m^3	Sand/Gravel kg/m^3		Sand /LWA kg/m^3			W/C	Fresh Density kg/m^3	28 d Comp. Str. MPa
				Sand 0–8 mm	Gravel 8–16 mm	Sand 0–4 mm	LWA 2–4 mm	LWA 4–12 mm			
Normal weight concrete	N	–	500	930	750	–	–	–	0.45	2400	45.0
	NA	CEMOS 1.5	500	930	750	–	–	–	0.41	2180	33.2
LWAC	L	CEMOS 1.5	315	–	–	305	120	285	0.60	1247	18.0
	LB	CAEA 0.05	315	–	–	305	120	285	0.55	1350	20.4

N — Normal concrete
NA — Normal concrete with CEMOS
L — 3L concrete (LWAC with CEMOS)
LB — LWAC with conventional air-entraining agent (CAEA)

2.1 Hydrochloric Acid (HCl) Attack

Hydrochloric acid (HCl) attacks hardened concrete through a dissolution process, forming soluble salts; leaching also takes place. During this process, the pH of the acid solution is increased. Consequently, hydrolysis is resumed, and eventually Si, Al, and Fe gels are produced. During the test, it was observed that the outer surface of the specimen was yellow, whereas the interior was brown. This is caused by the difference in the $Fe(OH)_3$-content as confirmed by Rubetskaya, et al.[3] Chandra[1] described an HCl attack as a reaction that occurs in layers forming distinct zones.

The results of concrete deterioration in terms of percent weight loss, are shown in Fig. 8.1 and the physical appearances of the specimens are shown in Fig. 8.2. These results show that the minimum damage occurred in the LWAC with the polymer micro-particle (3L-concrete) and the maximum in the normal concrete. Further, the difference is more pronounced in the normal concrete without the polymer micro-particles.

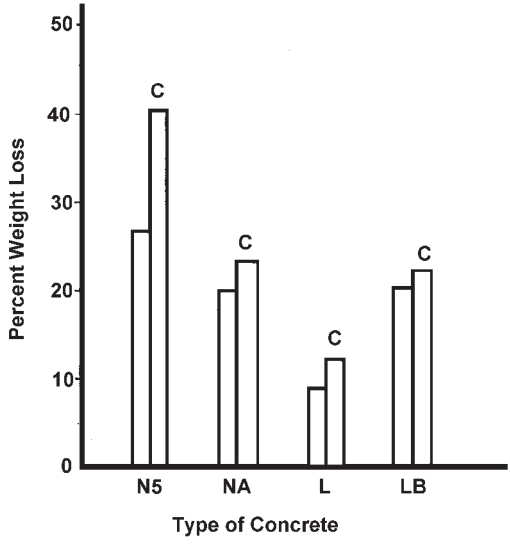

Figure 8.1. Percent weight loss of concrete after storing in 15% hydrochloric acid solution for 3 months; size of the specimens 6 × 6 × 12 cm, C-cut surfaces, LB-lightweight aggregate concrete with conventional air intruder, L-3L concrete, NA-normal concrete K50 with CEMOS 110, N5-normal concrete K50.[1]

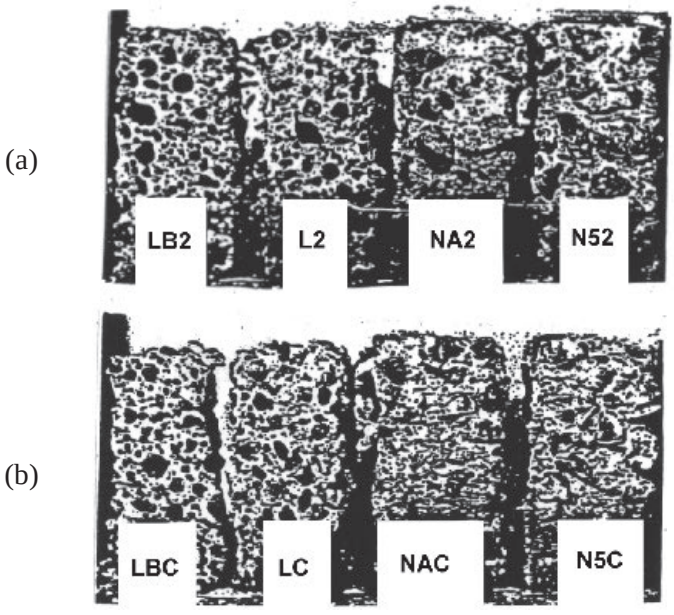

Figure 8.2. Physical appearance of the specimens after storing in 15% hydrochloric acid solution for 3 months; *a)* cast surface, *b)* cut surface, LB-LWAC with air-entraining agent, L-3L concrete, NA-normal concrete K50 with CEMOS 110, N5-normal concrete K50 without CEMOS 110.[1]

The 3L concrete is damaged less than the LWAC with the conventional air-entraining agent. The reason for this is attributed first to the change in the structure of the concrete because of the addition of the micro-particles, providing a more compact structure, and second, to the hydrophobic character that the micro-particles have imparted to the concrete which reduces the absorption property.[1] Due to this, the penetration of the acid was slower than without micro-particles. A third reason is the complex formation due to the reaction between calcium hydroxide and carboxylate ions of the polymer particles.[4][5] The calcium complex is hydrophobic in nature, therefore the availability of free calcium hydroxide in concrete vulnerable to acid attack is less.

The damage was more pronounced in cut sections than in uncut ones. In the first case, the cement mortar is damaged on the aggregate surface whereas, in the latter case, the damage occurs directly on the cement paste between the aggregate particles. Moreover, due to the formation of the hydroxide layer on the surface of the uncut specimens, the

acid penetration is delayed. These results reported by Chandra[1] are in agreement with the observations made by Romben,[6] Dehler,[7] and Biczok.[8] The damage to the concrete as observed was in the following order: N5 > NA > LB > L.

2.2 Sulfuric Acid (H_2SO_4) Attack

Attack of hydrated portland cement by sulfuric acid is two-fold. The first one is by acid attack or hydrogen ions and the second is by the sulfuric ions. Two salts are formed: namely calcium sulphate from sulphate ions, and calcium hydroxide and ettringite from calcium sulphate and calcium aluminate. These are expansive salts and the pressure produced during their formation causes concrete to crack and disintegrate.

The results of concrete deterioration in terms of percent weight loss are shown in graphical form in Fig. 8.3 and their physical appearance is shown in Fig. 8.4a for the normal specimens and in Fig. 8.4b for the cut surface specimens.

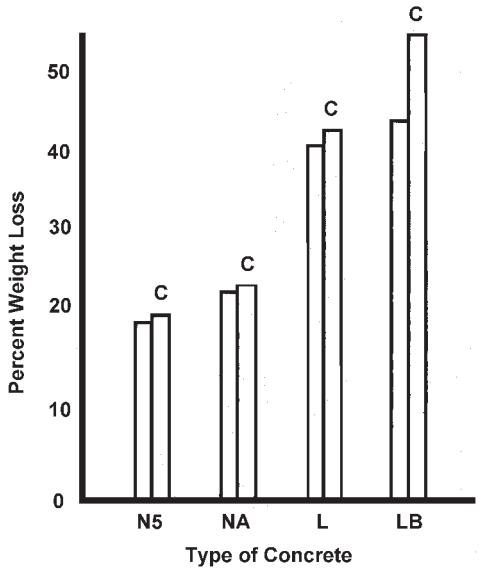

Figure 8.3. Percent weight loss of concrete after storing in 5% sulfuric acid for 6 weeks; size of the specimens is 6 × 6 × 12 cm, C-cut surfaces, LB-lightweight aggregate concrete with conventional air intruder, L-3L concrete, NA-normal concrete K50 with CEMOS 110, N5-normal concrete K50 without CEMOS 110.[1]

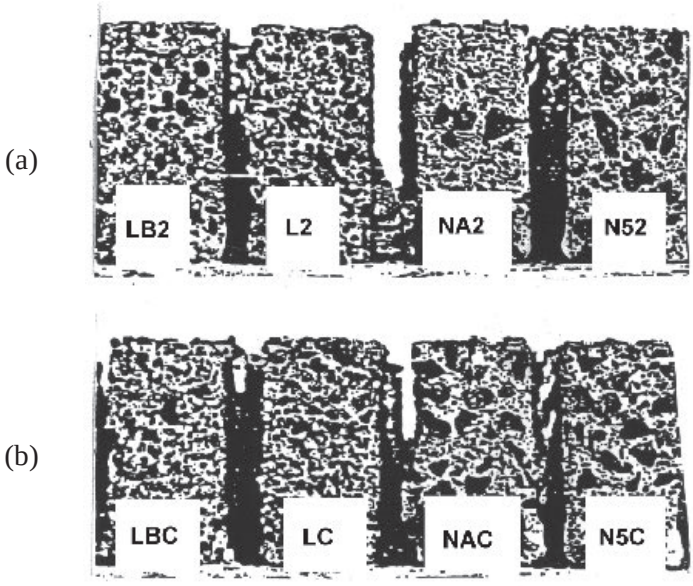

Figure 8.4. Physical appearance of specimens after storing in 5% sulfuric acid solution for 3 months; *a)* cast surface, *b)* cut surface, LB-LWAC with air-entraining agent, L-3L concrete, NA-normal concrete K50 with CEMOS 110, N5-normal concrete K50 without CEMOS 110.[1]

Sulfuric acid caused more damage to the LWAC than to the normal concrete. The maximum damage noticed was in the LWAC with a conventional air-entraining agent. The damage to the lightweight aggregate concrete appeared on the cementing edges, and the aggregates were also affected. The expansion of cement paste in the concrete of insoluble sulfate may have crushed the LWA and increased the permeability of the concrete.

In normal weight concrete, CEMOS did not increase the resistance against sulfuric acid. The deterioration of the concrete occurred in the following order: LB > L > NA > N5.

2.3 Lactic Acid (CH_3 CHOH COOH) Attack

Lactic acid attacks are due to the formation of calcium lactate. The calcium lactate formed may dissociate easily giving more ions and increasing the conductivity. The solubility of $Ca(OH)_2$ and C_3S in lactic acid is high. During the test, Chandra[9] observed the growth of a hard, white

insoluble material in the matrix between the aggregates. This increased the weight of the concrete. These results parallel the observations made by Dehler.[7]

The results of the concrete deterioration in terms of percent weight loss are reported in graphical form in Fig. 8.5 and their physical appearance in Fig. 8.6a for normal specimens and in Fig. 8.6b for the cut surface specimens. The results clearly show that minimum damage occurred in the lightweight aggregate concrete with the CEMOS addition.

The samples under the lactic acid solution did not deteriorate much. However, while the samples were in the drying state, a white precipitate appeared on the surface in the matrix between the aggregates and mortar. It looked like a precipitate of calcium lactate, which forms according to the following reaction.[10]

$$2CH_3CHOHCOOH + Ca(OH)_2 \rightarrow Ca\begin{matrix}\diagup \\ \diagdown\end{matrix}\begin{matrix}COOCHOHCH_3 \\ COOCHOHCH_3\end{matrix} + H_2O$$

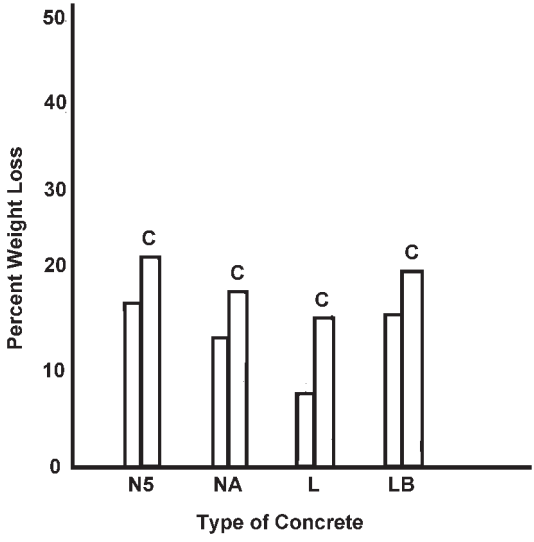

Figure 8.5. Percent weight loss of the concrete after storing in 5% lactic acid solution for 3 months; size of the specimens 6 × 6 × 12 cm, C-cut surfaces, LB-lightweight aggregate concrete with conventional air intruder, L-3L concrete, NA-normal concrete K50 with CEMOS 110, N5-normal concrete K50.[9]

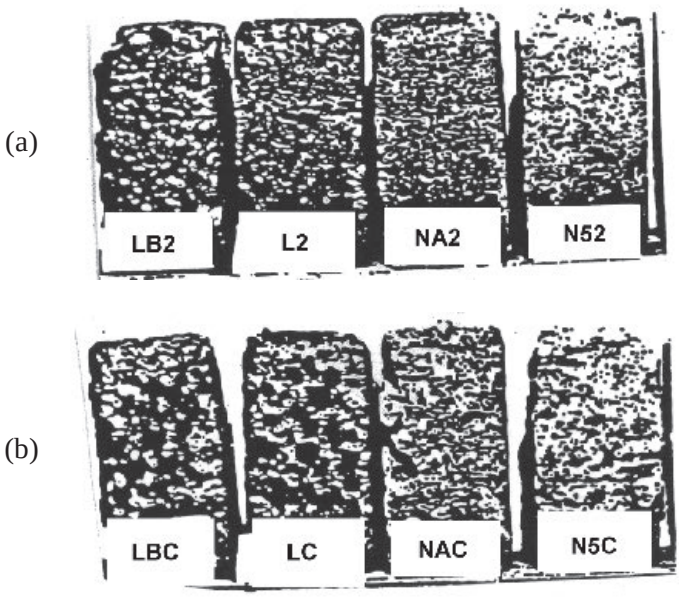

Figure 8.6. Physical appearance of the specimens after storing in 5% lactic acid solution for 3 months; *a)* cast surface, *b)* cut surface, LB-LWAC with air-entraining agent, L-3L concrete, NA-normal concrete K50 with CEMOS 110, N5-normal concrete K50 without CEMOS 110.[9]

Calcium lactate, thus formed, may dissociate easily giving more ions and increasing the conductivity. The solubility of $Ca(OH)_2$ and C_3S in lactic acid is higher. The destruction observed was in the following order: L<NA<LB<N5. The cut surfaces were more damaged than the cast surfaces. Lightweight aggregate concrete, in this case, was also less damaged than the normal concrete as was the case with the hydrochloric acid attack. The reason for this is the same as is explained in the case of hydrochloric acid.

2.4 Concluding Remarks

Tests have demonstrated that the lightweight aggregate concrete with CEMOS is the most resistant to hydrochloric and lactic acid. This is because of the hydrophobic property introduced by the polymer CEMOS in the lightweight aggregate concrete. It correlates to the cement content in the concrete. Normal weight concrete, both with and without an air-entraining

agent, was more damaged than the LWAC. Normal weight concrete had more cement compared to the lightweight aggregate concrete. It produces more $Ca(OH)_2$ which reacts with HCl and forms $CaCl_2$, which leaches away. Concrete, in this way, loses strength. Besides, the attack of acidic dissolution increases porosity which provides easy access for further penetration of the acid. Apart from this, the bond between the lightweight aggregates and the cement is not just on the surface like in normal weight concrete. Because of the porous nature of the aggregate, the binder penetrates inside the aggregates. This makes the bond much stronger. It means that, with the action of the acid on the surface, the aggregates do not fall apart as in normal weight concrete.

However, in the case of sulfuric acid, expansive salts, i.e., ettringite and gypsum, are formed which produce substantial stresses. Lightweight aggregate concrete, which is lower in strength than normal weight concrete, becomes more damaged.

3.0 ALKALI-AGGREGATE REACTION

Alkali ions present in portland cement, in the binder used, or from other sources outside concrete, may react with some of the siliceous constituents that may be present in some of the aggregates. This leads to expansion and cracking. The phenomenon, called an alkali-silica reaction, can influence the strength and elasticity of concrete. Pop-outs and a white deposit on the surface are other signs of an alkali-silica reaction. Three types of alkali-aggregate reaction can occur:

- Alkali-silica reaction.
- Alkali-carbonate reaction.
- Alkali-silicate reaction.

3.1 Alkali-Aggregate Reaction in LWAC

Normal weight concrete is made using natural stone aggregates, which can be sensitive to the alkali. Concrete deteriorates due to the alkali-aggregate reaction. In the case of lightweight aggregate concrete, a part of the regular aggregates, depending upon the type of concrete produced, are replaced by lightweight aggregates. Lightweight aggregates are of different

types. Some of them are of natural origin like volcanic sources and the others are man made in factories; examples include expanded clay aggregates like Leca™, in Sweden and Norway, and Liapor™ in Germany; sintered fly ash aggregates; Lytag™; expanded slag aggregates; etc. These aggregates are not alkali sensitive. With the partial replacement of the normal aggregate, the risk of alkali-aggregate reaction is decreased.

The high performance concretes are made with the addition of mineral admixtures like silica fume and chemical admixtures, i.e., superplasticizer. This makes it possible to produce concrete with a low water-to-binder ratio. A low water-to-binder ratio produces concrete of low permeability. Apart from this, these additions dilute the effect of the alkali on portland cement. A decrease in the permeability and the dilution effect further reduce the risk of damage to concrete due to the alkali-aggregate reaction.

3.2 Indirect Tensile Test

An alkali-aggregate reaction causes cracking of the structure. When internal distress is associated with expansive reactions, testing in compression may fail to diagnose the problems because many of the cracks that have formed will close during the compression testing procedure. Quite the opposite occurs when concrete is tested in tension. The largest and least favorably-oriented cracks and tensile stress components form the nucleus for failure of the specimen. Concrete cylindrical specimens made with and without reactive aggregates were tested by an indirect tensile test.[11] For almost one year, expansions and compressive and tensile strengths were measured. While compressive strengths were modestly reduced by cracking due to deleterious expansion caused by alkali-aggregate reactivity, profound reductions occurred in companion tensile strength specimens. For the structures containing reactive aggregates, both compressive and tensile strengths should be measured. The indirect tensile test is especially suited to testing of cores from structures. Because it seeks out the weakest link, it appears to give a more accurate indication of the concrete deterioration than measurements of compressive strength.

Further, the inclusion of a Solite aggregate in the lightweight concrete has several beneficial effects on concrete containing reactive aggregates. The pozzolanic activity created by the surface of the expanded shale can improve the internal integrity beyond that expected from concrete containing non-reactive aggregates. As well, inclusion of lightweight

aggregate moderates and maintains compressive strength and tensile strength loss, and reduces the disruptive expansion experienced by concrete containing reactive coarse aggregates. By providing additional pore space to relieve the pressures developed during the AAR, the lightweight aggregate is capable of reducing the severity and the extent of the reaction itself. Expansions of similar concrete mixtures have also demonstrated significant reductions in deleterious expansions caused by reactive normal weight coarse aggregates. With appropriate addition rates of expanded shale aggregates, there has been no evidence of cracking or degradation of engineering properties. It appears that the Solite aggregate plays a duel role, as both an accommodation mechanism and as a relatively slow acting, but significant pozzolan.

3.3 Concluding Remarks

Research shows that lightweight aggregate concrete does not contain alkali-sensitive aggregates as in the case of normal weight concrete. Hence, an alkali-silica reaction is avoided to a great extent. Nevertheless, it was demonstrated that the inclusion of expanded shale aggregates in the lightweight concrete has several beneficial effects on concrete containing reactive aggregates. The pozzolanic activity created by the surface of the expanded shale can improve the internal integrity beyond that expected from concrete containing non-reactive aggregates. As well, inclusion of lightweight aggregate moderates and maintains compressive strength and tensile strength loss, and reduces the disruptive expansion experienced by concrete containing reactive coarse aggregates. By providing additional pore space to relieve the pressures developed during the AAR, the lightweight aggregate is capable of reducing the severity and the extent of the reaction itself. Expansions of similar concrete mixtures have also demonstrated significant reductions in deleterious expansions caused by reactive normal weight coarse aggregates. With appropriate addition rates of expanded shale aggregates, no evidence of cracking or degradation of engineering properties has been found.

4.0 CARBONATION AND CORROSION

Concrete, when exposed to the atmosphere, interacts with carbon dioxide which is found in nature. The interaction is mainly with the calcium

hydroxide that was produced during the hydration of portland cement. The calcium silicate hydrate also reacts with carbon dioxide. This process is known as carbonation. Calcium hydroxide exists in the pores of concrete. It provides alkalinity to the concrete and protects the reinforcement bars from corrosion. In concrete, the pH is normally 13.5, which is from the alkalis in cement. When carbon dioxide reacts with calcium hydroxide, the alkalinity is reduced from 12.5 to 8.5, which is measured by determining the change in the pH value. Carbonation depth is determined by measuring the pH value of the liquid phase in equilibrium with the solid mass. The carbonation process is shown schematically in Fig. 8.7.[12]

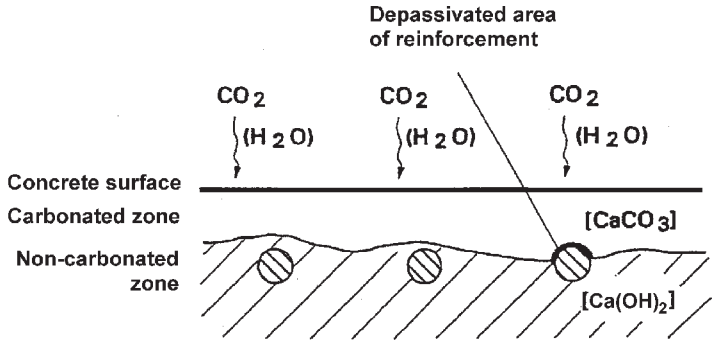

Figure 8.7. Schematic representation of the carbonation process.[12]

4.1 Chemical Interaction

The basic chemical reaction involved in the carbonation process is as follows:

$$Ca(OH)_2 + CO_2 \rightarrow CaCO_3 + H_2O + q \text{ joules}$$

where q = 2430 J/g of reacted CaO.

This reaction takes place in the presence of moisture,[13] that is, the adsorbed CO_2 gas, coming into contact with water, gets dissolved and then penetrates further; while this reaction dominates, others also take place. Berger, et al.,[14] reported the following reaction:

$$C_3S + yH_2O + (3\text{-}x)\ CO_2 \rightarrow CSyH + (3\text{-}x)\ CaCO_3$$

$$C_2S + yH_2O + (2\text{-}x)\ CO_2 \rightarrow CSyH + (2\text{-}x)\ CaCO_3$$

Carbon dioxide lowers the pH value by forming carbonic acid. It interacts and forms highly insoluble calcium carbonate. Water containing aggressive carbon dioxide causes the carbonate in the outer layer to transform into soluble calcium bicarbonate.[15]

$$Ca(OH)_2 + CO_2 \rightarrow\ CaCO_3 + H_2O$$

$$C_3S_2H_3 + 3CO_2 \rightarrow CaCO_3 + S_2 + 3H_2O$$

$$CaCO_3 + CO_2 + H_2O \rightarrow Ca(HCO_3)_2$$

Some of the bicarbonate that is formed leaches out, whereas a small amount penetrates further to react with $Ca(OH)_2$.

$$Ca(HCO_3)_2 + Ca(OH)_2 \rightarrow 2CaCO_3 + 2H_2O$$

All these reactions take place only in the presence of water. In the dry state, the reaction will not take place. This supports the argument that the carbon dioxide must be dissolved before taking part in the carbonation reaction. Verbeck[16] reported that the rate of carbonation is extremely high at relative humidities of 50 to 75% and practically nil at 25 and 100%. At 100% RH, the pores are almost full and dispersion of CO_2 becomes slower than when the pores are not as full of water. Nevertheless, in the latter case carbon dioxide can be dispersed into the interior as a gas. Concrete can also get damaged under water because of dissolved carbon dioxide. There can be high levels of carbon dioxide due to decay of plants in water.[17] In that case, the damage is caused by the interaction of carbonic acid.

Apart from the interaction with calcium hydroxide, carbon dioxide also interacts with hydrated aluminates and calcium sulfoaluminates.[18][19]

$$C_4AH_{13} + 4CO_2 \rightarrow 4\ CaCO_3 + 2Al(OH)_3 + 10\ H_2O$$

While the calcium compounds are converted to carbonates, sodium and potassium hydroxides released during the cement hydration also react in a similar manner.[20]

Normal atmospheric concentration of CO_2 is 0.03%, but it can be higher depending upon location, for example, in industrial areas, garages, etc.

4.2 pH Profile

As the carbonation proceeds, different zones are formed and the pH varies accordingly. A pH profile is shown in Fig. 8.8.[21] Carbonation depth is generally measured by noting the change in color using a phenolphthalein indicator. It indicates the change in the pH value and is the measure of neutralization depth up to a certain pH value (approximately 9.5), but it is not a measure of carbonation depth. For this reason, when the carbonation reaction is in progress, pH is between 9.5 and 12.5, farther than the boundary shown by the color change. It will not be detected by the phenolphthalein indicator. The pore water in equilibrium with non-carbonated concrete has a pH that lies in the range of 12.5 to 13.5 due to the dissolved alkalis. The pH falls as the carbonation proceeds so that a totally carbonated layer may have a pH of about 8.3. The intermediate layer between the carbonated and non-carbonated areas might have extra calcium hydroxide, which flows in from the non-carbonated zone due to the concentration gradient. This zone is actually very susceptible from the durability point of view.

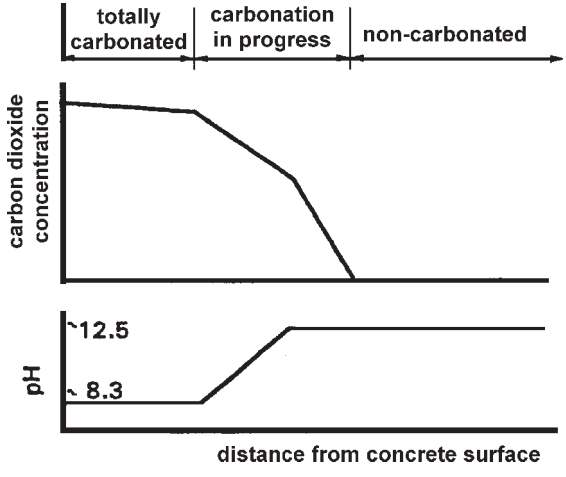

Figure 8.8. Profile of pH in carbonated and non-carbonated concrete.[21]

4.3 Effect of Cracks

Carbonation can occur in two ways:

1. Surface carbonation.
2. Carbonation through cracks.

The behavior of carbon dioxide in a crack is different from the behavior of carbon dioxide in contact with a concrete surface. However, there are similarities in the sense that the chemical reaction will take place under particular conditions. It will depend upon the concentration of carbon dioxide, which subsequently will depend upon the source of the carbon dioxide supply. The diffusion coefficient in the crack will be different from that in the air, and further, it may not be constant. It can vary depending upon the crack width and the rate of carbon dioxide penetration through the crack. The depassivation will follow the crack path, and the rebars will be corroded in the nearby areas, whereas away from the crack, there will be no corrosion. Therefore, during inspection and control a very careful mapping is to be done. Strunge and Chatterji[22] have shown that the corrosion proceeds along the cracks (Figs. 8.9 and 8.10) in areas with a high number of air voids, along the cracks between aggregates and paste, and through porous areas where water and oxygen, necessary for corrosion, can reach the reinforcement.

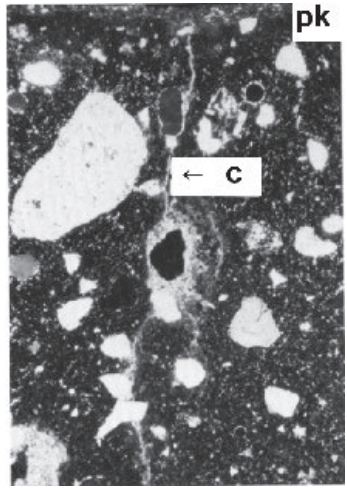

Figure 8.9. Surface of concrete, at the top, a very narrow zone of carbonated paste is seen (*pk*). Along crack (*c*), perpendicular to the surface, the cement paste is carbonated, (area 3.7 × 2.8 units).[22]

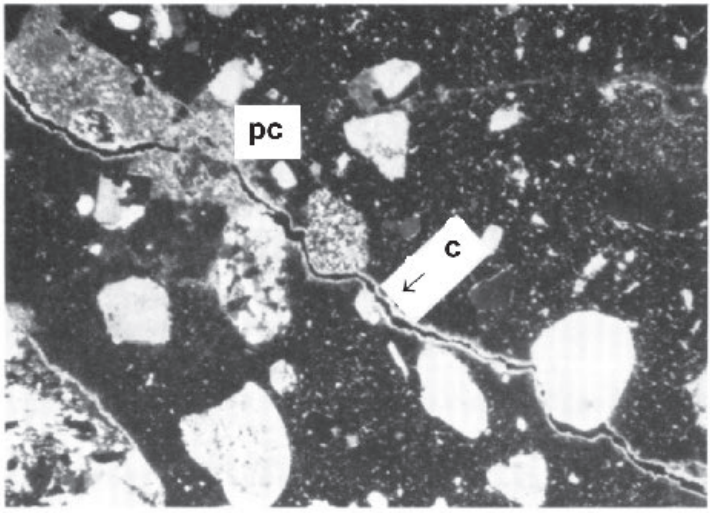

Figure 8.10. Area of the sample about 20 mm from the surface. The paste (*pc*) is carbonated along crack (*c*), (area of 3.7 × 2.8 units).[22]

Thus, the carbonation process depends upon the rate of carbon dioxide penetration into the concrete structure. This will be governed by the porosity of concrete, i.e., the microstructure of concrete.

Unlike normal concrete, the microstructure of LWAC depends not only on the composition of cement paste, but also on the type of lightweight aggregates used. Because the sintered lightweight aggregates have pozzolanic reactivity, calcium hydroxide produced during cement hydration interacts with the pozzolanic material and produces calcium silicate hydrates. The microstructure is densified, and the free calcium hydroxide decreases. Different types of aggregates have different reactivities, accordingly the carbonation varies from aggregate to aggregate. LWAs are porous, thereby they absorb water. Thus, the moisture in the structure of concrete is higher, which favors carbonation. Due to this, the carbonation in the LWAC is higher than that of normal concrete. High strength LWAC has a very dense matrix which consequently decreases the permeability. Hence, the carbonation depth significantly decreases and so does the reinforcement corrosion. Another method of decreasing the carbonation is to increase the thickness of the reinforcement cover over concrete.

The depassivating action has been well documented by many authors.[21][23] The carbonation depth increases with time, but most of the studies have been made over a short time.[24][25] Nevertheless, analytical approaches based on short-term test results have also been developed to predict the rate of carbonation as a function of these primary variables.[26]

Most of the carbonation tests are performed in the laboratory for a short time. The samples are normally cured and the carbonation depth is measured at different intervals. Sometimes, accelerated tests are done where the test specimens are steam cured and are placed in a chamber in an atmosphere of carbon dioxide. The carbonation depth is measured on the fractured surface of the samples at any particular time.

Accelerated tests may change the mechanism of the reaction, partly due to the change in the microstructure by steam curing and partly due to the forced carbonation. What is missing very often is the verification of these predictions of carbonation with the mature concretes in service.

Apart from phenolphthalein, carbonation is also assessed by determining the free calcium hydroxide. The more carbonation, the less free calcium hydroxide there will be. This is determined by measuring the amount of soluble calcium hydroxide in an ethylene glycol solution.[27]

4.4 Determination of Free Calcium Hydroxide

As described earlier in Sec. 3.3, the pozzolanic reaction and the microstructure of lightweight aggregate concrete depends upon the type of aggregate, cement-to-aggregate ratio, water-to-binder ratio, and the curing conditions. A study was made by Bremner, et al.,[27] where mortar specimens were made with two fractions of LWA, 0–1.2 mm and 1.2–5 mm, which were combined in the ratio of 2:1. The fine aggregates were produced in St. Petersburg and Moscow. Comparison was done with the mortar samples made using quartz sand. The composition of the aggregates is shown in Table 8.2.

Mortar cubes were made with a cement-to-sand ratio of 1:1 and 1:5. Water was added to obtain the same relative flow for all mixes. After 24 hours, half the cubes were stripped and then cured at 100% RH for 14 days and at 75% RH thereafter. The other half of the cubes was subjected to the standard steam-curing cycle, typical of plants producing precast concrete housing components, and was cured at 75% RH at room temperature.

Table 8.2. Composition of Cement and Fine Aggregates[27]

	Cement	LWA-St. Petersburg	LWA-Moscow
Loss on ignition	3.25	0.47	4.8
SiO_2	24.0	63.68	71.0
Fe_2O_3	3.4	7.61	4.7
Al_2O_3	3.67	17.96	13.5
CaO	62.21	1.53	1.0
MgO	4.26	3.9	1.6
SO_3	2.06	0.08	—
K_2O	0.44	5.19	—
Na_2O	0.1	0.06	—
Free CaO	Trace	0	4.0

The kinetics of bonding of calcium hydroxide as an index of reduced pH was used to evaluate the corrosion potential of steel in the concrete. The ethylene glycol test method was used to determine the amounts of calcium hydroxide present and, for convenience, expressed as a percentage of total CaO present in the mix. After 28 days and after 3 years curing, the amount of calcium hydroxide was determined. The results of these tests are shown in Table 8.3.

Table 8.3. Ca Soluble in Ethylene Glycol Expressed as Percent[27]

Mix No.	Cement/ Fine Aggr.	Curing Method	Fine Aggregate					
			Quartz		LWA St.P		LWA Moscow	
			28 days	3 years	28 days	3 years	28 days	3 years
1	1:1	Moist	6.0	3.8	3.7	2.0	4.5	3.0
2	1:5	Moist	—	—	0.2	0.2	0.8	0.8
3	1:1	Steam	8.7	8.0	4.1	3.5	3.0	2.5
4	1:5	Steam	—	—	1.6	1.2	0.9	0.4

Table 8.3 shows that with the increase in the proportion of fine LWA, mixes 2 and 4, the free calcium hydroxide decreases when the cement content is the same.[28][29] It is because of the increased pozzolanic reaction. The steam-cured sample decreased the carbonation because of the drying effect during the steam curing. That is, the samples have a lower moisture content. This agrees with the hypotheses mentioned in Sec. 4.1. Table 8.3 also shows that the carbonation did increase with time as there is no change in the amount of soluble calcium hydroxide. In the case of steam curing, the reaction occurs to a greater extent over time. Further, the aggregates from St. Petersburg reacted more when moist-cured compared to the samples having quartz sand and the samples made with the aggregates from Moscow. This is indicated by the presence of more soluble calcium hydroxide. But in steam curing, the reaction increased with time for all the aggregates, except in the case of the aggregates from Moscow where the free calcium hydroxide decreased to half after 3 years compared to 28 days. The major difference is in the silica, alkali, and free CaO contents in the fine LWA. Though the silica content is higher in the aggregates from Moscow, there is more free CaO, whereas in the aggregates from St. Petersburg the free CaO content is zero. This makes the aggregates from St. Petersburg more reactive.

In addition to the loss of pH due to the pozzolanic action of the LWA, the effect of various environments on concrete carbonation was studied. The composition of concrete and the pH after different intervals is shown in Table 8.4.

The 100 mm cubes were steam-cured and placed in an accelerated test chamber with a carbon dioxide content of 10% by volume and an RH of 75%. All the concretes were mixed so as to produce the same slump as the concrete made from the normal weight aggregates and with a water-to-cement ratio of 0.4. The depth of carbonation after 30 days in the test chamber is given in Table 8.5.

The concrete with a low density had a higher carbonation (Mix A) because of the more open pore structure. Replacement of quartz in the concrete having the same strength increases carbonation. It may be due to the increase in the air void volume which aids the penetration of carbon dioxide.

Table 8.4. Concrete Composition, Compressive Strength, and pH Measured in Fluid Phase[27]

Mix No.	Comp. Str.[c]	Cement	Quartz	Granite	Lightweight Aggregate		pH			
			FA[a]	CA[b]	FA	CA	Mixing	Steam Curing	9 months	1.5 years
1	10	250	—	—	395	515	12.8	11.5–11.8	10.8–11.0	10.5–10.8
2	20	300	—	—	445	595	12.8	11.8–12.0	10.8–11.5	10.5–11.2
3	20	300	530	—	—	595	13.0	11.8–12.2	10.8–12.3	11.8–12.1
4	30	380	—	—	445	595	12.8	12.5–13.0	11.9–12.2	11.9–12.1
5	30	380	530	—	—	595	13.2	12.8–13.5	12.0–12.1	12.0–12.1
6	20	307	830	1240	—	595	13.8	12.8–13.5	12.2–12.5	12.0–12.5

a–FA-fine aggregates, b–CA-coarse aggregates, c–Comp. Str.-compressive strength in MPa

Table 8.5. Compressive Strength, Type of Aggregates, and Carbonation Depth Sites[27]

Mix	Compressive Strength, MPa	Type of Aggregate		Carbonation Depth, mm
		Fine, FA	Coarse, CA	
A	10	Lightweight	Lightweight	>30
B	20	Lightweight	Lightweight	15
C	20	Quartz	Lightweight	20
D	30	Lightweight	Lightweight	13
E	30	Quartz	Lightweight	17
F	20	Quartz	Granite	18

The results from the accelerated test were substantiated by exposing a 100 × 100 × 300 prism of the same composition as tested earlier, but with reinforcing bars. These were placed in three different places. The first was placed on the roof of a research institute in Moscow and evaluated after 5 years of exposure (Exposure A). A second set of specimens was placed in a building confining dairy cattle (Exposure B). A third set was placed in a chemical plant (Exposure C). The second and third sets of specimens were evaluated after three years of exposure. Average ambient relative humidity in Moscow is normally about 75%, in the agriculture building about 80%, and in the chemical plant about 95%. The results are shown in Table 8.6.

Table 8.6. Carbonation Depth in mm for Field Exposure Sites

Mix No.	Exposure A Roof 75% RH	Exposure B Agriculture 80% RH	Exposure C Chem. Plant 95% RH
1	45–50	6	35–40
2	4	0.5	2.5
3	6	2.0	1.0
4	4	0.5	1.5
5	2	0.5	1.0
6	6	2.5	5.0

As in the previous work, the specimens were broken at the end of the test program and the steel examined for corrosion. Only the concrete with mix no. 1 had significant corrosion. Some pitting was noted in the concretes made with mixes no. 2 and 6. For mix no. 2, the specimen appeared to be improperly consolidated in the region where corrosion had taken place.

Both the accelerated and the field tests have shown that the carbonation depth is less with lightweight aggregate concrete compared with normal concrete. This is attributed to a good quality of matrix (high strength concrete with a low water-to-cement ratio). This is essential if corrosion of steel is to be avoided.

4.5 Carbonation Test in the Laboratory

Carbonation depths of lightweight aggregate concrete of category X-concrete and 3L-concrete, developed at Chalmers University, was measured on 15 cm cubes. These cubes were cured at 20°C and 55% RH for 1 year. Carbonation depth was measured by phenolphthalein. The composition of concretes and the carbonation depths are shown in Table 8.7.

Table 8.7. Composition and Carbonation Depths of LWAC[30]

Ingredients	**K40**	**XL**	**XT**	**XB**	**3L**
Cement	399	270	310	300	342
Water	184	133	156	149	176
CEMOS	0	3	3	3	3
Aggregate: 0–8	988	0	0	0	0
Stones: 8–16	749	0	0	0	0
Sand: 0–2	0	184	246	257	422
Leca™: 2–4	0	0	0	0	241
Leca™: 4–8	0	0	0	0	165
Pumice	0	483	538	485	0
Polystyrene	0	7	4	5	0
Strength	46.4	7.3	10.7	9.6	25.4
Density	2335	870	1050	1015	1360
Carbonation depth	3	8	10	11	2
The ingredients mentioned are in kg/m^3 and carbonation depth in mm.					

The carbonation depth of 3L concrete is lower than that of the normal K40 concrete even though the density and the strength are lower than the normal K40 concrete. This is attributed to the modified pore structure achieved by the addition of polymer CEMOS and the pozzolanic reaction between the cement and Leca™ sintered clay aggregates. But this does not hold true in the case of concretes XL, XT, and XB, the concretes made with the volcanic aggregate pumice and polystyrene. It may be because of the very high suction of water and carbon dioxide by the pumice and carbon dioxide by polystyrene aggregates.

4.6 Field Performance

The above laboratory work was supplemented by a field study of structures made some 16–18 years ago where brick, normal weight concrete, and structural grade LWAC were used at various locations for exterior wall panels for chemical plants producing potassium fertilizer for agriculture.

The structural lightweight aggregate concrete panels were in good condition, whereas the brick and normal weight concrete panels were in various states of distress.

Field studies of some of the ships and bridges incorporating structural LWAC were done by Holm, et al.,[31] McLaughlin,[32] and Ohuchi, et al.,[33] for durability with particular attention given to depth of carbonation. The profile of the carbonation front was determined for these mature structures in or over sea water.

Location of the samples from the structures, concrete data, and the depth of carbonation are shown in Table 8.8. Both fine and coarse lightweight aggregates were used in making LWAC.

The relationship between density, strength, and carbonation depth can be clearly seen. Higher density and higher strength concretes, which generally indicates dense pore structure, have less permeability and hinder the penetration of carbon dioxide. The carbonation depth is much higher in the samples from Japan even though the concrete had higher density compared with the concrete in the bridge at Annapolis. This must have something to do with the environmental conditions.

Table 8.8. Field Measurement of the Depth of Carbonation[34]

Location and Reference	Structure and Age	Concrete Data (Strength and Density)	Depth of Carbonation, (mm) (in)	K_c (mm/√yrs)
Cape Charles, VA[32]	World War II Concrete Ships 43 Years	All LWC (35 MPa, 1730 kg/m^3)		
		(A) Hull Bulkhead	1 (.04)	0.2
		(B) Wing-Wall	1 (.04)	0.2
		(C) Superstructure Deck-Top	1 (.04)	0.2
		(D) Superstructure Deck-Bottom	2 (.08)	0.3
Annapolis, MD Chesapeake Bay[35]	4 Mile Multi-span Bridge 35 Years	All LWC (24 MPa, 1650 kg/m^3)		
		(A) Top Surface, Truss Span	1 (.04)	0.2
		(B) Bottom Surface, Truss span	5 (.20)	0.8
		(C) Top Surface, Approach Span	8 (.31)	1.4
		(D) Bottom Surface, Approach Span	13 (.51)	2.2
Coxsackie, NY[31] (Not over Seawater)	NY Thruway Interchange Bridge 15 Years	Sanded LWC (27 MPa, 1760 kg/m^3)		
		(A) Exposed Top Deck	5 (.20)	1.3
		(B) Bottom Surface	10 (.39)	2.6
Japan[33]	Bridges Viaducts, 19 Years	Sanded LWC (23 MPa, 1820 kg/m^3)	16 (.63)	3.7
		Sanded LWC (26 MPa)	18 (.71)	4.1

From Table 8.9, the insulating concrete is more carbonated than the other structural concretes. This effect is more pronounced in the outdoor exposure of non-structural lightweight aggregate concrete. It is attributed to the higher water-to-binder ratio leading to a more open structure, making penetration of carbon dioxide easy.

4.7 Measurement of Carbonation Depths: Field and Laboratory Studies

Outdoor exposure testing of the rate of carbonation has been carried out by Grimer[24] and Shulze and Gunzler.[25] Their results are summarized in Table 8.9. These results essentially confirm the data in Table 8.8, with respect to tests on structures, in that carbonation rates are low in high strength concretes. Nevertheless, their carbonation coefficients are slightly higher than those given in Table 8.8, probably reflecting the lower moisture environment at the sites. It is mentioned in Sec. 4.1 that moisture is essential for carbonation to proceed.

To provide information on the behavior of low moisture exposure, a sanded lightweight concrete (made with natural sand for the fine aggregate fraction and expanded aggregate for the coarse) cylinder from the Newburgh-Beacon Bridge in New York was stored in laboratory air for over four years (Table 8.9). Even with relatively severe drying conditions the carbonation coefficient K_c was only 3 for this moderate-strength concrete, indicating that neither very dry nor very damp conditions are conducive to rapid carbonation.[36]

The effect of strength and density on carbonation depth can be seen in the last part of Table 8.9, which covers specimens stored in a laboratory, in Richmond, VA, for over 20 years. Physical and engineering properties are shown in Table 8.10. The carbonation depth was measured on the fractured surfaces according to ASTM 496. The results clearly indicate that an increased rate of carbonation occurs in low-strength concrete in a dry environment.

The Building Research Establishment (BRE) in the UK carries out long time performance tests at Shoeburyness,[37] which is situated four miles (6.5 km) east of the river Thames eastuary in the UK. The BRE marine site has spray, tidal, and full immersion zones. The pH of the sea water varies between 7.9 and 8.2. The details of the test method and environmental conditions are described by Osborne.[35]

Table 8.9. Laboratory Studies of the Depth of Carbonation

Study and Reference	Concrete Data	W/C	Density, kg/m^3 (pcf)	Comp. Strength, MPa (psi)	Years Age	Depth of Carbonation, (mm) (in)	K_c, (mm/√yrs)
UK BRE[24] Grimer[24] Outdoor Exposure Site	Structural						
	1:5 Sand and Gravel	0.6	2350 (147)	30 (4350)	6	3 (.12)	1.2
	1:5 Structural LWC	0.9	1710 (107)	27 (3920)	6	3 (.12)	1.2
	1:5 Insulating LWC	0.8	1620 (101)	22 (3190)	6	4 (.16)	1.6
	Non-Structural						
	1:9 Sand & Gravel	0.95	2290 (143)	15 (2180)	6	15 (.59)	6.1
	1:9 Structural LWC	1.42	1630 (102)	18 (2610)	6	15 (.59)	6.1
	1:9 Insulating LWC	1.4	1500 (94)	7 (1020)	6	20 (.79)	8.2
East Germany[25] Outdoor Exposure Site	LWC A Cement 550 kg/m^3	0.5	1680 (105)	44 (6380)	1	2 (.08)	2
	LWC A 430	0.65	1620 (101)	35 (5080)	1	4 (.16)	4
	LWC A 355	0.8	1600 (100)	30 (4350)	1	7 (.28)	7
	LWC B 430	0.5	1420 (89)	30 (4350)	1	1.5 (.06)	1.5
	LWC B 360	0.65	1380 (86)	24 (3480)	1	5 (.20)	5
	LWC C 475	0.5	1580 (99)	40 (5800)	1	2.5 (.10)	2.5
	LWC C 380	0.65	1560 (97)	34 (4930)	1	4 (.16)	4
	LWC C 330	0.8	1520 (95)	28 (4060)	1	7 (.28)	7

(Cont'd.)

Table 8.9. *(Cont'd.)*

Study and Reference	Concrete Data	W/C	Density, kg/m^3 (pcf)	Comp. Strength, MPa (psi)	Years Age	Depth of Carbonation, (mm) (in)	K_c, (mm/√yrs)
Newburgh-Beacon Bridge, NY Lab Air	150 ∅ × 300 mm Test cylinder						
	Sanded LWC Bridge Deck	0.5	1800 (112)	31 (4500)	4	2 (.08)	1
			1800 (112)	31 (4500)	4	6 (.24)	3
Richmond, VA Solite Corp. Lab Air (Table 3.10)	Sand & Gravel Str. Concrete	0.54	2200 (137)	24 (3480)	20	23 (.91)	5.1
	All LWC Str. Concrete	0.5	1600 (100)	23 (334)	20	23 (.91)	5.1
	Sanded LWC Str. Concrete	0.53	1810 (113)	25 (3630)	20	24 (.94)	5.4
	High Air Ex. Sh. Ins. Concrete	0.6	1310 (82)	9 (1310)	20	32 + (1.26+)	7.2 +
	Perlite Insulating Concrete	1.35	600 (37)	2 (290)	20	32 + (1.26+)	7.2 +

Table 8.10. Carbonation Depth Studies of Twenty Year Old Concrete of Varying Compositions and Materials

Concrete Type Mix Composition	Mix Number				
	1	2	3	4	5
	Structural Concrete	Structural Concrete	Structural Concrete	Insulating Concrete	Insulating Concrete
Coarse Aggregate Type (kg/m^3) (pcy)	Gravel 1068 (1800)	SLWA 445 (750)	SLWA 549 (925)	SLWA 415 (700)	—
Fine Aggregate Type (kg/m^3) (pcy)	Nat Sand 712 (1200)	Nat Sand 718 (1210)	SLWA 771 (1300)	SLWA 653 (1100)	ILWA 142 (240)
Cement (kg/m^3) (pcy)	335 (564)	377 (635)	335 (564)	223 (376)	335 (564)
Water (kg/m^3) (pcy)	182 (307)	178 (300)	178 (300)	135 (228)	452 (762)
W/C	0.54	0.47	0.53	0.61	1.35
Fresh Density (kg/m^3) (pcf)	2290 (143)	1730 (108)	1870 (117)	1420 (89)	920 (57)
Density 28 days (kg/m^3) (pcf)	2240 (140)	1610 (100)	1820 (114)	1322 (82)	660 (41)

(Cont'd.)

Table 8.10. *(Cont'd.)*

Concrete Type Mix Composition	Mix Number				
	1	2	3	4	5
	Structural Concrete	Structural Concrete	Structural Concrete	Insulating Concrete	Insulating Concrete
Air Content (%)	5	7	5	21	—
Slump (mm) (in)	125 (5)	125 (5)	125 (5)	125 (5)	125 (5)
Strength at 28 Days (MPa) (psi)	25.2 (3650)	25.4 (3680)	23.8 (3450)	9.4 (1360)	1.9 (280)
Carbonation Depth ave. (mm) (in)	23 (.91)	23 (.91)	24 (.94)	32+(1.26+)	32+(1.26+)
Carbonation COEF. K_c	5.1	5.1	5.4	7.2+	7.2+

Structural high-strength concretes tested by Osborne,[38] after 5 years of exposure in the spray zone at Shoeburyness, showed very low depths of carbonation, generally below 1 mm, with the exception of the low cement content (280 kg/m^3) sintered fly ash aggregate concrete, which has carbonated to a depth of 3.5 mm. However at 10 years, carbonation had only progressed to 4 mm in this concrete, with all other lightweight and dense aggregate concretes just over 1 mm. These data indicate that for all concretes, even the lower cement content PFA aggregate concrete, carbonation is not likely to be a problem in fairly high humidity environments such as a spray zone site. Little or no carbonation was observed in the tidal zone. Concrete prisms containing rebar for 15 years had some rusting at the ends of some of the rebar, due to chloride corrosion.

Bilodeau, et al.,[39] have also shown that the carbonation depth of high strength lightweight aggregate concrete is very low. The depth of carbonation of the concrete was determined on broken portions of the prisms used for drying shrinkage measurements after 448 days of air drying, using the phenolphthalein test.

The depth of carbonation, as determined by the phenolphthalein test, was negligible for all the concretes investigated. This is due to the low permeability of the concrete resulting from its low W/C, and the use of a blended cement incorporating silica fume. The depth of carbonation for the laboratory specimens and the exposed lightweight structures are illustrated in Figs. 8.11 and 8.12.

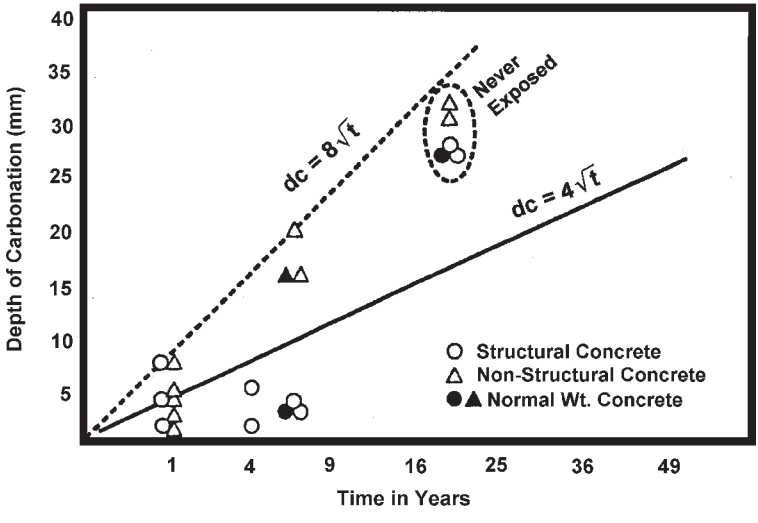

Figure 8.11. Measured depth of carbonation (mm) of lightweight concrete, laboratory samples.[34]

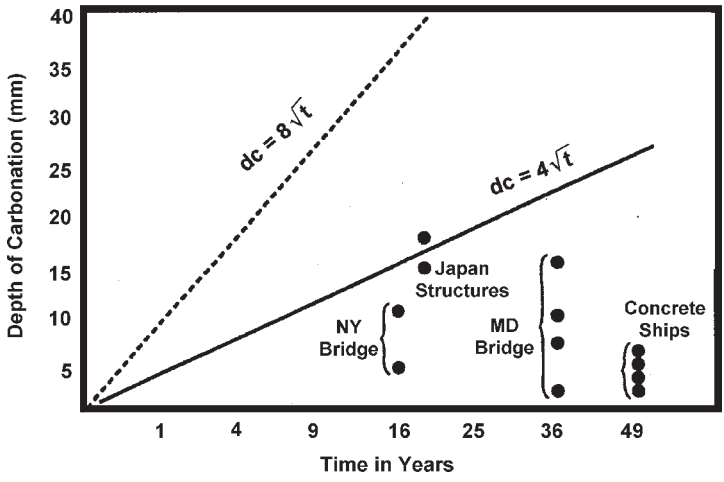

Figure 8.12. Measured depth of carbonation (mm) of exposed lightweight concrete structures.[34]

4.8 Permeability and Corrosion Protection

Laboratory testing of normal weight and lightweight concrete indicates that, in the unstressed state, the two concretes are about equal. However, at higher levels of stress, the lightweight concrete can be loaded to a higher percentage of its ultimate compressive strength than normal weight concrete can, before the microcracking causes a sharp increase in permeability.[14][15] Laboratory testing fails to take into account the more robust conditions that exist in the field, particularly at an early age. In the laboratory, the concrete is maintained at a constant temperature, there is no significant shrinkage restraint, and field-imposed stress is absent, all of which need to be accounted for. The water initially absorbed by the lightweight aggregate prior to mixing can provide water for extended moist curing. The water tends to wick out from the course aggregate pores into the finer capillary pores in the cement paste, thereby extending moist curing.

4.9 Concluding Remarks

Carbonation depends upon the type of cement, cement-to-aggregate ratio, type of aggregates, type of curing conditions, and the environmental conditions to which the concrete is exposed. It also depends upon the reactivity of the aggregates, especially if they are used as fine aggregates. The carbonation lowers the pH value of the pore solution, neutralizes the protective film, and may lead to the corrosion of the reinforcement.

The carbonation depths registered in Table 8.10 are summarized in Table 8.11.[34] The time needed for carbonation depth to reach the reinforcement steel is related to the thickness of the concrete cover. The greater the thickness, the longer the time required for reinforcement corrosion. Further, insulating and non-structural concretes have higher carbonation rates. The higher water-to-cement ratio leads to a more open structure, which enhances the penetration of carbon dioxide.

Table 8.11. Estimate of Time in Years for Carbonation to Reach Reinforcing Steel[34]

Concrete Applications	**Exposed Mature Marine Structures, Bridge Decks**	**Insulating and Non-Structural Concretes**
Concrete Inspection	Continuous	No
Concrete Quality	High	Low
As Measured by W/C Ratio	< 0.45	> 0.65
As Measured by Compressive Strength	> 30 MPa (4350 psi)	< 20 MPa (2900 psi)
Maximum Rate of Carbonation $K_c = dc/\sqrt{t}$ in (mm/$\sqrt{}$yrs)	4*	8**
Concrete Cover of 20 mm (0.78 in)	25 Years	6 Years
Concrete Cover of 30 mm (1.18 in)	56 Years	14 Years
Concrete Cover of 40 mm (1.58 in)	100 Years	25 Years

* As observed from field measurements of mature marine structures.
** As observed from laboratory specimens.

The quality of concrete, with respect to its resistance to the penetration of carbonation, may be categorized by maximum anticipated carbonation coefficients of 4 and 8. This approach, for specific depths of cover, can give an estimate of the period during which corrosion will not be initiated by carbonation factors. The rates of carbonation are shown in Figs. 8.11 and 8.12.

5.0 CHLORIDE ION PENETRATION

Chloride ions penetrate concrete and react with calcium hydroxide and calcium aluminate. With calcium hydroxide, the reaction forms calcium chloride which, being soluble in water, leaches out. With calcium aluminate, it forms the expansive double salt $C_3A \cdot CaCl_2 \cdot H_2O$ if the concentration of $CaCl_2$ is higher than the surroundings. It leads to microcrack formation making easy penetration of chloride ions. The chloride penetration is fast in the beginning, later it slows down. In an experiment the Cl:CaO ratio stabilized after three months of exposure to salt solution.[40] The levels reached were proportional to the chloride content of the aggressive solution used in the test. They showed that it is not only the chloride that plays a role, it is the pH of the solution that is responsible for the binding of chlorides and leaching of $Ca(OH)_2$. At pH 13, the leaching of $Ca(OH)_2$ was very small and the amount of bound chloride did not vary much. At pH 11.5, there was simultaneous dissolution of chloride and calcium ions.

In the case of simultaneous CO_2 and sulfate attack, these salts decompose and chloride ions are released. There are some synergetic effects of carbonation and chloride ion ingress that lead to much more rapid corrosion than would be caused by these two phenomena individually.[41] Corrosion of reinforcement steel occurs in the presence of oxygen and water, but the saturation degree of oxygen decreases in the presence of the chloride ions. This could be a reason why there is a lack of corrosion of steel reinforcement even in the presence of the high chloride concentration.[42] The existence of crevices at the steel/concrete interface provides a low-pH condition. This is presented as a possible explanation for corrosion without oxygen. The process is summarized below:

- Differential aeration cells are generated in crevices where oxygen is consumed.

- Cl^- migrates into crevices, offsetting Fe^{2+} ions and acidification of crevices.
- Passivity is destroyed with the acidification.
- Corrosion continues due to the cyclic catalytic mechanism. The presence of oxygen is necessary only to initiate the process and chloride is necessary to cause the acidification.

In the presence of chloride, a basic iron chloride is formed, $3Fe(OH)_2 \cdot FeCl_2$, which later decomposes and forms β-FeO·OH (akaganite).[43] Leaching of salt increases the porosity and permeability of concrete and weakens the bond between the aggregate and the cement paste. Consequently, the strength of concrete decreases. An increase in porosity and permeability accelerates the anodic and cathodic reactions. Excluding all other factors, chloride alone is not sufficient to initiate steel corrosion.

Due to these reactions, $Ca(OH)_2$ is removed from the vicinity of the reinforcing steel, pH falls below 11, hydroxide protective films are destroyed, and the anodic process progresses.

In practice, the interaction between oxygen, water, and chloride ions is complex. Different chloride salts behave in different ways. For example, $CaCl_2$ creates a more open pore structure, allowing an easier diffusion and reduction in pH of the pore solution, whereas other alkali chlorides (NaCl and KCl) enhance the porosity to a lower extent and, in general, increase the pH of the pore solution. There is also a possibility that ion exchange will take place with K and Na ions. Therefore, $CaCl_2$ is considered to be more deleterious than NaCl or KCl. The diffusion coefficient of chloride ions depends on the cation and decreases in the following order:

$$MgCl_2 > CaCl_2 > KCl > NaCl$$

5.1 Lightweight Aggregate Concrete

Lightweight aggregate concrete, due to its low density, is becoming attractive in off-shore construction. However, it requires concrete of high strength and good durability, especially a resistance to chloride ion penetration as the atmosphere is chloride-laden. Although LWAC has shown good performance,[44] there is reluctance to use it because of durability problems. The obvious reason for this reluctance is most often the assumed higher

permeability of the LWAC, hence, the expected lower resistance against chloride ion penetration. High strength structural LWAC can be produced either by using high strength mortars which will compensate for the low strength of the LWA, by using high strength LWA, or both. High strength mortars are dense, thus have low permeability. This is expected to enhance the resistance to chloride ion penetration.

Most of the tests for measuring chloride ion penetration are performed in the laboratory. These results are difficult to translate to the chloride ingress in concrete exposed to the natural environmental condition where, apart from other parameters, temperature and humidity frequently vary. This is one of the reasons why, in spite of the excellent laboratory test results, concrete gets damaged on outdoor exposure. The problem seems to be that it is not easy to make a test procedure which resembles the field conditions, i.e., the size of the specimens, exposure conditions, and the testing time.

The problem of chloride ingress of normal aggregate concrete is not resolved where the aggregates do not interfere in the hydration process and in the building of the microstructure. It is more difficult to understand this in the case of LWAC as the concrete is made of aggregates which vary in their material and structural properties such as density, voids, and absorption. Chloride ingress has been tested on the LWAC made with different types of aggregates produced in different ways. Some of the tests have been performed in the laboratory on small samples for a short time and some tests have been carried out on the beams which have been exposed to temperature and humidity cycles for a long time. Tests have also been performed in field conditions for longer time. Some of the tests are described here.

5.2 Laboratory Tests

Bilodeau, et al.,[39] tested chloride ion permeability of LWAC made with different types of aggregates. The maximum size of the aggregate was 12.5 mm and the grading was in accordance to the ASTM 330, the standard specification for LWA for structural concrete. The properties of LWA are given in Table 8.12. The fine aggregate was a natural sand having a specific gravity of 2.70 and a water absorption of 0.8%. The concrete was made using a sulfonated naphthalene formaldehyde condensate liquid superplasticizer and an air-entraining agent. Polypropylene fibers, 20 mm in length, were used in one batch. Canadian blended cement incorporating 8% silica fume was used in this investigation.

Table 8.12. Physical Properties of LWA[39]

No.	Dry Rodded Unit Weight, kg/m^3	Void Content, %	Specific Gravity			Absorption, %
			Bulk	Bulk SSD	Apparent	
I	850	42.7	1.48	1.56	1.60	5.2
II	910	37.1	1.45	1.64	1.79	13.1
III	780	42.8	1.37	1.55	1.68	13.4
IV	870	39.4	1.44	1.59	1.70	10.3
V	760	41.0	1.29	1.58	1.81	22.6
VI	860	42.2	1.49	1.67	1.82	12.6

The mixture proportion of concrete is shown in Table 8.13 and the physical properties are shown in Table 8.14. Altogether, six mixes were made of each mixture, but only two are presented here, Batch A and Batch EF—with and without fibers. The samples were cast, demolded after one day, and transferred to 100% relative humidity until the test. At 28 days, rapid chloride ion permeability was tested according to ASTM 1202 on discs cut from 102 × 203 mm cylinders from Batch A.

The resistance of concrete to the chloride ion penetration, expressed in coulombs, ranged from 265 to 742.[39] The concrete made with aggregate I demonstrated the highest resistance (lowest coulomb value), whereas the concrete made with aggregate V showed the lowest resistance (highest coulomb value). Nevertheless, according to the ASTM C 1202 rating system, all the concretes investigated demonstrated very low permeability to chloride ions with values lower than 1000.

These excellent results are probably due to the high density of the aggregate, which has a dense structure and less void contents. This reflects on the absorption characteristics of the aggregate (Table 8.12). It subsequently influences the effective water-to-cement ratio, as can be seen from the slump (Table 8.13) and the compressive strength (Table 8.14). Densification of the microstructure is also due to the use of silica fume, which works partly as a pozzolanic material and partly as a filler.

Table 8.13. Mixture Proportion of LWA Concrete[39]

No.	Batch	LWA[a]	AEA,[b] ml/m^3	SP,[c] l/m^3	Fibers, kg/m^3	Slump, mm
1	A	I	85	8.9	0	90
	EF		55	5.0	1.5	135
2	A	II	55	5.9	0	190
	EF		45	4.5	1.5	80
3	A	III	40	6.2	0	100
	EF		45	4.4	1.5	115
4	A	IV	40	5.8	0	140
5	A	V	40	3.3	0	170
6	A	V	165	7.0	0	145

a-LWA–lightweight aggregate, b-AEA–air-entraining agent, c-SP–superplasticizer

Table 8.14. Physical Properties of Concrete[39]

No	Batch	LWA	Air, %	Density, kg/m^3	Compressive Strength, MPa				
					1 d	7 d	28 d	91 d	365 d
1	A	I		1917	52.4	61.1	63.3	67.9	71.3
	EF		5.5	1922			63.2		
2	A	II		1947	48.9	59.4	67.7	72.7	76.0
	EF		5.5	1885			71.9		
3	A	III	5.5	1900	41.4	52.1	56.3	59.6	61.3
	EF			1895			53.9		
4	A	IV	5.3	1935	42.7	53.2	61.6	61.6	63.3
5	A	V	4.5	1920	41.1	48.3	50.1	50.8	52.4
6	A	VI	4.5	2000	40.7	51.4	57.5	59.8	na

The results of the concrete made with aggregate I is probably an indication that the concrete had the lowest effective water-to-cement ratio (lowest absorption of aggregates, Table 8.12) and low slump (Table 8.13. No. 1, Batch A) and the densest cement mortar. Table 8.14 shows the high compressive strength, and the lowest coulomb values, i.e., the highest

resistance to the chloride ion penetration. Similarly, the concrete made with the aggregate V had the highest coulomb values, i.e., the lowest resistance to the chloride ion penetration. This is attributed to the low density of the aggregates, high void contents, and high absorption resulting in high slump and low strength. Concrete of high permeability is produced.

In the tests carried out by Bilodeau, et al.,[39] the chloride ions were measured at one temperature and the concrete was cured at room temperature. In an experiment performed under the LightCon project,[45] the samples were cured at 20°C, and semi-adiabatically cured up to a maximum temperature of 65°C and 95°C, respectively. The samples were then submerged into indoor tanks of sea water. The chloride ion penetration was measured at different intervals up to two years. The curing temperature of concrete did not have a significant impact on the chloride ingress (Fig. 8.13 and 8.14). These results seemed to be surprising, prompting further investigation.

Further investigation was done in another project under LettKon.[45] This entailed both laboratory tests and tests performed in connection with the construction of the Stolma bridge and Rostsundet bridge. The mix proportion of concrete is shown in Table 8.15. The samples were cured at 35–40°C (to be called "cold") and at 70°C (to be called "warm"). A chloride profile is made through measurement of the chloride concentration in concrete taken in increasing depths, measured from the concrete surface. Based upon the time of exposure, the diffusion coefficient (D) is calculated using Fick's second law. The calculation also gives C_s, which is the theoretical chloride concentration in the surface of concrete.

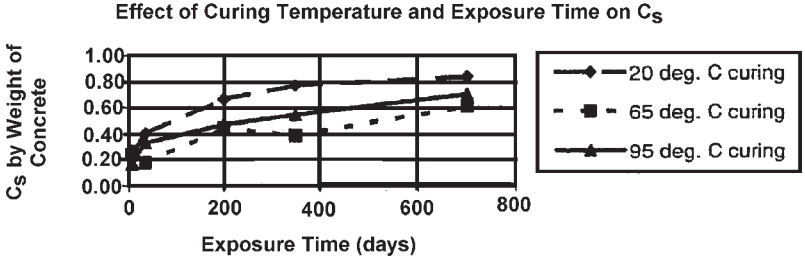

Figure 8.13. Effect of curing temperature conditions and exposure time on surface chloride content C_s, mean values from different mixes.[45]

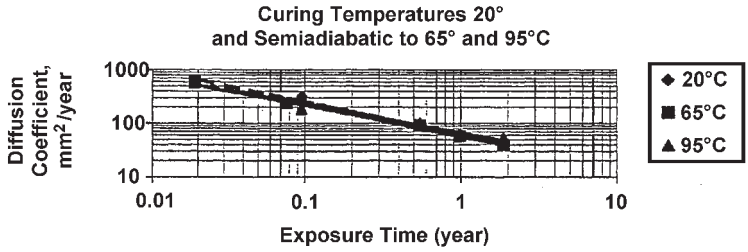

Figure 8.14. Effect of curing temperature on diffusion coefficient D.[45]

Table 8.15. Mixes in the LettKon Project[45]

Mix Name	LA0	LA8	LN	LS	Stolma Bridge	Rostsundet Bridge
Cement, NORCEM, anlegg	475	410	400		422	430
Silica fume	0	33	32		37	25
Slag cement				475		
Sand	663	685	900	663	784	774
LWA, Leca™	510	520		510	510	584
Normal WA			880			
Effective water	190	190	190	190	173	173
Effective water/binder ratio	0.33	0.33	0.45	0.33	0.36	0.36
Density	1900	1900	2400	1900	2000	200
The values given are in kg/m^3						

Note that for the separate mixes, C_s and D diverge for the tests which have been warm and cold cured. There is a tendency that C_s and D diverge in both directions. C_s was, in general, higher for cold than warm curing, which makes the warm curing best. On the other hand, D was, in general, lower for cold than for warm curing, which makes the cold curing the best. See Figs. 8.15 thru 8.22 for the results from the laboratory and Figs. 8.23 and 8.24 for the results from the bridges. Since the variations of C_s and D proceed in opposite directions for cold and warm curing, the following is done for comparison.

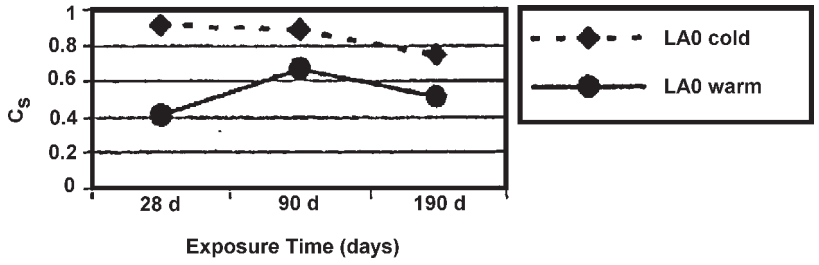

Figure 8.15. C_s for LA0, cold and warm curing.[45]

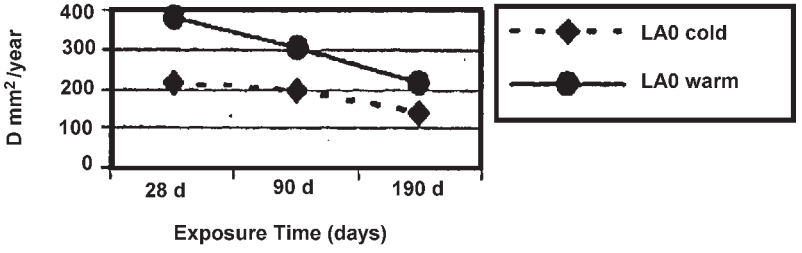

Figure 8.16. D for LA0, cold and warm curing.[45]

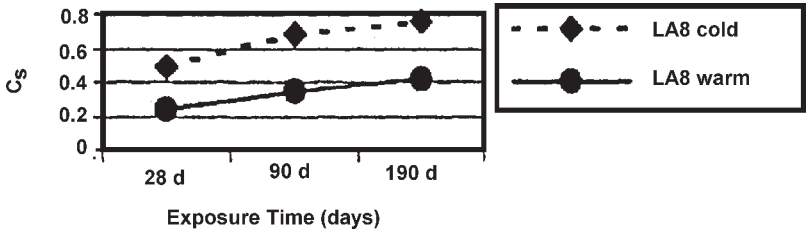

Figure 8.17. C_s for LA8, cold and warm curing.[45]

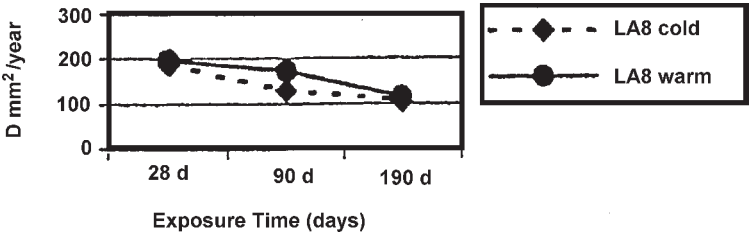

Figure 8.18. D for LA8, cold and warm curing.[45]

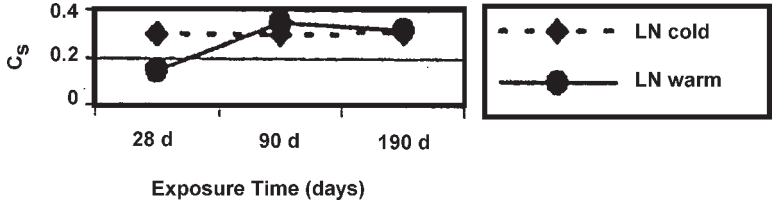

Figure 8.19. C_s for LN, cold and warm curing.[45]

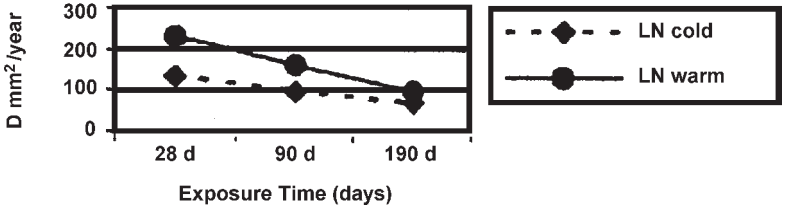

Figure 8.20. D for LN, cold and warm curing.[45]

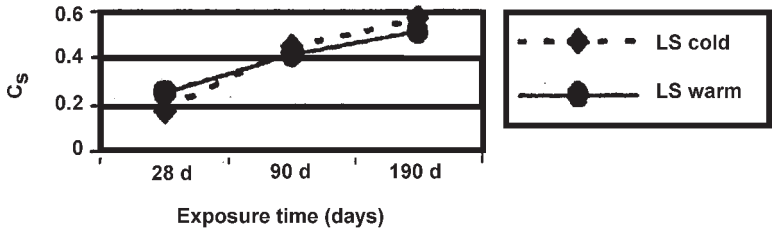

Figure 8.21. C_s for LS, cold and warm curing.[45]

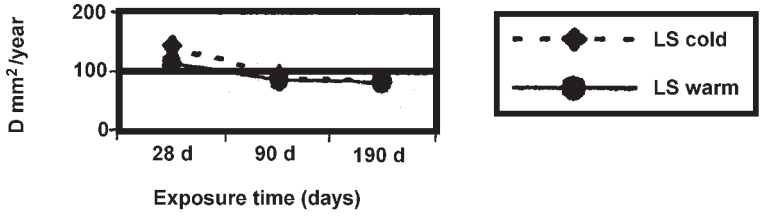

Figure 8.22. D for LS, cold and warm curing.[45]

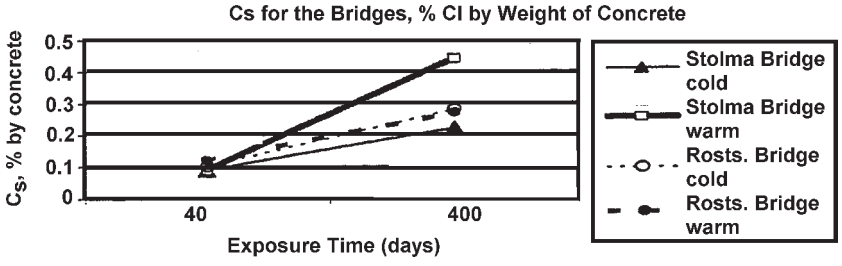

Figure 8.23. C_s for the Stolma and Rostsundet bridge, cold and warm curing.[45]

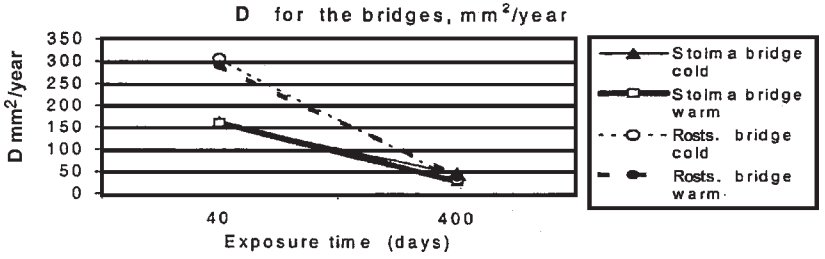

Figure 8.24. D for the Stolma and Rostsundet bridge, cold and warm curing.[45]

The measured values for C_s and D are used together with a chosen joint α equal to 0.5. The depth of ingress for the chloride level 0.07% of concrete weight was calculated for 1, 10, and 100 years of exposure. The results are shown in Fig. 8.25. This comparison shows that the calculated depths of chloride ingress for cold and warm curing for the separate mixes is quite similar at different exposure times. For most of the mixes the difference was 5–10%, the largest variation was approximately 20% at 100 years exposure.

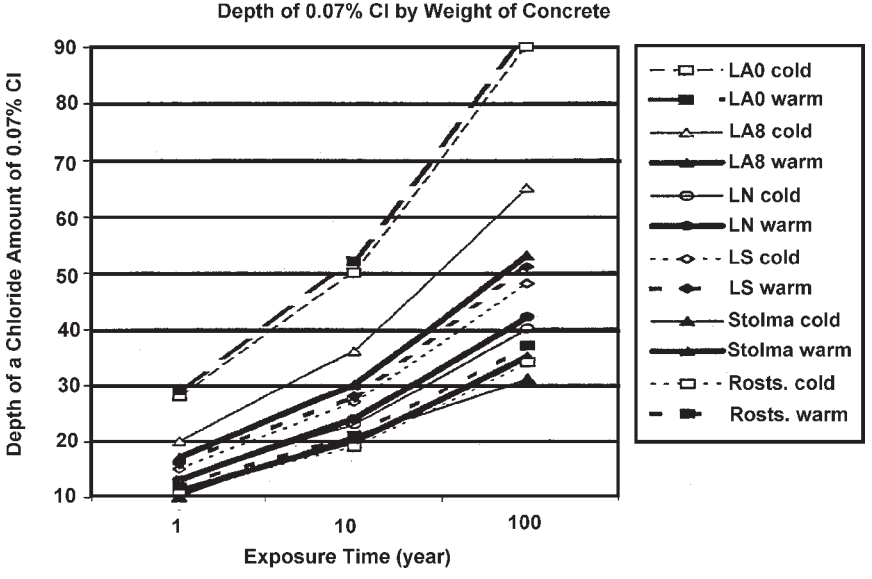

Figure 8.25. Calculated depth where 0.07% of chlorides appear after increasing exposure time. Four mixes from laboratory and the mixes from Stolma and Rostsundet bridges.[45]

The measurements of chloride ingress are based on exposure times of a maximum of 1/2 to 1 year, which is too short a time to draw firm conclusions. Nevertheless, the results show the same tendency as in the LightCon project, e.g., the curing temperature plays a very little role in the chloride penetration into the concrete.

The third project, environmental-friendly concrete, was to measure the chloride ingress into concrete with a cement blended with 20% fly ash. Samples were made from three concrete qualities and were cured for 28 days either at 20°C or semi-adiabatically at 60°C. A comparison is done with normal weight concrete; the composition is shown in Table 8.16.

Table 8.16. Mixes with NORCEM Standard Fly Ash (FA) Cement[45]

Name	**NW045**	**NW040**	**NW038**
NPRA concrete quality term	SV50	SV40	SV30
Water/binder ratio	0.45	0.40	0.38
Silica fume (%)	0	5	10
NORCEM standard FA cement	370	360	370
Silica fume (kg)	0	18	37
Sand: 0–8 mm	1050	1050	1050
Gravel: 8–11 mm	790	810	774
Plasticizer (P)	1.85	1.80	1.85
Sikament 92	1.8	2.3	2.3
Water, total	166.5	158	169
Weight total (kg)	2376	2396	2400

The results in Figs. 8.26 and 8.27 were specifically done to show that the same tendencies yield for normal weight concrete as for the LWAC. The results from curing at 20°C are denoted “cold” and the results for the semi-adiabatic curing are denoted “warm.” The measurements of the chloride ingress are based on the exposure times of a maximum of two

years. This is a short exposure time to draw firm conclusions. Nevertheless the results support the previous findings reported in the LightCon and LettKon project. The curing temperature does not have significant influence upon the chloride ion penetration.

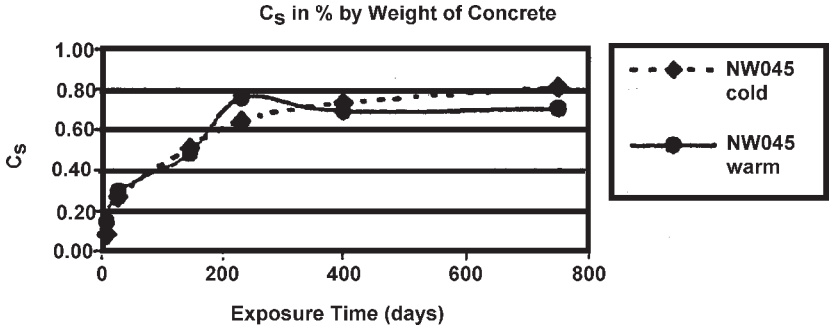

Figure 8.26. Cs for NW045, cold and warm curing.[45]

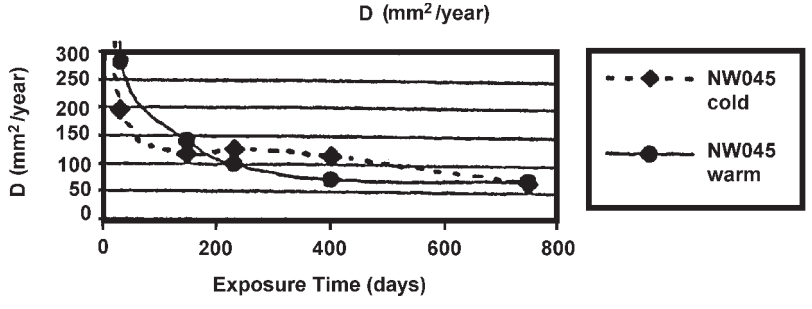

Figure 8.27. D for NW045, cold and warm curing.[45]

In the tests performed by Bilodeau, et al.,[39] and Carlsson[45] for chloride ion penetration, the LWAC used was cured at 20°C and 60–95°C but the tests were carried out at room temperature and constant humidity. In real practice, the humidity and temperature vary frequently. The exposure conditions are more aggressive and the penetration of chloride is faster. The chloride ion penetration in LWAC beams exposed to alternating

moisture and temperature cycling has been studied by von Breugiel and Taheri.[46] They used large beams and exposed the tops to thermal and humidity cycles. They expected to generate small strains and stresses, providing conditions close to the natural climate. A cross section of a beam is shown in Fig. 8.28 with a climate chamber on top, which provides alternating temperature and drying and wetting regimes. The thermal loading (ΔT) can be split into three parts, average temperature (ΔT_{av}), temperature difference (ΔT_{fl}), and self-equiliberating temperature (ΔT_{eigen}). In view of the stress-generating strain, self-equiliberating temperatures being predominent, these cause eigen-stresses, which in massive structures are the major reason for surface cracks in concrete.

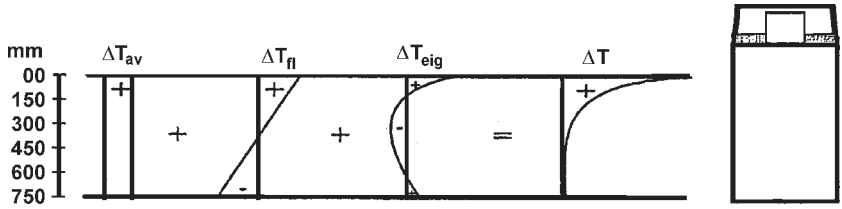

Figure 8.28. Imposed temperature distribution ΔT in the beam and its components ΔT_{av}, ΔT_{fl} and ΔT.[46]

Concrete beams were exposed to a simulated marine environment with thermal and humidity cycles. The hypothesis in this test is that, by applying thermal and humidity cycles at the top surface of thick beams, eigen-stresses, either tensile or compressive, are generated in the top layer of the beams. If the tensile stresses exceed the tensile strength, the concrete will crack. These cracks may grow because of the alternating character of the loading and may promote the penetration of chloride into the concrete.

Chloride penetration tests were carried out on beams. Three large beams of 6 m long, 0.4 m wide, and 0.75 m thick were made. Each beam consisted of three parts, each 2 meters in length and made with different concrete types. Two parts of each beam were made with LWA; Liapor™ F8, Lytag™, and the third one with normal weight aggregate (NWA). Portland cement used was CEM 1 32.5 R; its dosage was 361 kg/m^3, 17 kg/m^3 silica fume (5% CSF) was also used. The superplasticizer used was

1% by weight of the cement and the water-to-cement ratio was 0.45. The fraction of the aggregate was 4–8 mm. In the NWC, or reference concrete, crushed aggregate 4–16 mm was used. In all the mixtures, 0–4 mm sand was also used. The physical properties of the concretes at 28 days are shown in Table 8.17.

Table 8.17. Physical Properties of Concrete Mixtures at 28 days[46]

	NWC, MPa	**Liapor™, MPa**	**Lytag™, MPa**
Compressive strength of 150 mm cubes	62.51	59.78	61.16
Splitting tensile strength of 150 mm cubes	3.91	3.69	4.29
Modulus of elasticity of 100 × 100 × 100 mm prism	34500	25687	26803

The beams cast were cured in different ways. They were covered with plastic to prevent plastic shrinkage and subsequent microcracking. The second day after casting, the first and the third beams were subjected to "standard curing conditions," i.e., sealed curing under plastic foil for two weeks at a temperature of 20°C. The second beam was exposed to elevated temperature curing, which is denoted by "poor curing." This constituted 38°C temperature and 50% RH for two weeks. The three beams were left in the open air after the curing period of two weeks for further hardening.

After curing, the top surfaces of all three beams were subjected to wetting and drying cycles. For wetting, a 5% NaCl solution was used. Apart from this, the top surfaces of the first and second beams were also exposed to thermal cycles. The third beam, acting as the reference, was exposed to the laboratory temperature. The set up is shown in Fig. 8.29.

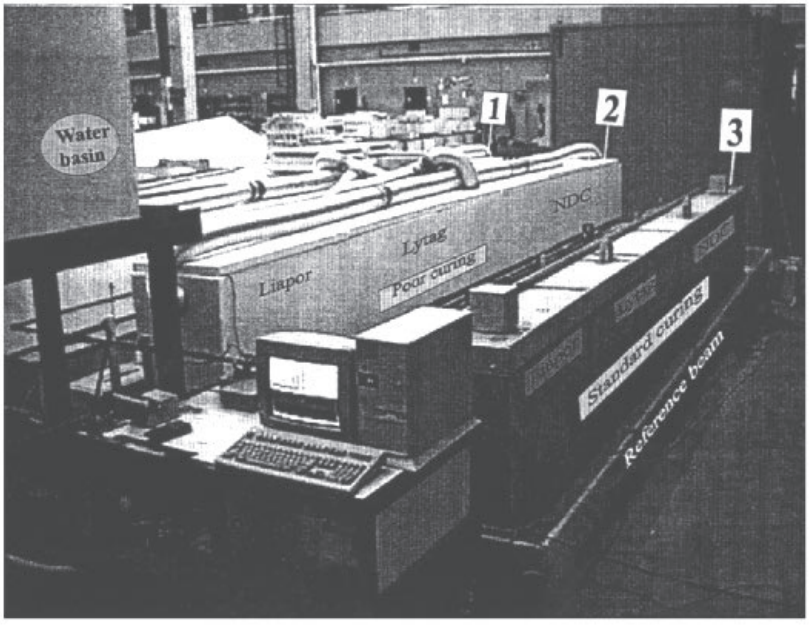

Figure 8.29. Overview of the experimental set up for large scale chloride ion penetration test.[46]

The chloride concentration at different depths was measured by chemical analysis. The procedure for the estimation of chloride penetration and determination of the chloride profile is shown in Fig. 8.30. Fifty-millimeter diameter cylinders were drilled from all three beams before starting the test to investigate the effect of restraint. These cylinders were left in their position during the test. The gap between the drilled cylinder and the adjacent concrete was filled with an elastic material to prevent chloride ion containing water from penetrating into this space. These pre-drilled cores, named "stress free specimens," are supposed to develop few or no microcracks when exposed to temperature cycles. These are denoted by unrestrained specimens. This allows a comparison of the rate of chloride ingress in "restrained" beam sections and "unrestrained cylinders." The first measurement was carried out after one month, i.e., after eighteen complete exposure cycles. The final measurement was carried out at the end of the test.

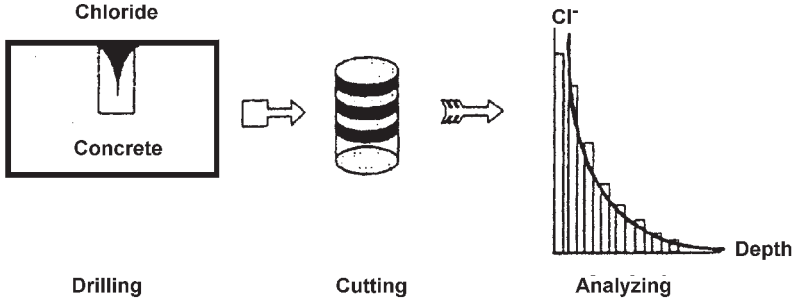

Figure 8.30. Procedure for measuring the chloride profile.[46]

5.3 Effect of Restraint

The effect of restraint on the chloride penetration depth was clearly observed after 1 and 6 months. As an example, the lightweight concrete beam, made with Lytag™ aggregates, was cured at an elevated temperature, viz., "poor cured" as shown in Fig. 8.31. A similar effect of restraint on the chloride profiles was observed for other concretes, but the effect was less pronounced. In the case of beam 3, which is not subjected to thermal curing, the effect of restraint is still very evident for all three concrete mixtures.

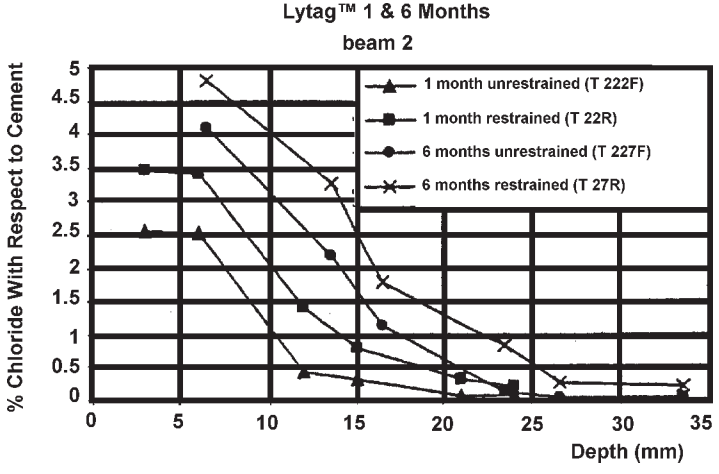

Figure 8.31. Effect of restraint on chloride ion penetration, Lytag™ beams "poor curing."[46]

For the Lytag™ mixture shown in Fig. 8.32, the drying/wetting cycles promote the chloride ion penetration in concrete.

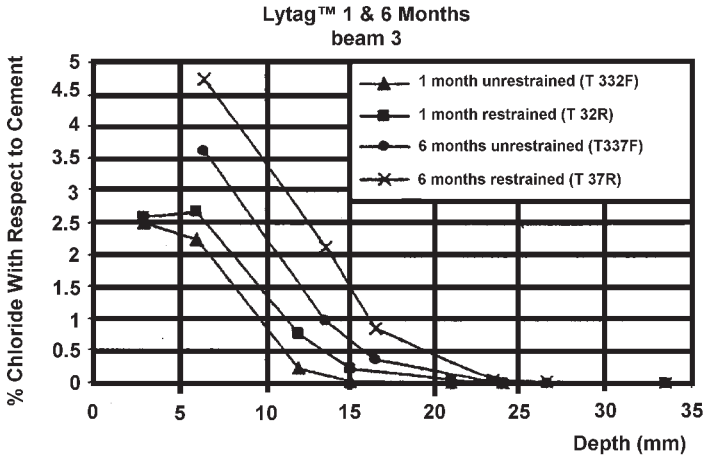

Figure 8.32. Effect of restraint on chloride penetration, LWAC-Lytag™, only dry-wet cycles, standard curing.[46]

5.4 Effect of Aggregate Type on Chloride Ion Penetration

It is a general belief that the LWAC is less susceptible to temperature-induced microcracking due to the lower stiffness and a smaller difference in the stiffness between the matrix and the aggregate. But these tests show that there is hardly any difference in the chloride profile between the NWA and the two LWACs (Figs. 8.33 and 8.34). Further, the three concretes respond to the restrained conditions in the same way. The chloride profile measured in reference beam number 3, the beam which is not subjected to thermal cycles, shows the same shape for all three concretes (Figs. 8.35 and 8.36). All concretes appear to suffer from the drying and wetting cycles in the same way, viz., due to the imposed humidity cycles, the chloride penetration is promoted. The LWACs do not behave better than NWC, but they are not worse. The test results are summarized as follows:

- *During the test, the maximum temperature measured at a depth of 50 mm reached up to 33°C. It is obvious from this observation that there are steep temperature gradients in the concrete cover.*

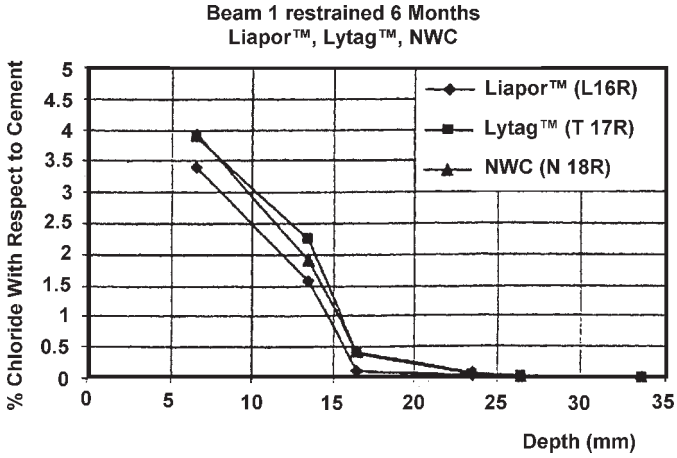

Figure 8.33. Chloride profile in three types of concretes—restrained condition, thermal and humidity cycles during 6 months standard curing.[46]

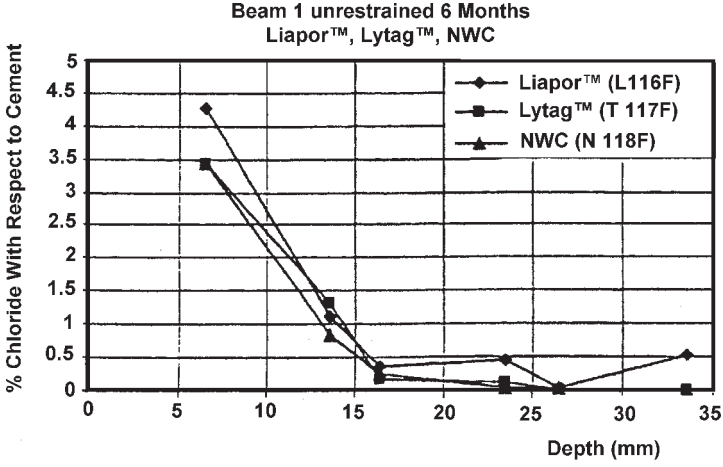

Figure 8.34. Chloride profile in three types of concretes—unrestrained condition, thermal and humidity cycles during 6 months standard curing.[46]

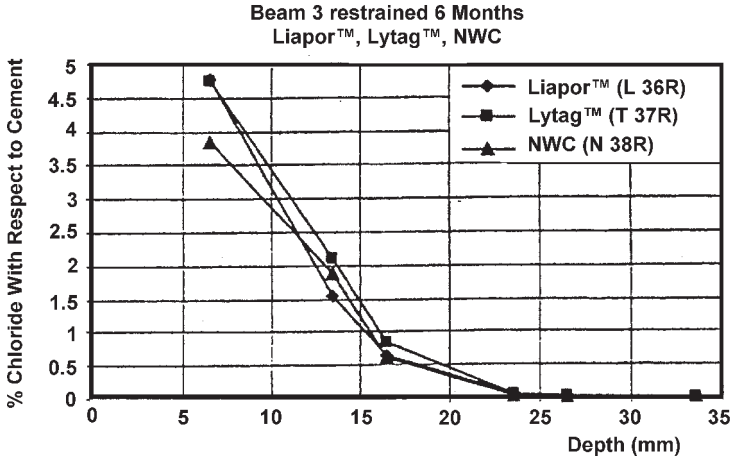

Figure 8.35. Chloride profile in three types of concretes—restrained conditions, humidity cycles during 6 months standard curing.[46]

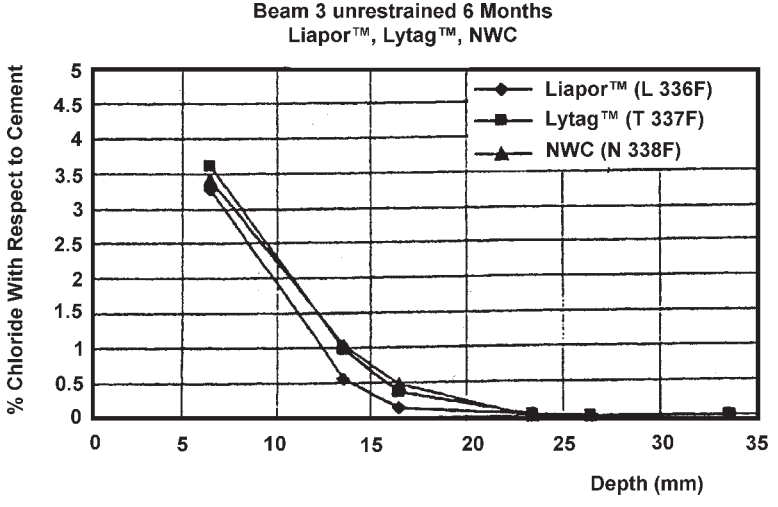

Figure 8.36. Chloride profile in three types of concretes—unrestrained condition, humidity cycles during 6 months standard curing.[46]

From a comparison of the observed deformations of the beam, i.e., axial length changes and bending with calculated free deformation of the beams, the degree of restraint could be deduced. These analyses have resulted in calculated stresses in the top layer of the beams between 9 and 10.5 MPa in compression and between 3.5 and 4.5 MPa in tension. These tensile stresses could have been high enough to cause fine cracks in the cover concrete.

After one month of testing, the results show that LWAC tends to have a higher surface concentration of chloride. However, the shape of the chloride profile is identical with that of NWC. After six months of testing, the results show that the initial higher surface concentration of chloride was leveled out. LWAC seems to perform as good as NWC, based upon a six month test period. This is mainly attributed to the better compatibility between the aggregate and the matrix, due to LWAC being less susceptible to temperature-induced microcracking. No appreciable influence of the type of lightweight aggregates could be seen.

5.5 Field Test

The tests described above were performed under laboratory conditions where, in spite of the variation of the temperature and humidity, the conditions are far from the actual atmosphere prevailing in the field. Besides, the tests performed were up to six months in time, which is too short. It is important to test the durability for a longer period of time. Osborne[38] tested LWAC made with pelletized slag and sintered fly ash. A comparison was done with concrete containing normal weight aggregates.

The specimens were exposed in the tidal zone at the marine exposure site for more than 15 years. The chloride ingress was determined in accordance with procedure mentioned in BS 1881; part 124, 1988.[47] The results are shown in Table 8.18.

The chloride contents were very similar at all depths of ingress for both LWA concretes of 460 kg/m^3 cement content. At the depth of 11 and 16 mm, the chloride concentrations calculated on the mass of dry concrete were 0.75 and 0.58–0.59%. These results, translated to Cl^- per mass of cement, give about 2.7 and 2.0%, respectively, which is somewhat higher than for the gravel aggregate concrete. These are the chloride levels present around the rebar at nominal depths of 10 mm and 20 mm, respectively, and would normally provide more than a sufficient concentration of Cl^- to induce corrosion of the reinforcing steel.[48] A comparison of two years

data,[36] indicated that the diffusivity of chloride decreased with increased exposure time. This is in agreement with the results of Dhir, et al.,[49] who observed that it takes a long time to establish a steady state of chloride intrusion.

Resistance to attack by soft acid water was good for both LWA concrete and was superior to that of the equivalent dense aggregate concrete.

Table 8.18. Chloride Ingress of Reinforced Concrete Prisms Stored in Marine Tidal Zone for 15 Years[46]

Depth (mm)	Pelletized Slag	PFA	Gravel
1.6	1.25	1.01	0.66
6.11	0.97	0.85	0.53
11.16	0.75	0.75	0.42
16.21	0.58	0.59	0.39
21.26	0.53	0.50	0.36
26.31	0.41	0.44	0.37
31.36	0.37	0.38	0.33
36.41	0.34	0.35	0.33
Percent of chloride at different depths (Cl^- as mass of sample)			

5.6 Concluding Remarks

Chloride ion penetration is related to the properties of the aggregate, its density, void content, and absorption, which influence the effective water-to-cement ratio. This subsequently influences the pore structure and permeability of concrete which principally control the penetration of chloride ions.

The performance of LWAC using various types of aggregates is equal to the normal weight concrete in the marine environment, which is laden with the chloride-rich air. Further, the LWAC also performed well in varying temperature and humidity conditions. This is attributed to the better compatibility of the lightweight aggregates to the matrix. This makes the LWAC less susceptible to the temperature-induced microcracking.

REFERENCES

1. Chandra, S., Acid Resistance of 3L Concrete, Internal Report, Div. of Building Materials, Chalmers University of Technology, Göteborg, Sweden (1982)
2. De Puy, G. W., Freeze-thaw and Acid Resistance of Polymer Impregnated Concrete, ACI Publication, SP 47 (1975)
3. Rubetskaya, T. V., Bubnova, L. S., Gronchar, U. F., Ljuberskaya, G. V., and Fedorchenco, V. O., A Concrete in Corrosion Conditions, *Beton i Zhelezobeton,* (10):3 (Oct. 1971)
4. Chandra, S., Berntsson, L., and Flodin, P., Behavior of Calcium Hydroxide with Styrene-methacrylate Polymer Dispersion, *Cement and Concrete Research,* 11:125–129 (Jan. 1981)
5. Chandra, S., Flodin, P., and Berntsson, L., Interaction between Calcium Hydroxide and Styrene-methacrylate Polymer Dispersion, *3rd Int. Congress on Polymers in Concrete,* pp. 125–130, Koriyama, Jpn (May 13–15, 1982)
6. Romben, L., *Aspects on Testing Methods for Acid Attacks on Concrete—Further Experiments,* Swedish Cement and Concrete Research Institute, Report F09:79, Stockholm (1979)
7. Dehler, E., Betongzusatzmittel und Aggressive Beständigkeite, *Betongteknik,* (3):20–22 (Jun. 1980)
8. Biczok, I., *Concrete Corrosion-Concrete Protection,* Akademia Kiado, Budapest, p. 149 (1972)
9. Chandra, S., Frost Resistance and Other Properties of Cement Mortar With and Without Admixtures, Internal Report, Div. of Building Materials, Chalmers University of Technology, Göteborg, Sweden (1982)
10. Singh, N. B., and Sarvahi, R., Effect of Lactic Acid on the Hydration of C_3S, *Il Cemento,* 4:197 (1991)
11. Bremner, T. W., Boyd, A. J., Holm, T. A., and Boyd, S. R., *Indirect Tensile Testing to Evaluate the Effect of Alkali-Aggregate Reaction in Concrete,* T192-2, Elsevier Science Ltd. SEWC (1998)
12. Richardson, M. K., Carbonation of Reinforced Concrete: Its Causes and Management, *CITIS, Dublin* (1988)
13. Lea, F. M., *The Chemistry of Cement and Concrete,* Edward Arnold, London (1971)
14. Berger, R. L., Young, J. F., and Leung, K., Acceleration of Hydration of Calcium Silicates by Carbon Dioxide Treatment, *Nat. Phys. Sci.,* 20(97):16 (1972)

15. Aschan, N., Thermogravimitric Undersökning av Karbonatiserings-fenomenet i Betong (Thermogravimetic Investigation of Carbonation Phenomenon in Concrete), *Nordic Betong,* 17(83):275–283 (1963)

16. Verbeck, G. J., Carbonization of Hydrated Portland Cement, Am. Soc., Test Mat. Spec. Tech. Publ. 205, PCA, Res. Dep. Bull. 87, pp. 17–36 (1958)

17. Mehta, P. K., Durability of Concrete in Marine Environment, A Review, *ACI Spec. Publ. 65,* p. 1 (1980)

18. Venuat, M., and Alexandre, J., De la Carbonation du Beton (On the Carbonation of Concrete), *Rev. Mater. Constr.,* 638, p. 421 (1968)

19. Bennison, P., The Repair and Protection of Reinforced Concrete, *Corros. Prev. Control,* 31(3):5 (1984)

20. Steinor, H. H., Influence of the Cement on the Corrosion Behavior of Steel in Concrete, Portland Cement Association, Res., Dep. Bull., 1:168 (1964)

21. Schiessl, P., Corrosion of Reinforcement, *Durability of Concrete Structures,* (S. Rostam, ed.) CEB-RILEM Int. Workshop, Copenhagen, pp. 73–93 (May 18–20, 1983)

22. Stunge, H., and Chatterji, S., Microscopic Observations on the Mechanism of Concrete Neutralization, *Durability of Concrete, Aspects of Admixtures and Industrial By-Products, 2nd Int. Seminar,* Chalmers University of Technology, Doc, D9-1989, p. 229, Swedish Council of Building Research, Stockholm (1989)

23. Meyer, A., Investigations of the Carbonation of Concrete, Supplementary paper III-52, *Proc. 5th Int. Symposium on the Chemistry of Cement,* Tokyo, pp 394–401 (1968)

24. Grimer, F. J., The Durability of Steel Embedded in Lightweight Concrete, *Concrete,* pp. 125–131 (Apr. 1967)

25. Schulze, W., and Gunzler, J., Corrosion Protection of the Reinforcement in Lightweight Concrete, *Proc. 1st Int. Congr. On Lightweight Concrete,* pp. 111–122, London (May 1968)

26. Allen, R. T. L., and Forrester, J. A., The Investigation and Repair of Damaged Reinforced Concrete Structures, *Corrosion on Reinforced Concrete Construction,* pp. 223–234, (A. P. Crante, ed.) Ellis Harwood Ltd. (1983)

27. Bremner, T. W., Holm, T. A., and Stepanova, V. F., Lightweight Concrete—A Proven Material for Two Millenia, *Advances in Cement and Concrete,* pp. 37–51, (S. L. Sarkas, and M. W. Grutzeck, eds.) Durham, NH (Jul. 24–29, 1994)

28. Stepanova, V. F., Durability of Lightweight Concrete Structures, Internal Report, *Concrete and Reinforced Concretes,* p. 16, NIIZhB, Russia (1991)

29. Stepanova, V. F., Durability of Normal Weight and Lightweight Concrete with Low Cement Content, *Concrete and Reinforced Concrete Magazine*, Moscow, (9):29–31 (1988)

30. Rodhe, M., X-Betong, Properties of Fresh and Hardened Concrete, Report P86:3, p. 30, Chalmers University of Technology, Dept. of Building Materials (1986)

31. Holm, T. A., Bremner, T. W., and Newman, J. B., Lightweight Aggregate Concrete Subject to Severe Weathering, *ACI Concrete Int.*, 6:49–54 (1984)

32. McLaughlin, P. E., Powered Concrete Ships, *Engineering News Record*, pp. 94–98 (Oct. 19, 1944)

33. Ohuchi, T., Hara, M., Kubota, N., Kobayashi, A., Nishioka, S., and Yokoyama, M., Some Long-term Observation Results of Artificial Lightweight Aggregate Concrete for Structural Use in Japan, II:274–282, *Int. Symp. Long-term Observation of Concrete Structures*, Budapest, Hungary (Sep. 17–20, 1984)

34. Holm, T. A., Bremner, T. W., and Vaysburd, A., Carbonation of Marine Structural Lightweight Concrete, *2nd Int. Con. Performance of Concrete in Marine Environment*, p. 11, St. Andrews, N. B., Canada, ACI, SP 109, (Aug. 21–26, 1988)

35. Holm, T. A., Three Decades of Durability, *The Military Engineers* (Sep.–Oct. 1983)

36. Swenson, E. G., and Sereda, P. J., Mechanism of the Carbonation Shrinkage of Lime and Hydrated Cement, *J. Appl. Chem.*, 18:111–117 (1968)

37. Osborne, G. J., The Durability of Lightweight Concrete Made with Pelletized Slag as Aggregate, *Durability of Building Materials*, pp. 249–263, Elsevier (1985)

38. Osborne, G. J., The Durability of Lightweight Aggregate Concretes after 10 Years in Marine and Acid Water Environment, *1st Int. Symp. Structural High Strength Lightweight Aggregate Concrete*, pp. 591–603, Sandefjörd, Norway (1995)

39. Bilodeau, A., Chevrier, R., and Malhotra, M., Mechanical Properties, Durability and Fire Resistance of High Strength Lightweight Concrete, *Int. Symp. Structural Lightweight Aggregate Concrete*, pp. 432–443, Sandefjörd, Norway (1995)

40. Gergout, P., Rivertegat, E., and Moine, G., Action of Chloride Ions on Hydrated Cement Pastes: Influence of Cement Type and Long Time Effects of the Concentration of Chlorides, *Cement Concrete Research*, 22:451–457 (1992)

41. Roper, H., and Baweja, D., Carbonation Chloride Interaction and their Influence on the Corrosion Rates of Steel in Concrete, *Durability of Concrete, 2nd Int. Conf.*, p. 295, (V. M. Malhotra, ed.) Montreal, ACI Special Publication, SP-126-1 (1991)

42. Durwkovic, A., and Calogovic, V., Investigation of Concrete from a Bridge Support after 11 Years of Exposure to Sea Water; *Durability of Concrete, 2nd Int. Conf.*, p. 627, (V. M. Malhotra, ed.) Montreal, ACI Special Publication, SP-126-1 (1991)

43. Figg. J., Salt Surface Rust and Other Chemical Effects, *Proc. Symp. Prof. Gerwick, Jr. Int. Experience with Durability of Concrete in Marine Environment,* p. 49, (P. K. Mehta, ed.) University of California at Berkeley, Dept. of Civil Engineering (Jan. 16–17, 1989)

44. EuroLightCon, LWAC Material Properties, State of the Art, Document BE96-3942/R13, p. 37 (1998)

45. Carlsson, J., E., The Influence of Curing Conditions on the Chloride Diffusion in Lightweight Aggregate Concrete, *2nd Int. Symposium Structural Lightweight Aggregates Concrete,* pp. 866–873, Kristianstad, Norway, (Jun. 2000)

46. von Breugiel, K., and Taheri, A., Chloride Penetration in Lightweight Aggregate Concrete Beams Exposed to Alternating Moisture and Temperature, *2nd Int. Symp. Structural Lightweight Aggregates Concrete,* pp. 856–865, Kristianstad, Norway (Jun. 2000)

47. British Standard Institution, BS 1881, Testing Concrete; Methods for Analyses of Hardened Concrete, BSI, London (1988)

48. British Standard Institution, BS 6349; Part I, Code of Practice for Maritime Structures, Part I; General Criteria, Incorporating Amendment NO. 4, AMD 6159, Published July 31, 1989, BSI, London 1984 (1989)

49. Dhir, R. K., Jones, M. R., and Ahmed, E. H.,Concrete Durability; Estimation of Chloride Concentration During Design Life, *Magazine of Concrete Research,* 43(154):32–44 (Mar. 1991)

9

Fire Resistance of Lightweight Aggregate Concrete

1.0 INTRODUCTION

The performance of building materials under fire exposure is of significant importance. One phenomenon that must be considered during fire is the risk of explosive spalling, which may cause much of the concrete cover to disappear leaving the reinforcing bars directly exposed to fire. This may happen in a very short time in parts or in all of the structure. Prestressed concrete structures with thin webs are more liable to spalling and explosions, and may collapse suddenly. Therefore, it is of great importance to diminish or overcome this problem. The design of the concrete mixture itself directly influences the risk of spalling at high temperature. During fire, the water in concrete transforms to steam. If the pore system of concrete is not sufficient to transport this steam, a pressure builds up and causes spalling of concrete. The other cause is the thermal expansion of the aggregates used. Thus, the fire endurance is related to the pore structure of concrete and to the thermal properties of the aggregates used for making it.

The thermal behavior of concrete, its relative humidity, the thermal properties of aggregates and concretes, the pore structure of the concrete in respect to fire endurance, and fire testing methods are described in this chapter.

2.0 BEHAVIOR OF CONCRETE AT ELEVATED TEMPERATURE

2.1 Sorption Characteristics of Building Materials

The *thermal fire endurance* is the time at which the average temperature on one side of a construction exceeds its initial value by 139°C when the other side is exposed to a standard fire specified by ASTM Method E119.

The effect of moisture on the fire endurance of building elements is, of course, closely related to the amount of moisture, and, in turn, to the sorption characteristics of materials. The amount of moisture held by a solid at various vapor pressures, in other words, the shape of sorption isotherms, depends on the specific surface, the effective porosity, and the pore geometry (basic pore-shape, pore size distribution, etc.) of the solid, and, in the domain of capillary condensation, marked sorption hysteresis can be experienced.

Figure 9.1 shows the moisture sorption isotherms of a certain type of clay brick obtained by calculations. The shape of the curves can be regarded as typical of building materials in general with an important exception for concrete. In the case of concrete, the hysteresis loop extends to a pressure range of $0 < p < p_0$.[1] To understand the cause of this behavior, one should realize that the binding energy of some water molecules held in the portland cement paste by chemical bonds is less than the energy needed to dislodge the most firmly held adsorbed molecules during drying. Consequently, at some advanced stage of drying, desorption and partial dehydration will take place simultaneously. Since the amount of water held by adsorption cannot be determined exactly, part of the water, which is dislodged by some standard drying procedure, is more accurately called *evaporable water* rather than *moisture*. For similar reasons, the amount of water retained by the hydrated cement throughout drying should be termed *non-evaporable water*.

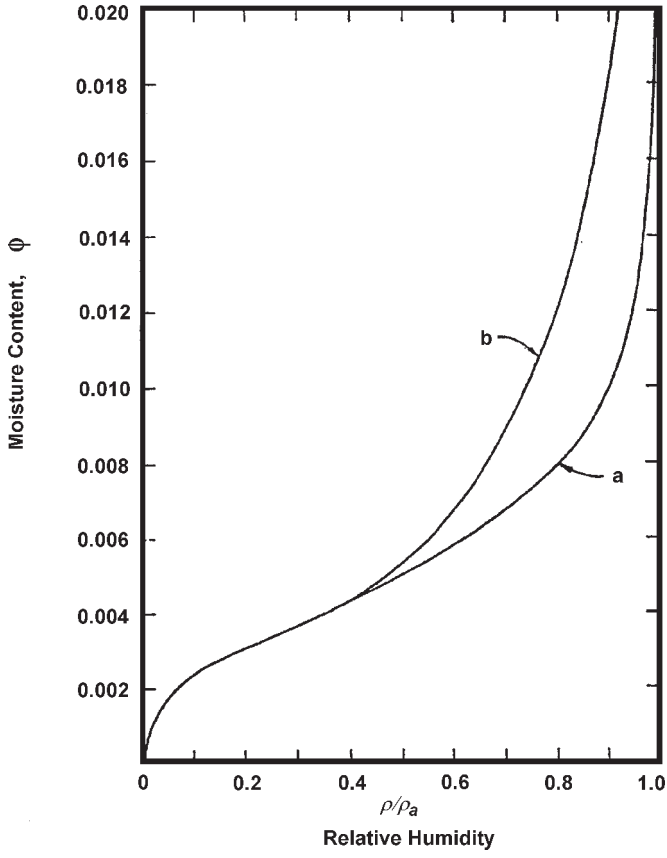

Figure 9.1. Calculated sorption isotherm of a certain clay brick, (a) adsorption branch, (b) desorption branch.[1]

In the case of concrete, the reference state of the material is not its "dry" state, but a state determined by some standard drying procedure. Among the various drying techniques, two are taken as standard:

1) D-drying.

2) drying in an oven at 105°C.

- D-drying: The sample is dried over ice at –79°C (sublimation temperature of CO_2) by continuous evacuation with a rotary pump through a trap cooled in a mixture of solid CO_2 and ethanol. The partial pressure of water is 5×10^{-4} torr.
- Drying in oven: Heating to constant mass at 105°C in an atmosphere of controlled humidity, but free from CO_2, reduces the water content approximately to the same value, although it is not a strictly defined drying condition.

In view of these discussions, it seems most probable that the unusual shape of the sorption isotherm of concrete is due to partial or complete rehydration, during adsorption, of the water of constitution lost at very low pressure during desorption.

The sorption characteristics of portland cement paste and concrete depend very strongly on the degree of hydration[2]-[4] and thus on the age, curing procedure, and some other factors. Under ordinary circumstances, a sufficiently large mass of concrete can retain enough water in its pores to ensure the progress of hydration for a very long period after the removal of forms and protecting covers. If, however, the concrete is subjected to forced drying, the hydration slows down considerably as the RH in the pores becomes lower than 95% and stops completely at 80%.[5]

2.2 Spalling

Because of the marked differences in the sorption characteristics of various building materials, the amount of moisture that these materials hold at normal atmospheric conditions may be very significant in certain cases, or barely noticeable in others. The presence of moisture is the major source for building up vapor pressure causing explosion spalling of concrete at an early stage of fire exposure.

A probable mechanism of spalling of concrete, called *moisture clog spalling*, during fire exposure is described by Shorter and Harmathy.[6] When heat begins to penetrate into the concrete slab, desorption of moisture starts in a thin layer adjoining the surface exposed to fire. A major portion of the released vapors move toward the colder regions and become reabsorbed in the pores of some neighboring layer. As the thickness of the dry layer gradually increases, a completely saturated layer of considerable

thickness (called a moisture clog) builds up at some distance from the exposed surface. A little later, a sharply defined front forms between the dry and saturated layers (Fig. 9.2). Further desorption will obviously take place from this frontal area, indicated by line *CD*.

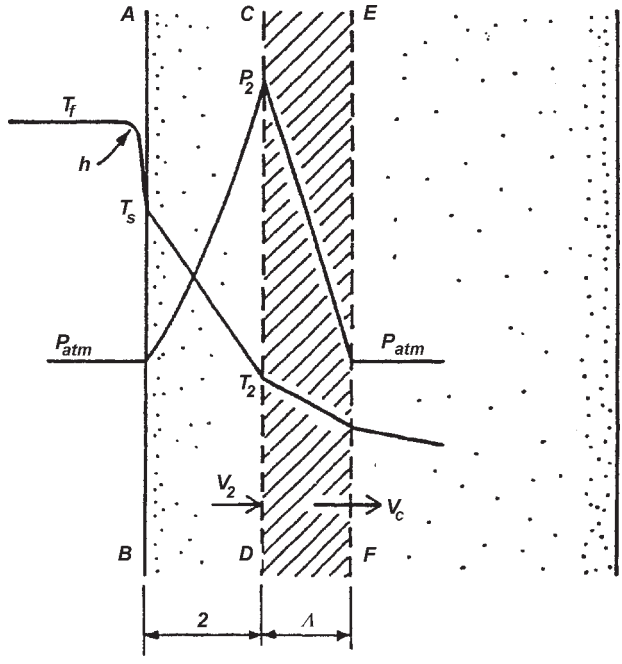

Figure 9.2. Diagram of moisture clog formation.[6]

In the meantime, the temperature of the exposed surface keeps rising, and a very steep temperature gradient develops across the dry layer resulting in a high heat flow and intensified desorption at the *CD* plane. Having little passage toward the colder regions, the vapors have to leave through the dry layer, gradually expanding and meeting increasing resistance along the flow path. With further steepening of the temperature gradient, there will be a rapid pressure build up at the plane *CD*.

If the resistance of the pores to moisture flow is not too high, under the effect of the large pressure difference, the moisture clog (region *CDEF*) begins to move towards the colder regions and the pressure buildup soon levels off. If, on the other hand, the permeability of the materials is low, the pressure at the plane *CD* continues to grow and will eventually exceed the ultimate tensile strength of the material. When this condition is reached, a layer of thickness approximately equal to that of the dry layer separates from the material.

If this suggested mechanism is correct, one could expect that material properties such as porosity, permeability, ultimate strength, and thermal conductivity (by effecting the heat flow through the dry layer) will play an important role in moisture clog spalling. With advancement in the hydration, the pore structure of concrete becomes dense. The permeability of mature portland cement paste, for example, is several orders of magnitude lower than that of fresh cement.[1][3] This makes the concrete more vulnerable with age to moisture clog spalling.

2.3 Gain in Thermal Fire Endurance

If spalling is not expected to take place, the presence of moisture in building materials is beneficial for fire endurance. The primary reason is the absorption of heat, associated with the desorption of moisture, checks the rise of temperature in a building element during fire exposure, delaying the development of various phenomena which may lead to failure during fire exposure.

2.4 Thermal Compatibility of Aggregates and Cement Paste

When concrete is heated, physical and chemical changes take place in the cement paste and the aggregate. This results in a weakened structure and the strength of the cement paste decreases. The effect of temperature on the thermal expansion of granite aggregates, cement paste, and concrete is shown in Fig. 9.3.[7] This illustrates the thermal incompatibility between the cement paste and the aggregate. The incompatibility creates internal stresses and microcracks and weakens the concrete. Internal stresses can also develop partly due to nonuniform temperature distribution and partly due to vapor pressure (developed during the transformation of water to steam). These stresses can contribute to explosive spalling.

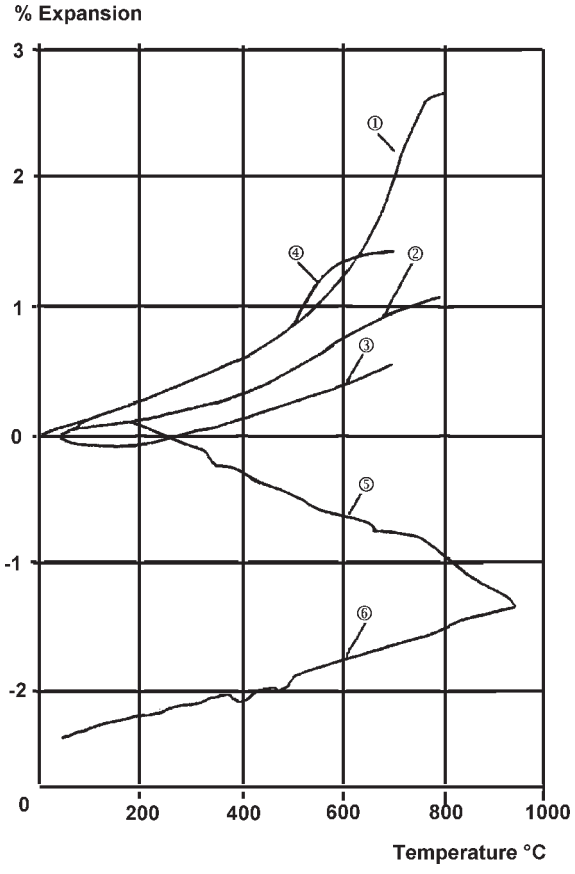

Figure 9.3. Effect of temperature on thermal expansion of *1)* granite, *2)* concrete made with granite aggregate, *3)* limestone, *4)* sandstone, *5)* cement paste in process of heating, *6)* cement paste in the process of cooling.[7]

This phenomenon has been described by Nekrasov and Zhukov[8] by the inequality:

Eq. (1) $$(P+\sigma)K < R_p^t$$

where P is the pressure of the steam in the concrete, σ is the tensile temperature stress in the concrete or the tentative stress corresponding to deformation force, K is the coefficient taking into account the approximation of the formula, and R is the tensile strength of the hot concrete. The inequality [Eq. (1)] can be described in the form:

Eq. (2) $$\left(\frac{P}{E_{bt}}+\varepsilon\right)K<\varepsilon_p^t$$

where ε is the deformation of the concrete due to the tensile temperature or other stresses, E_{bt} is the elastic modulus of the hot concrete, and ε_p^t is the deformation limit of the heated concrete due to the tensile stresses. If during heating and cooling, the inequality [Eq. (1) and (2)] is maintained, no cracks or other faults should develop in the block. Another formula is given by Nekrasov and Zhukov[8] for measuring the total flux of the moisture through the cross-section of the block:

Eq. (3) $$f=-\lambda m\left(\nabla\theta+\delta\nabla t\right)-K\nabla P$$

where λm is the coefficient of mass conduction, θ is the mass transfer potential, t is the heat transfer potential, δ is the thermal gradient, and K is the coefficient of liquid or steam filtration.

The principal condition of the temperature and moisture state in the one dimensional case of a heated wall is illustrated in Fig. 9.4.[9] Three zones are created there, a dried zone, a vaporization zone, and one zone only A_1-A_1, where the temperature lies between 100–200°C.

The steam pressure, P, and thermal gradient, δ, depend mainly on the pore system of the concrete. The more open the structure, the lower will be the steam pressure and the thermal gradient. Here, most of the stress is due to the thermal incompatibility of the aggregates and cement paste and the vapor pressure.

The difference between thermal spalling and moisture clog spalling occurring during a standard fire endurance test is easily recognizable. Moisture clog spalling is generally more violent and the thickness of the dislodged layers is greater, about 1 inch (2.54 cm). Spalling of concrete may also be due to other factors such as excessive deformation, expansion of reinforcement, or crystalline transformation in certain aggregates, especially with a high quartz content.

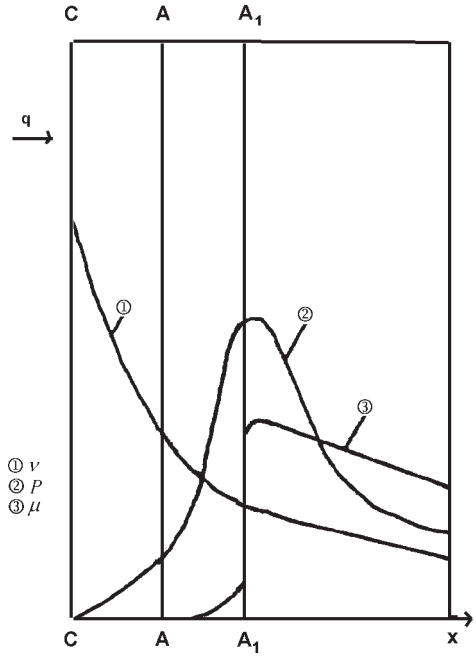

Figure 9.4. Distribution of temperature (v), vapor pressure (P), moisture content (μ), in a concrete section during heating from one side; q = heat flow, C-C = warm side, A_1-A_1 = vaporization front, A-A = border of dry concrete.[9]

3.0 FIRE TEST OF LIGHTWEIGHT AGGREGATE CONCRETE

Fire endurance tests of four types of concrete were conducted in a gas-oil furnace.

- The first type was LWAC, "3L-concrete," developed at the Chalmers University of Technology[10] with a density of 1100–1200 kg/m^3. The lightweight aggregates used were Swedish Leca™.
- The second type was the structural LWAC with a density of 1650 kg/m^3 and 15 cm cube compressive strength of 35 MPa.[11]

- The third type was structural LWAC modified with chemical admixtures.[12]
- The fourth type was a high strength LWAC made with the addition of condensed silica fume.[13]

Type one and two lightweight aggregate concretes were made using LWA, Swedish Leca™. A comparison was done with normal weight concrete made with the addition of a polymer.[14] The densities of LWAC and normal concrete were 1100 and 2310 kg/m^3, respectively. A fire test was performed on:

- 2.5 cm thick plates of normal concrete
- 2.5 cm thick plates of LWAC
- 5.0 cm thick slab of LWAC
- 15 cm thick reinforced concrete beam of LWAC

The test specimens were cured under laboratory conditions, i.e., 40% RH and 20°C. A gas-oil fired furnace with an opening of 2.5 × 0.3 m^2 was used for heating the test specimens. The tests were performed by one-side and two-side heating. The position of the test samples in the furnace is shown in Fig. 9.5 and the results are shown in Figs. 9.6 thru 9.10. The test results revealed that thin plates of normal concrete and LWAC do not show any spalling when heated from one side.

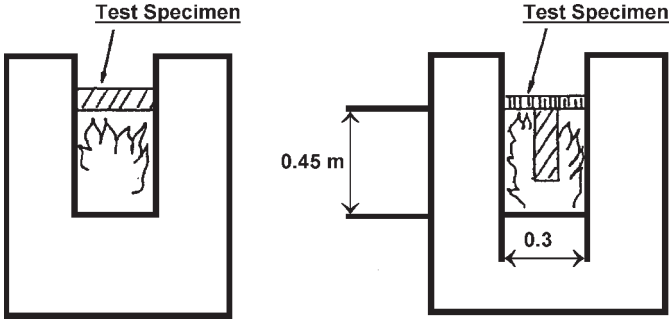

Figure 9.5. Position of the samples in the furnace *(a)* one-side exposure, *(b)* two-sides exposure.[14]

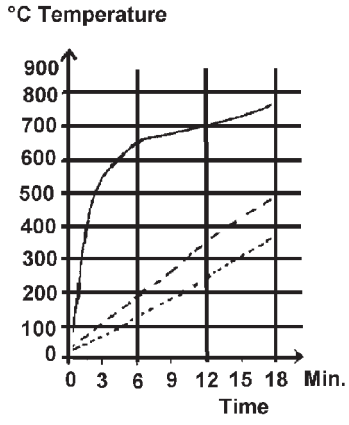

(a)

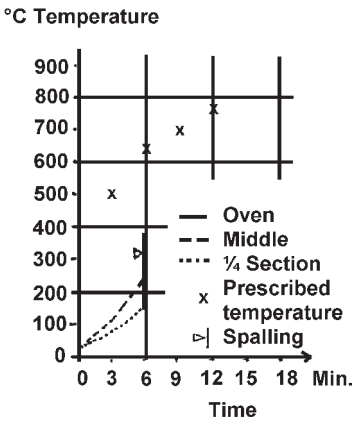

(b)

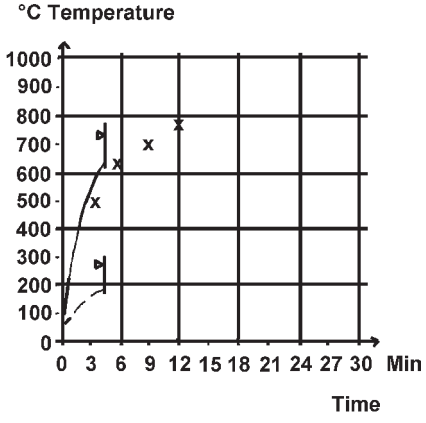

(c)

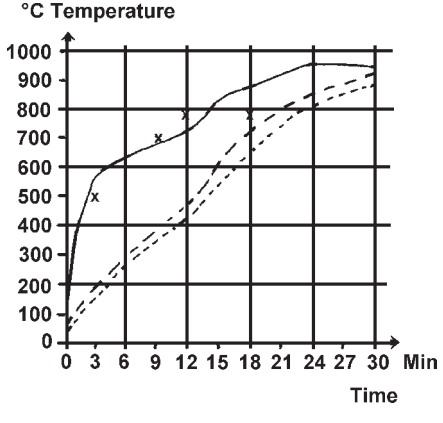

(d)

Figure 9.6. Temperature curves for *(a)* one and *(b), (c), (d)* two-side heated plate (2.5 cm in thickness) of normal concrete, *(b)*and *(c)*show the temperature at which normal concrete specimens made without a polymer have shown destructive spalling, whereas *(d)*made with a polymer has shown no spalling.

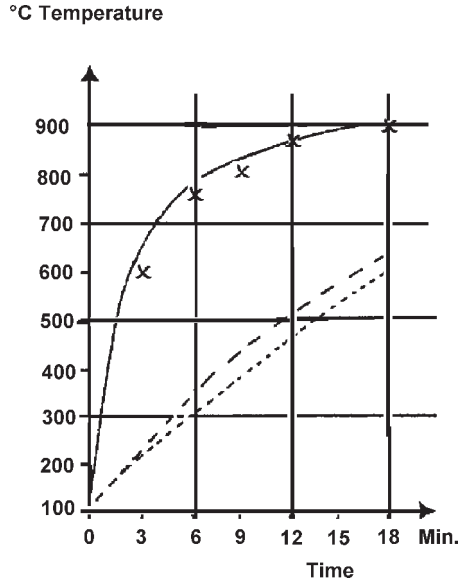

(a)

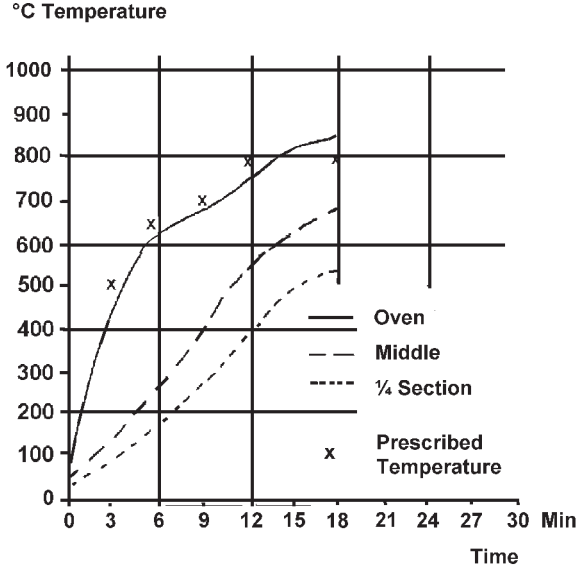

(b)

Figure 9.7. Temperature curves for *(a)* one-side fire exposure, *(b)* two-sides fire exposure of the LWAC thin plates.[14]

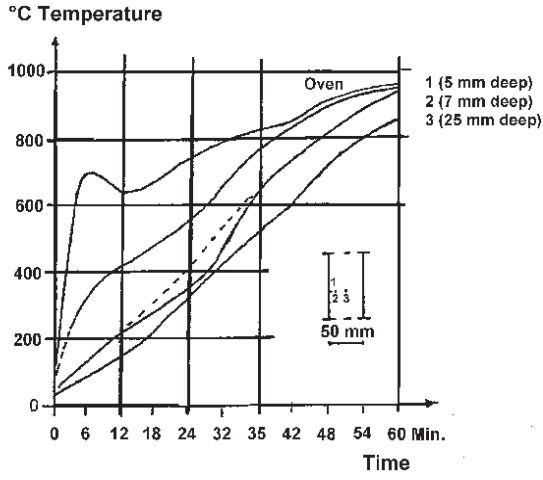

Figure 9.8. Temperature curves for two-sides fire exposure of the LWAC slab (thickness 50 mm).[14]

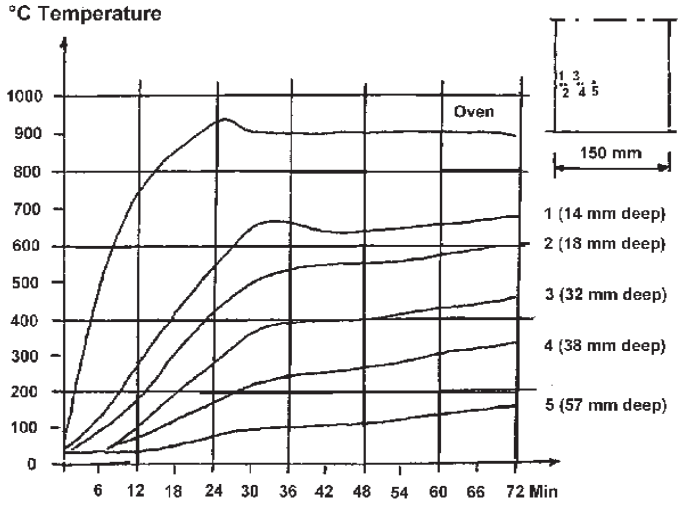

Figure 9.9. Temperature curves for two-sides fire exposure of the reinforced LWAC beam (thickness 150 mm).[14]

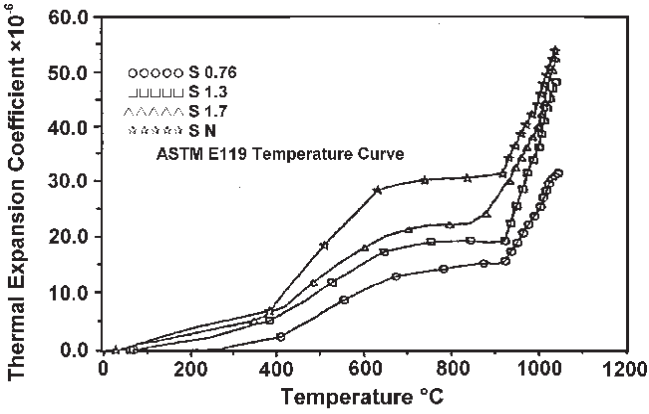

Figure 9.10. Thermal expansion coefficient of various types of concrete.[16]

Heating the normal concrete plates (Fig. 9.6) from two sides resulted in destructive spalling at about 125–175°C. In the concretes made with the polymer addition, no spalling was observed when heated from both sides, even after 30 minutes. Tests performed on the 5 cm slabs and the LWAC reinforced beam ($b \times h = 0.15 \times 0.3$ m^3) did not show any damage for 1 hour after heating when the temperature in the middle of the specimens observed was 850°C (Figs. 9.8 and 9.9).

The residual strength after the fire exposure test was less for normal concrete than for the LWAC showing more damage to the normal concrete. These results are in agreement with those reported by Malhotra.[15] Jau and Wu[16] have studied the performance of 15 cm thick LWAC panels under fire. They reported that the LWAC showed low thermal conductivity and a low thermal expansion coefficient at any temperature other than that of normal weight concrete.

The thermal expansion coefficient for concrete of different specific weights is shown in Fig. 9.10, and the residual compressive strength after heating to different temperatures is shown in Table 9.1.

Table 9.1. Residual Compressive Strength after Exposure to High Temperature, kp/cm^2[16]

Specific Weight	0.75	1.3	1.7	Normal Weight
Temp. °C	Compressive Strengths			
22	161	283	291	323
518	131	264	260	302
704	121	219	236	276
843	86	138	169	195
927	74	112	120	131
1010	38	42	44	50
1052	32	33	30	33

The thermal expansion coefficient is higher for the concrete with a higher specific weight compared to the one with lower specific weight. Residual compressive strengths show the same tendency. However, the decrease in the strength of the normal weight concrete is much greater compared to the lightweight concretes. It is due to the fact that the cement paste expands during heating, up to 150°C; with a further temperature rise it shrinks substantially.

Thermal expansion curves are well illustrated in Fig. 9.3.[7] As the temperature increases, the volume of the aggregate increases with the different intensities, depending upon the coefficient of thermal expansion of the aggregates and the cement-to-aggregate (sand-to-Leca™) ratio.

According to the FIP/CEB manual of lightweight aggregate concrete,[17] the coefficient of thermal expansion of lightweight expanded clay aggregate Leca™ is 50–70% lower than that of gravel (approx. 12×10^{-6}/K). There is a much greater volume expansion of silica due to its transformations at higher temperatures to cristobolite and trydymite. In the lightweight concrete made here, the amount of sand used is one-fourth of the aggregate used in normal concrete. This reduces the possibility of lightweight concrete expansion to approximately one-fourth.

The improvement is attributed to the LWA and, in the case of normal concrete, to the polymer addition which has entrained air, and has made possible the transport of vapor hindering the build up of steam vapor pressure.

The fire resistance test of structural LWAC was done on a normal reinforced concrete plate of the size 6.0 m × 2.60 m × 0.2 m. Four cubic meters of concrete was mixed in a free-fall mixer and was cast with the help of rod vibrators.

The 28 day density and the 15 cm cube compressive strength were 1660 kg/m^3 and 35.2 MPa. The beam was cured for 3 months, then was tested at the Swedish National Testing and Research Institute.[18] The fire test was performed according to SIS 024820 (NT FIRE 005, ISO 834). Heating was from one side. The plate was loaded under the test with two linear loads of 9.2 kN/m placed on the plates at quarter points. The total of the load, including the dead load of the slab, was 7.0 kN/m^2. After eight minutes, the plate started deteriorating and after 23 minutes the test was stopped. The basic composition of the lightweight aggregate concrete was:

Portland cement		425 kg/m^3
Sand		850 kg/m^3
Swedish Leca™	: 2–6	310 kg/m^3
	: 4–10	310 kg/m^3
W/C		0.39
Mighty 100™		1% of the weight of cement

The strength of the concrete was high which was achieved by making very high strength cement mortar in order to compensate for the lower strength of the LWA. The strength of the mortar was about 80 MPa. It implies that the mortar was very dense and had a very low permeability. This dense structure did not provide adequate conditions for moisture transport. The moisture content determined after the test was 6.1%, which is equivalent to the 95% RH during testing. The relative humidity during the test should not exceed 75%.[19] Due to the dense structure, the plate could not dry fast enough to have the requisite relative humidity. This high inner water content, which was not uniformly dispersed, transformed to steam and built up pressure differentials in the plate during the fire test. This happened due to the inability of steam to be transported out due to the dense concrete structure. It is the same phenomena which hindered fast drying of the concrete plate. Consequently, the steam pressure built up resulting in the spalling of the plate.

3.1 Modified Structural Lightweight Aggregate Concrete

Structural lightweight aggregate concrete developed by Berntsson and Chandra[11] has a very dense cement mortar matrix, which compensated for the low strength of the lightweight aggregate. This created difficulties in the transportation of vapor/steam and resulted in the spalling of concrete.

This concrete structure was modified using superplasticizers, air-entraining agents, and polymers. The aim was to have an air void system adequate for the transport of the steam build up during the heating of concrete. This would hinder the formation of steam vapor pressure and would not cause spalling of concrete.

Concretes were made with the addition of superplasticizers, air-entraining agents, and polymers. The basic composition was the same as described earlier, except some chemical admixtures were used. Ten centimeter diameter cylinders were cast and cured for 6 days under water after demolding and for 22 days at 55% RH and 20°C temperature in the climate room. The fire resistance was tested in a Superkanthal furnace.

The compositions and the fire test results are shown in Table 9.2. The physical condition of the samples after the test is shown photographically in Fig. 9.11 for normal concrete and in Fig. 9.12 for the LWAC.

Mercury porosimetry was used to analyze pore size distribution of LWAC made with the addition of superplasticizers naphthalene formaldehyde condensate (Mighty M™) and melamine formaldehyde condensate (Peramine F) and the air-entraining agent, Sika Aer™. The pore volume is shown in Table 9.3.

Table 9.3 shows that the samples made with the addition of the superplasticizer Mighty 100™ (marked M) spalled at the RH 85%, whereas no damage could be seen at 82% RH and lower. The same concrete with AEA (MS) did not show explosion spalling as was the case with sample MS at a RH more than 85%; instead cracks on the surface were noticed.

This is because the air-entraining agent has created a more open pore structure. The pore volume in this case is 19% more than that of the sample M. The samples made with the addition of SP Peramine marked PER spalled at a RH of more than 88%, whereas no damage could be seen at 84% RH and lower. The PER with AEA (PERS) sample had not shown any explosion spalling even at 89% RH; only crack formations on the surface of the sample were noticed, whereas no damage could be noticed at 85% RH. It is obvious that PERS has a more open pore structure. The pore

Table 9.2. Fire Test of Lightweight Aggregate and Normal Weight Concrete[12]

No.	Admixture	RH	Remarks in Fire Test
K25	Nil	98	Expansion spalling from hot end
		94	Numerous expansion cracks from hot end
		65	Numerous expansion cracks from hot end
M	Mighty	94	Explosion spalling
		89	Explosion spalling
		85	Explosion spalling
		82	No damage
		75	No damage
MS	Mighty + SikaAer	94	Explosion spalling
		88	Explosion spalling
		85	Crack formation on the surface
		82	No damage
		75	No damage
PER + P	Peramine	93	Explosion spalling
		89	Explosion spalling
		87	Crack formation on the surface
		82	No damage
		74	No damage
PER + S	PER + S	94	Explosion spalling
		88	Crack formation
		86	Few cracks
		84	No damage
		74	No damage
MP1	M + P 1%	83	Explosion spalling
	M + P 5%	75	No damage
MP		82	Explosion spalling
		60	No damage
MF	M + F 0.18%	81	No damage

K25 - normal weight concrete; others are lightweight aggregate concrete, M - Mighty 100™ (SP), PER - Peramine (SP), S - Sika Aer™ (AEA), P - Mowiton (Polymer), F - polypropylene fibers.

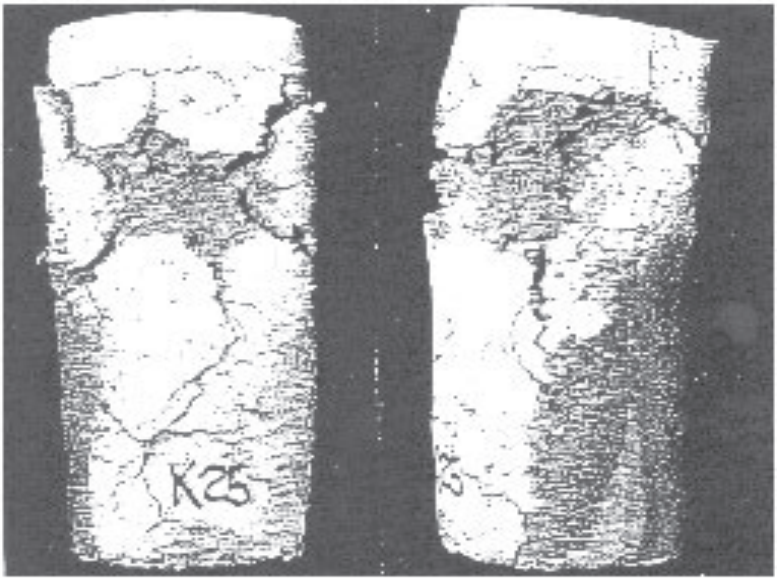

Figure 9.11. Normal concrete K25 after the fire test.[12]

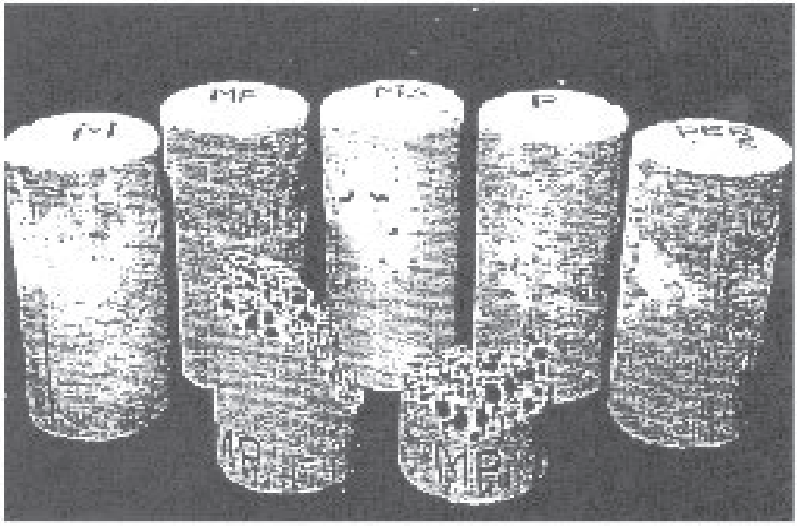

Figure 9.12. Lightweight aggregate concrete after the fire test, M - Mighty™, MF - Mighty™ + Fiber, P - Peramine F, PERS - Peramine + Sika Aer™, MP - Mighty™ + Polymer.[12]

Table 9.3. Pore Volume of Lightweight Aggregate Concrete[12]

No.	Symbol	Pore Volume kg/m^3	Remarks
1	M	0.140	
2	MS	0.167	19% more than M
3	PER	0.164	17% more than M
4	PERS	0.193	18% more than PER 16% more than M
M - samples with Mighty™, MS - samples with Mighty™ and AEA, PER - samples with Peramine, PERS - samples with Peramine and AEA			

volume is 18% more than that of the sample PER without AEA and 16% more than those marked MS (Mighty™ and AEA). Besides the pore volume, the pore structure is more refined in this case which makes the vapor transport easier during heating of the concrete. Thus, the pressure is not built up and explosion spalling does not take place, even at a higher relative humidity.

The polymer sample, MP made with a 5% polymer addition, was broken in two pieces after 15 minutes exposure to 81% RH. The polymer interacts with calcium hydroxide and forms complexes and a film. The complexes can fill up the pores or can seal them from the surface. On the other hand, the film forms on the surface of the pores and capillaries. These pores and capillaries create barriers for moisture and vapor transport. Consequently, the drying of the concrete will be slow and nonuniform, and the water dispersion in the structure will not be homogeneous. The water accumulates in pockets in the concrete structure and the water, thus locked in, transforms to steam during heating. Due to the difficulties in the steam transport, pressure builds up and causes explosion spalling of the concrete cylinders during the fire test. The samples with the 5% polymer addition from the same series were tested after 56 days and no damage could be noticed. Over time, the drying took place and the water which was locked in passed by diffusion through the polymer complexes. The relative humidity of the sample decreased. Consequently, the vapor pressure which builds up is not high enough to cause spalling of the sample.

Other samples, even without the air-entraining agent addition, had pore structures sufficient for steam transport at this RH and there was no hinderance due to the polymer addition, film formation, etc., and they passed the fire test.

The tests were performed on small cylinders and not on the big plates under load. However, it seems that the moisture in the lightweight aggregate concrete tested earlier had a moisture ratio that was too high, although there is no direct relation between the RH and moisture ratio. The RH in the middle of the plate was expected to be high, and this should have been the major cause of explosion spalling of concrete. The optimum RH for good fire resistance seems to be less than 80%.

The moisture content in the concrete and the pore structure are the deciding factors for the fire resistance of concrete. Distribution of the moisture also plays a very important role. Moisture content depends upon the drying time and the relative humidity of the surrounding air. An open pore system facilitates faster dying and the transport of the steam during the fire test. Therefore, the steam pressure does not build up and the resistance to fire is enhanced.

3.2 High Strength Lightweight Aggregate Concrete

The fire resistance tests have been carried out generally on low and medium strength concretes, but not much attention has been given to the fire resistance of high strength concrete. However, with an increase in strength, the mortar matrix in concrete becomes richer and denser in order to compensate for the lower strength of the aggregates. This makes moisture movement in the concrete difficult and has a deleterious effect on the fire resistance. This effect can be improved to some extent by using chemical admixtures such as superplasticizers and an air-entraining agent. The use of fibers also improves fire resistance. Another factor which needs special attention is the resistance of concrete to hydrocarbon fires. This effect must be considered while designing concrete structures for special industrial production systems and offshore installations. Hydrocarbon fires are characterized by high temperatures and a very rapid temperature rise.

Jensen, et al.,[13] studied the fire resistance of high strength LWAC exposed to hydrocarbon fire. The compressive strength and E-modulus at elevated temperatures were determined for LWA and normal density

concrete (ND) on cylindrical specimens of approximately 100 mm diameter. The lightweight aggregate concrete was LWA 75 with an intended mean cube strength of 75 N/mm^2. The concrete had the following composition:

Cement	416 kg/m^3
Condensed silica fumes	22 kg/m^3
Water	193 kg/m^3
W/(C + S)	0.36 kg/m^3
Gravel: 0–8 mm	700 kg/m^3
LWA: 4–8 mm	313 kg/m^3
LWA: 8–16 mm	313 kg/m^3
Superplasticizer	5.5 kg/m^3
AEA	0.4 kg/m^3
Slump	150 mm

The tests included reinforced pre-stressed beams (150 × 200 × 2800 mm) of four different concrete types. Three of them had passive fire protection consisting of several cement-based mortars containing expanded polystyrene.

Concrete types:

ND95	Normal density concrete (reference).
LWA75	Lightweight aggregate concrete.
LWAF75	Lightweight aggregate concrete with polypropylene fibers (Liapor™ aggregates, Fibrin fiber type 1823).
LWAF75P	LWA aggregate concrete with polypropylene fibers and protected with LightCem LC5 passive fire protection.
LWA50	LWA concrete (LightCem, Leca™ aggregate).

The effects of the compressive strength level (i.e., water-to-binder ratio and silica fume content) were examined on the following:

ND concretes:

ND65:W/(C + S) = 0.50, 5% SF.

ND95:W/(C + S) = 0.36, 5% SF.

ND95-0:W + /(C + S) = 0.36, 0% SF.

ND115:W/(C + S) = 0.27, 5% SF.

The strengths of normal density and LWA concrete were 65–115 MPa and 75 MPa, respectively. The targeted temperatures during testing were 20, 100, 200, 300, 400, and 600°C. The results show a reduction in compressive strength and the E-modulus by 25–40% at temperatures in the range of 200–300°C (Figs. 9.13 and 9.14).

A further strength reduction with concrete temperatures higher than 300°C is not apparent. In fact, the results showed a slight increase between 300° and 450°C. The total mean loss of strength at 600°C was in the range of 60 percent. No effect of W/(C + S) on the temperature development strength loss was apparent, since the results did not distinguish significantly between concretes between W/(C + S) = 0.27, 0.36, and 0.50 (ND115, ND95, and ND65), respectively. In some cases, concrete without silica fume shows better performance in terms of the somewhat lower loss of strength. This may be due to less densification and the reduced brittleness of the concrete. The replacement of normal coarse aggregate with LWA does not seem to affect the temperature-dependent loss of strength.

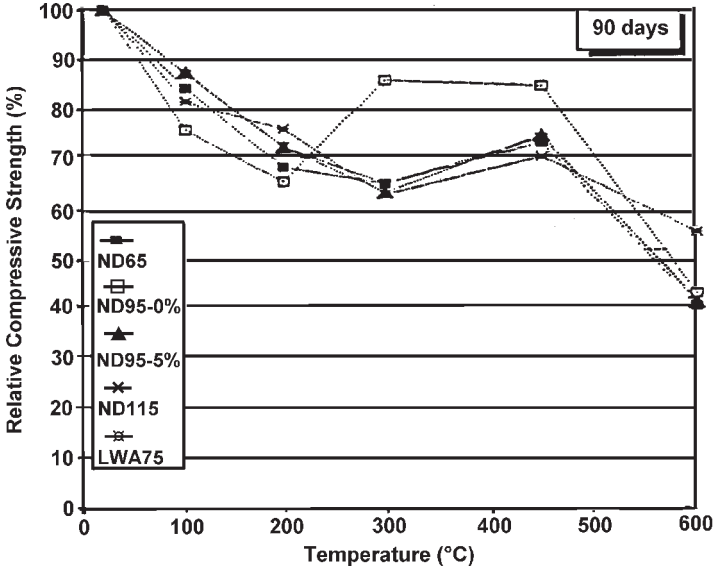

Figure 9.13. Relative compressive strength versus target temperature of specimens during testing.[13]

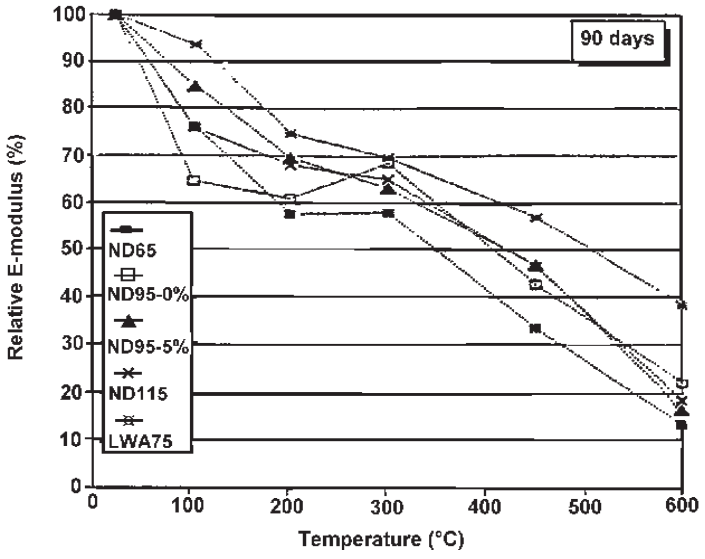

Figure 9.14. Relative E-modulus versus target temperature of specimens during testing.[13]

The reduction in the E-modulus at temperatures higher than 300°C is very clear. There is a linear reduction in the temperature range of 300–600°C. The maximum reduction without any clear effect of the water-to-binder ratio (0.50–0.36) was in the range of 75–87% for ND concretes, and 60–70% for the LWA concrete.

Hydrocarbon fires may cause serious damage to concrete structures. The question which arises after the fire is whether or not the structure has enough residual strength for continued unaltered use or use after minor repairs.

A considerable decrease in the compressive strength and E- modulus, even at relatively low temperatures, i.e., 100–300°C, was noted (max 40% reduction). The loss in strength and E-modulus at 600°C was in the range of 60% and 60–87%, respectively. Spalling was highly dependent upon the high moisture content. The following observations were made:

- LWA75: These beams showed severe spalling. The damage was considered to be too extensive to permit further experimental investigation, i.e., the residual strength was assumed to be zero.

- LWAF75: Only minor spalling was observed in these beams. However, cracks were observed. The residual strengths was calculated according to NS 3473.[20] In some of the beams, the failure mode changed from an intended flexural failure in tension to a flexural failure in compression, indicating an even more serious reduction in the concrete strength than that due to the reduced load-carrying capacity.
- LWAF75P: These beams withstood the exposure to fire extremely well, i.e., no visual damage could be observed, except for one beam which was loaded during the fire exposure. A permanent deflection was observed in this beam. The residual strength was somewhat above the estimates based on NS 3473 with the initial material parameters.
- ND95 and LWA50: The results were similar to LWAF75. The addition of 0.1–0.2 vol% polypropylene fibers in the LWA mix resulted in a significant reduction in spalling. This was confirmed by the structural beam tests.

Fire tests on beams confirm the previous findings that severe spalling occurred at reinforced and pre-stressed LWA beams. Reduced spalling occurred on ND concrete beams. Reduced or no spalling was observed on LWA beams with passive fire protection.

The positive effect of using fire protection (a special cement-based mortar with expanded polystyrene beads) to prevent spalling and reduce the temperature rise is obvious, and should, therefore, be considered in the design evaluation.

Ultimate strength tests on beams after fire exposure showed that, even if the structural elements only show minor spalling after exposure, the reduction in concrete strength and, thus, in the load-bearing capacity may be severe.

3.3 Fire Resistance of High Performance Lightweight Aggregate Concrete (HPLC)

Expanded shale has a linear stress-temperature relationship, whereas most silicious types of natural aggregates are nonlinear and may expand about three or four times as much as expanded shale when heated to 900°C.

When incorporated in a concrete mixture, these two types of aggregates (expanded shale and silicious) resist the propensity of the cement paste matrix to contract when heated above 300°C. The vesicular shale lightweight aggregate expands less, thereby the concrete incorporating this type of aggregate tends to expand less. As a result, internal disruption is reduced so that the concrete's loss in strength at high temperatures is decreased. Also, with reduced expansion in the concrete, the bowing of walls exposed to fire on one side is lessened and, as a consequence, structural stability in terms of resistance to buckling of the wall is greater, leading to high performance compared to normal concrete.[21]

4.0 FIRE PROTECTION

The heating of the lightweight aggregates to about 1200°C during manufacture preconditions them to perform better than normal weight aggregate when concrete made from them is subjected to fire. Building codes normally require about 30% less thickness for a floor slab to achieve a two hour fire separation. This, combined with the fact that there is about 30% reduction in density when LWC replaces NC, has enabled lightweight concrete to capture much of the market for concrete floor toppings over steel decking in steel-framed buildings.

4.1 Insulating Properties

In the production of lightweight aggregates, a vesicular structure is produced that acts as an excellent insulator. When used in concrete, they reduce the thermal conductivity of the concrete by about a factor of two when the density of the concrete is reduced from 2400 to 1800 kg/m^3.[21] Lightweight aggregates can be made of clay with an additional expanding agent added to them such that when they have been fired and cooled, the dry particle relative density is as low as 0.5, and when they are incorporated into concrete, a density of about 800 kg/m^3 is produced with a thermal conductivity about one order of magnitude less than NC.[22]

4.2 Resistance to Petrochemical Fires

Concrete that is moisture saturated and exposed to a fire in which the temperature increases more rapidly than the concrete can dry out produces an explosive type failure. At about 300°C, the vapor pressure of the water is 8.6 MPa and this is sufficient to cause tensile failure of the concrete. In petrochemical fires or in marine terminals and platforms, the concrete is usually saturated and the heat rise is rapid. The result is explosive spalling which is a severe and potentially lethal problem. By incorporating plastic fibers into the concrete mixture, this problem is alleviated. Apparently the plastic fibers melt providing relief channels through the concrete that relieve the internal pressure and allow the concrete to resist the effect of the fire in a manner similar to dry concrete or saturated concrete heated at a very slow rate.

5.0 CONCLUDING REMARKS

The moisture content in the concrete and the pore structure are the deciding factors for the fire resistance of concrete. Distribution of the moisture also plays a very important role. Moisture content depends upon the drying time and the relative humidity of the surroundings. An open pore structure facilitates faster drying and the transport of steam during the fire test. This hinders the build up of steam pressure during the fire. Consequently, fire resistance is enhanced.

The addition of polymers and fibers modifies the pore structure and helps in moisture transport. They are aids for increasing the fire resistance. The LWA expands less, thereby, the concrete incorporating these aggregates tends to expand less. As a result, internal disruption is reduced such that the loss of strength of concrete at high temperature is decreased, therefore, the fire resistance is increased.

Hydrocarbon fires may cause serious damage to concrete structures. The question which arises after the fire is whether the structure has enough residual strength for continued unaltered use or needs repairs. The residual strength after fire exposure of normal strength concrete is lower than that for LWAC. This is due to the higher thermal expansion coefficient for normal weight concrete compared to the LWAC.

REFERENCES

1. Powers, T. C., Copeland, L. E., and Mann, H. M., *Journal, Research Development Laboratories,* Portland Cement Association, 1(2):38 (1959)
2. Powers, T. C., and Brownyard, T. L., *Proc. American Concrete Institute*, 43:101, 249, 469, 549, 669, 849, 933 (1946–1947)
3. Powers, T. C., *Proc. 4th Int Symp. Chem. Cement*, 2:577, National Bureau of Standards (1962)
4. Copeland, L. E., Kantro, D. L., and Verbeck, G., *Proc. 4th Int Symp. Chem. Cement*, National Bureau of Standards, 2:429 (1962)
5. Copeland, L. E., and Bragg, R. H., ASTM Bulletin 204, ASTM, p. 34 (Feb. 1955)
6. Shorter, G. W., and Harmathy, T. Z., *Proc. Institute of Civil Engineers*, 29:313 (1961)
7. Thelandersson, S., Effects of High Temperature on Tensile Strength of Concrete, *Nordisk Betong* 2 (1972)
8. Nekrasov, K. D., and Zhukov, V. L., Investigation of Heating Large Blocks of Refractory Concrete, translated from *Ogneupory*, 6:21–27 (1967)
9. Thelandersson, S., Concrete Structures at High Temperatures - A Review (in Swedish), *VAST* (Sep. 1974)
10. Berge, O., 3L Concrete, An Attractive New Building Material, *Nordisk Betong* 6, (in Swedish) (1978)
11. Chandra, S., and Berntsson, L., *Lightweight Aggregate Concrete for Inside House Construction*, R13:1994, Swedish Council for Building Research (1994)
12. Chandra, S., *Development of Fire Resistant Structural Lightweight Aggregate Concrete*, Chalmers University of Technology (Apr. 1996)
13. Jensen, J. J., Hammer; T. A., Opheim, E., Hansen, P. A., Fire Resistance of Lightweight Aggregate Concrete; *Proc. Int. Symp. Structural Lightweight Aggregate Concrete, Sandefjörd, Norway*, (I. Holand, T. A. Hammer, and F. Fluge, eds.) pp. 192–203 (Jun. 20–24, 1995)
14. Chandra, S., Berntsson, L., and Andersberg, Y., Some Effects of Polymer Addition on the Fire Resistance of Concrete, *Cement and Concrete Research*, 10:367–375 (1980)
15. Malhotra, H. L., The Effect of Temperature on the Compressive Strength of the Concrete, *Magazine of Concrete Research*, 8(23):85 (1956)

16. Jau, W. C., and Wu, G. G., Performance of Lightweight Concrete Panels Subjected to Fire, *Proc. Int. Symp. Structural Lightweight Aggregate Concrete, Sandefjörd, Norway,* (I. Holand, T. A. Hammer, and F. Fluge, eds.), pp. 180–191 (Jun. 20–24, 1995)
17. *CEB/FIP Manual of Lightweight Aggregate Concrete, Design and Technology*, The Construction Press Ltd., Lancaster (1977)
18. SP, Borås, Fire Test of Concrete Plate Under Load, Provningsrapport 92R12201, *SP, Brandteknik* (1992)
19. *Moisture in Materials in Relation to Fire Tests*, ASTM Special Technical Publication 385, ASTM, p. 60 (1964)
20. NS 3473, Norwegian Standard, *Design of the Concrete Structures*, Norwegian Standardization Association (1989)
21. Bremner, T. W., Holm, T. A., and Valsangkar, A. J., Structural Integrity of Fire Walls at High Temperature, *Proc. 5th North American Masonry Conf.*, III:237–264, University of Illinois (Jun. 1990)
22. *Design and Control of Concrete Mixtures*, 6th ed., p. 199, Portland Cement Association, Ottawa (1995)
23. Harmathy, T. Z., *Symp. on Fire Test of Materials,* ASTM STP 301, ASTM (1961)

10

Freeze-Thaw Resistance of Lightweight Aggregate Concrete

1.0 INTRODUCTION

In cold countries, the temperature varies during winter from several degrees below 0°C to a few degrees above 0°C, and water freezes to ice and ice melts to water. Consequently, concrete undergoes a thermal shock along with a volume change due to the freezing of water. This process is called the freeze-thaw cycle. Concrete deteriorates as a result of these temperature cycles. When deicing salts are used, the deterioration becomes more severe. This is known as *freeze-salt resistance*. The freeze-thaw cycle and the freeze-salt resistance of concrete can interact at the same place and, in actual practice, it is difficult to separate them. On roads and pavements, deicing salts are used. In the marine environment, air is laden with salts. In polluted areas, salts can be formed when pollutant gases interact with the alkalis in concrete. These factors interact, subsequently or simultaneously, and it is not easy to divorce them from each other.

Concrete contains a certain amount of water which changes to ice in the winter. It is logical to think that the transformation of water to ice results in a 9% by volume expansion and is one of the major causes of damage due to freezing and thawing. Actually, the mechanism of concrete deterioration is not that simple. Therefore, the mechanisms involved in freezing and thawing of concrete, in general, with and without deicing salt, must be considered before addressing the freezing and thawing of a particular LWAC.

In order to understand the mechanisms of freezing and thawing within the cement paste, an understanding of the constitution of the paste itself is essential. Portland cement is a mixture of several compounds, among which the most important ones are two calcium silicates— tri-calcium silicate ($3Ca{\cdot}SiO_2$) and di-calcium silicate ($2Ca{\cdot}SiO_2$). These silicates constitute about 75% of the portland cement by weight. In the hydration reaction, the two silicates produce similar calcium silicate hydrates and different amounts of calcium hydroxide. The silicate hydrate is similar to the natural mineral tobermorite and is called tobermorite gel. This gel is the most important constituent and plays a dominant role in the setting and hardening of the paste and governs the strength development and dimensional stability of hardened paste and concrete.

The term *gel* was given to the part of the hardened cement paste that determines surface area and porosity. The gel pores are believed to average approximately 15 to 20 Å in diameter. The concrete microstructure constituents of solid, water, and air are divided among the tiny pores of molecular dimension between particles of tobermorite gel. The larger pores between aggregations of gel pores are capillary cavities. The capillary cavities are estimated to average 500 nm in diameter. Then, there are bubbles of entrained air, which are larger and vary from a few microns to a few millimeters in diameter.

The freeze-thaw resistance of concrete is related to its air void system. Specifically, it means the pore size distribution, i.e., the size of the pores, their distribution, and the pore-spacing factor, which is defined as half of the average distance between two pores. This factor is an index of the maximum distance of any point in the cement paste from the periphery of a nearby air void. While the air content is the same, the pores' size and distribution can vary. In one experiment,[1] 5 to 6% air was incorporated into concrete by using one of the five different air-entraining agents, which produced 24,000; 49,000; 55,000; 170,000; and 800,000 air voids per cubic

centimeter of hardened cement paste. The corresponding concrete specimens required 29, 39, 82, 100, and 550 freeze-thaw cycles, respectively, to exhibit 0.1% expansion.

The air void system is related to the water-to-cement ratio. Concrete with a high water-to-cement ratio leads to shrinkage problems, lower strength, and the loss of air leading to an uneven pore structure. On the other hand, concrete with a low water-to-cement ratio, which is possible to achieve with the use of high-range water-reducing agents, does not always produce concrete with an adequate air void system. Theoretically though not easy to do, the addition of an air-entraining admixture and a dispersing agent and high-range water reducers, can provide a pore structure suitable for reasonable frost resistance.

Though there are serious problems with the freeze-thaw damage of concrete, there is no earmarked standard for the pore size distribution and the pore-spacing factor. On the contrary, there are controversies which are debatable. One concept is that if the concrete has a 15 cm cube compressive strength of 25 MPa and the spacing factor is 0.2 mm, it should be immune to freezing and thawing,[2] whereas according to Chatterji, even if the concrete possesses these properties, it is damaged in freezing and thawing.[3]

The other concept is that to have good freeze-thaw resistance, one should have 4–6 vol% air.[4] However, experience has shown that a concrete with 4% air and a spacing factor of 0.16 mm also deteriorates in freezing and thawing.[3] Chandra and Aavik[5] have also shown that concrete with 4% air damages during freezing and thawing. This implies that besides pore size and the pore-spacing factor, there must be something more which damages concrete during freezing and thawing. In this context, two factors seem to be relevant:

- The bond between the aggregates and matrix.
- The character of the pore.

As stated earlier, it is a general and logical belief that one of the major causes of damage to concrete during freezing is the volume expansion caused by the freezing of water. This does not seem to be the sole reason for the expansion causing deterioration. Beaudoin and McInnis[6] reported expansion even when benzene was used for the pre-saturation of concrete after drying. Thus, the concrete was not pre-saturated with water, and it was far below the degree of critical saturation. It must also be noted that water-free benzene contracts upon freezing instead of expanding. This

makes it more difficult to understand the mechanism of freeze-thaw, freeze-salt attack on concrete, especially when the theory of critical saturation[7] also fails. Thus, there must be some other factors involved in this deterioration mechanism. Some of the possible causes are hydraulic pressure, osmotic pressure, chemical interaction, thermal compatibility of the aggregates, etc.

2.0 HYDROSTATIC PRESSURE

The pore structure of portland cement paste is shown by a schematic diagram in Fig. 10.1,[8] wherein gel pores and capillary cavities are marked. The gel particles and gel pores are indicated as a heterogeneous mass. The larger empty spaces indicate capillary cavities and the curved boundary at the left represents a part of the wall of an air void.

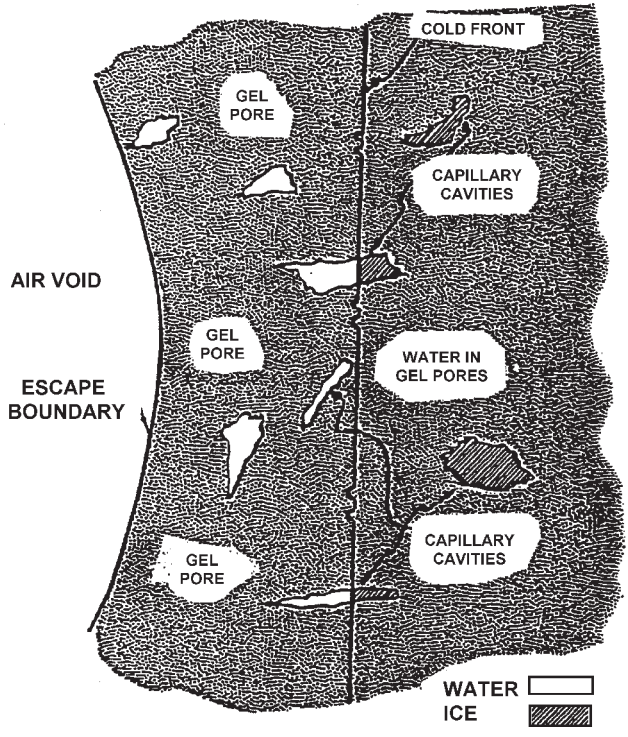

Figure 10.1. Schematic diagram of the pore structure of portland cement paste.[8]

When water begins to freeze in a capillary cavity, the increase in the volume due to ice formation forces the excess water out through the boundaries of the specimen. It works like a pump and generates pressure. It is called *hydraulic* or *hydrostatic pressure*. The magnitude of the pressure depends on the distance to an "escape boundary," the permeability of the intervening material, and the rate at which freezing occurs. When this pressure is high enough to stress the surrounding gel beyond its elastic limit or its tensile strength, it will cause permanent damage.

The hydrostatic pressure will be higher farther from the escape boundary; thus, to prevent the disruptive pressure development, the capillary cavities need to be close. Experience shows that these should not be farther than 80–100 μm from the nearest escape boundary.

2.1 Infiltration of a Concrete Structure by Ice

The freezing of water in a porous body is different from that of bulk water. Ice infiltration can only continue if the local size of the pore is lower than the equilibrium size of the ice crystal. Ice infiltration can occur by two processes:

- Ice infiltration due to the supercooling of water.
- Ice infiltration under pressure.

Under atmospheric pressure, only a macroscopic ice crystal is in thermodynamic equilibrium with a saturated porous body at 273°K. However, a microscopic ice crystal requires supercooled water to penetrate a porous body. The size of a microscopic ice crystal is related to the temperature of supercooled water.[9] At any given degree of supercooling, ice will infiltrate only interconnected pores that are equal to or larger than the critical diameter of a capillary. The relationship between supercooled temperatures and the diameter of a capillary is shown in Fig. 10.2.[10]

At any given pressure, ice crystals will infiltrate interconnected pores that are equal to or larger than the critical diameter. Pore size needed for ice penetration at different restraining pressures is shown in Fig. 10.3. A high ice-concrete bond between the concrete and the external ice and snow may act as the initial restraining pressure. The high tensile strength of ice infiltrated concrete, due to either of the above two reasons, will ensure continuing restraining pressure.

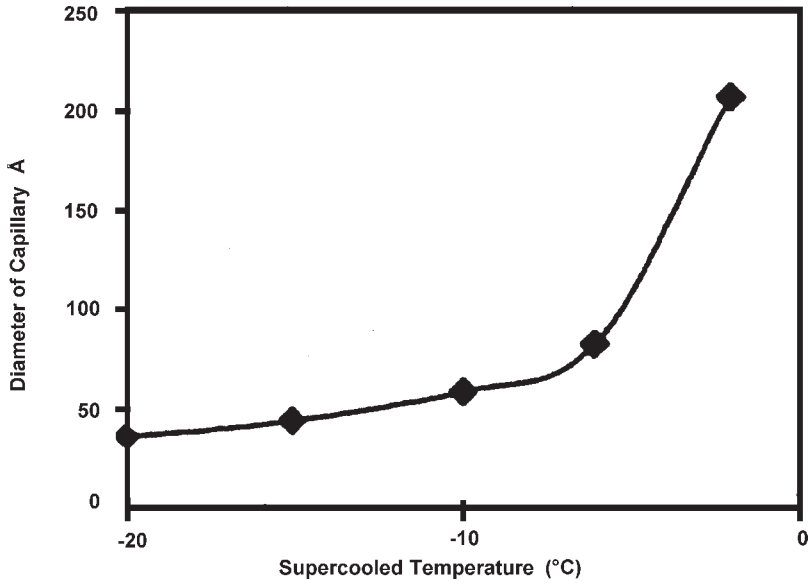

Figure 10.2. Capillary size needed for ice penetration.[10]

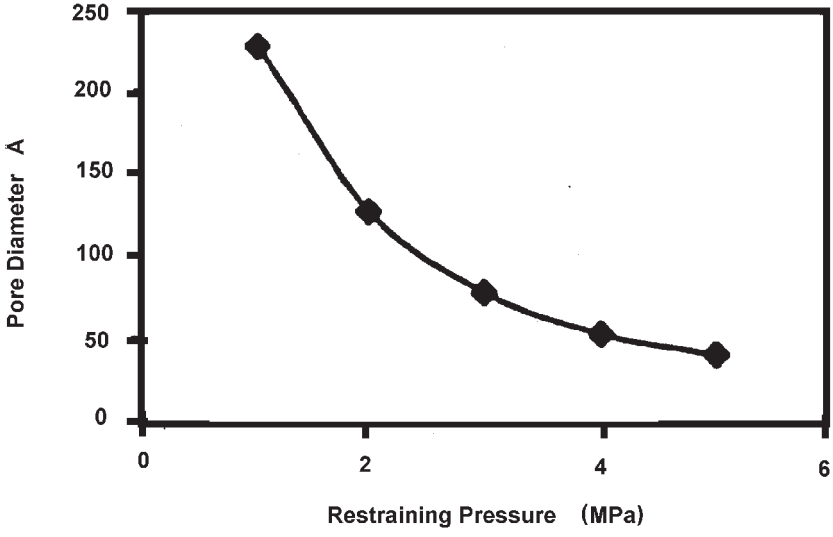

Figure 10.3. Pore size needed for ice penetration at different restraining pressures.[10]

2.2 Magnitude of Required Pressure for Frost Damage

To cause damage to a freezing concrete by an internally generated pressure, the pressure's magnitude needs to be about two times the tensile strength of the frozen part of concrete.[11] The tensile strength of a reasonable quality, saturated concrete is about 2.5 MPa at room temperature. This means the tensile strength of the same concrete will be about 4 MPa at -10°C and 6 MPa at -20°C. However, the exact temperature in the freezing cycle at which damage occurs is rarely known. The damage-producing pressure can, therefore, be between 8 and 12 MPa or approximately 10 MPa. The mechanism of concrete deterioration is to be examined with this in mind.[10]

Powers' Hydraulic Pressure Mechanism. In Powers' theory, the strength of frozen concrete was never considered. It is difficult to visualize a realistic situation where the required pressure of 10 MPa would be generated by this mechanism. Furthermore, Powers' suggested equation for calculating the hydraulic pressure predicts a pressure of only about 91.7% saturation.[13] Concrete samples show damages below this degree of saturation.

Litvan's Mechanism. Litvan[13] also did not consider the strength of frozen concrete. He did not propose any method for calculating the pressure generated from his proposed mechanism.

Chatterji's Mechanism. Chatterji[10] proposed two mechanisms which are capable of producing disruptive pressure, causing damage to concrete:

- *The mechanism of micro-lens formation.* Movement of water through concrete is very restricted, and, as such, it behaves like a closed system during freezing. It resembles micro-lens formation. In a closed system, the pressure generation due to the formation of ice may be calculated using the Clapeyron equation. The calculated pressure is 1.25 MPa/°C.[14] According to this concept, about 8°C supercooling is required to cause any damage. It is a more realistic temperature, one which occurs during the freezing and the thawing of concrete.
- *Freezing of entrapped water.* It is of interest to note that a pressure of about 7.6 MPa has been measured in freezing water drops of 7–8 mm size with very little supercooling, and higher pressure development is expected in a

larger volume of water.[15] A similar pressure generation may occur in entrapped water in freezing concrete.[16] This mechanism is in accordance with Litvan's theory.

3.0 OSMOTIC PRESSURE

In winter, when deicing salts are used, salt gets dissolved and penetrates inside the concrete. This creates a salt concentration gradient in the capillaries. This concentration increases as the water begins to freeze, so the water being forced from the capillaries has a higher concentration of salt than the surrounding gel pore water. A pressure differential develops in the direction toward the capillary pore and opposite to the flow of water. This creates *osmotic pressure*. The pressure required to overcome osmotic pressure in the capillary is a combination of the hydraulic pressure required to force capillary water into the gel pore structure and the osmotic pressure which resists this flow. The use of salt may also increase the concentration in the pore structure of surface concrete to a point where the salt solution would act as antifreeze and increase the availability of moisture for saturation of the concrete.

3.1 Sodium Chloride Solutions

Experience has shown that 2–4% sodium chloride solution has the most disruptive effect.[17] This is mainly due to its higher partial vapor pressure than sodium chlorides of higher concentrations. It causes the greatest deterioration of concrete due to the optimum combination of freezable water and the osmotic pressure it develops. If the concentration increases above 4%, there is a decrease in deterioration. The higher concentration of salt lowers the freezing temperature of the salt solution, which would give the water in the capillary cavities an antifreeze effect and reduce the amount of freezable water.

4.0 SCALING MECHANISM

4.1 Salt Scaling Mechanism

The salt scaling mechanism is best illustrated by a natural phenomenon shown in Fig. 10.4. When fresh concrete remains in a plastic state, the density of the particles of aggregate and portland cement will cause them to settle and the water will tend to rise to the surface. This phenomenon, known as *bleeding*, creates a film of water on the freshly placed concrete. As long as this water film is on the surface, the only natural compacting force is the force of gravity. Rapid drying of the surface moisture may lower the water level so that particles of cement and aggregate are exposed as indicated in Fig. 10.4.[18] At this point, capillary forces resist further lowering of the water surface. The magnitude of the capillary forces depends on the diameter of the capillary. These forces are significant, however, and may result in a compacting force computed to be from 500 to 1400 psf.[19][20] Moreover if this mechanism develops before the concrete has set, bleed water will continue to rise, but will be trapped beneath the compacted surface layer on concrete pavements with a less dense surface layer immediately underneath. The only condition needed to separate the compacted surface from the pavement in freezing weather is sufficient moisture to permit the growth of capillary ice in the porous layer.

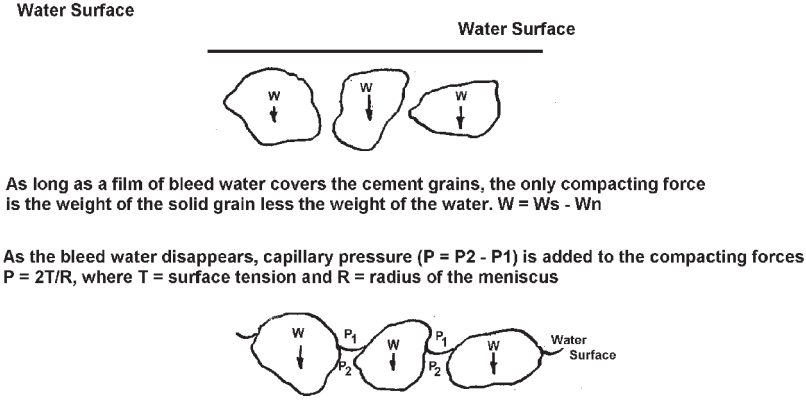

Figure 10.4. Compacting forces caused by the rapid drying of fresh concrete.[18]

This mechanism of *accretion* will provide for continued growth of the ice crystals as long as moisture is available. Deicing salts not only create additional forces through osmosis, but also provide an additional source of surface moisture in freezing weather by melting the ice and snow. As deicing salts melt snow and ice, the temperature immediately below the surface is significantly reduced because of the comparatively large heat of fusion of ice. This may cause a damaging temperature drop in the saturated zone immediately beneath the surface.[21] Thus, the deicing salts may cause concrete to scale by any combination of the following:

- By providing moisture from the melting of ice and snow in freezing weather.
- By causing additional freezing through lowering the temperature in the subsurface zone (ice cream freezer principle).
- By creating a system which develops osmotic pressures.
- By building salt crystals in subsurface voids.

Young concrete is more susceptible to scaling than mature concrete. This is attributed to the following:

- Partially-hydrated portland cement contains more capillary voids.
- Partially-hydrated paste has a greater degree of saturation since portland cement draws water from adjacent capillaries as it hydrates.
- In addition to dimensional changes due to drying shrinkage and thermal contraction, additional shrinkage results from the diffusion of unused water in the gel structure to the capillaries. This is undoubtedly another cause of crazing of new concrete in cold weather.
- Young concrete has less strength and, therefore, has less resistance to the disruptive forces of freezing.

Chemical Interaction. Sodium chloride can interact with the cement hydration products, making very soluble salts which leach out, reducing the strength of concrete. This creates a more porous structure and makes it easy for the penetration of salt. Further, it can interact with calcium to form very expansive double salts; Friedel's salt for example, which creates cracks and thus causes damage to the concrete.

$$Ca(OH)_2 + 2NaCl \rightarrow CaCl_2 \text{ (leaches out)} + 2NaOH$$

$$C_3A + CaCl_2 \rightarrow C_3A{\cdot}CaCl_2{\cdot}10H_2O \text{ (Friedel's salt)}$$

Capillary Effect. Analogous to the formation of ice lenses in soils, a capillary effect[22] involving the large scale migration of water from small pores to large cavities, is believed to be the primary cause of expansion in porous bodies. According to the theory advanced by Litvan,[23] the rigidly held water by the C-S-H (both in interlayer and adsorbed in gel pores) in cement paste cannot rearrange itself to form ice at the normal freezing point of water because the mobility of water existing in an ordered state is rather limited. Generally, the more rigidly water is held, the lower the freezing point. Three types of water are physically held in cement paste. In order of increasing rigidity, these are: the capillary waters in small capillaries (10–50 μm), the adsorbed water in gel pores, and the interlayer water in the C-S-H structure.

It is estimated that the gel pores do not freeze above -78°C. Therefore, when a saturated cement paste is subjected to freezing conditions, while the water in large cavities turns into ice, the gel pore water continues to exist as liquid water in a supercooled state. This creates a thermodynamic disequilibrium between the frozen water in capillaries, which acquires a low energy state, and the supercooled water in gel pores, which is in a high-energy state. The difference in entropy of ice and supercooled water forces the latter to migrate to the lower energy sites (large cavities), where it can freeze. This fresh supply of water from the gel pores to the capillary pores increases the volume of ice in the capillary pores steadily until there is no room to accommodate more ice. Any subsequent tendency for the supercooled water to flow toward the ice-bearing regions would obviously cause internal pressures and expansion to the system. Further, according to Litvan,[13][23] the moisture transport associated with the cooling of saturated porous bodies may not necessarily lead to mechanical damage. Mechanical damage occurs when the rate of moisture transport is considerably less than demanded by the conditions (large temperature gradient, low permeability, and high degree of saturation).

It may be noted that during frost action on cement paste, other regions undergo contraction (e.g., loss of adsorbed water from C-S-H balance the tendency for certain regions to expand). The net effect on a specimen is, obviously, the result of two opposite tendencies. This explains why the cement paste containing no entrained air showed a large elongation (Fig. 10.5), while the cement paste containing 10% entrained air showed contraction during freezing (Fig. 10.6).

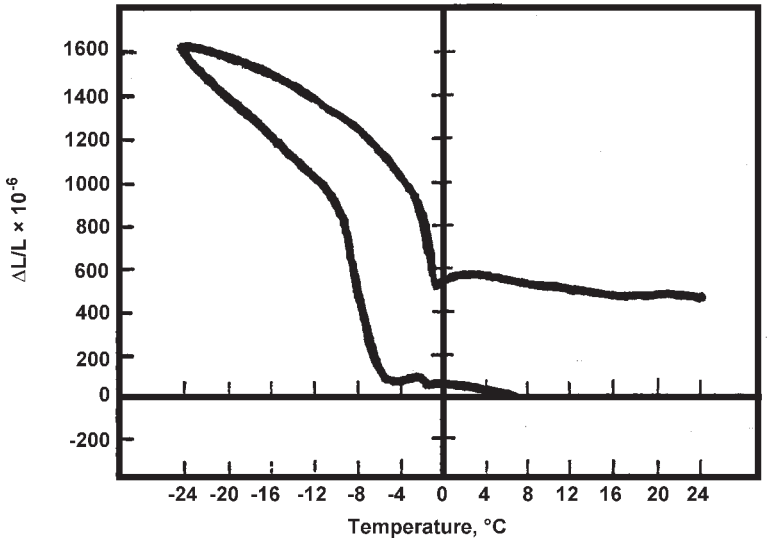

Figure 10.5. Cement paste with no entrained air, showing long elongation.[4]

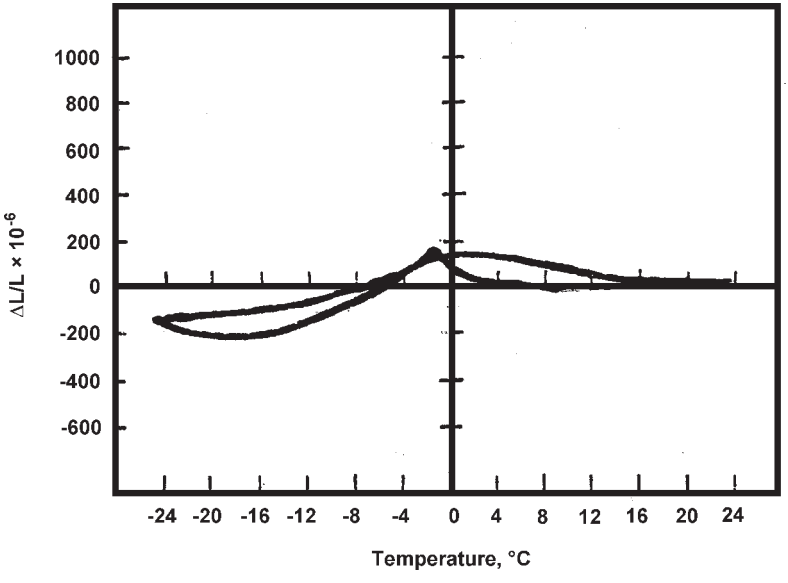

Figure 10.6. Cement paste containing 10% air, showing contraction.[4]

4.2 Influence of Rate of Cooling

Pigeon investigated the influence of the rate of cooling for normal concrete exposed to freeze-thaw cycles. He showed that the critical spacing factor decreased very significantly as the freezing rate increased from 2 to 6°C/h (Fig. 10.7).[24] This indicates that most of the difference between the value of 680 μm at 2°C/h and that of 250 μm at 11°C/h can be explained by the effect of the freezing rate. It is possible that freezing in water, rather than in air at 100% relative humidity, also has some effect on the value of $\bar{L}$, critical spacing factor. The main difference between the two types of tests is probably not the intensity of internal cracking caused, but the surface scaling. When concrete freezes in water, scaling is often very important, but does not always occur when the freezing takes place in air.

The influence of the freezing rate was analyzed by Powers[25] in his hydraulic pressure theory. It is very interesting to note that although this theory is not considered valid by most of the researchers, it can still explain the results shown in Fig. 10.7. Considering the 250 μm value to be correct for a rate of 11°C/h, a value of 600 μm was obtained by Powers equation for 2°C/h. A value of 450 μm for 6°C/h is obtained if the calculations are based on the value of 680 μm for 2°C/h.

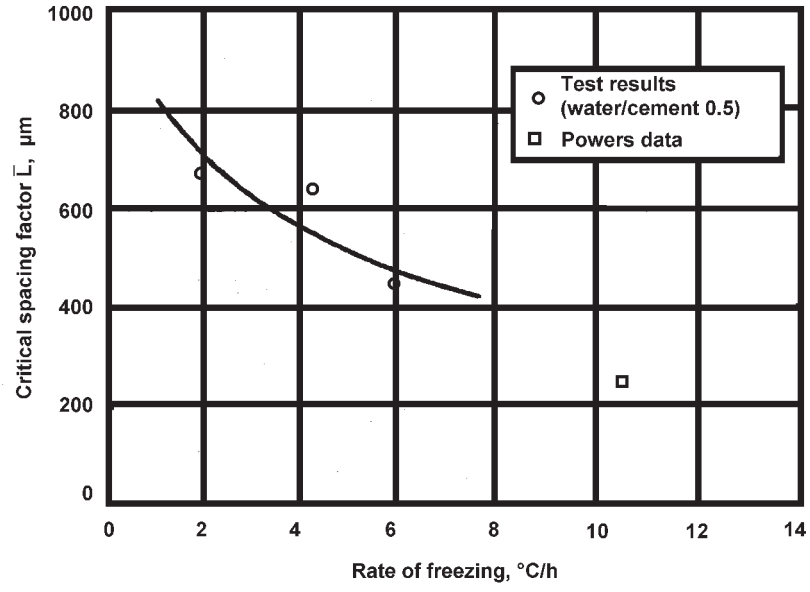

Figure 10.7. Critical air void spacing factor versus rate of freezing for concretes with a water-to-cement ratio of 0.5.[24]

4.3 Influence of Water-to-Cement Ratio

The influence of the W/C ratio on freeze-thaw durability was studied on concretes made with different W/C ratios,[26] which were cured in two ways:

- Moist cure until the start of the test,
- Continuously exposed to air with 80% RH from the day they were cast.

Further, the concrete age was varied from 7 days to 91 days. The scaling increased with an increase in W/C even though the air content and the concrete consistency was almost the same. This is explained as follows:

- An increase in W/C increases permeability, that is, the air pores easily become water filled.
- An increase in W/C produces a coarsened pore structure (Fig. 10.8a). Similar observations were made with the addition of the air-entraining agent vinsol resin (Fig. 10.8b).

It can be concluded that a reduction of W/C is a very positive measure since the probability of obtaining an air pore structure that secures a good salt scaling resistance becomes higher with a low W/C. Thereby, the specific surface of air pores is increased and the spacing factor is decreased.

A comparative study of different Swedish portland cements has shown that the low alkali/low C_3A cement (A-cem: C_3A = 2%, and Na_2O = 0.5%) gives the lowest scaling and the smallest spread between individual specimens. It also seems to give concretes that are less affected by different types of admixtures and admixture combinations.[26] It has been found in other investigations that the spacing factor becomes lower with a lower free alkali content in the pore water.[27]

4.4 Densification with Condensed Silica Fume

High strength concretes, both lightweight aggregate and normal weight, are generally made with the addition of condensed silica fume. The mechanism of freeze-thaw damage in the presence of a deicing salt is different than without condensed silica fume.

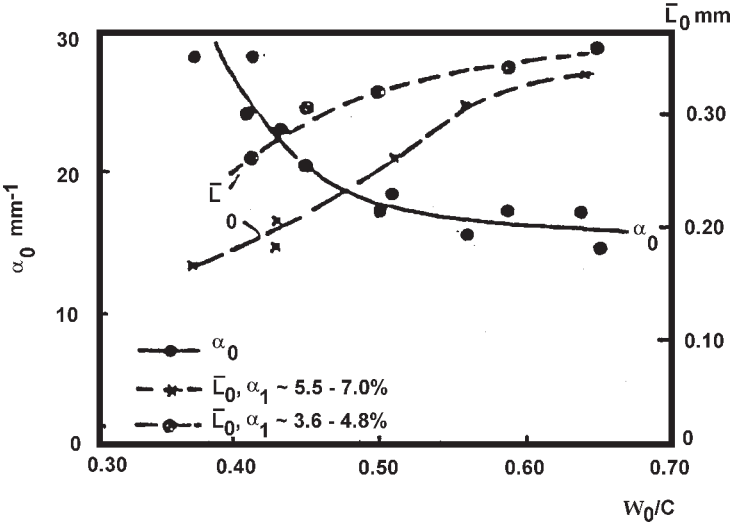

(a)

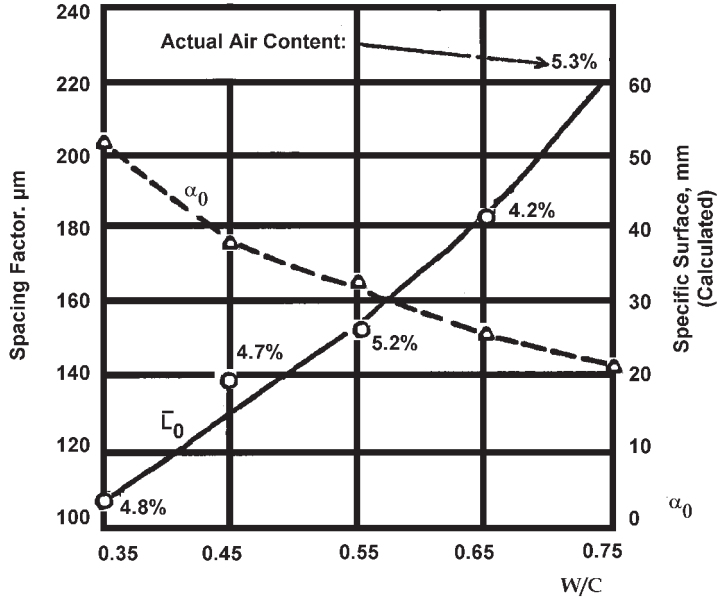

(b)

Figure 10.8. Relationship between the structure of the air pore system and the water-to-cement ratio, *(a)* tensoid, *(b)* neutralized vinsol resin.[26]

The salt frost attack seems to consist of two phases. During the first phase, the combination of salt plus water gives rise to surface scaling. The scaling starts during the first cycle. The second phase, with accelerated deterioration, probably takes place when the critical degree of saturation is reached in the complete material volume, after a number of cycles and a certain time of water absorption.

Concrete, for example, without silica fume seems to be more sensitive to the first phase, while concrete with silica fume is much more sensitive to the second phase. The second phase is, in some respects, more "dangerous" than the first phase due to the rapid development of damage with internal cracking of high strength concrete during a freezing and thawing test.

When silica fume is used in concrete, the water demand is increased. To maintain the W/C, superplasticizers are used. This influences the air void system, which is maintained by using air-entraining agents.

The freeze-salt resistance is lower with the simultaneous use of AEA (air-entraining agent) and plasticizer than with using AEA only. Air-entraining agents do not work the same way with the superplasticizers as they work alone. This is because of the variations in the surface charges of the two chemical admixtures. The variations produce a more uneven and a coarser pore structure and often cause more damage to the concrete (Fig. 10.9).

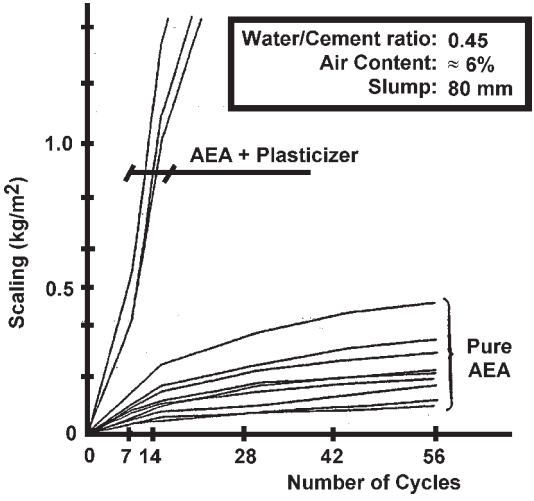

Figure 10.9. Scaling resistance curves for air-entrained concretes. The air-entraining agents (AEA) used are pure AEA and AEA-containing plasticizers, respectively.[28]

An ordinary scaling test of up to 56 cycles showed that a concrete with a W/C of 0.35, with and without the addition of condensed silica fume, behaves quite differently[28] (Fig. 10.10). Material *A* shows scaling, whereas Material *C* shows excellent resistance. There is a dramatic change in the situation at about 110 cycles when the sample breaks into two pieces. This is attributed to the internal damage of the concrete which was not visible from the outside (microcrack development). A decrease in the W/C ratio produces concrete of high strength, therefore, the brittleness of the concrete is increased.

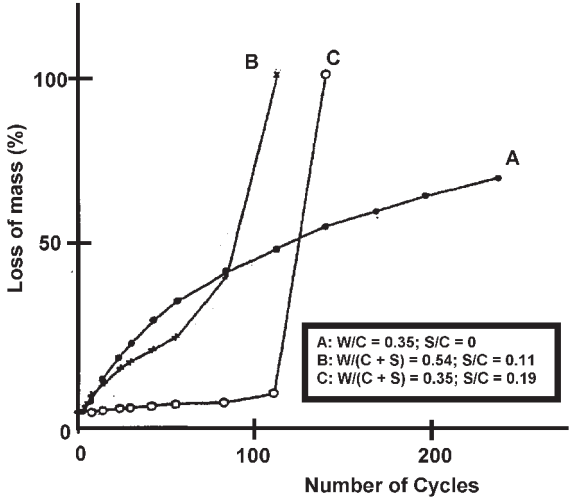

Figure 10.10. Scaling resistance curves (loss of mass) for concretes without *(A)* and with *(B)* and *(C)* silica fume as functions of freeze-thaw cycles (W = water, C = cement, S = silica fume).[28]

5.0 FREEZE-THAW RESISTANCE OF LIGHTWEIGHT AGGREGATE CONCRETE

Klieger and Hanson[29] did a comprehensive study of freezing and thawing tests of LWAC. Nine lightweight aggregates and one normal weight aggregate (No. 8) were used. Out of the lightweight aggregates, five were expanded shale (aggregates number 2, 3, 10, 11, and 12), an expanded

slate (aggregate 5), an expanded clay (aggregate 4), a shale expanded by the sintering process (aggregate 7), an expanded blast-furnace slag (aggregate 6), and the normal weight sand and gravel (aggregate 8). Vinsol resin was used as the air-entraining agent.

All the aggregates except expanded shale (10, 11, and 12) were air dried and screened into the various size fractions. The fine aggregate fractions for aggregates 2, 3, 4, 5, 6, and 7 were recombined to provide a grading recommended in ASTM.

The normal weight sand and gravel grading were according to the requirement of ASTM 33. The absorption, unit weights, and specific gravity of these aggregates are shown in Table 10.1. Concrete prism samples of 3 × 3 × 11¼ inches were cast equipped with stainless steel gauge studs for length change measurement. Slabs for surface scaling tests were 3 × 6 × 15 inches.

Concretes were prepared at two levels of compressive strength, 3000 psi and 4500 psi. Both non–air-entrained and air-entrained concrete were prepared. The average strength of non-air concrete was 2910 psi and that of the air-entrained concrete was 2600 psi. For 4500 psi concrete, the average strength of the non–air-entrained concrete was 5700 psi, and that of the air-entrained concretes was 4750 psi. The concrete compositions, compressive strengths, and durability factors at 300 cycles are shown in Tables 10.2 to 10.5.

Prisms and slabs were cured 14 days in the moist room at 73°F (22°C) and 100% RH, followed by 14 days in the air of the laboratory at 73°F and 50% RH. The prisms were then immersed in water for 3 days prior to the start of the freezing and thawing test. The surfaces of the slabs were covered with water, one-quarter inch (6 mm) in depth, for 3 days prior to the start of surface scaling tests.

The prisms were frozen and thawed in tap water at all times. Two cycles of freezing and thawing were obtained every 24 hours, 7 days per week. The minimum specimen temperature attained was approximately -10°F (-23°C) and the maximum was approximately 55°F (13°C).

In the surface scaling tests, which were conducted on concrete slabs made with three lightweight aggregates, the slabs with a quarter inch layer of water on the surface (equal to 250 ml) were placed in a cold room maintained at 0°F (-18°C) overnight. The slabs were removed the following morning and stored for 6 hours in a room maintained at approximately 70°F (21°C). Flake calcium chloride (7% $CaCl_2$) was applied directly to the ice on the surface at the rate of 2.4 lb/yd^2 (1.2 kg/m^2) of surface area. At the end of the thaw period, the solution of calcium chloride and water was poured

Table 10.1. Absorption, Specific Gravity, and Unit Weight of Aggregates[29]

Aggr. No.	Size	Absorption by Weight			Specific Gravity		Apparent	Unit Wt., lb/cu ft	
		1 hr	4 hrs	24 hrs	Bulk			Dry Loose	Dry Rodded
					Oven Dry	S. S. D			
2	Fine	2.2	4.1	6.8	1.75	1.86	1.98	52	56.2
	Coarse	11.3	12.6	14.9	1.17	1.34	1.41	42.1	45
3	Fine	2.1	3.6	4.8	1.91	2	2.1	72	77.2
	Coarse	6.6	8	9.7	1.21	1.33	1.37	43.7	45.4
4	Fine	9.6	11.1	13.5	1.76	2	2.34	57.8	63.7
	Coarse	11.3	12.7	15.6	1.5	1.73	1.96	49.6	54.2
5	Fine	3.4	4.4	6.6	1.97	2.1	2.26	62.7	68.6
	Coarse	8.1	9.2	11	1.3	1.44	1.54	43.9	47.3
6	Fine	2.3	2.9	4	2.1	2.19	2.3	64.2	70.2
	Coarse	6.2	6.6	7.1	1.46	1.56	1.62	44.2	47.3
7	Fine	5.6	6.3	7	1.91	2.05	2.21	64	68
	Coarse	6.5	7	7.3	1.59	1.72	1.52	45	48
1 kg/m^3 = 15.8 lb/cu ft									

(Cont'd.)

Table 10.1. *(Cont'd.)*

Aggr. No.	Size	Absorption by Weight			Specific Gravity		Apparent	Unit Wt., lb/cu ft	
		1 hr	4 hrs	24 hrs	Bulk			Dry Loose	Dry Rodded
					Oven Dry	S. S. D			
8	Fine	—	—	2.2	—	2.65	—	108.2	112.7
	Coarse	—	—	2.1	—	2.65	—	100	108.2
10	Fine	5.1	7.1	9.5	1.72	1.88	2.06	62.5	65.3
	Medium	7.4	9.6	11.8	1.37	1.53	1.63	50.2	53.6
	Coarse	7.7	9.4	12.3	1.28	1.43	1.51	43.8	47
11	Fine	7.9	10	11.7	1.61	1.8	1.98	56.2	65.2
	Coarse	11.8	12.7	15.6	1.44	1.66	1.85	47.1	51.8
12	Fine	8.8	10.1	11.8	1.57	1.76	1.93	53.4	62.8
	Coarse	5.4	6.7	7.7	1.32	1.42	1.47	44.1	49.6
1 kg/m^3 = 15.8 lb/cu ft									

Table 10.2. Composition and Properties, Non–Air-entrained Concrete, 3000 psi[29]

Aggregate		Quantity per Cubic Yard						Slump in.	% Air Content	Unit Wt. lb/cu ft	DF 300 cycles	Relative DF	Comp. Str. psi
No.	State	Cement		Water	Aggregate*		AEA						
		sack	lb		Fine	Coarse							
2	D	6.39	601	493	818	673	0	2.3	4.5	95.8	85	142	3200
	W	6.4	602	591	820	675		2.3	2.7	99.5	45	161	2980
3	D	5.28	496	361	996	782	0	2.5	4.0	97.7	92	154	3330
	W	5.3	498	433	1000	784	0	2.8	3.8	101.0	59	210	2710
4	D	4.54	425	536	1077	759	0	2.9	2.8	104.2	81	134	2840
	W	4.55	427	665	1082	763		2.4	2.0	100.2	42	150	2830
5	D	6.36	598	461	1183	654	0	2.5	3.5	107.1	89	148	3230
	W	6.21	584	540	1159	639		2.1	3.8	108.2	29	104	3030
6	D	6.99	657	462	1283	704	0	2.7	3.0	115.0	15	25	2860
	W	6.92	651	505	1268	696		2.4	2.3	115.3	5	18	2500
7	D	6.51	612	514	1232	716	0	2.7	2.0	113.8	5	8	2650
	W	6.51	612	545	1233	716		2.3	1.5	115.6	2	7	2730

* = Air-dried weight: kg = 2.204 lb: inch = 2.54 cm: meter = 3.28 ft: yard = 3 feet: kg/cm^2 = 1/14.22 psi: kg/m^3 = 15.8 lb/cu ft: D = Air dried: W = water saturated for 24 hrs.

(Cont'd.)

Table 10.2. *(Cont'd.)*

Aggregate		Quantity per Cubic Yard						Slump inch	% Air Content	Unit Wt. lb/cu ft	DF 300 cycles	Relative DF	Comp. Str. psi
No.	State	Cement		Water	Aggregate*		AEA						
		sack	lb		Fine	Coarse							
10	D	4.53	426	390	921	707	0	2.8	4.0	90.6	82	136	2460
	W	4.42	416	504	920	702		2.0	3.6	94.1	7	25	1760
11	D	5.51	518	527	1105	639	0	2.0	2.8	103.2	48	80	3350
	W	5.53	520	619	1113	644		2.3	2.0	107.4	24	86	3930
12	D	4.97	467	417	1108	601	0	2.0	3.5	96.1	43	72	3300
	W	5.06	476	514	1129	612		2.5	1.5	101.1	7	25	2630
8	D	3.97	373	339	1628	1763	0	2.2	1.5	152.0	60	100	2740
	W	3.97	373	339	1626	1761		2.0	1.7	151.8	28	100	2910

* = Air-dried weight: kg = 2.204 lb: inch = 2.54 cm: meter = 3.28 ft: yard = 3 feet: kg/cm^2 = 1/14.22 psi: kg/m^3 = 15.8 lb/cu ft: D = Air dried: W = water saturated for 24 hrs.

Table 10.3. Composition and Properties for Air-entrained Concrete, 3000 psi[29]

Aggregate		Quantity per Cubic Yard						Slump inch	% Air	Unit Wt. lb/cu ft	DF at 300 cycles	Relative D.F	28d Comp. Str. psi
No	State	Cement		Water	Aggregate*		AEA						
		sack	lb		Fine	Coarse							
2	D	6.16	579	445	766	630	2660	3.3	5.5	89.6	88	98	2030
	W	6.46	607	549	783	645	1810	2.4	6.5	95.6	90	94	2740
3	D	5.35	503	343	950	755	1588	2.3	7.0	94.2	94	104	3190
	W	5.31	499	392	944	740	2085	2.8	8.0	95.5	89	93	2690
4	D	4.62	434	498	1042	734	1380	2.3	7.0	100.1	73	81	3020
	W	4.64	436	630	1047	738	1255	2.6	5.7	105.4	90	94	2600
5	D	6.23	586	421	1108	611	1510	2.6	7.7	101.1	94	104	2800
	W	6.21	584	510	1137	610	1635	2.7	7.7	103.4	91	95	2510
6	D	6.95	654	418	1213	666	2435	2.9	6.6	109.6	95	106	2550
	W	7.20	677	446	1250	686	2206	2.2	6.0	113.2	95	99	2780
7	D	6.39	601	450	1150	668	4000	4.4	7.0	106.2	61	68	1770
	W	6.64	624	480	1198	693	3115	2.1	5.0	110.9	41	43	2660

* = Air-dried weight; D = Air dried; W = water saturated for 24 hrs; + = Extrapolated values

(Cont'd.)

Table 10.3. *(Cont'd.)*

Aggregate		Quantity per Cubic Yard						Slump inch	% Air	Unit Wt. lb/cu ft	DF at 300 cycles	Relative D.F	28d Comp. Str. Psi
No.	State	Cement		Water	Aggregate*		AEA						
		sack	lb		Fine	Coarse							
10	D	4.49	422	351	888	679	990	2.6	8.0	86.8	90	100	2500
	W	4.52	425	469	890	679	865	2.8	6.6	91.1	45+	47	1990
11	D	5.45	512	459	1082	625	1245	2.2	6.7	99.3	41	46	2660
	W	5.35	522	567	1093	632	1135	2.0	4.8	104.3	60+	63	3320
12	D	4.97	467	395	1073	582	810	2.4	6.6	93.3	89	99	2440
	W	5.11	480	481	1102	597	710	2.5	4.4	98.5	36	38	2500
8	D	3.91	368	310	1570	1701	1250	2.8	4.5	146.3	90	100	2810
	W	3.91	368	310	1570	1700	1455	2.4	5.7	146.2	96	100	2590

* = Air-dried weight; D = Air dried; W = water saturated for 24 hrs; + = Extrapolated values

Table 10.4. Composition and Properties, Non–air-entrained Concrete, 4500 psi[29]

Aggregate		Quantity per Cubic Yard						Slump inch	% Air	Unit Wt. lb/cu ft	DF at 300 Cycles	Relative DF	28d Comp. Str. psi
No.	State	Cement		Water	Aggregate*		AEA						
		sack	lb		Fine	Coarse							
2	D	8.19	770	468	696	701	0	2.0	3.0	95.8	86	232	4890
	W	8.12	763	554	692	697		2.7	2.5	99.5	23	96	4720
3	D	7.54	709	371	861	825	0	2.2	2.6	102.4	90	243	5200
	W	7.24	681	420	818	783	0	2.7	2.2	100.1	20	83	4920
4	D	6.22	585	499	938	814	0	2.1	3.1	105.0	83	224	5680
	W	6.02	566	648	945	820		2.9	1.5	110.3	50	209	4920
5	D	7.74	728	439	1022	691	0	2.6	2.8	106.7	74	200	5320
	W	7.94	746	535	1019	689		2.5	2.1	110.7	16	67	4920
6	D	8.65	813	438	1100	736	0	3.0	2.6	114.4	28	76	4740
	W	8.79	826	465	1103	739		2.8	2.7	116.0	12	50	5040

* = Air-dried weight: D = Air dried: W = Water saturated for 24 hrs: ** = Repeat test of aggregate 10, using a lower cement content

(Cont'd.)

Table 10.4. *(Cont'd.)*

Aggregate		Quantity per Cubic Yard						Slump inch	% Air	Unit Wt. lb/cu ft	DF at 300 Cycles	Relative DF	28d Comp. Str. psi
No.	State	Cement		Water	Aggregate*		AEA						
		sack	lb		Fine	Coarse							
7	D	8.28	778	486	1075	766	0	2.6	1.5	115.0	7	16	4680
	W	8.19	770	512	1066	760		2.6	1.6	115.1	7	29	4550
10	D	6.79	638	379	661	949	0	2.8	1.7	97.3	41	111	6510
	W	7.00	658	494	668	959		2.9	1.5	102.9	8	33	6290
10**	D	5.85	551	381	681	975	0	2.0	2.3	95.9	52	140	6100
	W	5.79	543	508	680	975		2.3	1.6	100.2	8	33	4940
11	W	7.15	672	615	1000	628	0	2.6	2.1	107.9	21	88	4850
12	W	5.99	563	510	999	620		2.6	2.8	99.7	8	33	4750
8	D	4.90	461	239	1330	2081	0	3.0	1.0	152.2	37	100	5280
	W	4.95	465	247	1339	2095		2.4	0.7	153.6	24	100	5660

* = Air-dried weight: D = Air dried: W = Water saturated for 24 hrs: ** = Repeat test of aggregate 10, using a lower cement content

Table 10.5. Composition and Properties for Air-entrained Concrete, 4500 psi[29]

Aggregate		Quantity per Cubic Yard						Slump inch	% Air	Unit Wt. lb/cu ft	DF at 300 Cycles	Relative DF	28d Comp. Str. psi
No.	State	Cement		Water	Aggregate*		AEA						
		Sack	lb		Fine	Coarse							
2	D	8.05	757	438	644	648	2614	2.7	7.5	92.1	91	111	4550
	W	7.97	749	525	651	656	3607	2.4	6.5	95.6	93	100	4459
3	D	7.27	683	348	791	758	3706	2.4	5.7	100.9	93	114	4600
	W	7.12	669	398	770	738	3607	2.8	6.0	105.2	94	101	3940
4	D	5.87	552	475	908	789	1536	2.5	6.5	102.8	71	87	4990
	W	5.85	550	618	895	777	1513	3.1	5.4	108.1	82	88	4260
5	D	7.78	731	412	974	659	1862	2.8	6.1	110.6	97	118	4680
	W	8.07	759	507	986	667	1885	2.7	5.5	113.4	95	102	4780
6	D	8.77	824	403	1055	706	1644	2.5	6.5	110.0	98	120	4710
	W	8.68	816	427	1089	729	1648	2.1	5.7	111.2	99	106	4760

* = Air-dried weight: D = Air dried: W = Water saturated for 24 hrs: ** = Repeat test of aggregate 10, using a lower cement content

(Cont'd.)

Table 10.5. *(Cont'd.)*

Aggregate		Quantity per Cubic Yard						Slump inch	% Air	Unit Wt. lb/cu ft	DF at 300 Cycles	Relative DF	28d Comp. Str. psi
No.	State	Cement		Water	Aggregate*		AEA						
		Sack	lb		Fine	Coarse							
7	D	8.08	760	439	1032	736	2033	2.0	5.2	95.2	80	98	4540
	W	8.13	764	475	1029	734	2147	2.3	4.9	99.3	64	69	4460
10	D	7.00	658	355	639	918	1420	2.3	5.2	99.2	93	114	6280
	W	7.13	670	464	635	912	1411	2.7	4.6	98.0	92	99	6030
11	D	3.81	546	352	657	942	951	2.2	5.3	102.1	91	111	5380
	W	5.79	544	467	650	932	1058	2.9	5.4	95.5	91	98	4540
12	D	7.01	659	564	941	592	1676	2.7	7.1	145.8	48	52	4500
	W	5.97	561	467	957	594	1047	2.4	6.5	146.6	77	83	4040
8	D	4.83	454	202	1279	2001	1560	2.6	5.0	152.0	82	100	4600
	W	4.85	456	220	1280	2003	1561	2.5	4.6	151.8	93	100	4750

* = Air-dried weight: D = Air dried: W = Water saturated for 24 hrs: ** = Repeat test of aggregate 10, using a lower cement content

off the surface, the surface was rinsed with fresh water, and the quarter- inch (0.65 cm) layer of water added preparatory to repeating the daily cycle. Surface scaling was evaluated by visual examination and numerical ratings periodically. The numerical ratings and their descriptions are as follows:

Rating	Surface Condition
0	No scaling
1	Very slight scaling
2	Slight to moderate scaling
3	Moderate scaling
4	Moderate to bad scaling
5	Severe scaling

The individual durability factors were calculated using the number of cycles at which the relative dynamic modulus reaches 60% of the original at that time. The durability factor is as reliable an indicator of the distress due to freezing and thawing, as is expansion during the test. On the other hand, the relationships between expansion and weight change indicate weight change to be a relatively poor indicator of damage. For example many of the concretes showing marked reduction in dynamic modulus showed gains in weight rather than losses.

The durability factor is calculated by the following formula:

Eq. (1) $$\text{Durability factor} = \frac{\%\ \text{Original E}}{300} \times \text{No. of cycles}$$

where %Original E is the original modulus of elasticity at the end of the test.

5.1 Influence of Air Entrainment

In the case of air-dried aggregates (Table 10.3), aggregates 2 and 3 (expanded shale), 4 (expanded clay), possibly 5 (expanded slate), and 11 (expanded shale) show only minor changes in the durability factor with entrained air. The remainder of the aggregates, including the normal weight

sand and gravel, show substantial increases in the durability factor. For the soaked aggregates, however, marked increases in durability were attained by the use of entrained air. For example, for the 3000 psi concretes, non–air-entrained concrete made with aggregate 6 (expanded blast furnace slag) in the soaked condition had a durability factor of 5, whereas with entrained air the durability factor was 95. Similarly, the respective durability factors for aggregate 7 (expanded shale) in the soaked condition were 2 and 41. The data indicate that, for concretes of low durability, substantial increases in durability were effected by the use of artificially entrained air in amounts similar to those used in concretes made with normal weight aggregates. This is because of the refinement of air void systems. It is known that the cement paste in concrete is normally protected against the effects of freeezing and thawing if the spacing factor of the air void system is 0.008 inches (0.2 mm) or less.[30]

5.2 Influence of Moisture Content of Aggregate on Durability

Klieger and Hansen[29] showed that all of the concretes made with the air-dried aggregates showed greater durability than the non–air-entrained concrete made with aggregate 10 (expanded shale). The durability factor for the soaked aggregate was 7, whereas the durability factor for the air-dried aggregate was 82, a significant difference.

The air-entrained concretes made with nine of the 19 aggregates (dry and wet) showed slightly greater durability in the soaked condition than when air-dried (Table 10.3). In all but one of the nine cases, aggregate 11 at 3000 psi, the durability factors were already at a high level, therefore, the small differences were probably not significant.

In the case of aggregate 11 (expanded shale), the durability factor for the soaked aggregate was 60 compared to 41 for the air-dried aggregate. This particular behavior does not appear to be explainable in terms of air content or any of the other measured properties of these concretes.

5.3 Influence of Strength

For the non–air-entrained concretes (Tables 10.2 and 10.4), strengths did not appear to be of significant influence in determining the resistance of these concretes to freezing and thawing.[29] However, some aggregates

showed significantly higher durability at 3000 psi concrete strength than at 4500 psi. On the other hand, the reverse was true for an equal number of aggregates, although the differences were not as great. The leaner mixes in these non–air-entrained concretes generally had somewhat higher air contents than the richer mixes, and this may be the reason for some of the differences observed.

For air-entrained concretes (Tables 10.3 and 10.5), the durability factors of the 4500 psi concrete were generally greater than for the 3000 psi concretes made with the same aggregates. This was particularly marked for aggregates 7, 10, and 11 (all expanded shale aggregates) when used in a soaked condition.

5.4 Influence of Absorption on Lightweight Aggregates

The degree of saturation is a key parameter for the frost durability of concrete. When performing laboratory tests of LWAC, the moisture condition of LWA is of particular importance. Due to its porous nature, LWA can hold considerable amounts of water that may cause frost damage.

Klieger and Hanson[29] studied water absorption of 4500 psi concretes; absorption was determined in accordance with the procedure set forth in ASTM C330-53 T, on lightweight aggregates for structural concrete. For strength of 4000 psi, the absorption is limited to a maximum of 15%. Figure 10.11 shows the relationships between the absorption of the concretes made with the lightweight aggregates and their durability factor. The data shows that an absorption limitation is not a valid means of producing concretes resistant to freezing and thawing. The absorption of the concretes containing entrained air are quite similar to those for the non–air-entrained concretes, yet the durability is markedly different.

Jacobsen, et al.,[31] have shown that the water absorption of concrete is greater for LWA wet than LWA dry. The characteristics of the aggregates are shown in Table 10.6 and the physical properties of the concretes in Table 10.7. The results are surprising since one would expect the self-desiccation to suck at least some water from the wet aggregate particles, thereby reducing the amount of water absorbed externally. Further, air-entrained normal density aggregates (NDA) absorb more than the non–air-entrained concrete with normal density aggregates (ND), LWA dry, and LWA wet during curing. This is explained by the filling of the air voids in addition to the filling of the self-desiccation pores, in accordance with the findings of Helmuth.[9]

Table 10.6. Composition and Properties of Fresh Concrete[31]

Material	LWA dry	LWA wet	ND	NDA
Cement kg	428	426	440	401
CSF kg	36.9	36.7	37.9	34.5
Aggregates: ND kg	585	583	1765	1609
LWA kg	679 incl. 6.9% abs.	826 (water saturated)	-	-
SP kg	7.80	6.32	11.92	8.12
AEA kg	-	-	-	0.53
W/(C + CSF)	0.35	0.35	0.35	0.35
Density (kg/m^3)	1910	2020	2410	2160
Slump (mm)	90	120	210	150
Air (vol%)	2.4	2.8	1.4	11.8

LWA dry - oven dry LWA, LWA wet - vacuum saturated LWA, ND - normal density aggregate, NDA - normal density aggregate and air entrained.

Table 10.7. Compressive Strength, Density, Moisture Content, Absorption, and Air Void Characteristics[31]

Property	LWA dry	LWA wet	ND	NDA
f_{c28} (MPa)	74.5	72.3	104.7	65.2
Density (kg/m^3)	1920	2030	2470	2280
we (vol% of concrete)	14.4	28.5	11.1	12.2
Absorption at curing (vol% of paste)	3.1	5.0	4.5	8.1
Air voids (vol%)	1.7	1.9	2.0	13.2

we - moisture content (105°C). Absorption given is at water curing, air void characterstic is according to ASTM 457.

Compressive strength is 104.7 MPa for ND, and 72.3 and 74.5 MPa for LWA wet and LWA dry, respectively, indicating a somewhat lower water-to-cement ratio of the latter. NDA had a significantly lower strength than ND due to the high air void content.

The lightweight aggregates (dry) have shown excellent performance in the freeze-thaw resistance test according to ASTM C 666-54 and the salt-frost resistance test according to SS 1372 44 (Table 10.8). It shows that the LWA concrete can perform well in frost tests without air entrainment, in accordance with earlier experiences. Vacuum-saturated LWA (wet) results in severe internal cracking in both the scaling and cracking test after very few cycles. Table 10.8 shows that the internal cracking in LWA wet became severe very quickly, whereas it started more gently in ND. Obviously, the saturated LWA particles create a very destructive pressure upon freezing.

Surface scaling, on the other hand, was only a little higher in LWA wet than in LWA dry. The ND concrete required air entrainment to be durable in both the salt scaling and the internal cracking tests, in spite of a compressive strength of 104.7 MPa. In earlier studies of concretes of lower strength and higher water-to-binder ratio,[32] very good scaling durability was observed. Clearly, factors other than W/B may influence the need for air entrainment in these tests. Such factors include cement type, additional cementing materials, admixtures, aggregate, curing conditions, age, and preparation before frost testing and freeze-thaw cycling. By comparing the scaling results of ND (high scaling) and LWA wet (relatively low scaling), it appears that the paste quality cannot always guarantee good scaling durability. Apparently, the aggregate properties (porosity, stiffness, interface, etc.) play a role in the scaling process.

In addition to LWA dry, NDA also performed very well in both test methods. It was, however, noted that the degree of saturation increased continuously during the test for both concretes. That means that both air voids and LWA particles took up water during freeze/thaw when in contact with water. After 300 cycles, LWA dry and LWA absorbed 1.1 and 1.3%, respectively, of concrete volume without deteriorating. In both ASTM and SS tests, internal cracking was accompanied by an even higher absorption due to freeze/thaw which was also observed by Fagerlund[33] and Jacobsen, et al.[34]

Table 10.8. Results of Rapid Freeze-Thaw Test (ASTM C666 proc. A)[31]

	Concrete	Cycles							DF (Durability Factor)
		0	35	69	105	139	209	300	
Resonance frequency (Hz)	LWA dry	2625	2600	2590	2600	2610	2620	2610	99
	LWA wet	2500	0						2
	ND	2925	2830	1630					11
	NDA	2640	2590	2580	2610	2690	2560		94
Absorption (vol%)	LWA dry	0	0.2	0.3	0.4	0.5	0.7	1.1	
	LWA wet	0	3.7						
	ND	0	1.3	1.3					
	NDA	0	0.5	0.7	0.9	1.0	1.1	1.3	
Scaling (kg/m^2)	LWA dry	0	0.01	0.01	0.02	0.03	0.05	0.09	0.14
	LWA wet	0	0.12						
	ND	0	0.01	0.02					
	NDA	0	0.03	0.05	0.07	0.09	0.12	0.2	

5.5 Durability Relative to Normal Concrete

Klieger and Hanson[29] calculated the relative durability factor of lightweight aggregate concrete (Fig. 10.11). They showed that the relative durability factors of lightweight concretes ranged from a low of 7% to a high of 243% for the non–air-entrained concretes. For the air-entrained concretes, the range was 38 to 120%, a considerably smaller range in relative durability than for the non–air-entrained concretes. The results are quite similar to what would be obtained in a comparison of a number of normal weight aggregates of different types. Aggregate properties influence the durability of concrete. The use of air entrainment raises the durability of concrete markedly, but the aggregate properties may still operate to produce measurable differences in durability, even at relatively high levels of durability.

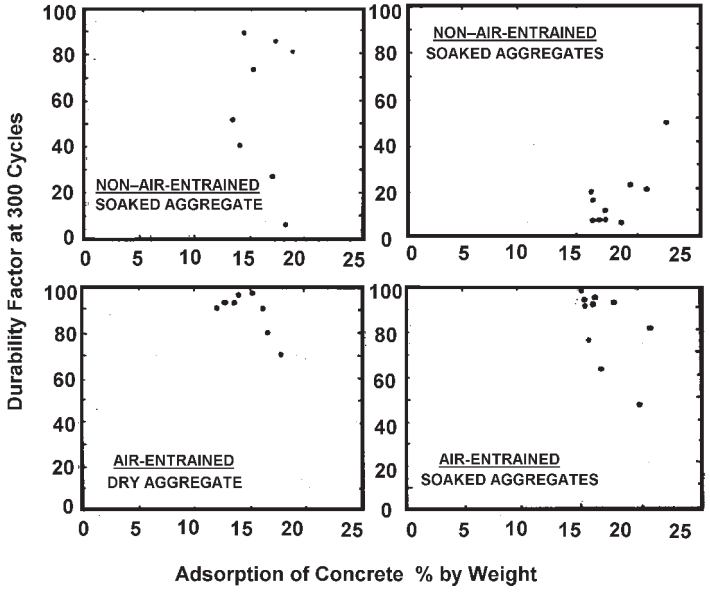

Figure 10.11. Relationship between absorption of concrete and durability factor.[29]

This comparison does not mean that air-entrained concretes made with lightweight aggregates, with relative durability factors lower than 100%, would not be suitable for use in exposed structures subjected to freezing and thawing. It does indicate the probable relative standing with regard to normal weight aggregate 8.

There are undoubtedly normal weight aggregates which, although inferior to aggregate 8, still have satisfactory field performance records. They would similarly show relative durability factors below 100% when compared with aggregate 8.

It is hard to establish a minimum relative durability factor using one normal weight aggregate as the basis for the relative values. It appears more desirable and defensible to establish a minimum durability factor for the particular concrete, say a value of 70 based on 300 cycles of freezing and thawing. If 70 was the durability factor selected, two of the aggregates in 3000 psi air-entrained concrete would not meet this requirement in either the air-dried or soaked condition, and an additional two aggregates would not meet this requirement when used in a soaked condition. For the 4500 psi air-entrainment concretes, two of the aggregates would fail to meet this requirement when used in a soaked condition, while all of the aggregates used in the air-dried condition would meet this requirement.

Chandra[35][36] has investigated the freeze-thaw resistance of LWAC with the addition of a conventional air-entraining agent, a polymer dispersion (CEMOS). The lightweight aggregate concrete was made with expanded clay aggregates Leca™. CEMOS contains soft microparticles of 0.1 μm diameter and has a film-forming ability. For comparison, normal weight concrete of 15 cm cube compressive strength was also tested. The composition is given in Table 10.9; 25 × 25 × 12.5 cube prisms were cut in two parts to get cut surfaces (area 25 × 12.5 = 312.5 cm^2). The specimens were stored for 28 days in a climate controlled room at 60% RH and 20°C temperature. Later, they were stored in water for 28 days.

A freeze-thaw test was performed by immersing the samples in a saturated NaCl solution at -20°C for 16 hours and thawing in tap water at room temperature.[36] The samples were weighed after a particular period and the weight loss was measured. The weight loss and the physical condition of the samples are shown in Fig. 10.12.

Results show the least damage in specimen M100 among the lightweight aggregate concrete cut specimens after 50 cycles. The normal weight concrete was badly damaged after 35 cycles only. The test was stopped for the normal weight concrete and continued for the other concrete

Table 10.9. Composition and Strength of Concrete for Freeze-Thaw Test[35][36]

No.	Sample No.	Adm %	Cement kg/m^3	Sand, Leca™, kg/m^3			Sand/Gravel kg/m^3		W/C	Fresh Den. kg/m^3	28d Comp. Str. MPa
				Sand (0–4)	Leca™ (2–4)	Leca™ (4–16)	Sand (0–8)	Gravel (8–16)			
1	M100	CEMOS 1.5	310	265	140	230	—	—	0.53	1020	10.4
2	M101	CEMOS 1	310	265	140	230	—	—	0.57	1100	14.6
3	M102	CEMOS 3	310	265	140	230	—	—	0.57	1190	15.5
4	M103	CAEA 0.05	310	265	140	230	—	—	0.51	1240	18.4
5	M104	CMT2 1	310	265	140	230	—	—	0.50	1280	18.9
6	M105	—	280	—	—	—	1180	665	0.75	2430	36.3
7	M106	CEMOS 1	280	—	—	—	1180	665	0.69	2170	28.0

CEMOS—Polymer dispersion with a film-forming ability
CMT2—Solid polymer microparticles
M105–M106—Normal weight concrete
CAEA—Conventional air-entraining agent
M100–M104—Lightweight aggregate concrete

types. The main reason for this damage was traced to the entrained air, as well as the hydrophobic, character of the polymer CEMOS. The damage was on the border of the aggregate and the cement paste. This indicates that the adhesion between the aggregate and the cement paste is weakened during the freeze-thaw test. This may be due to the development of hydraulic and osmotic pressures. The admixture, CEMOS, seems to coat the aggregate surface, thereby decreasing its water absorption and, consequently, increasing the freeze-thaw resistance.

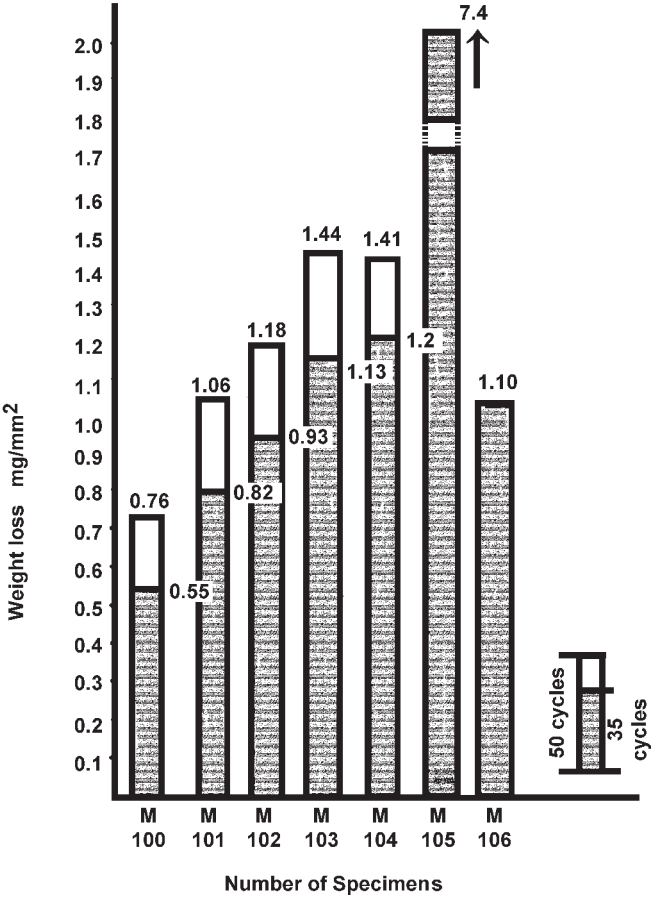

Figure 10.12. Mass loss of the samples during freezing and thawing.[35]

6.0 FIELD TESTS

The samples described in Sec. 5.0 of this chapter were put near the Göta River bridge (Göteborg) motorway in January, 1979. The specimens were placed on the ground with the cut surface down. The specimens were taken out after two years. In winter, deicing salt was used. The temperature record for this period as obtained from the Swedish Climate Office of the Swedish Institute for Meteorology and Hydrology is shown in Fig. 10.13.

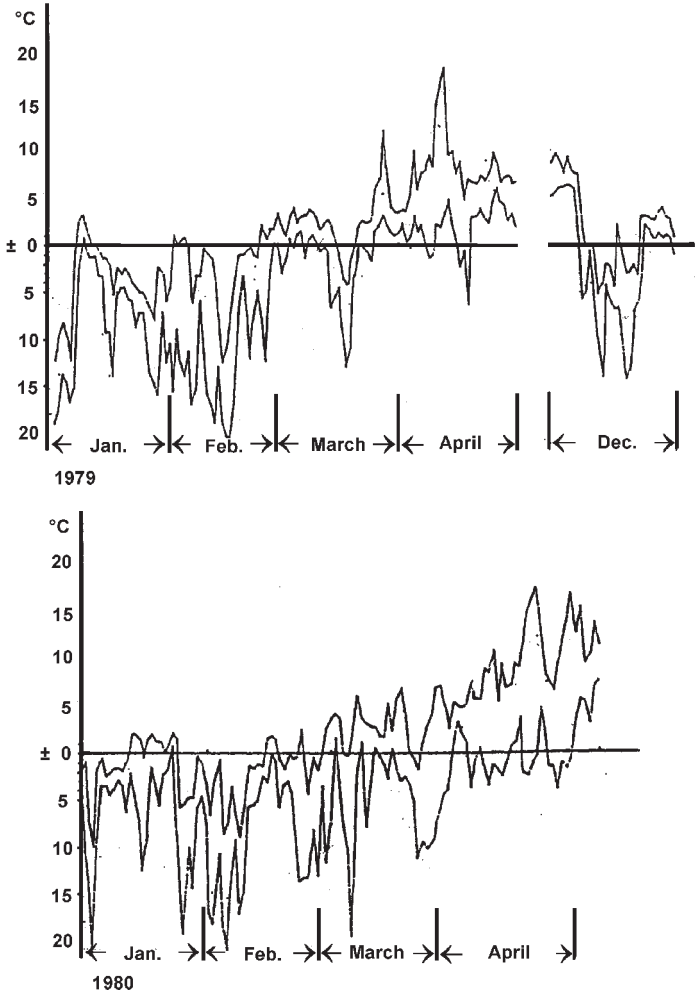

Figure 10.13. Minimum and maximum temperatures during the two winter periods 1979 and 1980.[36]

After the first winter no appreciable damages were noticed. It was observed during the inspection that the damage mainly occurred in the March-April period. From the temperature curve, this was the critical period as there was a maximum fluctuation of temperature, i.e., maximum freezing and thawing occurred in this period. More damages appeared after the second winter exposure. This may be due to the water saturation of the samples during rains. The results have a trend similar to the results obtained in the laboratory tests.

The samples after two winter exposures are shown photographically in Figs. 10.14 and 10.15. This implies that the results have something to do with the aggregate type as the paste was the same in both cases.

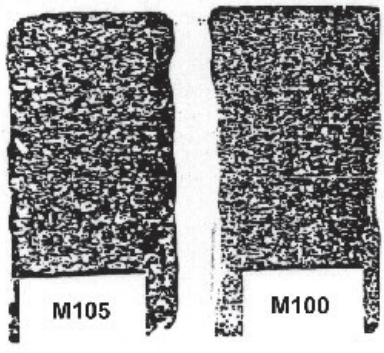

(a)

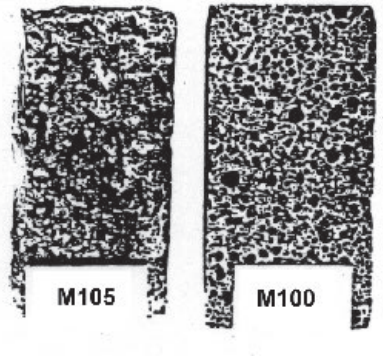

(b)

Figure 10.14. Lightweight aggregate concrete (M100) and normal concrete without air-entraining agent (M105) after two winters; *(a)* cast surface, *(b)* cut surface.[36]

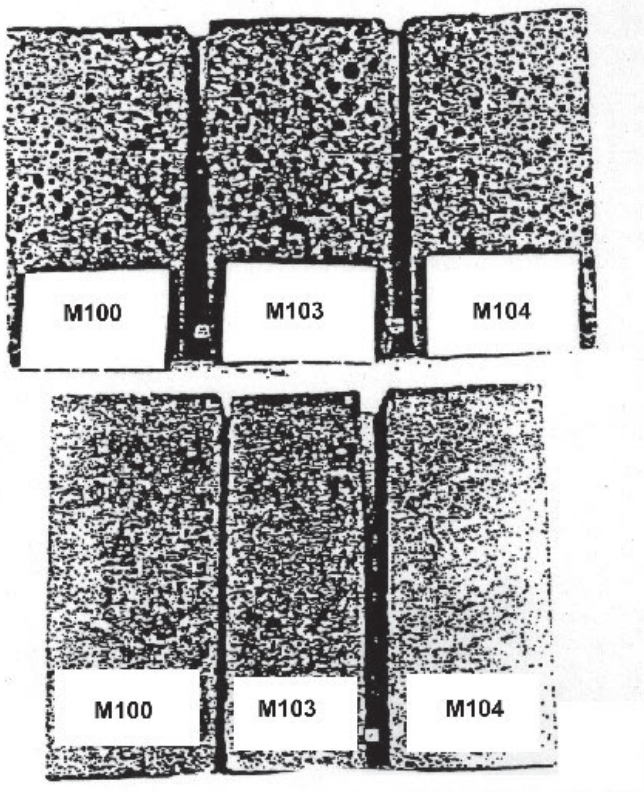

Figure 10.15. LWA concrete after two winters; M100 with 1.5% CEMOS, M103 with conventional air-entraining agent, and M104 with CMT 2; *(a)* cast surface, *(b)* cut surface.[36]

6.1 Internal Cracking During Freezing and Thawing

Increase in strength increases brittleness of the concrete. Consequently, concrete becomes less elastic. During freezing, when water transforms to ice, there is volume expansion. Brittle concrete is unable to accommodate this expansion, which leads to the formation of internal stresses. When these stresses exceed the tensile strength of concrete, cracks are developed. The modulus of elasticity is calculated by measuring the time taken by a sound wave to travel a particular distance. The time is

related to the microstructure of the concrete. If there are cracks, the time taken will be more, and the modulus of elasticity, which is inversely proportional to the time, will decrease. Durability factor is directly proportional to the modulus of elasticity and, therefore, will also decrease. Thus, the lower the durability factor, the higher the cracks, and the concrete is damaged even if there is no weight loss. Weight loss actually gives a sort of warning, and provides a possibility of repair. But, in the case of high strength concrete, one does not get this warning and the damage is more severe and costs more to repair, if repair is possible. In many cases it needs replacement.

$$C = \frac{L}{t}$$

where C = sound velocity
L = length of the sample
t = time

$$E = C^2 \cdot \rho$$

where E = modulus of elasticity
ρ = density of the material

$$DF = \frac{\%\ \text{original}\ E}{300} \times n$$

where DF = durability factor
%Original E = modulus of elasticity
n = number of cycles at the end of the test

Jacobsen, et al.,[31] have shown that the crack formation is lower in the case of lightweight aggregate concrete made with the expanded clay aggregate Leca™ compared to the high strength normal weight concrete. Cracks followed around most of the aggregate particles.

Whiting and Burg[38] investigated the internal cracking durability of various LWA concretes including some high strength LWA concretes. All concretes were air entrained. The test methods were ASTM C666 procedure A with various types of cycles, and Fagerlund's critical degree of saturation method.[33] Results of the ASTM C666 procedure A type testing showed very good durability for all the concretes tested. When using

more than 300 cycles or "Arctic" type freeze-thaw cycling (lower temperatures, higher number of cycles than the standard 300), internal cracking developed in some, whereas most concretes survived well. Failure occurred either at a high degree of saturation (few cycles), or after a high number of cycles at a comparatively low degree of saturation. In most cases, a clear correlation between the increased degree of saturation and frost damage due to internal cracking was found.

However, for the high strength LWA concrete, high scatter and no clear correlation between degree of saturation and internal cracking was observed. A variation in the degree of saturation was obtained by immersing concrete specimens for various periods of time under vacuum. Apparently, low paste permeability made uniform resaturation difficult. Various degrees of surface scaling were observed on all concretes at prolonged freeze-thaw cycling in water.

6.2 Resistance to Deicer Scaling

Concrete, when exposed to deicing salt during freezing and thawing, is damaged partly due to the chemical interaction of salts and partly due to freezing and thawing as was explained in Sec. 4.0 (Scaling Mechanism). Some of the LWAC with and without air-entraining agents were tested.[29] A comparison was done with normal weight concrete. Air-entrained concretes made with three of the lightweight aggregates were used to determine freeze-thaw resistance with deicing salt. The physical characteristics of these concretes and the surface scale ratings through 300 cycles of tests are shown in Table 10.3.

Non–air-entrained concretes (Tables 10.2 and 10.4) made with normal weight aggregates generally reached a scale rating of 5 at about 50 to 75 cycles of test. Air-entrained concretes made with these same aggregates showed surface scale ratings between 1 and 2 at 175 cycles of test, and between 1 and 3 at 300 cycles of test. On this basis, aggregate 3 would appear to be satisfactory in either the air-dried or soaked condition for an exposure involving the use of deicers. Similarly, aggregates 4 and 10, when used in the air-dried condition, would appear to be satisfactory, but possibly not when used in the soaked condition.

Zhang[39] investigated the salt scaling durability of non–air-entrained, high-strength LWA concretes with various types of LWA. The concretes had water/binder ratios in the ranges of 0.28 and 0.44 and were made with the addition of 0 and 9% silica fume. The concretes showed

excellent scaling resistance. The test was performed according to the Swedish Standard SS 1372 44. However, some acceleration of the scaling was observed for some of the concretes after approximately 50 cycles. Hammer and Sellevold[32] also obtained similar results.

Jacobsen, et al.,[31] investigated the interrelation between internal cracking and scaling of high strength lightweight aggregate concrete. Four concretes were tested; two with lightweight aggregate, LWA dry and wet, and two with normal density aggregate, ND dry and wet. All had a water-to-binder ratio of 0.35, and a silica fume-to-binder ratio of 0.08. The volume of the paste in concrete was kept constant at 32% of volume of concrete. The lightweight aggregates were Leca™ 800 with a particle density of 1425 kg/m^3 and a 28 day compressive strength of 72.3 and 74.5 MPa and densities of 2030 and 1920 kg/m^3 for wet and dry LWA concrete, respectively.

The aggregates used were either oven dried or vacuum saturated. The absorption of dry LWA from fresh cement paste was assumed to be 6.9% by mass. The normal aggregates were of granite origin.

The LWA dry concrete performed very well in frost resistance without air entraining, whereas the water saturated LWA concrete showed severe internal cracking in both the scaling and cracking test. The internal cracking in LWA wet concrete became severe very quickly (Fig. 10.16),[31] whereas it started more gently in ND concrete. This is because of the higher degree of saturation of the wet particles from the very beginning, as well as the significant increase in the water and/or salt solution at the start of the freeze/thaw testing compared to isothermal water storage/water absorption. This increases the degree of saturation in the beginning.

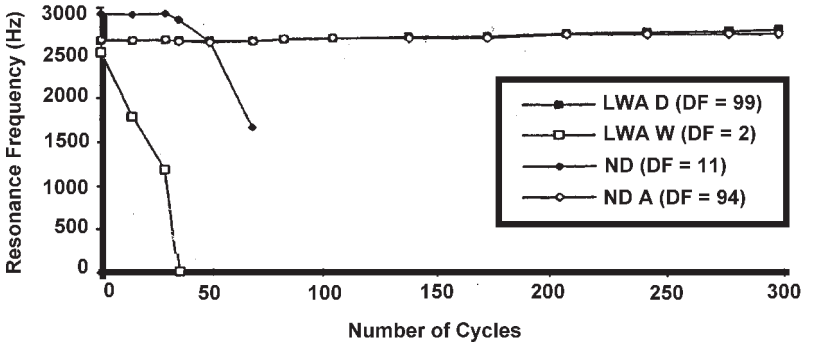

Figure 10.16. ASTM C 666 procedure A, resonance frequency versus the number of cycles in the beams.[31]

This seems to create a very destructive pressure on freezing. Surface scaling, on the other hand, was only somewhat higher in LWA wet concrete than LWA dry concrete (Fig. 10.17). ND concrete did not show good performance without air entrainment, even if the strength was as high as 104 MPa and the water-to-binder ratio was as low as 0.35. By comparing the scaling results of ND concrete (high scaling) with low scaling of LWA concrete, it can be concluded that the aggregate has an important effect on the frost-salt resistance.

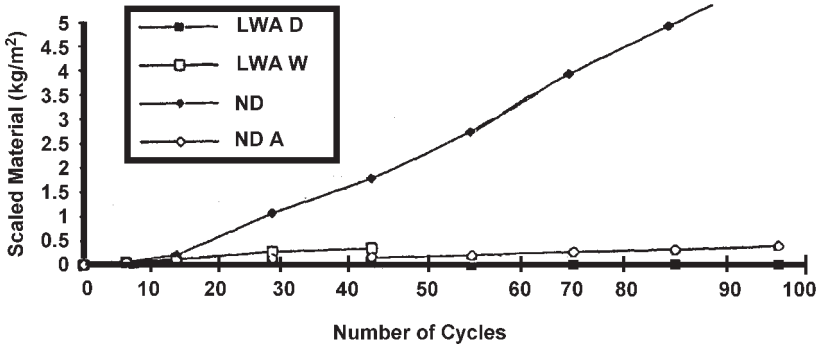

Figure 10.17. Swedish Standard SS 1372 44, scaling on the slab surfaces versus the number of cycles.[31]

7.0 CONCLUDING REMARKS

The freeze-thaw cycle test actually does not adequately represent natural freezing conditions. The freezing period, in practice, normally is much longer outdoors. The phenomenon of ice accretion in capillary cavities during the freezing period described by Powers, Helmuth, and others is possibly more important than the hydraulic pressure generated during the freezing of water. The critical spacing factors for concretes exposed to long freezing periods perhaps could be smaller than those for concretes submitted to usual freeze-thaw cycle tests.

A freeze-thaw test in water at freezing rates ranging from 2 to 6°C are required to determine the critical spacing factors when concrete is frozen in water at these low rates and also to evaluate the intensity of surface scaling in the absence of deicer salts. Scaling is a form of deterioration

different from internal cracking. The change in length and the loss of the dynamic modulus of elasticity from which $\overline{L}$ are determined are basically due to internal cracking.[40]

REFERENCES

1. Woods, H., *Durability of Concrete*, ACI Monograph 4, p. 20 (1968)
2. Mather, B., Durability of Concrete, Aspects of Admixtures and Industrial By-products, *Int. Seminar, Chalmers University of Technology, Göteborg, April 1986,* Swedish Council for Building Research, Document D-1, p. 159 (1988)
3. Chatterji, S., Durability of Concrete, Aspects of Admixtures and Industrial By-products, *Int. Seminar, Chalmers University of Technology, Göteborg, April 1986,* Swedish Council for Building Research, Document D-1, p. 309 (1988)
4. Powers, T. C., *The Physical Structure and Engineering Properties of Concrete,* Bulletin 90, p. 22, Portland Cement Association, Research and Development Laboratories, Skokie, IL (Jul. 1958)
5. Chandra, S., and Aavik, J., Influence of Black Gram on Protland Cement and Mortars, *Cement and Concr. Res.*, pp. 423–430 (1983)
6. Beaudoin, J. J., and McInnis, C., The Mechanism of Frost Damages in Hardened Cement Paste, *Cement and Concr. Res.*, 4:139–148 (1974)
7. Fagerlund, G., *Durability of Concrete,* ACI Special Publication, SP-47, pp. 13–66 (1975)
8. Powers, T. C., and Helmuth, R. A., Theory of Volume Changes in Hardened Portland Cement Paste During Freezing, *Proc. Highway Research Board,* 32:285–292 (1953)
9. Helmuth, R. A., Dimensional Changes of hpc Pastes Caused by Temperature Changes, *Proc. Highway Research Board,* 40:315–336, Washington, DC (1961)
10. Chatterji, S., Aspects of Freezing Process in Porous Material-Water System, Part 2, Freezing and Properties of Frozen Porous Materials, *Cement Concr. Res.*, 29(4):781–784 (1999)
11. Timoshenko, S., and Goodier, J. N., *Theory of Elasticity*, McGraw Hill, New York, p. 359 (1951)
12. Nerenst, P., Frost Action in Concrete, *Proc. 4th Int. Symp. Chem. Cement, Washington,* II:807–828 (1960)

13. Litvan, G. G., Particulate Admixture for Enhanced Freeze-thaw Resistance of Concrete, *Cement Concr. Res.*, 8(1):53–60 (1978)
14. Konrad, J. M., Frost in Soils; Concepts and Engineering, 16th Canadian Geotechnical Colloquium, *Canadian Geotechnic J.*, 31:2 (1994)
15. Chatterji, S., Aspects of Freezing Process in Porous Material-Water System, Part 1, Freezing and Properties of Water and Ice, *Cement Concr. Res.*, 29(4):627–630 (1999)
16. Chatterji, S., Jensen, A. D., Thaulow, N., and Christensen, P., Freezing of Aqueous Solutions in a Porous Medium, Part 2, *Cement Concr. Res.*, 15:729 (1985)
17. Verbeck, G. I., and Klieger, P., Study of Salt Scaling of Concrete, Bulletin 150, *Highway Research Board* (1957)
18. Cordon, W. A., *Freezing and Thawing of Concrete-Mechanism and Control*, ACI Monograph 3 (1967)
19. Kleiger, P., Effect of Atmospheric Conditions During the Bleeding Period and Time of Finishing on the Scale Resistance of Concrete, *ACI Journal Proc.*, 52:309–326 (Nov. 1955)
20. Powers, T. C., The Bleeding of Portland Cement Paste, Mortar and Concrete, *Bulletin 22,* PCA Res. Lab., Portland Cement Association (1939)
21. Emmons, W. J., *The Effect of Soft Particles of Coarse Aggregates on the Strength and Durability of Concrete*, Circular no. 6, National Sand and Gravel Association (1931)
22. Meier, U., and Harnik, A. B., The Freezing of Water in Hardened Cement Paste in Case of Prevented Evaporation, *Cement Concr. Res*., 8:545–551 (1978)
23. Litvan, G. G., Frost Action in Cement Paste, Materials and Structures, *Research and Testing,* RILEM, Paris, 6(34):293–298 (Jul.–Aug. 1973)
24. Pigeon, M., Prevost, J., and Simard, J. M., Freeze-Thaw Durability versus Freezing Rate, *ACI Journal*, pp. 684–692 (Sep.–Oct. 1985)
25. Powers, T. C., The Air Requirement of Frost Resistance Concrete, and Discussions, *Proc. Highway Research Board,* 29:184–202, 203–211 (1949)
26 Fagerlund, G., Effect of Air Entraining and Other Admixtures on the Salt-Scaling Resistance of Concrete, Durability of Concrete, Aspects of Admixtures and Industrial By-products, *Int. Seminar, Chalmers University of Technology, Göteborg, April 1986*, Swedish Council for Building Research, Document D-1, pp. 223–266 (1988)
27 Pistilli, M. F., Air Void Parameters Developed by Air Entraining Admixtures as Influenced by Soluble Alkalis from Fly Ash and Portland Cement, *ACI Journal,* pp. 217–222 (May–Jun. 1983)

28. Petterson, P. E., The Influence of Silica Fume on Salt Frost Resistance of Concrete, Durability of Concrete, Aspects of Admixtures and Industrial By-products, *Int. Seminar, Chalmers University of Technology, Göteborg, April 1986*, Swedish Council for Building Research, Document D-1, pp. 179–190 (1988)

29. Klieger, P., and Hanson, J. A., Freezing and Thawing of Lightweight Aggregate Concrete, *ACI Journal Proc.*, pp. 779–797 (Jan. 1961)

30. Powers, T. C., Void Spacing as a Basis for Producing Air Entrained Concrete, *ACI Journal Proc.*, 50(9):741–760 (May 1954)

31. Jacobsen, S., Hammer, T. A., and Sellevold, E. J., Frost Testing of High Strength Lightweight Aggregate Concrete; Internal Cracking vs. Scaling, *Proc. Int. Symp. Structural Lightweight Aggregate Concrete, Sandefjord, Norway*, pp. 541–554, (I. Holand, T. A. Hammer, and F. Fluge, eds.) (Jun. 20–24, 1995)

32. Hammer, T. A., and Sellevold, E. J., *Frost Resistance of High Strength Concrete*, ACI Special Publication, SP-121, pp. 457–489 (1990)

33. Fagerlund, G., The Critical Degree of Saturation Method of Assessing the Freeze-thaw Resistance of Concrete, *Materials and Structures*, 10:217–229 (1977)

34. Jacobsen, S., Gran, H. C., Sellevold, E. J., and Bakke, J. A., High Strength Concrete-Freeze/Thaw Testing and Cracking, *Cement Concr. Res.*, 25(8):1775–1780 (1995)

35. Chandra, S., *Freeze-Thaw Resistance of 3L-Concrete and Normal Concrete with Microparticles*, Report 82:4, Chalmers University of Technology, (Feb. 1982)

36. Chandra, S., and Aavik, J., Outdoor Freeze-Thaw Resistance of 3L-Concrete and Normal Concrete with Microparticles, Report 82:5, Chalmers University of Technology (Feb. 1982)

37. Deutscher Beton-Verein e.v., Verfahren zur Prufung des Frost und Tausalzwiderstandes von Beton fur Bruckenkappen und Änliche Bautelle, *Betonwerk + Fertigteiltechnik*, Vol. 1 (1976)

38. Whiting, D., and Burg, R., *Freezing and Thawing Durability of High Strength Lightweight Concrete*, ACI Special Publication, SP-126, pp. 83–100 (1991)

39. Zhang, M. H., Microstructure and Properties of High Strength Lightweight Concrete, Dr. Ing Dissertation 1989-5, The Norwegian Institute of Technology, Trondheim, Norway (1989)

40. Malhotra, V. M., Mechanical Properties and Freezing and Thawing Resistance of Non–Air Entrained, Air Entrained Superplasticized Concrete Using ASTM 666, Procedure A and B, *Cement Concr. Aggregates*, 4(1):3–23 (Summer 1982)

Glossary

1.0 TERMINOLOGY AND DEFINITIONS

Aardelite. Sintered fly ash aggregate, fly ash collected from the flue gas of thermal power stations is dampened with water and mixed with coal slurry in screen mixers. The material is then fed into rotating pans, known as pelletizers, to form special pellets. These are then sintered at a temperature of about 1400°C. This causes the ash particles to coalesce, without fully melting, to form a lightweight aggregate. These are known under the commercial name of "Lytag™."

Aglite. It is produced in the UK by mixing clay pellets or shale with ground coke, passing it over a sinter strand hearth, then through the crushers. These are angular because they are crushed and graded.

Exfoliated Vermiculite Aggregates. Vermiculite is a mineral of laminar formation, similar in appearance to mica, but unlike mica, it expands (exfoliates) rapidly when heated, thereby radically reducing the density.

Expanded Perlite Aggregates. Perlite is a glassy volcanic rock containing water. The aggregates are formed by crushing the material to graded sizes and rapidly heating it to the point of incipient fusion (approximately 1300°C). At this temperature, the water dissociates itself and expands the glass into a balloon-like formation of small bubbles to produce a cellular-type material with low density.

Expanded Slag Aggregate. See Foamed Slag.

Expanded Slate, Solite. When a certain type of slate is rapidly heated, a resulting generation of gases changes the characteristic laminar structure into a product containing large numbers of minute contours separated by glassy walls. The material is first crushed and then heated in a oil-fired rotary kiln. After cooling, the expanded slate is graded. The graded slate is known by the commercial name "SOLITE Aggregate."

Foamed Slag. Molten slag from a pig iron blast furnace is treated in the molten state (approximately 1300°C) with a controlled amount of water (or in some industrial processes by steam and compressed air) so that the steam is trapped in the molten mass to give the slag a porous structure, very similar to natural pumice. This is called "Foamed" or "Expanded Slag Aggregate."

High Strength Lightweight Aggregate Concrete (HSLAC). Lightweight aggregate concrete which has a cube compressive strength of 50 MPa and over is classified as High Strength Lightweight Aggregate Concrete.

Leca™, Light Expanded Clay Aggregates. These are produced from a special type of clay suitable for bloating. It is ground and pretreated before passing through a

rotary kiln. This forms a range of spherical pellets with a glazed but porous skin. These are made in Sweden and Norway and are called, for example, Swedish Leca™, and Norwegian Leca™.

Liapor™. These are also expanded clay aggregates. The process of their manufacture is different from the production of Leca™. They are first pressed into balls of a desired shape, dried, and then burned. Thus, unlike Leca™, their size and shape is very precise, there is no dust or 0–1 mm portion.

Lytag™, Sintered Fly Ash Aggregate. See Aardelite.

LWA, Lightweight Aggregate. The aggregates which are light and porous are called lightweight aggregates. They do not have any crystallized mineralogical composition. They have a glassy surface, cellular structure, and can be natural or man-made.

LWAC, Lightweight Aggregate Concrete. The concrete made by using lightweight aggregate is called lightweight aggregate concrete. It has low density and strength.

Pumice. These are volcanic aggregates and are formed when the SiO_2-rich molten lava cools. The molten magma has plenty of air and gases which get entrapped during sudden cooling of the magma. This makes the aggregates porous. The sudden cooling does not allow the crystallization of the minerals, so it attains glassy structure. It is found in Iceland, Italy, Greece, Turkey, and Germany.

Pellets. A ball-like form made from ash by moistening it, which is sintered for making lightweight aggregate.

Pelletization. This is a process for making pellets, a ball-like shape of ash made by moistening it, which is later sintered in the kiln for making lightweight aggregates

Ramtite. Sintered Fly Ash Aggregate. See Aardelite.

Rotary Kiln. It is a cylinderical kiln which generally has three sections: preheating, burning, and cooling. It is long and rotates and has a slope so that the material inside passes by itself. There are sometimes chains inside which break the clay into small pieces. When the clay passes the heating zone it expands and is cooled by air blowing into the cooling zone.

Scoria. Volcanic aggregates found, for example in Greece, Iceland, and Turkey. See Pumice.

Sintering. A process of burning aggregates in industrial furnaces to vitrification. They acquire a cellular structure, a porous structure where the pores are separated by the vitrified walls.

Structural Lightweight Aggregate Concrete. It is the lightweight aggregate concrete which is used for structural purposes. It has a particular strength which is recommended according to the standard of particular countries to qualify for use in the load-bearing structures. In Sweden, it should be equivalent to K8. The concrete should have a minimum, 15 cm, cube compressive strength of 10.5 MPa.

Tuff. A pyroclastic rock of consolidated volcanic fragments found in Yukon Canada and Eastern US.

2.0 ABBREVIATIONS

ASTM	American Society for Testing andMaterials Standard
BS	British Standard of Test Methods
DIN	German Standard of Test Methods
GOST	Russian Standard of Test Methods
ISI	Indian Standard of Test Methods
ISO	International Standard Organization for Test Methods
SS	Swedish Standard of Test methods
OPC	Ordinary Portland Cement
PFA	Pulverized Fly Ash
BFS	Blast Furnace Slag
CSF	Condensed Silica Fume
LWA	Lightweight Aggregate
LWAC	Lightweight Aggregate Concrete
LC	Lightweight Concrete
NC, NWC	Normalweight Concrete

3.0 SYMBOLS

C	CaO	Calcium oxide
A	Al_2O_3	Aluminium oxide
$\bar{S}$	$CaSO_4$	Calcium sulphate
H	H_2O	Water
F	Fe_2O_3	Iron (III) oxide
CH	$Ca(OH)_2$	Calcium hydroxide
CS	$CaO{\cdot}SiO_2$	Calcium silicate
CSH	$CaO{\cdot}SiO_2{\cdot}H_2O$	Calcium silicate hydrate:Tobermorite
C_2S	$2CaO{\cdot}SiO_2$	Di-calcium silicate

C_3S	$3CaO{\cdot}SiO_2$	Tri-calcium silicate
C_3A	$3CaO{\cdot}Al_2O_3$	Tri calcium aluminate
C_4AF	$4CaO{\cdot}Al_2O_3{\cdot}Fe_2O_3$	Tetra-calcium alumino-ferrite
	$C_6AS_3{\cdot}H_{32}$	Ettringite
	$K_2O{\cdot}Al_2O_3{\cdot}6SiO_2$	Potassium alumina silicate (Potassium feldspar)
	$CaCO_3$	Calcium carbonate (Calcite, Vaterite, Aragonite)
	Al_2O_3, Fe_2O_3	Amphoteric oxides
	NH_3(gas)	Ammonia
	$Na_2O{\cdot}Al_2O_3{\cdot}4SiO_2{\cdot}2H_2O$	Analcime
	$CaCl_2$	Calcium chloride
	KOH	Caustic soda
	H_2CO_3	Carbonic acid
	Cl	Chloride
	HCl(aq.)	Hydrochloric acid
	NO_x	Nitrogen oxide
	NO_3	Nitrate
	HNO_3(aq.)	Nitric acid
	NaOH	Sodium hydroxide
	SO_2(g)	Sulfur dioxide
	SO_4	Sulfate
	H_2SO_4	Sulfuric acid
	NaCl	Sodium chloride
	$R_2O{\cdot}RO{\cdot}R_2O_3{\cdot}(2\text{-}4)SiO_2{\cdot}nH_2O$	Natural zeolites

4.0 CONVERSION FACTORS

From	To	Divided By
LENGTH		
Centimeters	Microns	0.0001
Inches	Centimeters	0.3937
Feet	Meters	3.28083
Miles (English)	Kilometers	0.62137
AREA		
Square inches	Square centimeters	0.1550
Square feet	Acres	43560
Acres	Hectares	2.471044
Square feet	Hectares	107639
VOLUME		
Cubic yards	Cubic meter	1.3070
Gallons (US)	Liters	0.26418
Cubic feet	Gallons (US)	1.3368
Gallons (US)	Gallons (British)	1.20094
WEIGHT		
Pounds	Kilogram	2.204622
Tons (short)	Metric tons	1.10231
Tons (long)	Metric tons	0.98421
Barrels (376 pounds)	Metric tons	5.8633
Tons (short)	Tons (long)	1.12
Barrels (376 pounds)	Tons (long)	5.957
Barrels (376 pounds)	Tons (short)	5.3191
STRENGTH		
Pounds per square inch	Kilogram per square centimeter	14.2233
TEMPERATURE		
Degree Fahrenheit	Degrees Centigrade	(°C × 1.8 + 32)
HEAT		
Btu	Calories (kilogram)	3.96753
POWER		
Btu	Kilowatt hours	3413.44

Index

A

D

E

F

G

H

M

N

O

P

Q

R

S

T

U

V

W

X

Y